SEA SURFACE TEMPERATURE-RAINFALL RELATIONSHIPS AND ASSOCIATED OCEAN-ATMOSPHERE COUPLING MECHANISMS IN THE SOUTHERN AFRICAN REGION

by

Nan Delene Walker

A Thesis submitted to the University of Cape Town
in fulfillment of the requirements for the
degree of Doctor of Philosophy

April 1989

ABSTRACT

The relationships between interannual sea surface temperature variability (SST) of the oceans surrounding southern Africa and summer rainfall variations over South Africa are investigated using statistical, observational and mechanistic approaches. Positive correlations are identified between summer rainfall and SSTs of the Mozambique/Agulhas Current region, the Agulhas Retroflection region and the northern Benguela Current system. These relationships are stronger when rainfall anomalies associated with the Southern Oscillation are not considered. The observation of significant lag relationships involving temperatures of the Agulhas Current system suggests that future prediction efforts for summer rainfall will benefit from a consideration of SST anomaly patterns east and south of Africa, in combination with other atmospheric indices.

Surface winds, heat fluxes and atmospheric boundary layer characteristics are investigated using compositing analyses to assess pertinent ocean-atmosphere coupling mechanisms. Easterly wind anomalies across the southwest Indian Ocean and over source regions of the Agulhas Current accompany and precede the local oceanic "warm events" which correspond with higher rainfall. Thus a class of event is identified in which warmer waters along the east coast and stronger easterly wind forcing accompany wetter seasons over South Africa. The atmospheric boundary layer is considerably warmer and moister in association with positive SST anomalies along the east coast and increased tropical airflow. Consequently, moisture convergence and tropical convection are increased over the eastern interior near 20° to 25°S. South of Africa, positive SST anomalies generate surface heat flux anomalies, increasing instability and moisture levels within the boundary layer. Horizontal heat flux gradients are strengthened across the Agulhas/Subtropical Convergence SST front and the conditions necessary for cyclogenesis and westerly wave amplification are optimized. Tropical-temperate troughs account for most of the abnormal rainfall during local Agulhas "warm events". The presence of positive SST anomalies east and south of southern Africa increases the likelihood of their formation by intensifying tropical and temperate components. The contribution provided by each component is influenced by the position and magnitude of the SST anomaly as well as the season of occurrence. Conceptual models are presented which summarize the most important ocean-atmosphere coupling mechanisms associated with rainfall variations of southern Africa.

CONTENTS

CHAPTER Page

CHAPTER Page

PREFACE

The oceans and the atmosphere are intricately linked via complex coupling mechanisms involving transfers of heat, moisture and momentum at the air-sea interface. Temperature anomaly patterns of the surface ocean demonstrate considerable spatial coherency and temporal persistency, particularly when compared with the chaotic nature of the overlying atmosphere (Namias and Born, 1970). These characteristics suggest that the ocean provides some stability to the overlying atmosphere, thus increasing potential predictability within the ocean-atmosphere climate system. These concepts have given rise to numerous studies of air-sea interactions and their relationships to short-term climate variability.

Three main factors have hastened progress in this field over the past decade. One of the factors has been the increased interest shown in large-scale ocean atmosphere-interactions of the tropical Pacific Ocean, commonly termed the El Nino-Southern Oscillation Phenomenon (ENSO). The major Pacific warm event of 1982/3, which was associated with dramatic changes in tropical and extratropical weather and climate patterns across the globe, spurred renewed interest in the climatic implications of ocean-atmosphere interactions. The second important factor was the establishment of high-quality historical data bases of sea surface temperatures and other meteorological variables compiled from merchant ships' observations. The third factor was the development of general atmospheric circulation models through which the physical mechanisms linking the ocean and atmosphere can be tested and more throroughly evaluated.

The influence of sea surface temperature (SST) anomalies on atmospheric properties and circulations have been studied through the use of statistical, observational, theoretical and modeling approaches. The first three approaches were employed before general circulation and coupled ocean-atmosphere models had been developed (Priestley, 1964; Bjerknes, 1966; Bjerknes, 1969; Namias, 1973; Namias, 1976; Rogers, 1976; Davis, 1978) and their use has continued, as discrepancies exist between modeling results and the other approaches. The models have tended to underestimate the influence of SST anomalies, particularly in midlatitude regions (Chervin et al., 1980; Frankignoul, 1985; Shukla, 1986).

The identification of statistically significant links between oceanic and atmospheric properties has important implications for climate prediction. The use of rainfall as the climatic element improves the potential usefulness of the identified

statistical relationships. For this reason, investigations into the associations between interannual SST variability and continental rainfall patterns have increased in recent years (Namias, 1976; Markham and McLain, 1977; Weare, 1979; Nicholls, 1980; Barnett, 1981; Moura and Shukla, 1981; Streten, 1981; Hirst and Hastenrath, 1983; Lough, 1986; Folland et al., 1986; Nicholson and Entekhabi, 1987; Aceitano, 1988; Kershaw, 1988).

Research on SST-rainfall associations in the southern African region have been limited in comparison with other areas. Hirst and Hastenrath (1983) described ocean-atmosphere interactions in the tropical Atlantic in relation to Angolan rainfall and were able to attribute 30% of the rainfall variations to local SST influences. Nicholson and Entekhabi (1987) investigated rainfall of central and southern Africa in relation to SST variability from 10° to 30°S along the west coast. They discovered a 5-6 year periodicity in SST variability along the African west coast which was positively correlated with both rainfall variability and the Southern Oscillation Index. They concluded that rainfall and sea surface temperatures were simultaneously modulated by atmospheric forcing mechanisms, with little coupling between ocean and atmosphere pertinent to the associated rainfall variations. A 19-year oscillation has been identified in Agulhas Current temperature records spanning 131 years (Mason, 1988). Although the results are somewhat tenuous due to inadequacies in the long-term data set, the results are of interest as a quasi 18-year oscillation has been revealed in summer rainfall variations over South Africa (Tyson et al, 1975).

In this thesis the relationships between interannual surface temperature variability of the oceans surrounding southern Africa and summer rainfall variations over South Africa are investigated. The hypothesis to be tested is that interannual variations in sea surface temperatures within local ocean regions alter atmospheric boundary layer conditions and circulations, affecting rainfall processes over the interior of South Africa in summer. The study employs statistical, observational and mechanistic approaches to obtain insight into SST-rainfall relationships and the ocean-atmosphere coupling mechanisms pertinent to them. The primary objectives of this research were:

(1) to establish the nature of relationships between interannual variations of sea surface temperatures within the southeast Atlantic and southwest Indian Oceans and South African summer rainfall.

(2) to ascertain the stability of sea surface temperature-rainfall relationships involving the Mozambique, Agulhas and Benguela Current systems.

(3) to assess surface wind, heat flux and marine boundary layer variabilities as possible ocean-atmosphere coupling mechanisms contributing to contrasting rainfall regimes.

(4) to evaluate the role of air-sea interactions on atmospheric circulations and rain-producing synoptic systems in the presence of local oceanic warm events.

(5) to identify ocean-atmosphere feedback mechanisms pertinent to the SST-rainfall relationships.

The thesis is presented in seven chapters. CHAPTER 1 provides an introduction to atmospheric circulations affecting rainfall processes and rain-producing synoptic systems over southern Africa in summer. The dynamic ocean current systems surrounding Africa are also discussed with special emphasis on surface heat flux processes. CHAPTER 2 presents information on the data bases and analysis techniques used in the study. In CHAPTER 3, the statistical relationships between sea surface temperatures and summer rainfall over South Africa are established. CHAPTER 4 investigates ocean-atmosphere coupling mechanisms pertinent to the identified relationships by studying surface winds and heat fluxes corresponding to contrasting rainfall regimes. In CHAPTER 5, the rain-producing synoptic systems associated with oceanic warm events are identified and their developments are assessed in terms of local air-sea interaction processses. CHAPTER 6 presents conceptual models which show how positive SST anomalies and altered SST gradients affect atmospheric conditions, circulations and rainfall in the southern African region. The results of the analysis are summarized in CHAPTER 7.

Parts of the work presented in this thesis have been published during the course of the research. Concepts incorporated in Chapter 1 appeared in the preprints volume of the 2nd International Conference on Southern Hemisphere Meteorology, the South African Journal of Science, Deep-Sea Research, the South African Journal of Marine Science and the Journal of Geophysical Research. Parts of Chapters 3, 4 and 5 have appeared in the proceedings volume of Floods in Perspective and have been accepted for publication by both the South African Journal of Science and the Journal of Geophysical Research. Unpublished presentations have been made at the Conference on Long-term Data Series Relating to Southern Africa's Renewable Natural Resources and at the South African Society for Atmospheric Sciences.

Numerous people have assisted me through the course of this research and I acknowledge their contributions with gratitude. The staff of the South African Data Centre for Oceanography/CSIR supplied most of the marine data. Dr. J.A. Lindesay provided rainfall data over South Africa as well as data needed to compute the Southern Oscillation Index. Mr. I. Marais of the Satellite Remote Sensing Centre/CSIR furnished most of the satellite imagery and Dr. P. Arkin of the Climate Analysis Center provided the Outgoing Longwave Radiation data. Miss M. Kruger of the CSIR and her able library staff assisted greatly by obtaining publications quickly from around the world. The librarians of the South African Weather Bureau were also indispensable, sending needed information at short notice. Mr. W. Harmse and Miss U. von St Ange are gratefully acknowledged for their assistance with computer software development and the drawing office staff of the CSIR and Mrs S. Sayers for producing the high quality illustrations. Mr. P. Slevin is thanked for providing invaluable editing assistance. Mrs. J. van Heerden deserves special thanks for her expertise and enthusiasm in preparing the final typed version of this thesis. Colleagues at the CSIR are acknowledged for discussions, support and encouragement during the course of the work. Special thanks are extended to Mr. C. Stavropoulos, Miss R.D. Mey, Mr. R. van Ballegooyen, Mr. H. Valentine, Dr. J.R.E. Lutjeharms and Dr. M.L. Gründlingh. Discussions with other scientists during the course of the work are also greatly appreciated. Many thanks go to Dr. M.S.J. Harrison, Dr. J.A. Lindesay, Professor P.D. Tyson, Professor G.B. Brundrit, Professor L.V. Shannon, Dr. M. Jury, Professor J. van Heerden and Mr. D. Terblanche. Professors L. Underhill and W. Zucchini provided helpful discussions concerning the statistical analyses. Dr. F.A. Shillington is gratefully acknowledged for his supervision and encouragement throughout the research and during thesis preparation. My husband, Dr. I.L. van Heerden, is thanked for his helpful comments on the draft but, most of all, for his unfailing encouragement. This research was funded by the National Committee for Weather, Climate and Atmosphere Research/CSIR as well as the National Research Institute for Oceanology, now the Division of Earth, Marine and Atmospheric Science and Technology/CSIR.

LIST OF FIGURES

Figure | Page

Figure | Page

Figure **Page**

LIST OF TABLES

CHAPTER 1

INTRODUCTION

Atmospheric Circulations and South African Rainfall

The prominent surface circulation features influencing the weather over southern Africa are the subtropical anticyclones of the adjacent oceans and the circumpolar westerly circulation south of the subcontinent (Tyson, 1986). The oceanic anticyclones undergo major latitudinal and longitudinal displacements through the year (Figure 1.1).

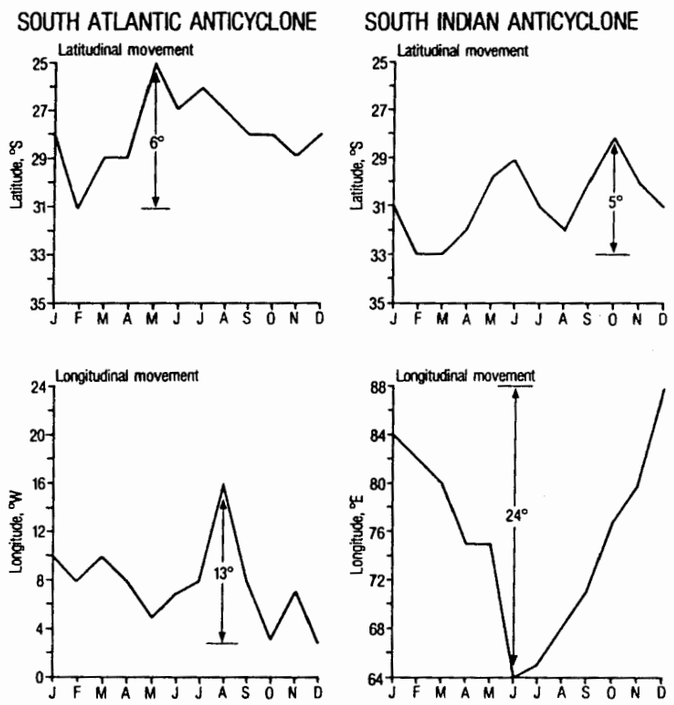

Figure 1.1 Annual variations in the latitudinal and longitudinal positions of the South Atlantic and South Indian Anticyclones (From Tyson, 1986 (after Vowinckel, 1955; McGee and Hastenrath, 1966)).

The South Atlantic Ocean Anticyclone moves through approximately 6° of latitude annually, reaching its southernmost position in mid-summer. Its mean position is closer to the African west coast during the early summer months (October through December) and several degrees further west from January to March (Vowinckel, 1955; McGee and Hastenrath, 1966; Tyson, 1986). The South Indian Ocean Anticyclone displays a semi-annual oscillation in its latitudinal position and is furthest south in August and

February-March. Longitudinally, it exhibits an extreme annual cycle moving 24° eastward from June to December. The poleward displacement of pressure systems from winter to summer is clearly indicated in Figure 1.2 which depicts the position of the Intertropical Convergence Zone (ITCZ) and near-surface streamlines within the tropics and subtropics. Marked seasonal changes occur over the western Indian Ocean region as a result of monsoon wind reversals which affect latitudes to 20°S (Ramage, 1984a). As a consequence, the ITCZ undergoes an average January to July latitudinal shift of approximately 30°. During summer, cyclonic flow over western Africa becomes established at the surface near 10°S. Anticyclonic circulation occurs along the east coast of southern Africa, despite the fact that the mean position of the South Indian Ocean Anticyclone is much further east.

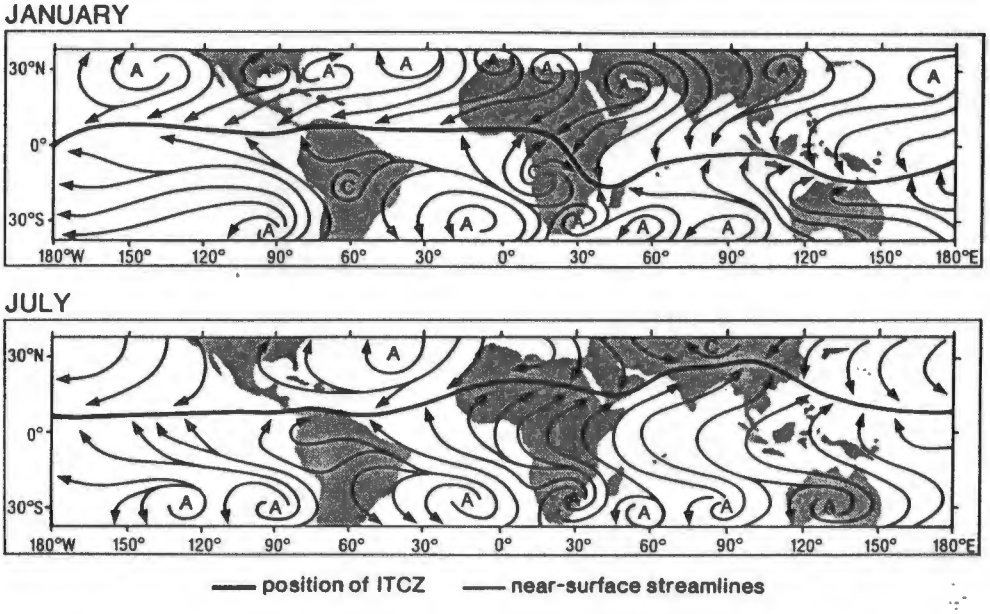

Figure 1.2 January and July near-surface streamlines in the global tropics illustrating the mean Intertropical Convergence. 'A' denotes an anticylonic center and 'C' denotes a cyclonic center (From Tyson, 1986 (after Hastenrath, 1985)).

The near-surface air flows and major convergence zones over the African subcontinent north of 25°S are shown in more detail in Figure 1.3. The northeast monsoon air of East Africa interacts with the deep tropical easterlies entering from the southwest Indian Ocean along the ITCZ (Torrance, 1979; Tyson, 1986). Further west, the tropical easterlies converge with the recurved South Atlantic air along the Zaire Air Boundary near 20°S. The Zaire Air Boundary fluctuates in position from day to day and marks a region where low pressure systems form preferentially during summer (Taljaard, 1972). Its position is a major factor influencing the location of air mass convergence and rainfall (Taljaard, 1986a). Most of the moisture contributing to precipitation over the country originates in the southwest Indian Ocean (Taljaard, 1986a). During winter, anticyclonic flow prevails over southern Africa at the surface, a

semi-permanent inversion develops and little moisture invades the plateau from the east (McGee and Hastenrath, 1966). In contrast to the seasonally varying surface circulation, the middle and upper troposphere circulations vary little throughout the year being anticyclonic and characterized by westerly airflow over most of the country in all seasons (Jackson, 1952; Schulze, 1965; Lindesay, 1988b).

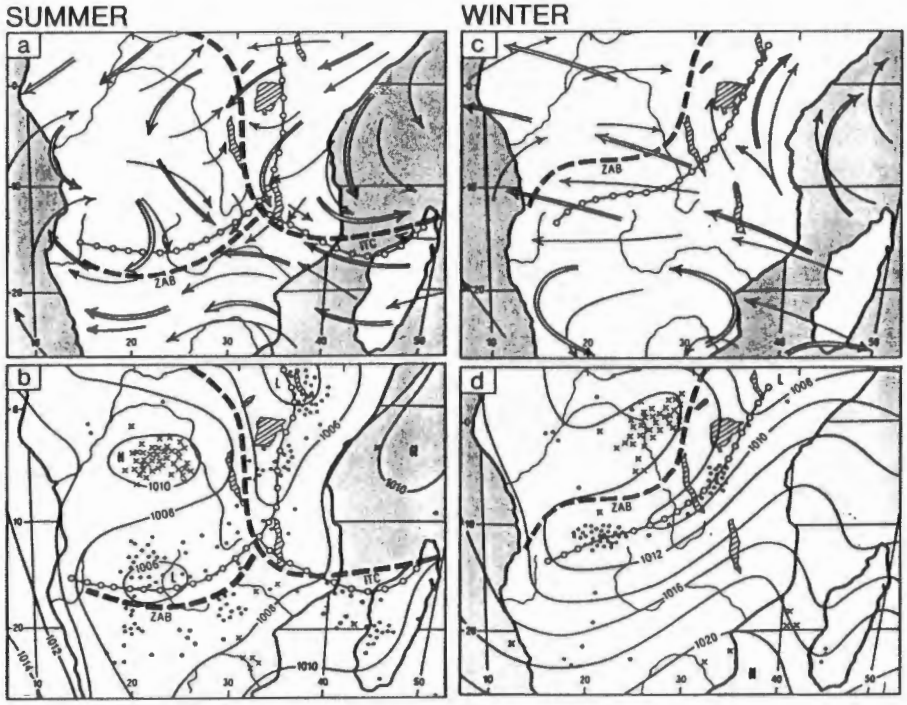

Figure 1.3 Mean locations of the Intertropical Convergence Zone (ITC) and Zaire Air Boundary (ZAB)(heavy dashed lines); a) and b) during summer (January and February 1958) and c) and d) during winter (July and August 1958). In a) and c) single arrows illustrate low-level flow and double arrows 3 km flow; linked circles mark the location of the major surface trough. In b) and d) crosses and dots mark centers of individual closed low and high pressure systems, respectively, and thin lines give mean sea level pressure in mb. (From Tyson, 1986 (after Taljaard, 1972)).

Regions south of the subcontinent are alternatively influenced by eastward moving anticyclones and baroclinic disturbances embedded in the circumpolar westerly air flow. These high frequency traveling eddies with periods of less than 2 weeks dominate the total variance and covariance fields of geopotential height, kinetic energy and mean eddy momentum flux (Trenberth, 1981; Tyson, 1986). Much of the low frequency atmospheric variability in midlatitudes is attributed to changes in either the frequency or the location of these transient disturbances. They track further south in

the summer in association with poleward displacement of the subtropical anticyclones and the subtropical jet stream.

Circulation controls on annual and interannual rainfall variations

Changes in the position and intensity of the subtropical anticyclones and associated changes in the tracks of low pressure systems south of the subcontinent have been viewed as the major controls on seasonal and non-seasonal rainfall variations over southern Africa (Schulze, 1965; Taljaard, 1972, 1986a, 1986b; Harrison, 1986a; Tyson, 1986). South Africa receives most of its rainfall during the summer months, with the exception of the relatively small winter rainfall area in the extreme southwest and the narrow all-year rainfall area along the south coast (Keen and Tyson, 1973; Schulze, 1984; Tyson, 1986; Taljaard, 1986a) (Figure 1.4). The largest portion of the summer rainfall region experiences a simple annual rainfall cycle with maximum rainfall occurring in January. The drier central interior of the country experiences two rainfall peaks during the year, the lesser occurring in November and the greater in February-March (Tyson, 1986; Taljaard, 1986a). These same areas exhibit similar non-seasonal rainfall variations (Keen and Tyson, 1973; Tyson et al., 1975; Tyson, 1986).

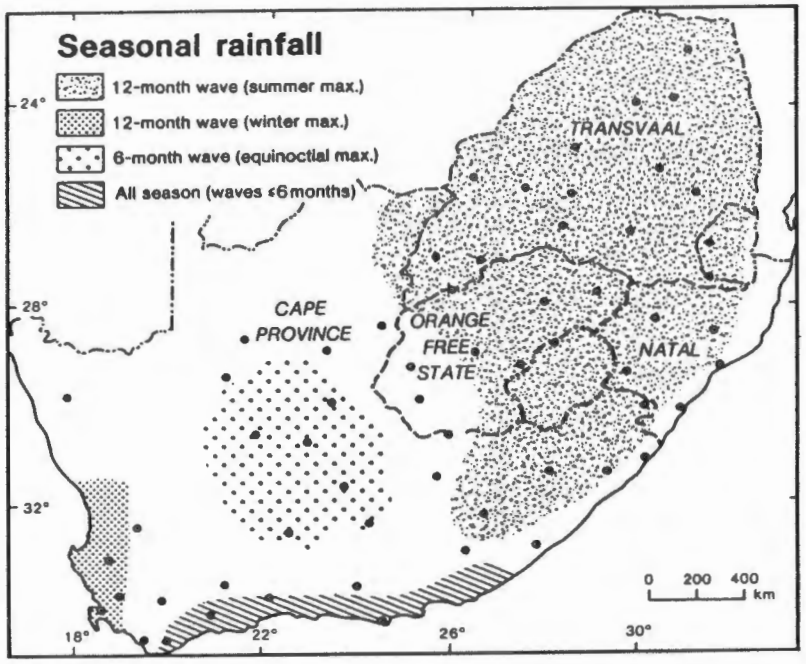

Figure 1.4 Map of South Africa showing the provinces, the seasonal rainfall regimes and the rainfall stations used in this thesis. (From Tyson, 1986 (after Keen and Tyson, 1973)).

In the search for controls on rainfall variations on interannual and longer time scales, Tyson (1981) demonstrated a close correspondence between wetter periods and higher sea level pressure southwest of the country near Gough Island (10°W) and lower pressure over the interior. This situation indicates intensification and poleward displacement of the South Atlantic Anticyclone and increased onshore airflow along the south coast. These relationships are not always observed during wetter months, however (Taljaard, 1986b; Terblanche and Taljaard, 1987).

An alternative control for South African rainfall variability on the interannual time scale is the Southern Oscillation (SO). Summer rainfall variability of South Africa is modulated to some degree by phases of the SO. Large-scale changes in atmospheric circulations related to alterations in the Walker Circulation across the Indian Ocean accompany the SO-rainfall relationships influencing the southern African region (Lindesay and Harrison, 1986; Tyson, 1986; Harrison, 1986a, Lindesay, 1988b). In addition, significant adjustments in the strength and location of the westerly wind maximum south of Africa are associated with alterations in SO index phases (van Loon and Madden, 1981; Harrison, 1986a; Tyson, 1986; Lindesay, 1988a,b). The SO-rainfall relationships are such that above-average rainfall over the summer rainfall region usually coincides with high index phases of the Southern Oscillation, whereas below-normal rainfall coincides with low index phases. Maximum variances of 20 to 30% have been attributed to this association (Lindesay, 1988a,b; van Heerden et al., 1988). Clearly, much of the interannual rainfall variability has yet to be explained.

Major rain-producing synoptic systems during summer

Harrison (1984) suggested that a clear picture of circulation controls on both the seasonal and non-seasonal variations in rainfall has not yet emerged because the interactions between individual synoptic events and period-mean atmospheric patterns have not been clearly established. Nevertheless, the conditions generally considered favorable for interior rainfall during summer include the presence of a tropical low pressure cell over the western interior, strong surface convergence of maritime air masses over the interior and the existence of a westerly wave along the west coast or overlying the subcontinent (Taljaard, 1986a; Tyson, 1986; Harrison, 1984; 1986a).

A classification of rain-bearing synoptic systems has been developed by Harrison (1984, 1986a) based on principal component analysis and satellite imagery (Figure 1.5).

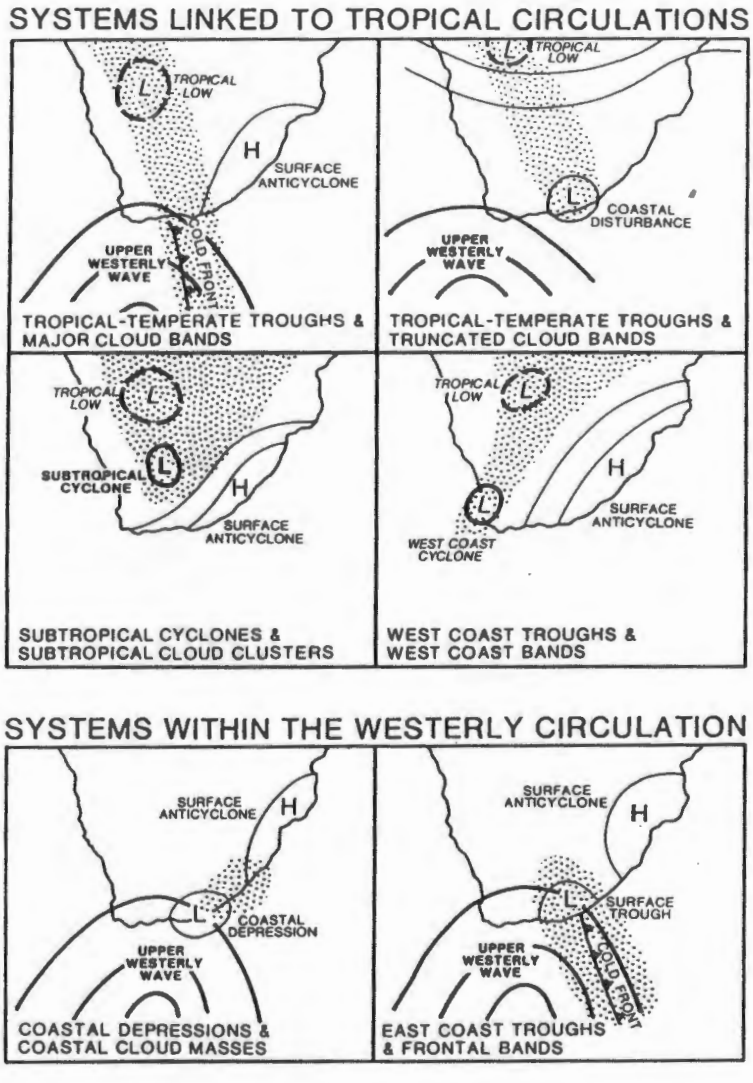

Figure 1.5 Generalized classification of circulation types and their attendant cloud systems. Lower-level circulation is shown by light lines; upper level by heavy lines. Cloud cover is shown by stippling. (From Tyson, 1986 (after Harrison, 1986a)).

The most important rain-producing system for the interior regions of the country is, by far, the tropical-temperate trough. It provides in excess of 40% of the interior's rainfall from November through April. It is readily apparent in thermal infrared satellite imagery as a distinctive cloud band connecting a tropical low or easterly wave over land with a westerly wave to the south of the continent (Harangozo and Harrison, 1983; Harrison 1984, 1986a; Tyson, 1986). The cloud bands develop in regions of forced low-level convergence between air flows around eastward moving anticyclones, in conjunction with a baroclinically unstable atmosphere on the leading edge of cyclone wave troughs (Johnson, 1969; Streten, 1973; Harrison, 1986a). Cloud bands are

characteristic features of the Southern Hemisphere circulation visible on satellite imagery and 3 to 4 are most frequently observed within the Southern Hemisphere (Streten, 1973). Harrison (1984, 1986a) has suggested that the tropical-temperate troughs are forced by tropical latent heat release over the subcontinent and provide a conduit for the poleward flux of momentum, heat and moisture from the tropics. Although the relative contributions provided by the tropical and temperate components have not been well documented, research has shown that tropical convection over southern Africa is intensified considerably by westerly waves intruding from the south (Bhalotra, 1973; Kumar, 1978; Acharya and Bhaskara Rao, 1981; Smith, 1985).

Tropical-temperate cloud bands are usually associated with temperate lows south of 40°S but can also be associated with coastal disturbances and west coast cyclones. Cloud bands linked to coastal disturbances have been termed truncated troughs and are most prevalent in early summer months with a peak frequency in November, as opposed to the tropical-temperate trough whose influence is maximal in January. West coast bands link tropical circulations with west coast cyclones which usually form over oceanic areas close to the west coast.

Strictly temperate circulations include coastal depressions and east coast troughs or frontal bands (Figure 1.5). Coastal depressions cause rainfall mainly along the south coast. They generally precede cold fronts and although most are shallow features (< 1500 m), some develop through a significant portion of the troposphere (Estie, 1984) and are marked by extensive cloud along coastal areas (Harrison, 1986a). They show similarities to truncated troughs and contribute most to rainfall during early summer months (October-December). Frontal bands or east coast troughs indicate the passage of low pressure systems and surface fronts along the south and east coasts. The associated rainfall is usually confined to coastal regions, however, during early summer their influence can extend into interior regions, explaining about 30% of the rainfall (Harrison, 1984; Tyson, 1986).

Cut-off lows were not specifically identified by the classification technique of Harrison (1984, 1986a), however, they contribute significantly to rainfall during the transitional months and are renowned for producing very high rainfall over limited areas, often resulting in flooding (Taljaard, 1985). These systems are essentially cold-cored lows within the mid-troposphere, cut off from their parent westerly wave trough by a strong ridge of high pressure.

Temperate forcing mechanisms exhibit more control over rainfall variations during early summer, whereas tropical systems exhibit more control during late summer. This was revealed by the detailed analysis of synoptic rainfall-producing systems over

southern Africa (Harrison, 1984; 1986a). An analysis of lower and upper tropospheric winds over the central interior confirmed these circluation changes, as equatorward flow was found to predominate in early summer and poleward flow in late summer. Such a change in the toroidal circulation forms an integral part of a local semi-annual cycle within which the Ferrel Cell dominates in the transitional seasons and the Hadley Cell in the high seasons (Harrison, 1986b).

Oceanographic Setting

Major ocean currents

Located at the southern tip of the African continent, South Africa is exposed to three distinct ocean current regimes; the warm Agulhas Current system to the east and south, the relatively cold Benguela Current system along the west coast, and the Subtropical Convergence near 38°-42°S (Figure 1.6). As a consequence of the termination of the African subcontinent near 35°S, a unique oceanographic situation is encountered where warm waters of a major western boundary current can directly influence temperature and flow characteristics of an eastern boundary current system.

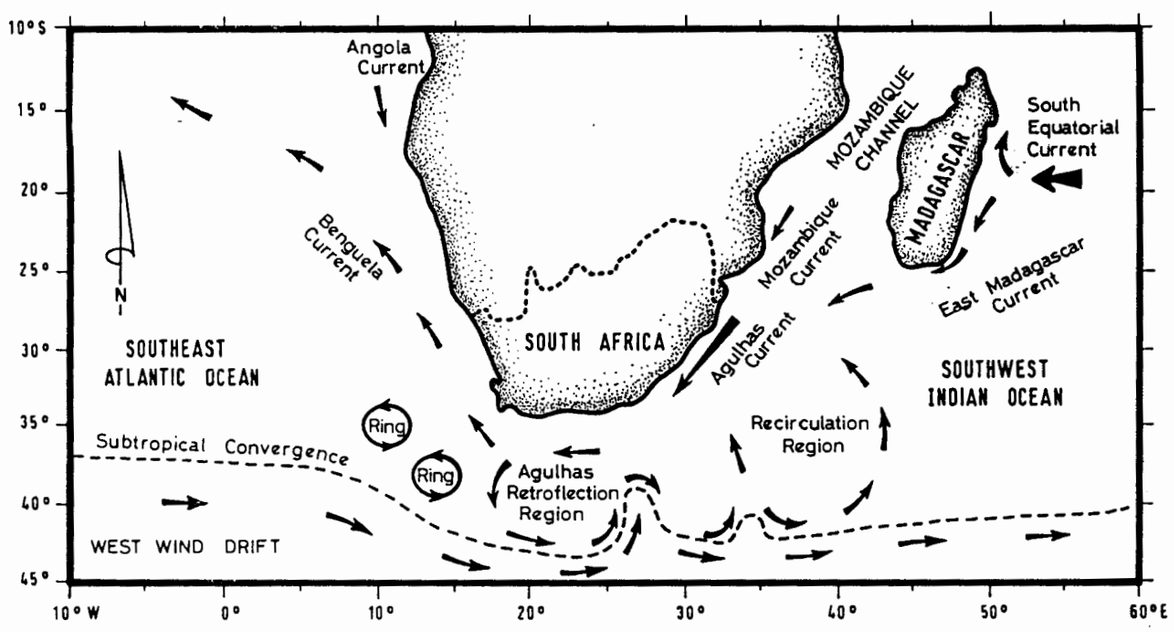

Figure 1.6 Location map of southern Africa and schematic representation of major ocean current sytems.

The Agulhas Current, which forms the western boundary of the South Indian subtropical gyre, flows southwestward along the east coast of southern Africa. Its source regions include the westward surface drift of the South Equatorial Current, the East Madagascar Current and the Mozambique Current (Harris, 1972; Lutjeharms et al., 1981). Although the width of the Agulhas Current core is only about 100 km (Pearce, 1977), a large portion of the southwest Indian Ocean is influenced by its expansive recirculation region to the southeast of the subcontinent (Gründlingh, 1978) (Figure 1.6). It also influences a considerable ocean area south of the African continent within the Agulhas Retroflection region, where much of the current executes an anticyclonic turn near 16°-20°E, 40°-42°S, subsequently flowing back into the southwest Indian Ocean along the northern edge of the Subtropical Convergence (Bang, 1970; Lutjeharms and van Ballegooyen, 1988) (Figure 1.7a). Retroflection generally occurs between 16°E and 20°E, however, extremes of 10°E and 25°E have been reported (Lutjeharms and van Ballegooyen, 1988). Warm Agulhas waters can extend considerable distances into the southeast Atlantic Ocean either as Agulhas rings shed at the western margin of the retroflection loop (Lutjeharms and Gordon, 1987), or as anomalous westward intrusions (Walker, 1986; Lutjeharms, 1988). Ring shedding from the western margin is followed by an eastward withdrawal of the retroflection. The temperature characteristics south of the subcontinent are thus highly dependent upon the dynamics of the southern section of the Agulhas Current system. South of Africa, Agulhas waters encounter cold sub-Antarctic waters at the Subtropical Convergence, near 40° to 42°S, where SST gradients in excess of 10^{o}C over 100 km can result (Lutjeharms and Valentine, 1984; Walker, 1986; Also see Figure 1.7a). A wave of 2-3° latitude is often encountered from 10° - 15°E in the Subtropical Convergence (Figure 1.7a).

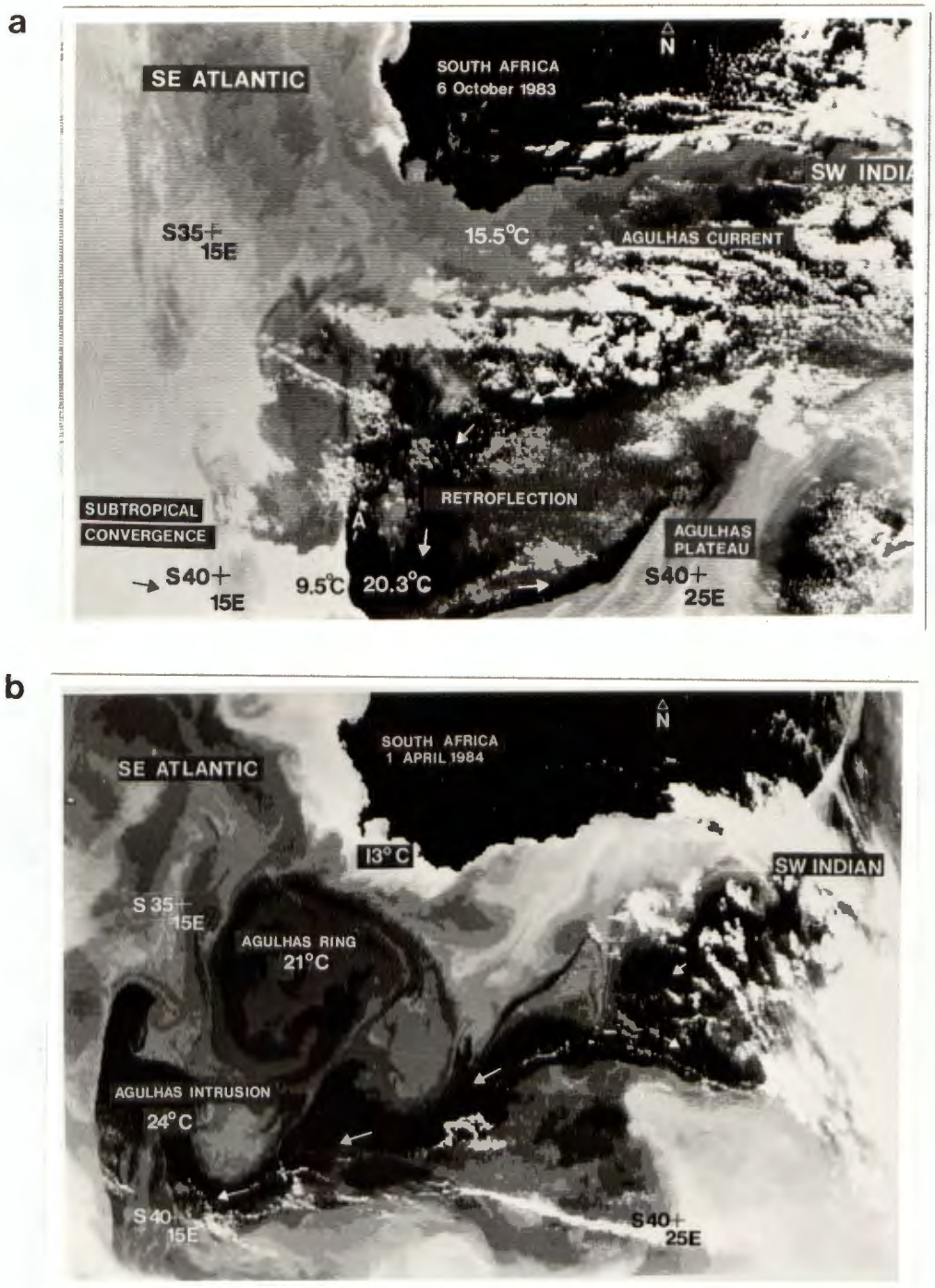

Figure 1.7 Temperature-corrected thermal infrared imagery of NOAA-7 illustrating sea surface temperature distributions south of Africa. a) 6 October 1983 (14h00 UTC) image, illustrating intense sea surface temperature gradients at the confluence of warm Agulhas Current waters and colder sub-Antarctic waters along the Subtropical Convergence (40°S, 16°E). b) 1 April 1984 (14h00 UTC) image showing an extreme westward penetration of Agulhas Current water into the South Atlantic (to 40°S, 13°E). Sample sea surface temperature values are shown. (From Walker and Mey, 1988).

West of the African subcontinent, between 15°S and 35°S, cold upwelled waters flank the coastline and contribute to equatorward surface flow of the Benguela Current system, the eastern boundary current of the South Atlantic Subtropical gyre. Considerable research has concentrated on this ocean region because of its importance to the commercial fishing industry. Upwelling increases in the southern and central Benguela in spring and summer in association with the poleward shift in the Anticyclone and prevailing equatorward winds (Parrish et al., 1983). In contrast, the northern Benguela experiences its highest temperatures in late summer when equatorward winds are weakest. A comprehensive review of the salient current features and seasonal variability within the system is found in Parrish et al.(1983) and Shannon (1985).

Interannual variability

Streten (1981) demonstrated the existence of pronounced interannual SST variability within both the Agulhas and Benguela Current systems (Figure 1.8). Of these, interannual variability within the Benguela current system has received the most attention (McLain et al., 1985; Shannon et al., 1986; Walker, 1987). Temperature anomalies of the Benguela current system are generally spatially coherent and also fairly long-lasting with the most pronounced anomalies occurring in the central and northern areas. Temperatures in the northern Benguela (north of 25°S) are out of phase with those in the southern and central Benguela on both annual and interannual time scales (Walker et al., 1984; Shannon, 1985; Walker, 1987). Warm events, analogous to Pacific El Ninos, have been reported in the northern Benguela (Shannon et al., 1986). They result from relaxation of easterly wind forcing in western parts of the tropical South Atlantic and poleward displacement of the Intertropical Convergence Zone (Hirst and Hastenrath, 1983; Shannon et al., 1986).

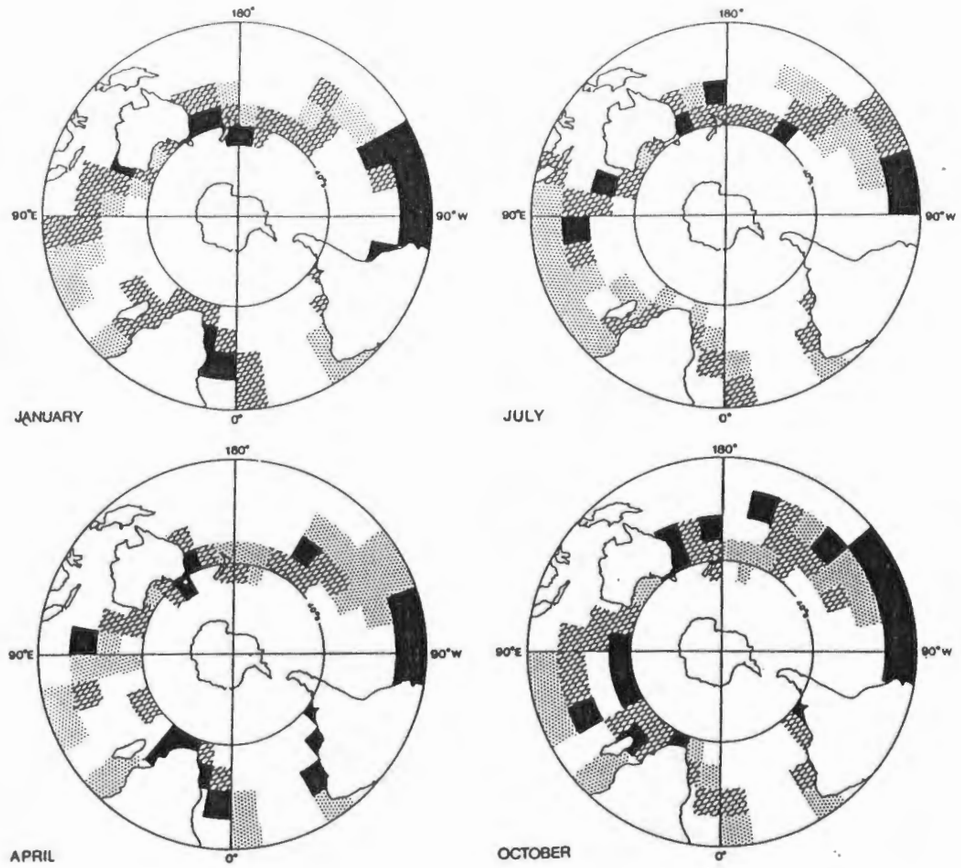

Figure 1.8 Regions of relative variability in SST over the Southern Hemisphere for midseason months. Black shading indicates 10° latitude by 10° longitude squares in which the percentage of observations of standard deviation of monthly mean SST > 1°C is more than one third higher than the zonally-averaged percentage for the 10° latitude zone; cross-hatching shows squares within plus or minus one third of the zonally averaged percentage, and stippling those less than one third of the zonally averaged percentage. Unshaded areas have less than 20 observations per 10° square. Data are for 1950-1969 (From Streten, 1981).

In contrast to the Benguela Current system, very little information has been published on interannual variability of the Agulhas Current system. Lutjeharms (1972) showed that the year to year variations in water movement in the western Indian Ocean were of similar magnitude to the seasonal variations. This observation may partially explain the absence of a clear annual cycle in Agulhas Current transport (Pearce and Gründlingh, 1982). South of the subcontinent near 40°S, 20°E, Gillooly and Walker (1984) identified pronounced SST variability on the interannual time-scale and attributed this to Agulhas Current influences. Modeling results have suggested that westward penetration of Agulhas Current waters into the southeast Atlantic is facilitated by a poleward shift of the wind stress curl zero line south of the subcontinent (de Ruijter, 1982; de Ruijter and Boudra, 1985), a shift which generally occurs from winter to summer (Hellerman and Rosenstein, 1983). Observational analyses have supported

the modeling results. Gillooly and Walker (1984) and Walker (1986) demonstrated that positive SST anomalies within the Agulhas Retroflection region are associated with above-average atmospheric pressure south of the subcontinent and increased easterly wind stress in the southwest Indian Ocean.

Ocean-atmosphere heat fluxes

Coupling between the surface ocean and the overlying atmosphere is a direct function of heat and water vapor fluxes at the air-sea interface. In the local ocean areas, maximum oceanic sensible and latent heat losses occur within the Agulhas Retroflection region, where the cool circumpolar westerly airflow first encounters relatively warm Agulhas waters at the western margin of the Agulhas Retroflection. A high heat flux core has been identified from 37° to 41°S and 16° to 22°E, within which combined latent and sensible oceanic heat losses are 200 W/m^2 during summer (Figure 1.9). Latent heat flux (evaporation) contributes approximately 85% to the total.

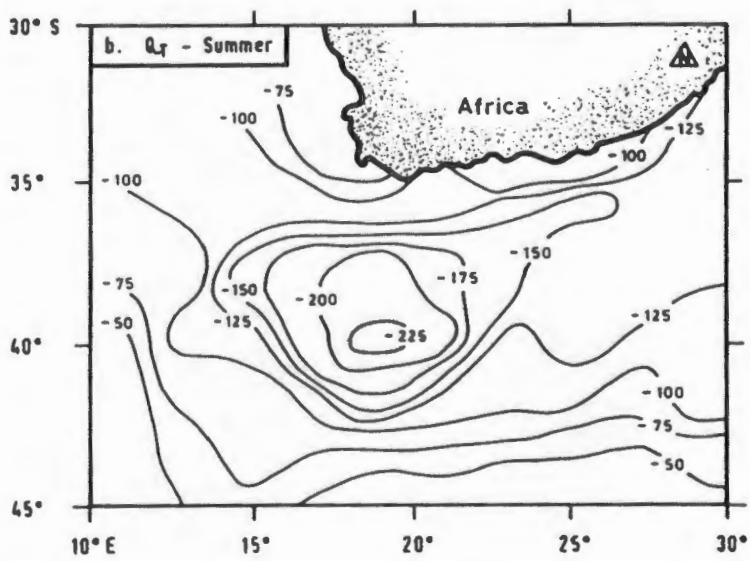

Figure 1.9 Combined sensible and latent heat fluxes (W/m^2) south of Africa during summer (December through February). A high heat flux core region is revealed from 37° - 41°S, 16° - 22°E within the Agulhas Retroflection region (From Walker and Mey, 1988). *Negative* values represent oceanic *losses*.

Monthly-averaged heat fluxes within the Agulhas Retroflection region vary little throughout the year as a result of prevailing westerly air flow and persistent air-sea temperature and humidity gradients (Walker and Mey, 1988). In contrast, the Northern Hemisphere western boundary currents experience distinct annual heat flux cycles with maximum heat losses occurring in winter (Bunker, 1976). The corresponding spatial heat

flux gradients at the Agulhas/Subtropical Convergence SST front are most pronounced during the summer months, a condition which would facilitate cyclogenesis southwest of the subcontinent. Harrison et al. (1989) has demonstrated a higher frequency of cyclogenesis along intense SST fronts southwest of the subcontinent during wetter summer months. In addition, explosive cyclogenesis has been documented near 10°E, 40°S (Jury et al., 1984) in close proximity to an SST anomaly exceeding +4°C in April 1984 (Walker, 1986) (Figure 1.7b). Cyclogenesis, often of an explosive nature, is a common occurrence over strong SST fronts of Northern Hemisphere western boundary currents (Sanders and Gyakum, 1980). The positioning of the Agulhas Retroflection high heat flux core region upwind of the tip of Africa would improve the chances of it influencing local weather and climate processes. This is in contrast to the Northern Hemisphere where the high heat flux regions are downwind from the proximate land masses.

Evaporation is relatively high within the southwest Indian Ocean. Along the east coast of southern Africa from 0° to 25°S, oceanic heat losses are approximatly 70 % of those within the high heat flux core of the Agulhas Retroflection region and little annual cycle is experienced in latent heat flux (Hastenrath and Lamb, 1979). Maximum values of both sea surface temperature and specific humidity occur during summer along the African east coast between 5°S and 22°S. Within the coastal upwelling region along the west coast (23°-35° S), surface waters gain rather than lose heat during summer (Figure 1.10). To the west of the cold coastal waters, oceanic heat losses occur but are relatively low in comparison with those of the southwest Indian Ocean and Agulhas Retroflection region.

The spatial distribution of rainfall over South Africa is closely related to sea surface temperature distributions and associated surface heat flux characteristics of adjacent oceans. The highest annual rainfall (100 cm/year) occurs along the eastern and southeastern coasts where both ocean temperatures and evaporation are relatively high. A strong negative rainfall gradient is observed from east to west and semi-desert conditions characterize the central and western interior. The northwest coastal area, adjacent to the central Benguela current system, experiences the least annual rainfall (10 cm/year) (Tyson, 1986).

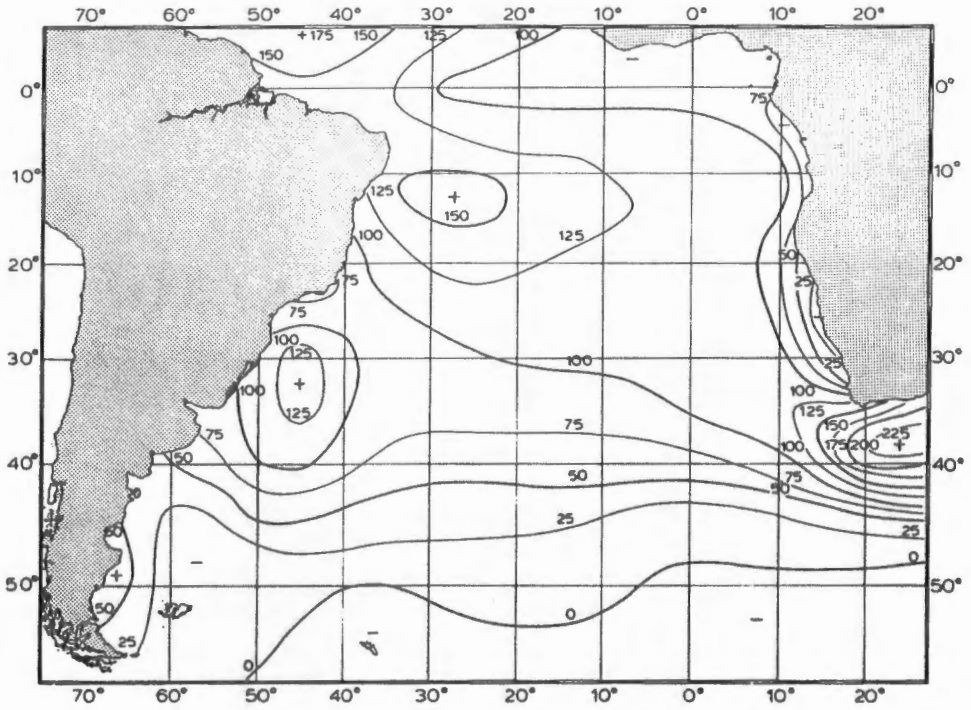

Figure 1.10 Combined sensible and latent heat fluxes from the sea surface during January (W/m^2) where *positive* values represent oceanic *losses* (From Hoflich, 1984).

CHAPTER 2

DATA AND ANALYSES

Data

Surface oceanographic and meteorological data

Voluntary Observing Ships (VOS) data have been used extensively for climate studies on various time-scales because they provide the longest available time series of surface oceanic and atmospheric measurements. The VOS data are considered most valuable for studies of annual and interannual climate variability (Bunker, 1976; Barnett, 1984; Wright, 1986) and the measurements most often used have been SST, wind speed and direction, dry bulb and wet bulb temperatures, atmospheric sea level pressures and total cloud cover (Bunker and Worthington, 1976; Weare, 1977; Lamb, 1978; Rasmusson and Carpenter, 1982; Hirst and Hastenrath, 1983; Barnett, 1983; Hastenrath, 1984; Cadet and Diehl, 1984; Lough, 1986; Nicholson and Entekhabi; 1987). These data are less than ideal, however, as they suffer from problems such as uneven spatial and temporal sampling, systematic errors due to instrumentation changes over time, and random errors caused by both instrument and human inaccuracies (Mobley and Preisendorfer, 1985). These potential sources of error can be reduced by averaging over relatively large space and time scales (Mobley and Preisendorfer, 1985; Wright, 1986).

The data used in this thesis were extracted from the South African Data Centre for Oceanography's Marine Climatology data base, which chiefly incorporates information from merchant ships collated at the United Kingdom Meteorological Office (Philips, 1986). As the observations had not been adequately quality-checked, a new marine data base was constructed for this research covering a large portion of the southeast Atlantic and southwest Indian Oceans from 0° to 40°S and 20°W to 70°E. The period of investigation was restricted to the years 1949 through 1984 as both the data quantity and quality increased after World War II (Barnett, 1984; Ramage, 1984b; Folland et al., 1984).

Measurement techniques for two key elements, SST and wind, have become more consistent since the late 1940's. Uninsulated buckets were replaced with insulated buckets near the beginning of the War. As uninsulated bucket temperatures were depressed below their true values as a result of evaporative cooling (Folland et al.,

1984), a potentially large source of error was eliminated from the analysis by excluding data before 1949. SSTs within the study period were measured with thermometers placed in insulated buckets or ships' engine intakes (Saur, 1963; Barnett, 1984; Folland et al., 1984). Whereas the former technique measures temperature within the top few meters, the latter technique samples from a range of depths, depending on the size and design of the ship. Despite the measuring depth differences, globally-averaged temperatures based on these two measurement techniques have yielded means which differ by less than 0.1°C (Folland et al., 1984).

Wind speed observations became more accurate after 1946 as a result of changes in wind recording and reporting instituted by the World Meteorological Organization (Ramage, 1987). Nevertheless, these data are still derived in two ways, from estimations based on sea state and from anemometer measurements. Both measurement techniques yield underestimates of absolute wind speed (Bunker, 1976; Graham, 1982). Analyses of Earle (1985) and Ramage (1987) have shown anemometer wind speeds to be higher than estimated wind speeds by 0.3 to 0.8 m/s.

As most merchant shipping is confined to major shipping lanes, the VOS data set is not spatially homogeneous. The existence of spatially coherent patterns of variables in data sparse regions increases confidence in the results. For this study, data were averaged within 5° latitude-longitude grid-squares on monthly and seasonal time scales. In Figure 2.1, the total number of quality-checked observations in each grid-square is displayed as a measure of spatial homogeneity within the study area. In general, 100 to 800 observations were available per season in a well-traveled grid-square. As an additional measure of data quality over the study region, the percentage of months for which data were available per grid-square compared with the total months in the time series is shown in Figure 2.2. VOS data were extremely scarce south of 40°S and thus were excluded from all statistical analyses. Although data coverage was poor within the 35°-40°S zone, an ocean area encompassing the Agulhas Retroflection region was included in some of the analyses because of its potential importance. Directly south of the subcontinent, a few grid-squares were reduced to 5° x 3° in order to exclude continental shelf temperatures which can differ dramatically from temperatures further offshore (Walker, 1986).

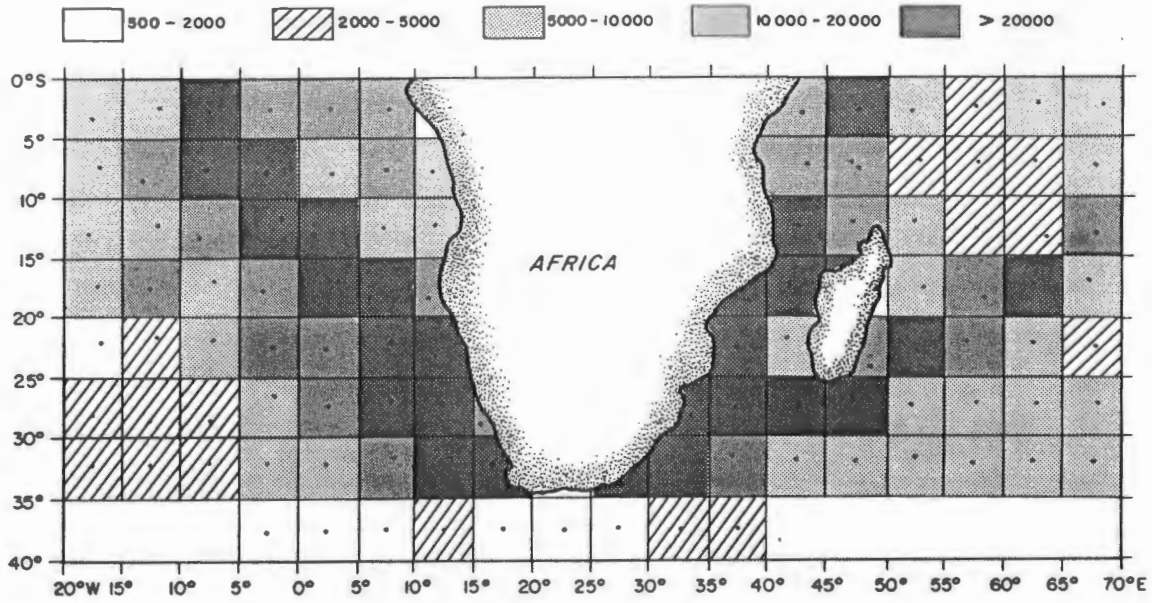

Figure 2.1 Voluntary observing ships' observations within each 5° latitude-longitude grid-square from 1949 through 1984.

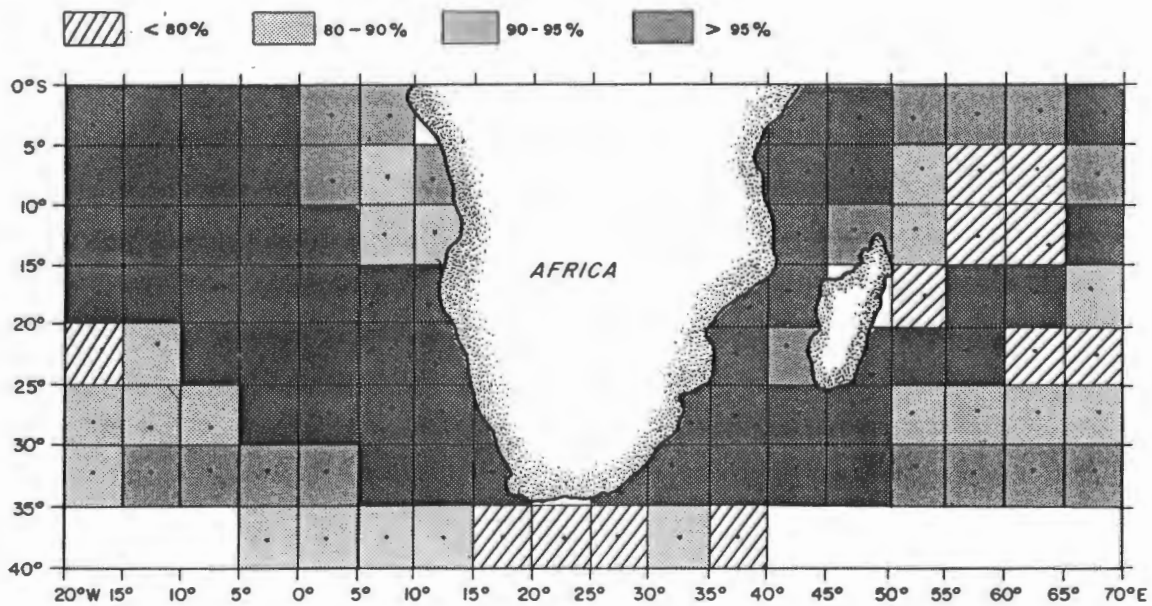

Figure 2.2 Percentage of the total months (432) for which monthly values from voluntary observing ships were available in each grid-square.

The marine data base was constructed from individual values of sea surface temperature (SST), sea level pressure (SLP), zonal (U), and meridional (V) wind components which were compiled into 5° x 5° grid-squares over the study area. Initially, long-term (36 year) monthly means of each parameter were calculated by grid-square. Quality-checking was then performed by comparing individual observations with the long-term means and deleting those which fell outside a 3.5 standard deviation limit from the appropriate long-term monthly mean. A similar procedure has been used by Weare (1979), Newell et al. (1982) and Cadet and Diehl (1984). The use of standard deviations in the quality checking enables elimination of erroneous data due to coding errors in the original ships' logs. After excluding the outliers, monthly means and revised long-term monthly means were computed for each of the 107 grid-squares. The annual and semi-annual cycles were removed from the data series by subtracting the long-term monthly means from the individual monthly means for each parameter. Where a monthly value was missing, the respective long-term monthly mean was used as a replacement. Seasonal means and departures from these means (i.e. anomalies) were obtained by averaging data for January-March, April-June, July-September and October-December. The choice of seasonal groupings is discussed in the next section. As no obvious trends were observed in the relatively short time series, de-trending was not performed.

In addition to the main marine database, satellite-derived SSTs were acquired in digital format for 2.5° latitude-longitude grid-squares from the National Environmental Satellite, Data, and Information Service (NESDIS), N.O.A.A., Washington, D.C. The satellite-derived SSTs were available from 1980 with the advent of the TIROS-series of environmental satellites and have an accuracy of about 0.5°C (Strong and McClain, 1984). They provided high quality information over ocean areas where merchant shipping is infrequent, and have been used as a source of more quantitative information within the southern reaches of the study region. Satellite derived SST data on a 1° x 1° grid-resolution were also obtained as weekly and monthly contour maps from NESDIS and the National Weather Service. Anomaly maps available from these groups were based on the National Center for Atmospheric Research (NCAR) 20-year climatology (Barbara Banks, personal communication).

Rainfall data

Monthly-averaged rainfall data for 59 selected stations were obtained from the Climatology Research Group, University of the Witwatersrand (Janette Lindesay, personal communication). These stations were chosen for their homogeneity and record

lengths and have been used in several previous studies concerning South African rainfall variations (Lindesay, 1984; Tyson, 1984; Lindesay et al., 1986; Lindesay, 1988a,b). There were no missing data during the 36-year period.

In all analyses, standardized rainfall departures (N_{ij}) were used and computed for each station from:

$$N_{ij} = (r_{ij} - r_i)/ \sigma_i$$

where r_{ij} is the seasonal rainfall total of station i in year j, r_i is the long-term seasonal mean and σ_i is the standard deviation of seasonal rainfall at station i. Standardizing the time series yielded a new time series with a mean of 0 and standard deviation of unity.

Use of this technique enables comparison and combination of station data with diverse statistics and reduces the contribution from stations with relatively high variability (Kraus, 1977; Nicholson, 1980). For most of the analyses, the standardized station rainfall departures were area-averaged for an eastern and western area within the summer rainfall region (Figure 2.3). These areas have been shown to exhibit coherent rainfall behavior based on seasonal data analyses (McGee and Hastenrath, 1966; Keen and Tyson, 1973) as well as non-seasonal analyses (Dyer, 1975; Tyson et al., 1975). Separation of the summer rainfall region into east and west was further motivated by their relative distances from the Atlantic and Indian Oceans. Rainfall stations over the entire country were incorporated in later analyses to resolve details on the spatial distribution of precipitation associated with specific SST anomaly patterns.

The statistical analyses were based on the use of seasonal means. Early summer was defined as October, November and December, and late summer was defined as January, February and March. These seasonal groupings conform with the well-documented semi-annual oscillations of atmospheric properties over the Southern Hemisphere and South Africa with turning points around November and February (van Loon, 1967; van Loon and Jenne; 1969,1970; Harrison, 1986a,b). As recent research on interannual rainfall variations over South Africa (Lindesay et al., 1986; Tyson, 1986; Lindesay, 1988 a,b) has been based to a large degree on these seasonal groupings, comparisons are facilitated with the present study. More emphasis has been placed on the late summer season when the bulk of the rain is experienced over the summer rainfall region. A rainfall failure during this season has the most serious implications as it is not recovered during any other part of the year.

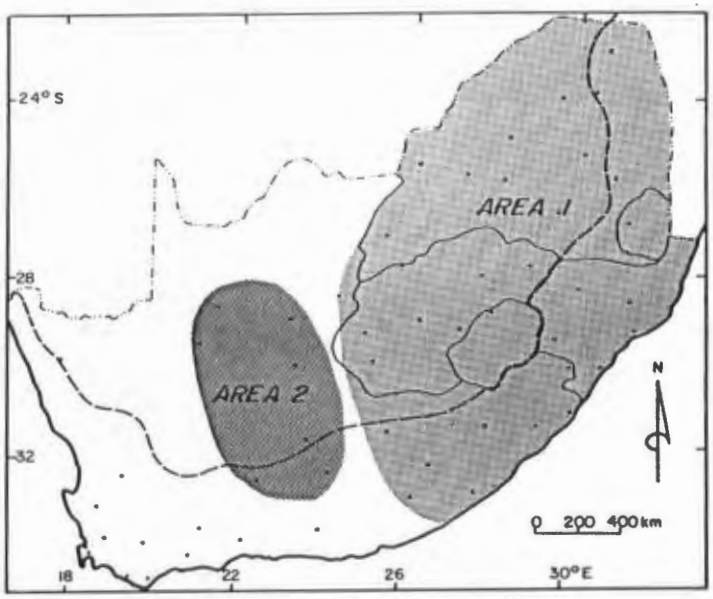

Figure 2.3 Locations of rainfall stations and delineations of areas 1 and 2. The escarpment (dashed line) separates high interior plateau areas from lower-lying coastal areas.

Surface vapor pressure data were used to investigate atmospheric conditions during contrasting rainfall regimes. Data for stations in Zimbabwe and South Africa were obtained as monthly-averages from *Monthly Climatic Data for the World*, published by the United States Department of Commerce, Washington, D.C.. In the case-study analyses, vapor pressure anomalies from the same source and wind data and anomalies (*Climate Diagnostics Bulletin*, Climate Analysis Center, N.O.A.A., Washington, D.C.) supplied additional atmospheric information.

The Southern Oscillation Index

Differences between standardized monthly mean atmospheric sea level pressures at Tahiti (17.5°S, 149.6°W) and Darwin (12.4°S, 130.9°E) were used as the Southern Oscillation Index. These stations are located within the South Pacific Ocean and the Indonesian centers of action of the Southern Oscillation respectively, and exhibit sea level pressure oscillations approximately 180° out of phase (Trenberth, 1976; Chen 1982). The Southern Oscillation Index (SOI) is thus considered most suitable for diagnostic studies (Chen, 1982) and has been used extensively in climatic research (Troup, 1965; Pittock, 1973; Trenberth, 1976; Horel and Wallace, 1981; Lindesay, 1988a,b).

In this study, the SOI was constructed from 3-month means (corresponding to the rainfall seasons) over the 36-year period. Monthly-averaged sea level pressure data were obtained from *World Weather Records* (U.S. Weather Bureau) and from the Department of Commerce publication, *Monthly Climatic Data for the World.* In the most recent years data was obtained from the *Climate Diagnostic Bulletin* published by the U.S. Department of Commerce, Washington, D.C.. The sea level pressure data were first standardized by month for each station, following the technique used with the rainfall data. After obtaining a time series of differences based on monthly values (Tahiti minus Darwin), the data were again standardized yielding what has been termed a double standardized Southern Oscillation Index. This is the standard technique in use by the Climate Analysis Center, Washington, D.C.. Finally, seasonal means were compiled based on the monthly data.

Satellite imagery

Extensive use has been made of satellite imagery (visible, thermal infrared and water vapor channels) to study the development and movements of rain-producing systems. Hemispheric mosaics of N.O.A.A. polar-orbiting satellite data were available from the National Climatic Center, Asheville, North Carolina, U.S.A. for the years 1978 to 1984. METEOSAT imagery was available for some of these years and for subsequent years from the Satellite Remote Sensing Centre/CSIR, Hartebeeshoek, South Africa.

Analysis Techniques

Several analysis techniques have been incorporated into this study, including principal component analysis, correlation analysis, superposed epoch methods, heat flux estimations and synoptic assessments. A brief description of each is given in this chapter, however in the interest of clarity, additional details are provided within the relevant chapters.

Principal component analysis

The technique of principal component analysis (PCA) has been widely used in the field of meteorology, oceanography and climatology (Kutzbach, 1967; Dyer, 1975; Davis, 1976; Weare, 1977; Horel, 1981; Harrison, 1984, 1986a; Tyson, 1984; Richman

and Lamb, 1985; Lough, 1986; Richman; 1986). It is a data transformation technique which can be used to satisfy a variety of objectives including pure data reduction, identification of relationships between different variables or identification of coherent modes of variability within a data field (Richman, 1986). This technique enables a large portion of the total variability of intercorrelated sets of variables to be represented by a smaller number of orthogonal variables. It was used in this study to identify ocean sub-areas where SST coherency was experienced over the 36 years. The resulting principal component time series were then used as input into correlation analyses with rainfall data to investigate SST-rainfall relationships on the interannual time-scale.

SST departures for each grid-square were used in the PCA. Through linear transformations of the data matrices (approximately 50 stations x 144 seasons), several principal components were extracted which summarized the input data with a minimal loss of information (Mardia et al., 1979). Each principal component is described by an eigenvalue which gives information concerning the proportion of data variance attributable to that component. The first component extracts a maximum amount of variance from the input matrix. The next component extracts a maximum amount of the remaining variance with the restriction of orthogonality with the first component and so on. The principal components are described by eigenvectors (loadings) in the spatial domain and PC amplitudes (scores) in the temporal domain (Lough, 1986). Spatial loadings on each component describe the correlations between the original SST time series and the principal component in question. The time series of scores for each component are derived mathematically from the spatial loadings and original time series of each grid-square. More comprehensive mathematical treatments of PCA can be found in Kendall (1975) and Mardia et al.(1979).

The principal components were rotated to avoid undesirable characteristics exhibited by non-rotated components such as domain shape dependence and subdomain instability (See review by Richman, 1986). The orthogonal varimax rotation (Kaiser, 1958) has become increasingly popular in recent years (Dyer, 1975; Walsh and Richman, 1981; Horel, 1981; Walsh et al., 1982; Tyson, 1984; Richman and Lamb; 1985; Richman, 1986) and was considered optimal for this study. It maximizes the variance rather than the sum of the squared correlation coefficients between each rotated PC and the original time series, thus giving a better definition of coherent areas of variability within the data field (Horel, 1981).

Correlation analyses

The strength of the relationships between the seasonal SST and rainfall departures were assessed using linear correlation analyses and superposed epoch analyses (next section). Linear correlations have been widely used in studies of interannual climate variability (Namias, 1976; Weare, 1979; Horel and Wallace, 1981; Walsh et al, 1982; Hirst and Hastenrath, 1983; Tyson, 1984; Cadet, 1985; Harnack and Harnack, 1985; Wright, 1986; Lindesay, 1988a,b; Aceitano, 1988). While the hazards of using correlation as a climatological tool have been pointed out (Ramage, 1983), the technique does provide a useful method for indicating statistical relationship between variables and for suggesting relationships for which physical explanations should be sought (Lindesay, 1988b). The SST departures exhibited near-normal distributions within the coherent sub-areas defined by the principal component analysis. Annual rainfall totals exhibit near-normal distributions over South Africa, except in the semi-arid northwest area (Dyer, 1974; Onesta and Verhoef, 1976). As the area-averaged rainfall departures of area 2 were not normally distributed, both the Pearson product-moment parametric test and the Spearman rank correlation test (non-parametric) were employed. The two tests yielded very similar results but where differences affected the analysis, they are discussed in the text. The Pearson product-moment correlation coefficient (r) is considered the more powerful (Shaw and Wheeler, 1985) and for this reason will form the basis for discussion in Chapter 3.

The product-moment correlation coefficient measures the covariance between two variables, in this case seasonal departure values of SST and rainfall. The correlation coefficient (r) is obtained by dividing the covariance of X and Y by the product of the standard deviations of the X and Y variables. Correlation coefficients can vary between -1.0, a perfect negative correlation, and +1.0, a perfect positive correlation. A correlation of zero indicates that the variables are independent of one another (Shaw and Wheeler, 1985). Local significance levels were determined using the T test with n-2 degrees of freedom. Since the time series subjected to correlation analyses comprised one season per year, auto correlation was not a problem and no reduction in degrees of freedom was performed. (Details in Appendix D). Results of tests for "field" significance are discussed in Appendix D.

Superposed epoch analyses

This analysis technique, commonly referred to as compositing, has been used extensively in the field of climatology (Lamb, 1978; Streten, 1981; Tyson, 1981; Rasmusson and Carpenter, 1982; Hirst and Hastenrath, 1983; Hastenrath, 1984;

Nicholson and Entekhabi, 1987; Lindesay, 1988 a,b). By using this method, stable ensembles can be derived from time series data, potentially yielding more valuable information on average changes than would be obtained by using individual years. It is particularly appropriate for use with the Voluntary Observing Ships data which suffers from data insufficiencies in time and space. This technique is exploratory and offers the advantage of reducing the number of maps and figures to be drawn when assessing relationships between climatic variables. It was used in this study to investigate monthly and seasonal differences in ocean temperatures, wind components, surface heat fluxes and atmospheric conditions under contrasting rainfall regimes. In making composites, it is possible that dissimilar patterns may be combined. Thus, the significance of differences between variables, composited according to WET and DRY seasons was determined with the non-parametric Kruskal-Wallis test (Shaw and Wheeler, 1985).

Heat flux computations

Ocean-atmosphere heat fluxes are the key energy transport processes linking the atmosphere and ocean and are thus crucial elements in investigating climatic variations (Bretherton, 1981). Surface heat flux processes and boundary layer modifications were investigated in this thesis to assess the possible role of local air-sea interactions on the rainfall variations over the subcontinent. As suggested by Ramage (1984b), only post-1960 data within the major shipping lanes were used and the calculations were made using original ships' observations rather than monthly-averaged data. The standard assumption was made that the measurements were obtained from a height of 10 meters. Potential errors resulting from the combination of estimated and measured winds, as well as day-time and night-time observations (Ramage, 1984b), have been reduced by using compositing techniques and focussing on interannual variability of parameters during the most recent years.

Bunker (1976) compared VOS data with Weather Ship data to obtain an estimate of error for heat flux calculations based on the former. He found the VOS wind data to be 0.2- 0.4 m/s lower than wind measurements obtained at Weather Ship stations, a difference he attributed to a fair weather bias. He found VOS SSTs to exceed Weather Ship measurements by a maximum of 0.2°C and dew point temperatures by 0.3°C - 0.5°C. From these comparisons, he estimated a probable error in heat flux calculations of less than 10%.

The turbulent fluxes of sensible and latent heat were estimated through the use of the standard bulk aerodynamic formulae (Malkus, 1962). Sensible heat fluxes were calculated from

$$Q_H = p\ Cp\ C_H\ U_{10}\ (SST - T)$$

where p is air density, Cp is the specific heat of air, C_H is the sensible heat transfer coefficient, U_{10} is wind speed at 10 m above the sea surface and T is the dry bulb temperature. The latent heat fluxes were determined from

$$Q_E = p\ C_E\ U_{10}\ L\ (Q_{SST} - Q_{AIR})$$

where C_E is the transfer coefficient for latent heat, L is the latent heat of vaporization, Q_{SST} is the specific humidity of air saturated over salt water at the SST, and Q_{AIR} is the specific humidity of air at 10 m.

The transfer coefficients were varied according to the atmospheric stability which was estimated from the sea-air temperature difference. Under neutral and unstable conditions, C_E was assumed equal to 1.3×10^{-3} and C_H to 1.2×10^{-3}. Under stable conditions (SST<T), a value of 0.85×10^{-3} was used for both transfer coefficients. This coefficient scheme is based on numerous observations over a wide range of environmental conditions (Kondo, 1975; Liu et al., 1979; Blanc, 1987) and has been used in previous research on heat fluxes locally (Walker and Mey, 1988; Jury and Walker, 1988; Mey et al., 1989).

Case-study analyses

As the synoptic systems responsible for rainfall over the subcontinent are not always reflected in monthly-averaged data (Jackson, 1952; Harrison, 1986a; Terblanche and Taljaard, 1987), a case study approach is adopted in Chapter 5 to assess the synoptic systems responsible for rainfall in the presence of "warm water events" surrounding southern Africa. In these case-studies, daily rainfall data were compiled for the eastern and western area using stations listed in the *Daily Weather Bulletin* (published monthly by the South African Weather Bureau). From these data, the nature of rainfall variability during the period was assessed and the main rainfall events isolated. The synoptic systems responsible for the abnormal precipitation were then identified and studied using satellite imagery and basic synoptic information (obtained from the South African Weather Bureau).

CHAPTER 3

STATISTICAL ASSOCIATIONS BETWEEN SEA SURFACE TEMPERATURES AND SUMMER RAINFALL

Spatial Coherency of Sea Surface Temperature Variability

Sea surface temperature departures within the southwest Indian Ocean and southeast Atlantic Ocean were subjected to principal component analysis (PCA) with the objective of identifying ocean sub-areas where interannual SST variability demonstrated spatial coherency over the study period. A separate analysis was performed on each ocean region. The two analyses included grid-squares north of 35° with the exception of 1 square in each ocean area where data availability was very low in comparison to other grid-squares (more than 25% of the seasonal data had to be replaced by the long-term mean). The correlation matrix was used as input to the PC analyses so that grid-squares characterized by higher variances were not over-emphasized in the results. The S-mode principal component analyses were performed (Richman, 1986) using seasonal SST anomalies. The Indian Ocean data matrix consisted of 47 grid-squares (stations) by 144 seasons (time) and that for the Atlantic Ocean consisted of 49 grid-squares by 144 seasons. The principal components were rotated using the varimax rotation (Kaiser, 1958; Horel, 1981; Richman, 1986) to enable a more accurate definition of coherent sub-areas. As this is an orthogonal rotation, the resulting PCs were uncorrelated in the time domain. Components whose eigenvalues exceeded 1 were considered significant (Guttman, 1954; Horel, 1981; Shaw and Wheeler, 1985) and rotated. Using this criterion, nine components in each ocean basin were rotated.

Results of the varimax rotations are given in Table 3.1. Within the Indian Ocean, 75% of the total original data variance was explained by the first 9 components, the first 5 explaining over 50%. Within the Atlantic Ocean, 79% of the variance was explained by the first 9 components, the first 4 accounting for over 50%. Using monthly data rather than seasonal data as input into the PC analyses resulted in less explained variance for both oceans, suggesting that averaging over 3 months helped to reduce "noise" inherent within the input time series.

The spatial loadings on each principal component were found to define unique ocean sub-areas as opposed to non-rotated solutions which have been shown to yield predictable positive/negative anomaly patterns regardless of the input data matrix

(Richman, 1986). As a result, the core areas for all components could be displayed on one diagram by illustrating loading values exceeding a chosen threshold value (Walsh et al. 1982; Richman and Lamb, 1985). Component loadings exceeding 0.7 were used to illustrate the core areas of most of the principal components. This means that the contours enclose grid-squares whose time-series exhibited linear correlations of 0.7 or more with the indicated component. This equates to an explained variance of 49%. In the case of PC 7, PC 8 and PC 9 within the Indian Ocean, loading contours of 0.6 and 0.4 were used because correlations between the grid-square SSTs and the principal components were comparatively low.

Table 3.1 Eigenvalues and variances associated with the first nine principal components describing non-seasonal SST variability within the a) southwest Indian Ocean and b) southeast Atlantic Ocean.

a

Principal Component	Eigenvalue	Variance (% of total)	Variance (Cumulative % of total)
1	7.1	15.1	15.1
2	5.5	11.7	26.8
3	4.8	10.2	37.0
4	4.4	9.3	46.4
5	3.5	7.4	53.8
6	3.4	7.2	61.0
7	2.5	5.3	66.3
8	2.2	4.7	71.0
9	1.7	3.6	74.6

b

Principal Component	Eigenvalue	Variance (% of total)	Variance (Cumulative % of total)
1	8.8	18.0	18.0
2	6.3	12.9	30.9
3	5.4	11.0	41.9
4	4.0	8.2	50.1
5	4.0	8.2	58.3
6	3.3	6.7	65.0
7	2.5	5.1	70.1
8	2.4	4.9	75.0
9	2.0	4.1	79.1

The 9 principal components extracted for each ocean area and their relative contributions to the total variance are displayed in Figure 3.1. Within the southwest Indian Ocean, PC 1 defined the Mozambique/Agulhas Current region along the east

coast from 15° to 35° S and captured 15% of the total variance. PC 2 was situated in the tropical Indian Ocean area at the extreme northeast corner of the study area and explained 11.7% of the total variance. Approximately 10 % of the variance was attributable to PC 3 in the western tropical Indian Ocean. PC 4 defined an area east of Madagascar in the vicinity of the Mascarene Islands, and captured 9.3% of the variance. The remaining components explained much less of the variance and were located in relatively data-poor regions.

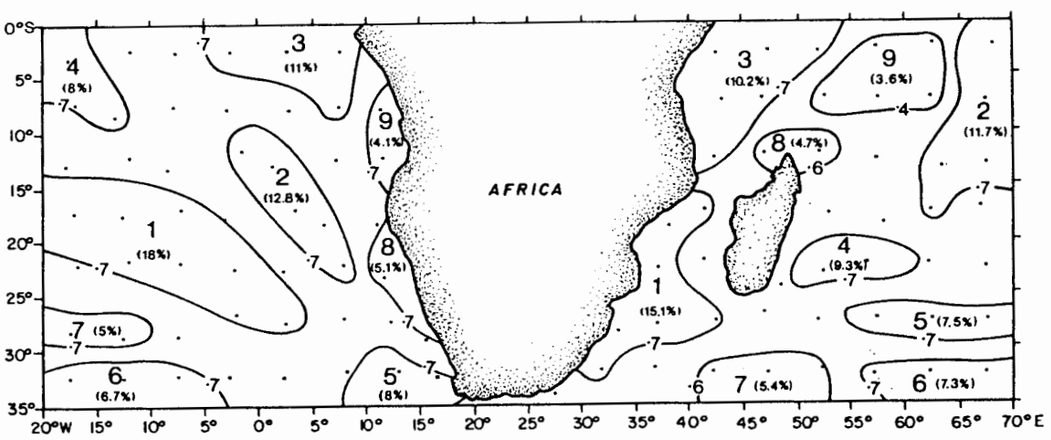

Figure 3.1 Core areas of SST coherence as determined from two principal components analyses with the varimax rotation. The loading value used to define each area is indicated and, where possible, a cut-off of 0.7 was used. The percent of the total variance explained by each component is shown in parentheses.

Within the Atlantic Ocean, PC 1 defined a large region in the subtropics across the central part of the study area and explained 18% of the total variance. PC 2 delineated a coherent area within the southeast trades from 10° to 25° S and accounted for 13% of the variance. PC 3, located in the eastern equatorial region, explained 11% of the variance, whereas PC 4 was confined to the extreme western equatorial region and explained 8% of the variance. PC 5 described SST coherence within the extreme southern part of the Benguela current system (8% variance explained) and PC 8 isolated coherent SST behavior within the northern Benguela region, centered on 20° to 25° S (5.1% variance explained). PC 9 described interannual SST variability along the Angolan coast from 5° to 15° S, explaining 4.1% of the variance. PC 6 and PC 7 were situated in the extreme southwest corner of the study area within a relatively data-poor region.

Relationships between SST and rainfall are examined in the next section by correlating the temporal amplitudes (scores) associated with each principal component with area-averaged rainfall during the early and late summer seasons. The scores for each PC are presented in Appendix A.

Sea Surface Temperature-Rainfall Associations During Late Summer: January-March

Correlation analyses

As a first step in the investigation of SST-rainfall relationships, linear correlations were determined between the temporal amplitudes of each PC and rainfall of areas 1 and 2. In Figure 3.2 the correlation coefficients significant at or above the 10% level are illustrated. Positive correlations of 0.31 and 0.35 (> 10% and 5% significance level) were determined between rainfall of both areas and SSTs within the Mozambique/Agulhas Current region (PC 1). In addition, a positive association of 0.36 (>5% significance level) was revealed between area 2 rainfall and SSTs in the far southeastern corner of the study area (PC 6). Stronger but opposite relationships (r= -0.44 and r= -0.45, > 1% significance level) were determined between rainfall of both areas and SSTs in the central tropical Indian Ocean (PC 2). This inverse correlation suggests that lower (higher) temperatures co-occurred with wetter (drier) seasons in both summer rainfall regions. A much less significant negative correlation was identified between area 1 rainfall and SSTs of the western tropical Indian Ocean (PC 3).

West of southern Africa, SSTs within 3 sub-areas demonstrated significant relationships with area-averaged rainfall. A significant positive correlation of 0.30 (> 10% significance level) was determined between SSTs of the northern Benguela region (PC 8) and area 2 rainfall. This result agrees with previous findings of Nicholson and Entekhabi (1987). Additional significant correlations involving Atlantic SSTs were negative. SSTs in the eastern tropical south Atlantic (PC 3) were oppositely correlated with area 1 rainfall, whereas SSTs in the subtropical Atlantic (PC 1) were oppositely correlated with area 2 rainfall.

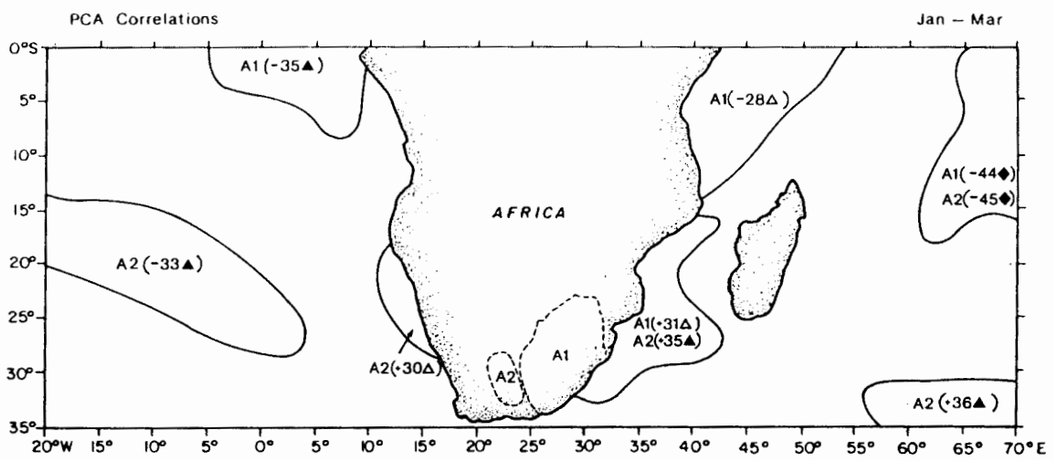

Figure 3.2 Linear correlations (x 100) between principal component amplitudes and area-averaged rainfall during late summer. Correlation coefficients (r) exceeding the 10% significance level are given in parentheses. Significance levels are as follows:
◆ > 1% ▲ >5% Δ >10%

A more detailed examination of SST-rainfall relationships was performed by correlating individual grid-square SST departures and area-averaged rainfall (Figure 3.3). For purposes of this analysis, SST data south of the subcontinent (35° - 40°S) were included, however, only for the most data-rich period of 1960-1984. Correlations significant at greater than the 10% level are shown.

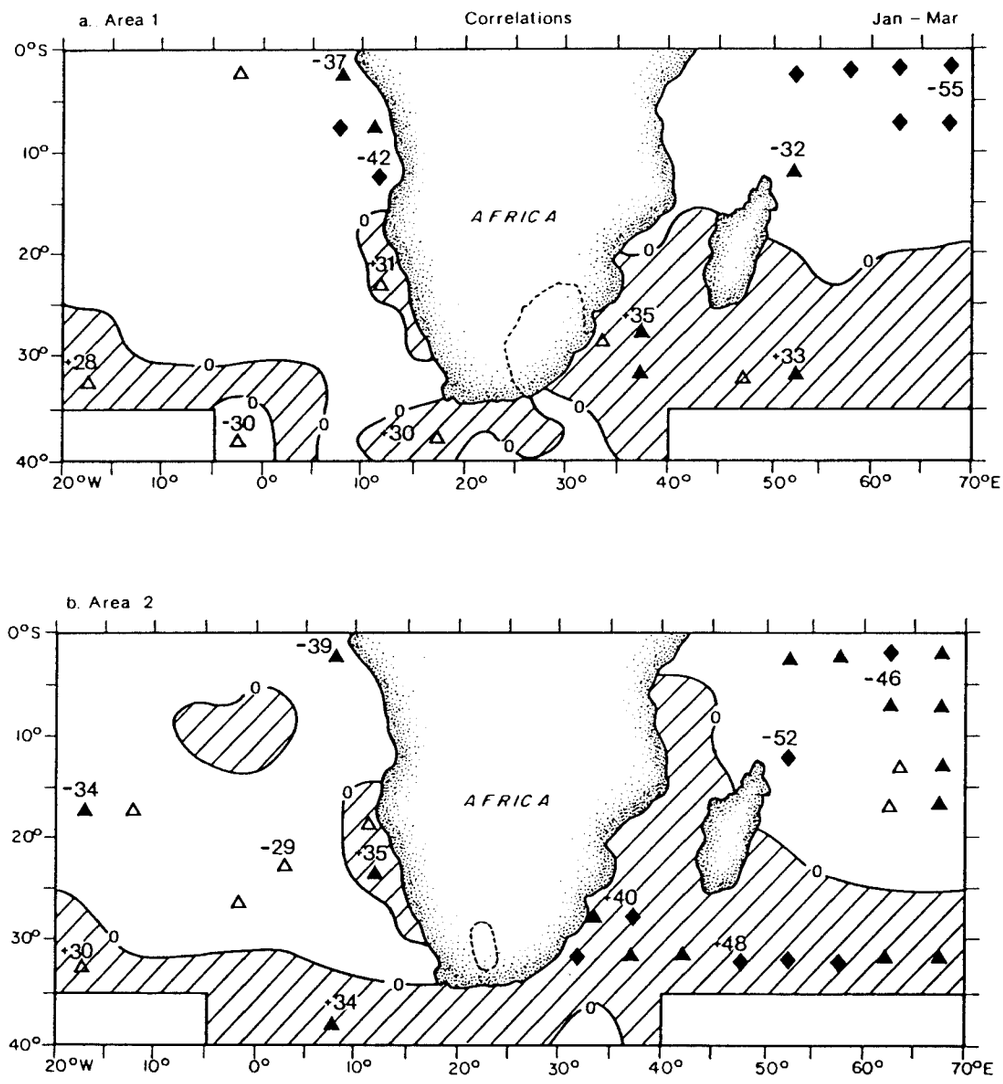

Figure 3.3 Linear correlations (x 100) between area-averaged rainfall of a) area 1 and b) area 2, and grid-square SST departures in late summer. Grid-square centers where correlations exceeded the 10% level are shown and significance levels are as in Figure 3.2. The highest correlations within each area are shown. Cross-hatching depicts areas of positive correlation. See Appendix D for results of "field" significance tests.

In general, these correlation fields confirmed the validity of the previous results obtained with PCA and gave more details of where the SST-rainfall associations were strongest in terms of the ocean's contribution. In regard to area 1 rainfall, strongest positive correlations (0.35, 5% significance level) were identified within the Agulhas Current system from 25° to 30°S. Area 2 rainfall exhibited even stronger correlations of 0.40 in the Agulhas system and 0.48 further east in the Indian Ocean subtropics (both significant above the 1% level). The strong correlations between area 2 rainfall and SSTs over a large ocean area south of Madagascar did not emerge from the previous PCA results. The positive correlation involving Benguela Current SSTs was strongest from 20° to 25°S. An additional positive SST-rainfall relationship was observed southwest of Africa in the 35° to 40°S zone where correlations with rainfall of areas 1 and 2 were 0.30 and 0.34 (> 10% and 5% significance level), respectively. The site of positive correlation was situated further west in correspondence with area 2 rainfall. Inverse relationships between SST and rainfall were observed over large areas of the tropical Indian Ocean northeast of Madagascar and the tropical Atlantic along the east coast.

In summary, the most significant correlations between rainfall and SSTs over the 36-year period were found to be indirect and involved ocean areas remote from the rainfall regions under consideration. Positive SST-rainfall associations were identified in local ocean areas including the Mozambique/Agulhas region, the western Agulhas Retroflection region and the Benguela region. Positive correlations involving Agulhas SSTs were the strongest and, in the case of area 2, the oceanic teleconnection area covered a large portion of the Indian Ocean south of Madagascar.

Compositing analyses

Sea surface temperature-rainfall relationships were further investigated by stratifying the SST data according to WET and DRY seasons for areas 1 and 2. Statistical significances of the SST differences for contrasting rainfall regimes were estimated using the non-parametric Kruskal-Wallis test. The upper and lower terciles of area-averaged rainfall were used as the basis for defining the WET and DRY seasons (Table 3.2). The SST field for WET (DRY) seasons was constructed by averaging SSTs within each individual grid-square over the 12 WET (DRY) seasons. The results are displayed as the differences between WET and DRY season SSTs (WET minus DRY) for each grid-square (Figure 3.4). Thus, a positive SST value indicates a direct (positive) association between SST and rainfall variations. In the interests of clarity and brevity, only the associations pertaining to wetter seasons will be discussed.

Table 3.2 Information pertaining to the upper and lower terciles of area-averaged rainfall departures during late summer which were used to define WET and DRY groupings of a) area 1 and b) area 2. Asterisks indicate years in which SO-rainfall associations were strongest.

a

WET SEASONS			DRY SEASONS		
Year	Rainfall	SOI	Year	Rainfall	SOI
*1976	1.72	1.46	*1983	-1.11	-3.38
*1967	1.26	1.44	*1970	-1.08	-0.36
*1974	1.20	2.00	*1965	-1.00	-0.35
*1955	1.11	0.30	1982	-0.68	0.29
*1972	0.94	0.33	1979	-0.60	-0.04
*1975	0.69	0.42	1968	-0.58	0.53
1981	0.50	-0.68	*1959	-0.50	-0.46
1978	0.38	-1.58	*1973	-0.45	-0.49
1977	0.36	-0.25	*1952	-0.42	-0.52
1963	0.35	0.17	*1966	-0.36	-1.36
*1956	0.31	1.27	1980	-0.34	-0.06
1958	0.10	-1.09	1951	-0.33	0.62

b

WET SEASONS			DRY SEASONS		
Year	Rainfall	SOI	Year	Rainfall	SOI
*1974	3.08	2.00	*1983	-1.11	-3.38
*1976	2.62	1.46	1964	-0.96	0.00
*1956	0.87	1.27	1984	-0.93	0.08
*1975	0.82	0.42	1982	-0.85	0.29
1963	0.71	0.17	*1970	-0.82	-0.36
1961	0.71	-0.72	1960	-0.70	0.00
*1972	0.48	0.33	*1966	-0.63	-1.36
1981	0.40	-0.68	*1965	-0.60	-0.35
1977	0.37	-0.25	1962	-0.59	0.64
*1950	0.35	1.51	1979	-0.55	-0.04
1954	0.16	-0.06	1951	-0.53	0.62
1973	0.13	-0.49	*1969	-0.40	-0.69

Spatially coherent SST anomaly patterns, which were strikingly similar for the two areas (Figure 3.4), were revealed by the compositing analysis. Wetter summers co-occurred with relatively high SSTs south of 20°S within the southwest Indian Ocean, west of the Agulhas Retroflection region and adjacent to the west African coast from 20° to 30°S. Similar SST patterns were revealed for the area 2 case, however, SST differences were somewhat greater in magnitude and covered larger ocean areas. In particular, the positive teleconnection area involving the Benguela current system expanded meridionally, whereas the teleconnection area west of the Agulhas Retroflection region experienced a zonal expansion, from 5° to 20° E (Figure 3.4b). In contrast, lower SSTs within tropical regions of the Indian Ocean were associated with higher rainfall over both areas. Likewise, large expanses of the tropical Atlantic harbored low SSTs during seasons of increased rainfall. SSTs for the WET and DRY cases were found to be significantly different (at the 10% level) in most of these areas (Figure 3.4).

Stratification of the data by contrasting rainfall regimes has revealed the existence of similar relationships to those determined from correlation analyses. Additional information was gained concerning the magnitudes and coherency of temperature patterns, particularly south of 35°S. Standard deviations of seasonal SSTs over the study area ranged from 0.5°-1.0° C and were highest along the west coast and south of 30°S. Thus, the largest SST differences were similar in magnitude to the standard deviations.

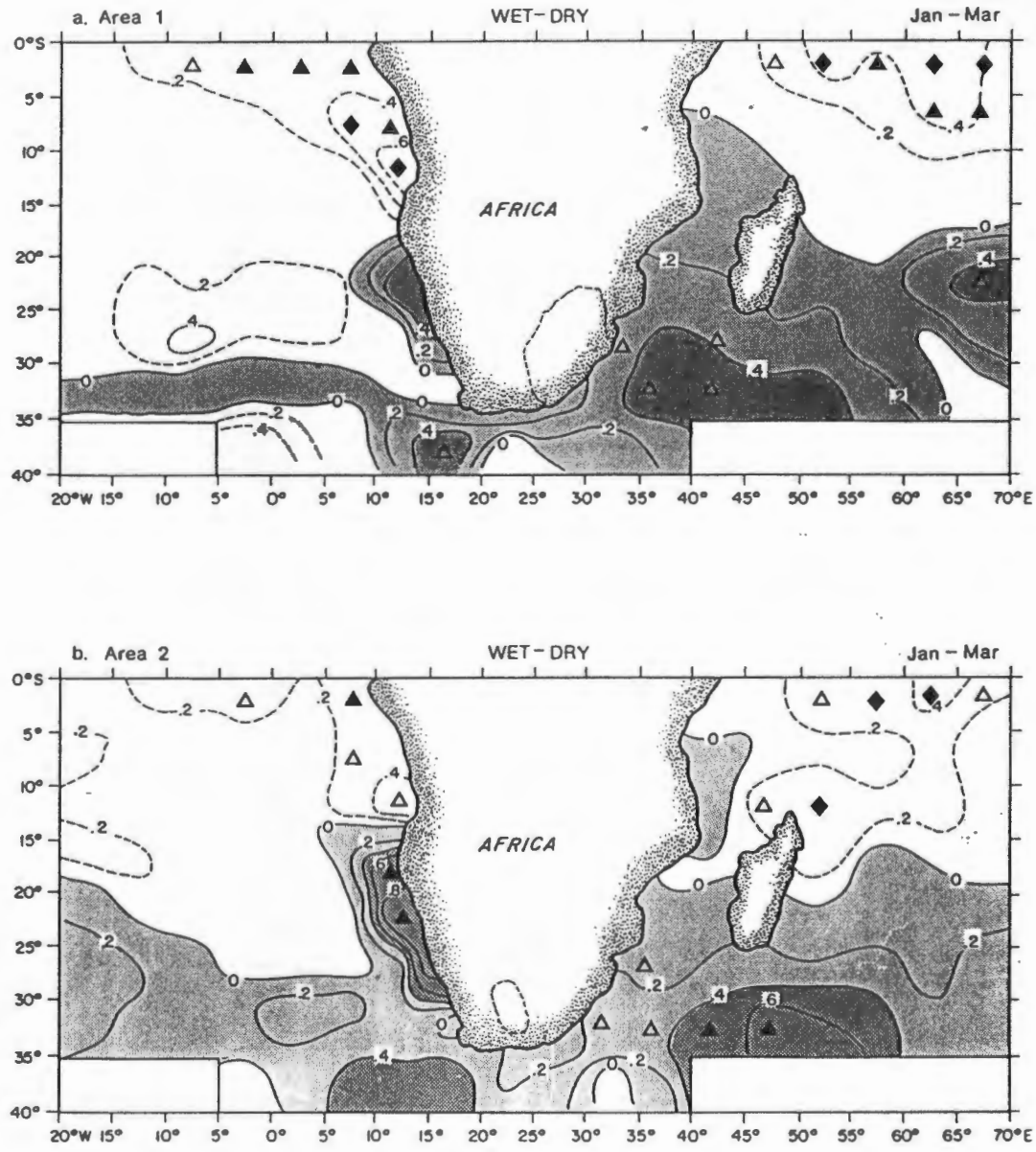

Figure 3.4 Composite SST differences (°C) between average WET and average DRY late summer seasons (WET minus DRY) for a) area 1 and b) area 2. Positive differences are shaded and differences exceeding 0.4°C are darkest. Dashed contours indicate negative differences. Differences significant above the 10% level are indicated and follow the convention given in Figure 3.2.

Sea Surface Temperature-Rainfall Associations During Early Summer: October-December

Correlation analyses

There were fewer significant SST-rainfall correlations during early summer as compared with late summer. The statistically significant linear correlations between the principal component scores and area-averaged rainfall are shown in Figure 3.5. A significant positive correlation (+ 0.32, > 5% significance level) was found between area 1 rainfall and SSTs of the Mozambique/Agulhas Current region (PC 1) which was similar in strength to that found later in summer. A positive correlation of similar strength was determined between area 2 rainfall and tropical SSTs north of Madagascar (PC 8). The strong inverse relationship between SSTs in the tropical Indian Ocean and rainfall of both rainfall areas during the late summer was weaker during early summer and only significant in terms of area 1 rainfall. A negative correlation involving area 1 rainfall was observed in the southeast Atlantic from 10° to 25°S where maximum southeasterly winds occur during early summer (Picaut et al., 1985).

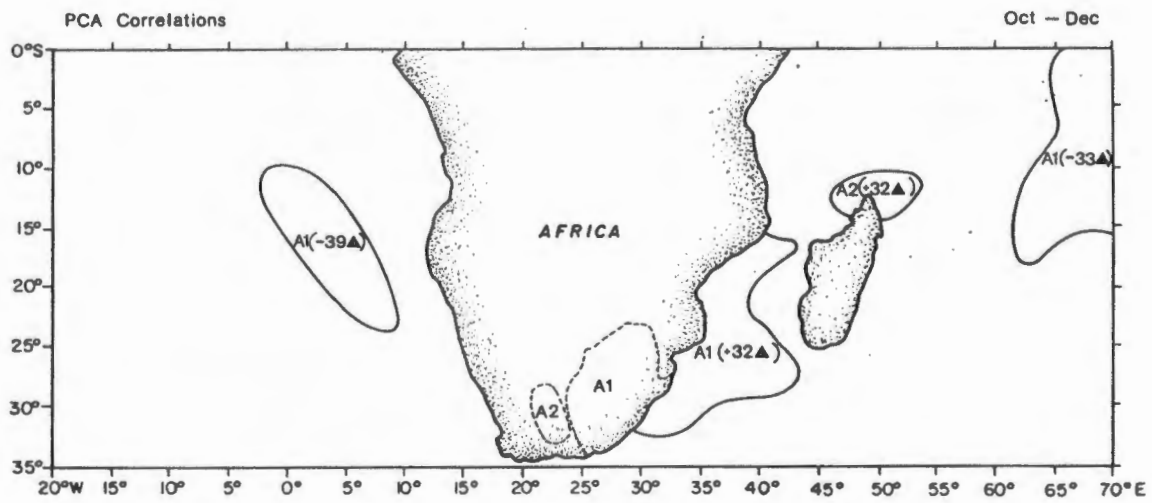

Figure 3.5 Linear correlations (x 100) between principal component amplitudes and area-averaged rainfall during early summer. Correlation coefficients (r) exceeding the 10% significance level are given in parentheses. Significance levels are as follows:
◆ > 1% ▲ > 5% △ > 10%

A correlation analysis performed with grid-square SST and area-averaged rainfall departures (Figure 3.6) confirmed many of the results of the previous correlation analysis using principal components. Correlations with area 1 rainfall were negative throughout the trade wind regions of both oceans. In addition, a significant negative correlation of -0.31 (>10% significance level) was noted southwest of the subcontinent between 10° and 15°E, west of the Agulhas Retroflection region. Only within the Agulhas Current system near 25° to 30°S were positive correlations observed (Figure 3.6a). Significant correlations involving area 1 rainfall were approximately double what would be expected by chance. In contrast, relatively few significant correlations characterized SST-rainfall relationships involving area 2 (Figure 3.6b).

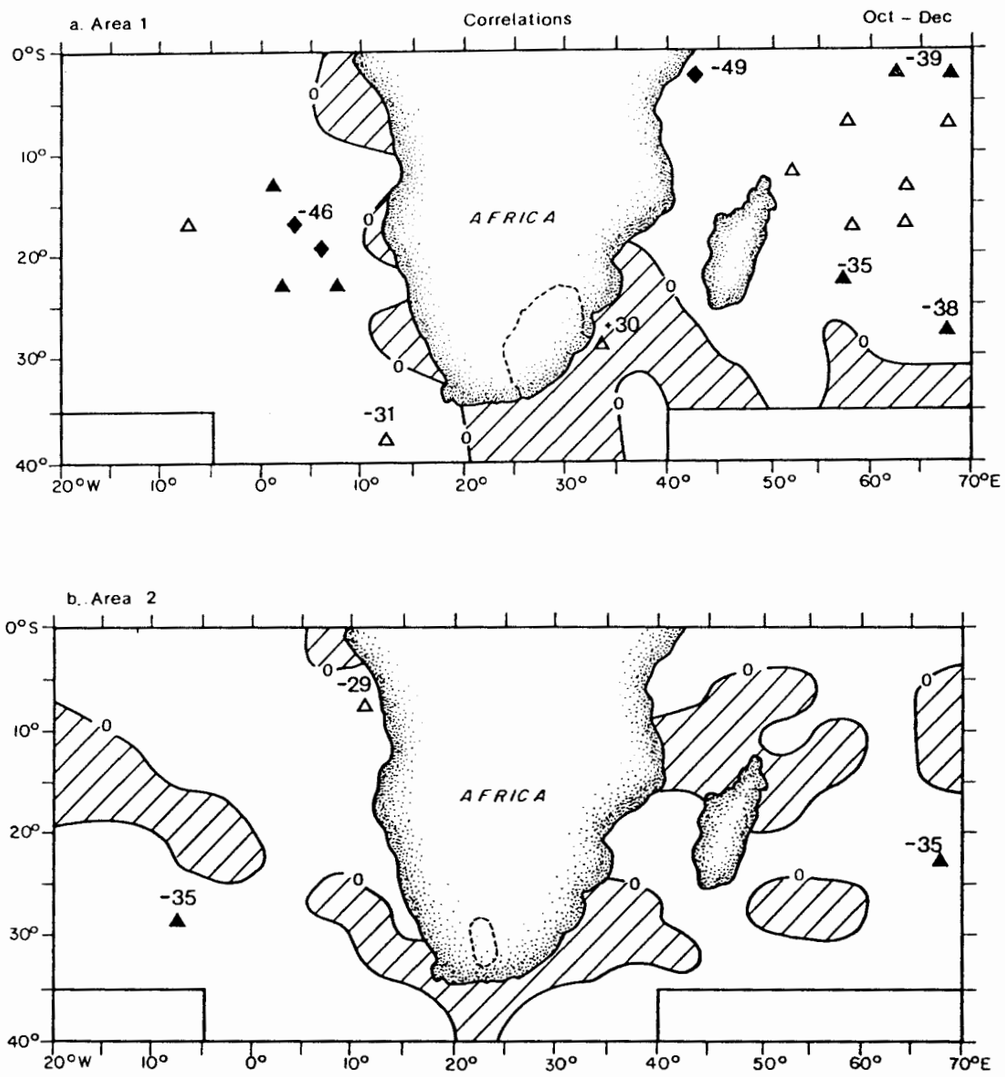

Figure 3.6 Linear correlations (x 100) between area-averaged rainfall of a) area 1 and b) area 2, and grid-square SST departures in early summer. Correlations exceeding the 10% level are shown and significance levels are as in Figure 3.5. The highest correlations within each area are presented. Cross-hatching depicts areas of positive correlation. See Appendix D for results of "field" significance tests.

Compositing analyses

Sea surface temperatures were stratified according to WET and DRY seasons as determined from area-averaged rainfall departures of the early summer season. The technique used was identical to that employed for the late summer analysis. The WET

Table 3.3 Information pertaining to the upper and lower terciles of area-averaged rainfall departures during early summer which were used to define WET and DRY groupings of a) area 1 b) area 2. Asterisks indicate years in which SO-rainfall associations were strongest.

a

WET SEASONS			DRY SEASONS		
Year	Rainfall	SOI	Year	Rainfall	SOI
*1960	1.09	0.58	*1972	-1.00	-1.18
*1956	1.06	1.08	*1965	-0.90	-0.86
*1975	0.77	2.00	*1951	-0.71	-1.30
1983	0.62	-0.04	1984	-0.64	-0.14
*1955	0.55	1.65	1968	-0.62	-0.15
1953	0.55	-0.05	*1982	-0.61	-2.99
1964	0.47	0.48	*1967	-0.61	-0.52
1958	0.45	-0.60	*1978	-0.45	-0.42
1949	0.40	0.26	1981	-0.44	0.21
1974	0.36	0.12	1954	-0.44	0.53
*1962	0.22	0.64	*1979	-0.28	-0.49
*1950	0.17	1.65	*1972	-0.27	-1.30

b

WET SEASONS			DRY SEASONS		
Year	Rainfall	SOI	Year	Rainfall	SOI
1953	1.79	-0.05	*1951	-1.38	-1.30
1963	1.41	-1.22	*1972	-1.19	-1.18
*1975	1.41	2.00	1954	-1.01	0.53
1983	1.32	-0.04	1960	-0.84	0.58
*1956	0.67	1.08	1969	-0.83	-0.40
*1955	0.67	1.65	1966	-0.61	-0.26
1982	0.59	-2.99	1984	-0.59	-0.14
1958	0.52	-0.60	1968	-0.53	-0.15
*1981	0.47	0.21	1949	-0.49	0.26
1957	0.47	-0.84	1962	-0.46	0.64
1977	0.43	-1.31	*1978	-0.45	-0.42
*1950	0.42	1.65	1980	-0.44	-0.15

and DRY seasons and their respective anomaly values are given in Table 3.3. SST means of the DRY group were subtracted from those of the WET group to yield the SST patterns shown in Figure 3.7. As in the previous compositing analysis, positive (negative) values indicated that SSTs in that region were higher (lower) during wetter (drier) seasons of the indicated area.

In general, the positive/negative SST patterns corresponded closely with those revealed in the previous correlation analyses (Figure 3.6a,b). Throughout extensive regions of the tropics and subtropics, lower SSTs were associated with higher rainfall of area 1. West of the Agulhas Retroflection region, lower SSTs were associated with higher rainfall during early summer. This relationship was stronger for rainfall area 1. Thus, there was a weak indication that SST gradients were enhanced at the Subtropical Convergence/Agulhas Retroflection front in correspondence with wetter seasons of both areas (Figure 3.7a,b).

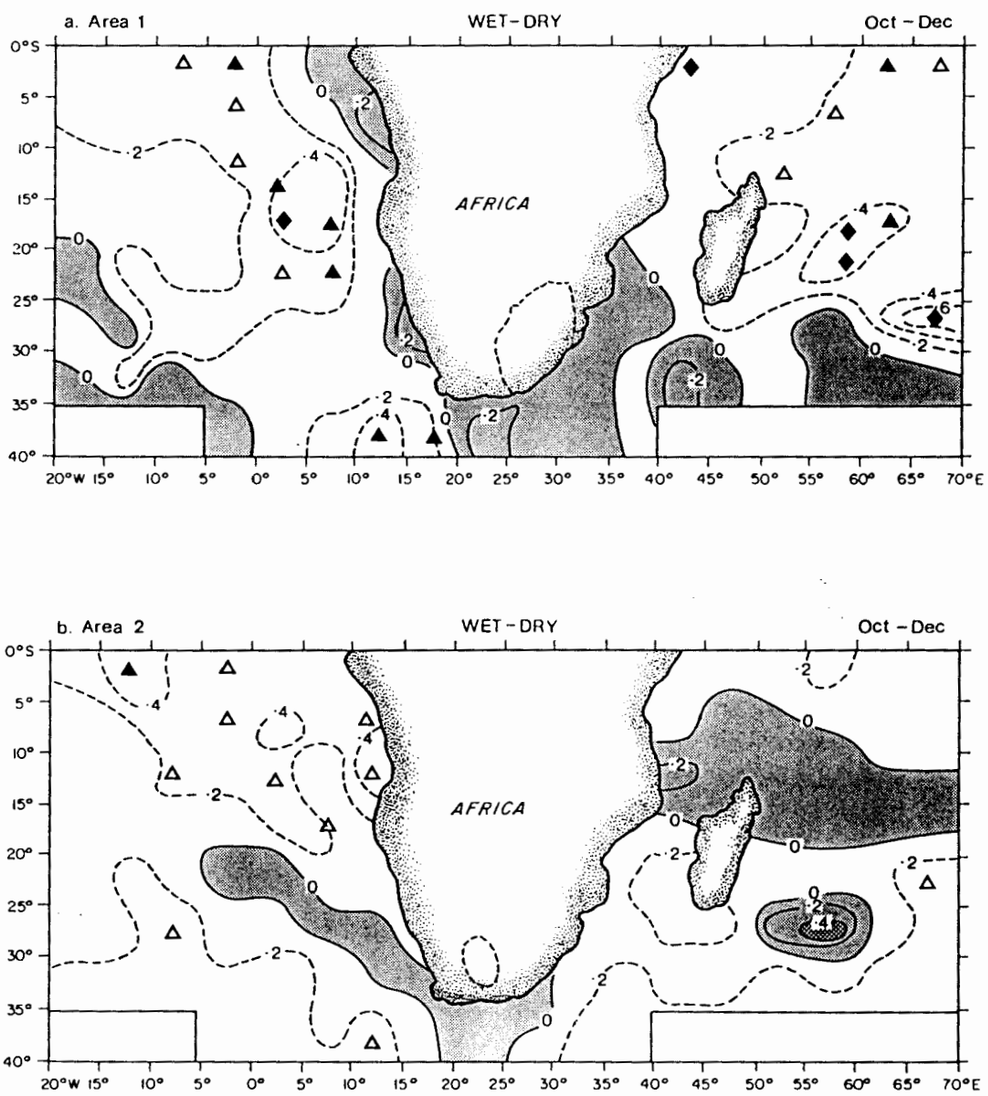

Figure 3.7 Composite SST differences (°C) between WET and DRY early summer seasons (WET minus DRY) for a) area 1 and b) area 2. Positive differences are shaded and differences exceeding 0.4°C are darkest. Dashed contours indicate negative differences. Differences significant above the 10% level are indicated and follow the convention given in Figure 3.5.

Sea Surface Temperature-Rainfall Relationships In The Absence Of Southern Oscillation-Rainfall Associations

Several researchers have investigated the associations between summer rainfall variations of southern Africa and the Southern Oscillation (SO). The associations are such that wetter (drier) periods correspond with higher (lower) index phases of the SO (Stoeckenius, 1981; Harrison, 1983; Lindesay et al., 1986; Lindesay, 1988a,b; van Heerden et al., 1988). Results of Lindesay (1988a) and van Heerden et al. (1988) have demonstrated that approximately 20 to 25 % of summer rainfall variations can be attributed to SO influences. Lindesay (1988b) has shown that the relationships were relatively strong during the 1960-1983 period.

It was postulated that local SST-rainfall relationships might differ in the absence of global-scale atmospheric anomalies associated with extreme phases of the Southern Oscillation. Therefore, in order to concentrate on local ocean-atmosphere interactions, it was necessary to exclude SO-rainfall associations from the analyses. The method employed was as follows.

High and low index phases of the SO were defined as the upper and lower terciles respectively, over the 36 years. Then all WET seasons which occurred during a high index phase season were excluded from further analyses. Similarly, all DRY seasons which occurred during a low index phase season were excluded from the analyses. This technique was used for the early and late summer seasons individually, the results of which are shown in Tables 3.2 and 3.3. Seasons exhibiting strongest SO-rainfall associations are marked with asterisks in the tables.

Correlation analyses: late summer

For area 1, five of the twelve wet seasons were not associated with SO high index phases. Similar results were obtained for the dry seasons and SO low index phases. For area 2, six of the wet seasons and seven of the dry seasons were found to be unassociated with SO high and low index phases respectively. These seasons are delineated in Figure 3.8, where the relationships between area-averaged rainfall and the SO index are schematically shown. This figure reveals that several WET seasons occurred during low index phases of the SO and vice versa. Therefore, removing the high and low index phases of the SO without regard for the associated rainfall variations would not have accomplished the desired result.

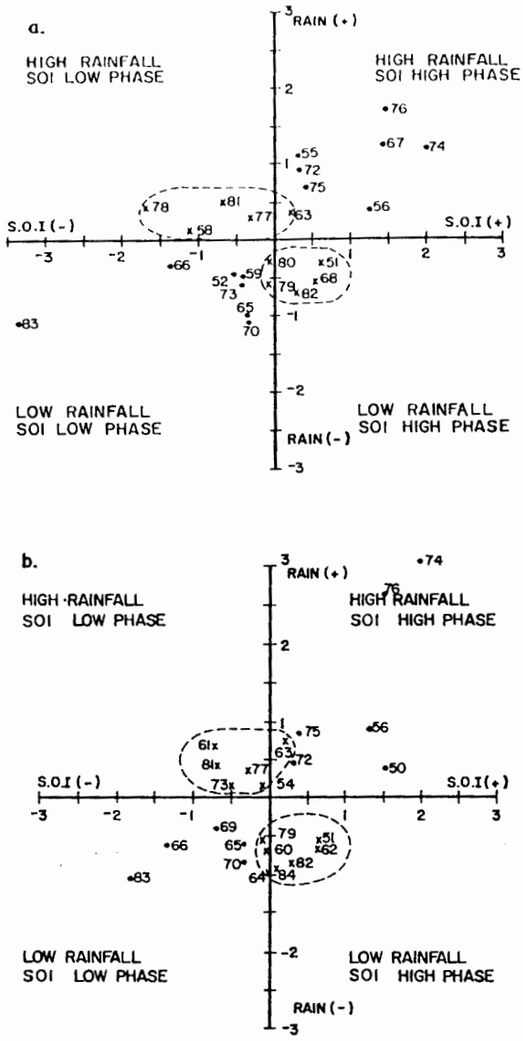

Figure 3.8 Scatter diagrams illustrating rainfall departures for WET and DRY *late summer* seasons of a) area 1 and b) area 2 and their relationships with the SOI. Seasons unassociated with SO-rainfall influences are circled. The values used to contruct the figure are given in Table 3.2.

After excluding seasons which demonstrated SO-rainfall associations, correlations between the principal component scores and area-averaged rainfall were determined (Figure 3.9). The strongest correlations were positive and involved local ocean areas. Positive correlations of 0.53 (> 1% significance level) and 0.39 (> 10% significance level) were determined between the Mozambique/Agulhas SSTs and rainfall of areas 1 and 2, respectively. Correlations between Benguela SSTs and area 1 and 2 rainfall were 0.46 (> 5% significance level) and 0.34 (> 10% significance level). In contrast to the correlation results obtained using the entire data set (Figure 3.2), these results have demonstrated that SST-rainfall relationships involving local ocean areas were stronger in the absence

of major SO-rainfall associations. Correlations involving area 1 rainfall were found to be strengthened to a greater degree.

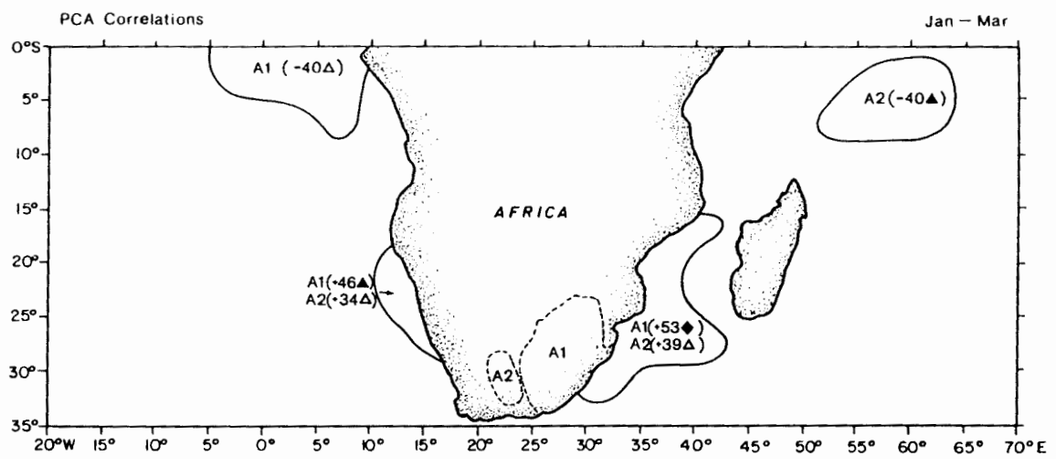

Figure 3.9 Linear correlations (x 100) between principal component amplitudes and area-averaged rainfall during late summer (*SO influences on rainfall excluded*). Correlation coefficients (r) exceeding the 10% significance level are given in parentheses. Significance levels are as follows: ◆> 1% ▲> 5% Δ> 10%

Negative correlations were again demonstrated between tropical SSTs and rainfall. In the Indian Ocean a significant relationship was only observed between tropical SSTs and area 2 rainfall and the oceanic teleconnection region had shifted westward (Compare Figures 3.2 and 3.9). The inverse relationship between area 1 rainfall and SSTs of the tropical Atlantic were increased in magnitude but not in significance as a result of the smaller data set. Several SST-rainfall relationships which appeared in the analysis of the entire data set (Figure 3.2) were not confirmed by this analysis.

Correlations between grid-square SSTs and area-averaged rainfall are illustrated in Figure 3.10. For area 1, a maximum positive correlation of 0.53 (> 1% significance level) was identified within the Mozambique/Agulhas Current system near 20° to 25°S. Significant positive SST-rainfall correlations were identified along the east coast from 10°to 35°S, with 4 grid-squares along the east coast illustrating significance above the 5% level (Figure 3.10a). Significant correlations involving area 2 rainfall were confined to the southern Agulhas area from 30° to 35°S (r= 0.58, > 1% significance level) and the northern Mozambique Channel from 10° to 15°S (r= 0.43, > 5% significance level)

(Figure 3.10b). Significant positive relationships were demonstrated between Benguela SSTs from 20° to 25°S and rainfall of area 1 (0.55, > 1% significance level) and area 2 (0.34, > 10% significance level). The South Atlantic grid-square at 20°-25°S, 20°-15°W (previously excluded from the PC analysis) was the site of a positive correlation with rainfall of both areas. This relationship was confirmed by the non-parametric Spearman rank correlation test. An additional positive correlation was observed involving area 1 rainfall and SSTs southwest of the subcontinent between 15° and 20°E. Negative correlations involving area 1 rainfall and two remote grid-squares were observed in the tropical and extratropical Atlantic (Figure 3.10a). Further confirmation of the reality of these relationships was obtained from the Spearman rank correlation test.

Compositing analyses: late summer

A compositing analysis was performed to further investigate SST-rainfall relationships after excluding SO influences. As in an earlier section, the SST data were stratified according to WET and DRY seasons (Table 3.2). SST means for the DRY group were subtracted from SST means of the WET group to yield the SST patterns displayed in Figure 3.11. The resulting SST patterns compared closely with those obtained from the corresponding correlation analysis. Significant differences were in evidence throughout the Mozambique/Agulhas region where higher temperatures co-occurred with wetter seasons. Near the western margin of the Agulhas Retroflection region, there was an indication that warmer waters were associated with wetter seasons of both areas. A significant WET-DRY difference was noted at 15° to 20°E (Figure 3.11a). This warm SST feature southwest of the subcontinent extended farther west into the South Atlantic and covered a larger area in the area 2 composite (Figure 3.11b), but did not attain significance at the 10% level. During wetter seasons, relatively low SSTs from 20° W to 10° E occurred to the west of relatively high SSTs near the Agulhas Retroflection region, thus indicating an intensification of SST gradients southwest of the subcontinent. Such a feature could increase the likelihood of local cyclogenesis.

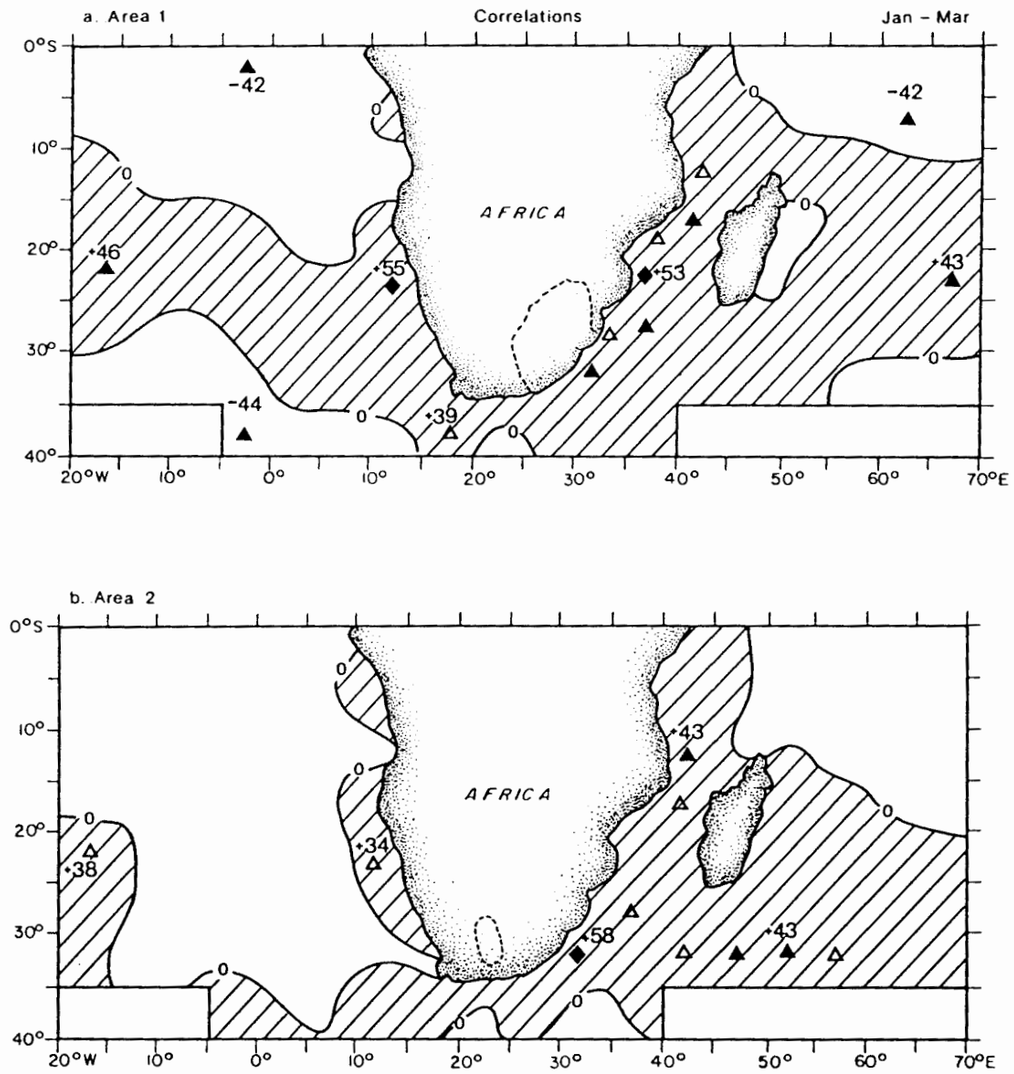

Figure 3.10 Linear correlations (x 100) between area-averaged rainfall of a) area 1 (n=22) and b) area 2 (n=25) and grid-square SST departures in late summer (*SO influences on rainfall excluded*). Correlations exceeding the 10% level are shown and significance levels are as in Figure 3.9. The highest correlations within each area are shown. Cross-hatching depicts areas of positive correlation. See Appendix D for results of field significance test.

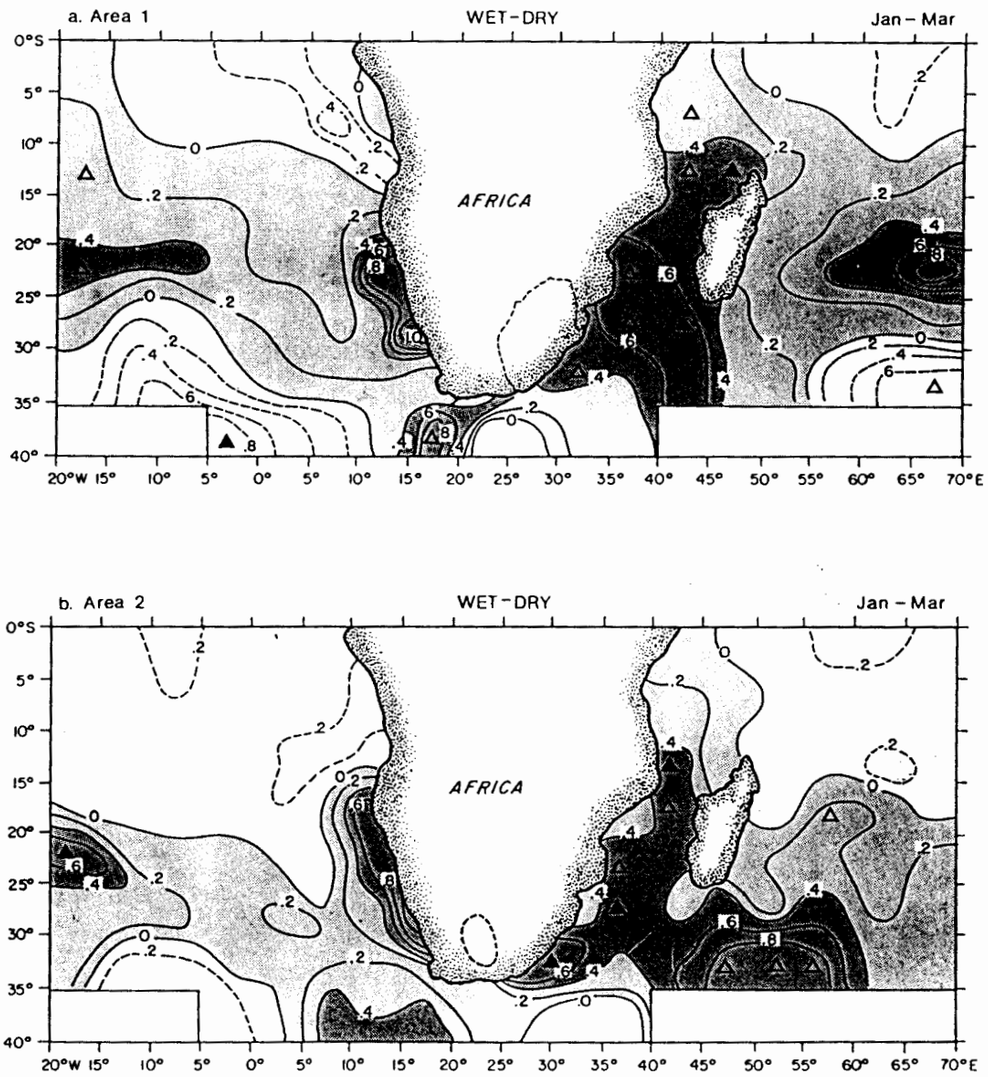

Figure 3.11 Composite SST differences (°C) between average WET and average DRY late summer seasons (WET minus DRY) for a) area 1 and b) area 2 (*SO influences on rainfall excluded*). Positive differences are shaded and differences exceeding 0.4°C are darkest. Dashed contours indicate negative differences. Differences significant above the 10% level are indicated and follow the convention given in Figure 3.9.

Within the Benguela system, spatially coherent SST differences were observed over a relatively large area, however the differences did not attain significance at the 10% significance level (Figure 3.11 a,b). The positive teleconnection involving SSTs in the central South Atlantic was revealed as significant in terms of rainfall of both areas, despite the relatively poor data characteristics in that grid-square.

After exclusion of major SO-rainfall associations, the negative correlations previously identified between tropical SSTs northeast of Madagascar and rainfall departures of both areas were found to be much less spatially extensive and, where present, less significant (Compare Figures 3.3 and 3.10). This was not an unexpected result as SSTs in this region were found to exhibit significant negative correlations with the SOI of -0.5 (>1% significance level), a relationship which has been previously demonstrated by Cadet (1985).

Lag associations

The simultaneous relationships between SST and late summer rainfall have been investigated in detail. In this section, the relationships will be studied with a lag of one season to assess their potential usefulness in rainfall prediction efforts. Correlations between October-December SST and January-March rainfall were computed based on the late summer seasons used in the previous section. Significant positive relationships involving SSTs along the east coast of Africa south of the equator were observed. In the case of area 1 (Figure 3.12a), the significant correlations were scattered with the highest correlation of 0.47 (> 5% significance level) occurring southeast of the subcontinent, within the Agulhas Current recirculation area. Positive correlations, significant at the 10% level, were observed in source regions for the Agulhas Current and an additional strong positive correlation (r= 0.42, > 5% significance level) was noted along the equator in the Indian Ocean. For the area 2 case (Figure 3.12b), strongest correlations were observed in the Mozambique Channel from 15° to 25° S (r= 0.50, > 5% significance level) and at 5° to 10°S (r= 0.44, > 5% significance level). In contrast, correlations were negative to the east of Madagascar for both rainfall areas. Strong negative correlations (-0.36, > 10% level and -0.40, > 5% level) were observed within trade wind regions of the South Atlantic.

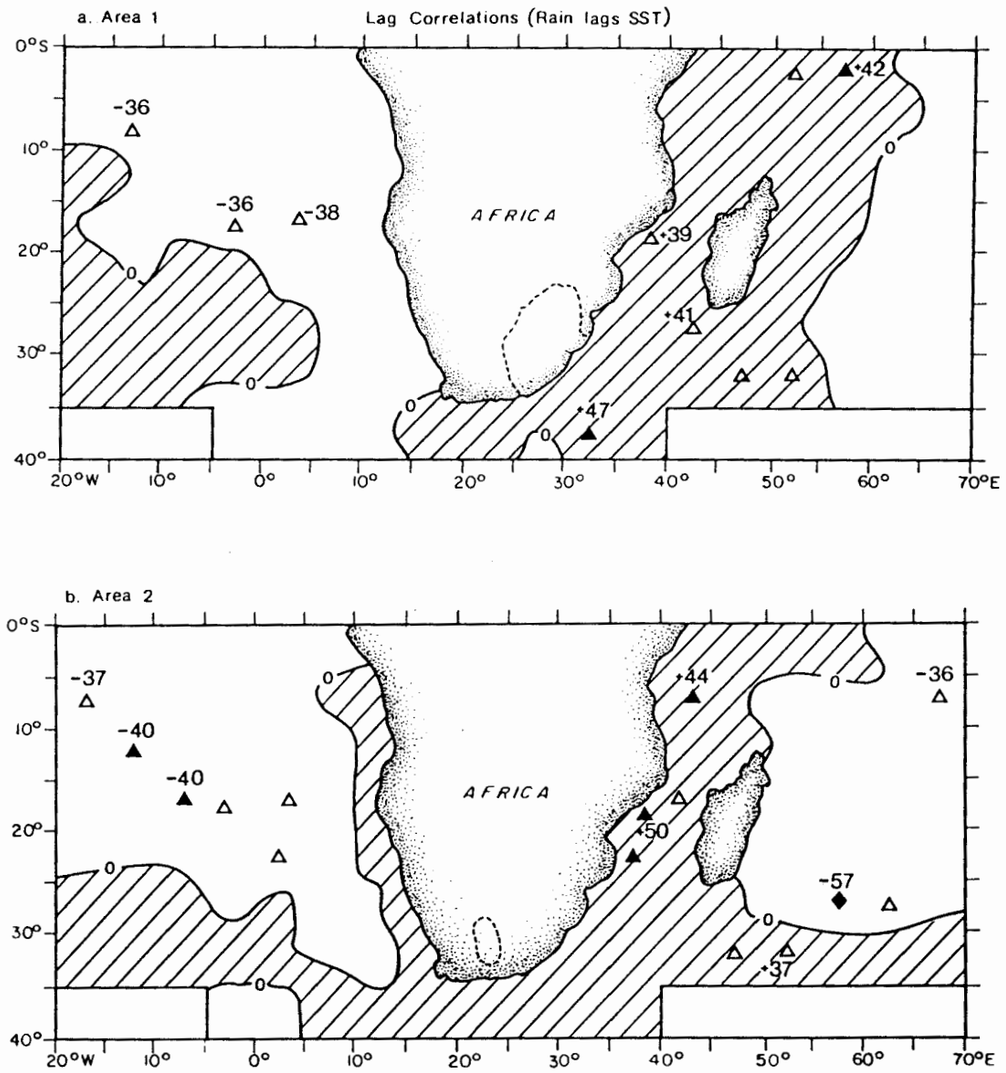

Figure 3.12 Linear correlations (x 100) between area-averaged rainfall of a) area 1 (n=22) and b) area 2 (n=25) in *late summer* and grid-square SST departures in *early summer*. Correlations exceeding the 10% level are shown and values for the highest correlations within each area are given. Significance levels are as in Figure 3.9. Cross-hatching depicts areas of positive correlation. See Appendix D for results of "field" significance tests.

These relationships were investigated further by stratifying the SST data for early summer seasons preceding WET and DRY late summer seasons. The results are displayed in Figure 3.13 as SST differences between the WET and DRY groupings. In the area 1 case, largest WET-DRY SST differences were located in the Agulhas system directly east of South Africa (Figure 3.13a). Significant differences were noted there and also further north along the equator. Results of the area 2 SST analysis (Figure 3.13b) corresponded closely with the correlation results (Compare Figures 3.12b and 3.13b), positive correlations occurring within the Mozambique Channel and further north in the tropics.

In addition, large ocean areas of relatively high temperatures west of southern Africa corresponded with wetter seasons (Figure 3.13 a,b). In the area 1 case, the WET-DRY differences within the South Atlantic were significant at the 5% significance level. Non-significant correlations were identified here in the previous correlation analysis. An additional significant difference worthy of mention was that situated southeast of Madagascar (Figure 3.13b), within a source region of the Agulhas Current. Here, lower temperatures in early summer corresponded with wetter late summer seasons and a relatively strong negative correlation (-0.57, > 1% significance level) was also observed (Figure 3.12 b). Low temperatures may reveal local effects from wind mixing due to intensification of the prevailing trade winds.

Results of this analysis have indicated that prediction efforts for late summer rainfall of the eastern and western portions of the summer rainfall region may benefit from a consideration of SST anomaly patterns surrounding southern Africa. With a lag of one season, SSTs of the Agulhas/Mozambique system and the tropical Indian Ocean would be most useful.

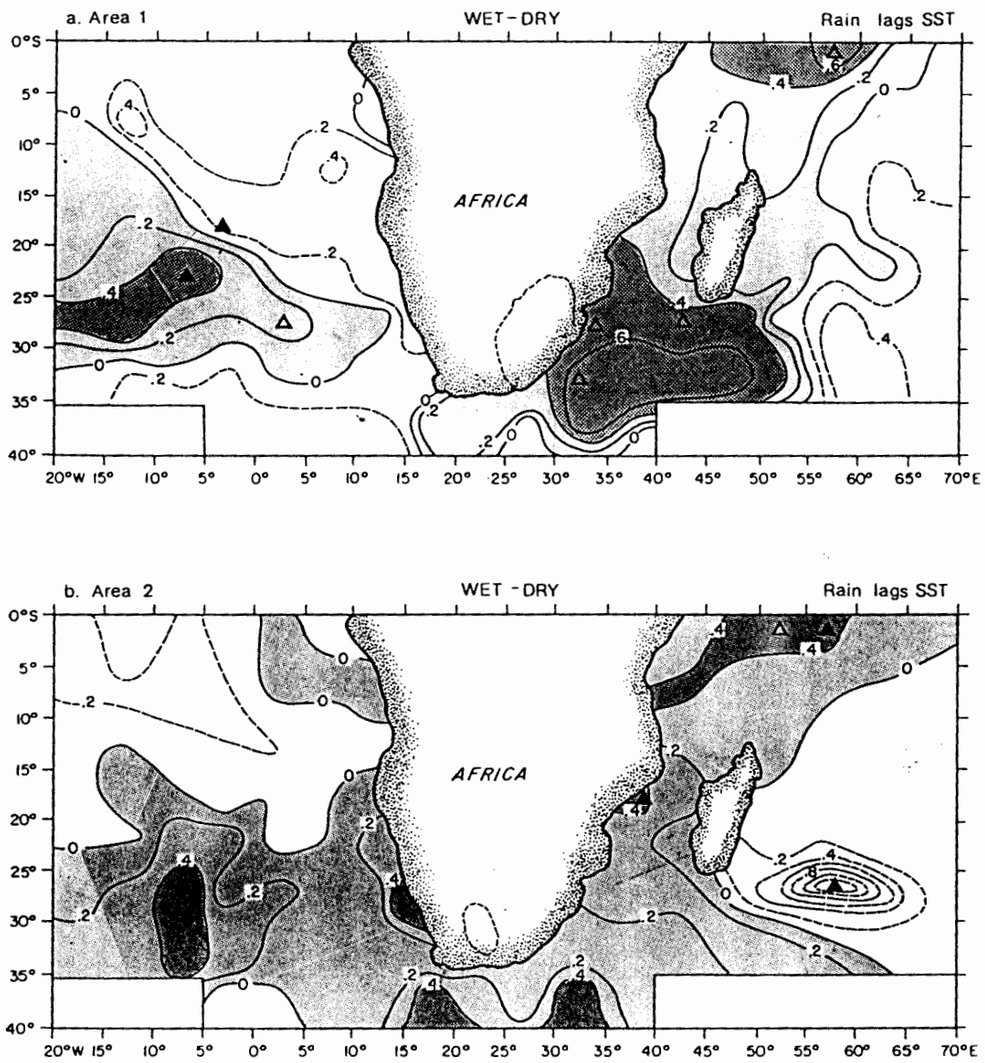

Figure 3.13 Composite early summer SST differences (°C) preceding average WET and average DRY late summer seasons (WET minus DRY) for a) area 1 and b) area 2. Positive differences are shaded and differences exceeding 0.4°C are darkest. Dashed contours indicate negative differences. Differences significant above the 10% level are indicated and follow the convention given in Figure 3.9.

Correlation analyses: early summer

Early summer rainfall variations demonstrate positive associations with the SOI, although to a lesser degree than those of late summer (Lindesay et al., 1986; Lindesay, 1988a; van Heerden et al., 1988). Major influences imposed by the SO on South African early summer rainfall variations were removed using the same methods described for the late summer rainfall period. WET seasons which fell within the upper tercile of the SOI were excluded from further analyses. Likewise, DRY seasons which fell within the lower tercile of the SOI were excluded. These seasons are marked with asterisks in Table 3.3. Fewer seasons were excluded during early summer as compared with late summer (Compare Tables 3.2 and 3.3), suggesting that early summer rainfall was less closely associated with the Southern Oscillation, an observation discussed in detail by Lindesay (1988a,b). In Figure 3.14, the SO-rainfall relationships are schematically illustrated and the rainfall seasons least effected by SO influences are circled.

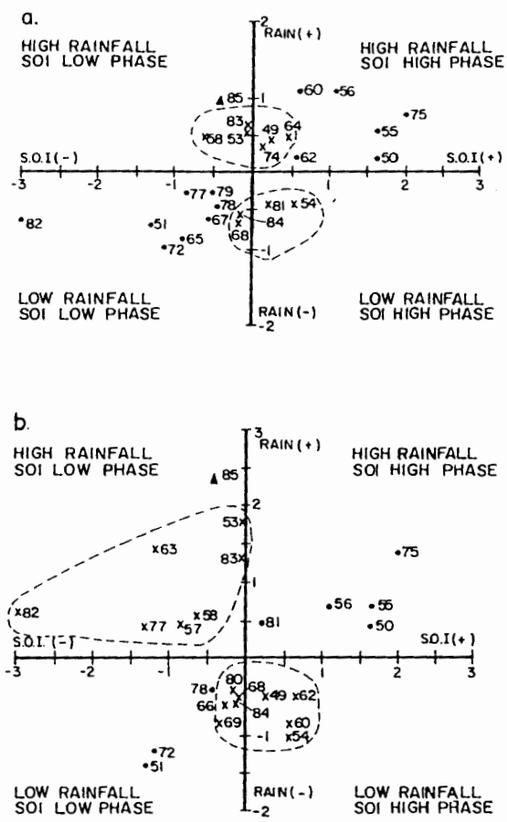

Figure 3.14 Scatter diagrams illustrating rainfall departures for WET nd DRY *early summer* seasons of a) area 1 and b) area 2 and their relationships with the SOI. Seasons unassociated with SO-rainfall influences are circled. The values used to contruct the figure are given in Table 3.3. Although not included in the 36-year period, the 1985 values are shown for later reference.

After exclusion of rainfall seasons most affected by the SO, correlations between the principal component scores and area-averaged rainfall were determined (Figure 3.15). The strongest positive correlations (r= 0.45, > 5% significance level) were observed within the Mozambique/Agulhas region (PC 1). This SST-rainfall relationship was considerably strengthened in comparison with correlation results using the entire data set in which correlations were 0.32 (> 5% significance level) (Figure 3.5). The previously identified negative correlation involving SSTs in the central tropical Indian Ocean was not observed. However, a new negative correlation was noted between SST in the far southeastern portion of the study area and area 2 rainfall. The previously observed negative correlation between area 1 rainfall and Atlantic SSTs within the southeast trade wind regions had shifted into equatorial regions and strengthened (-0.65, > 1% significance level).

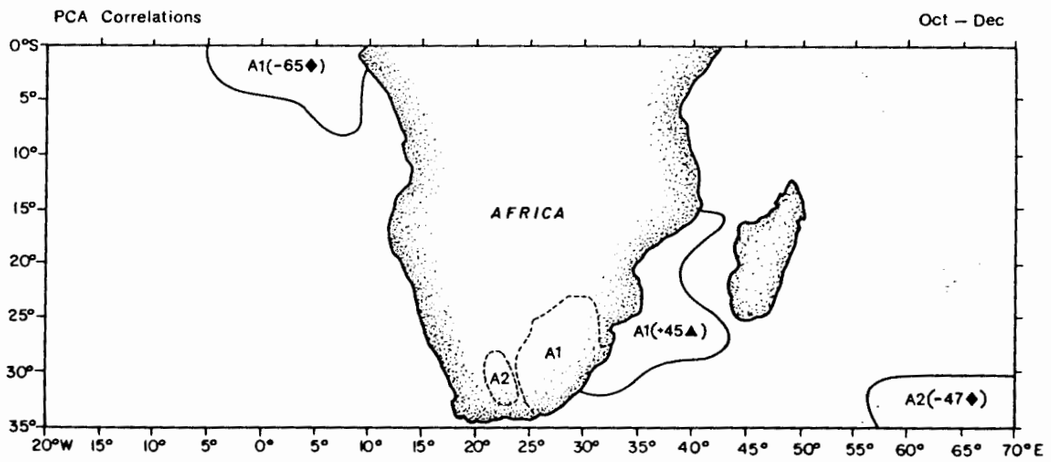

Figure 3.15 Linear correlations (x 100) between principal component amplitudes and area-averaged rainfall during early summer (*SO influences on rainfall excluded*). Correlation coefficients (r) exceeding the 10% significance level are given in parentheses. Significance levels are as follows: ◆> 1% ▲> 5% Δ> 10%

Correlations between grid-square SSTs and area-averaged rainfall are illustrated in Figure 3.16. The results are in agreement with those of the principal component analysis within the Mozambique/Agulhas region and also in the tropical Atlantic (Figure 3.16a). Several new significant correlations were also revealed. For area 1, negative correlations were noted west of southern Africa within subtropical ocean areas near 0°E. These

correlations revealed a correspondence between relatively low SSTs in the South Atlantic from 35° to 40°S and wetter seasons of both areas 1 and 2 (Figure 3.16). In terms of area 2, a large area of positive correlations was observed further north in the subtropics (Figure 3.16b). These newly discovered relationships were substantiated by the Spearman rank correlation test as well as from a compositing analysis based on WET-DRY differences (Figure 3.17). The compositing analysis also indicated a local enhancement of SST gradients along the Agulhas/Subtropical Convergence SST front near 15° to 20°E during wetter seasons, particularly for area 1 (Figure 3.17 a,b).

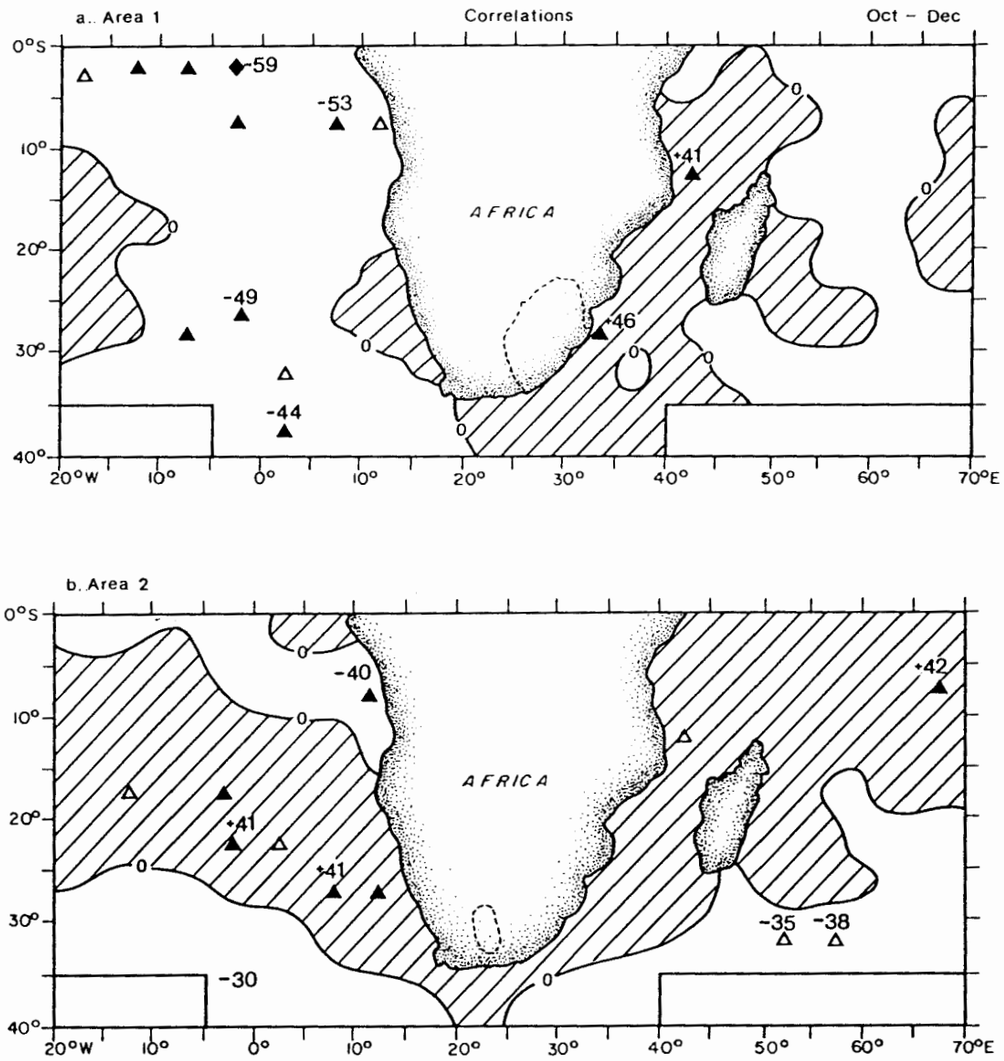

Figure 3.16 Linear correlations (x 100) between area-averaged rainfall of a) area 1 (n=22) and b) area 2 (n=28), and grid-square SST departures in early summer (*SO influences on rainfall excluded*). Correlations exceeding the 10% level are shown and the highest correlations within each area are presented. Significance levels are as in Figure 3.15. Cross-hatching depicts areas of positive correlation. See Appendix D for results of "field" significance tests.

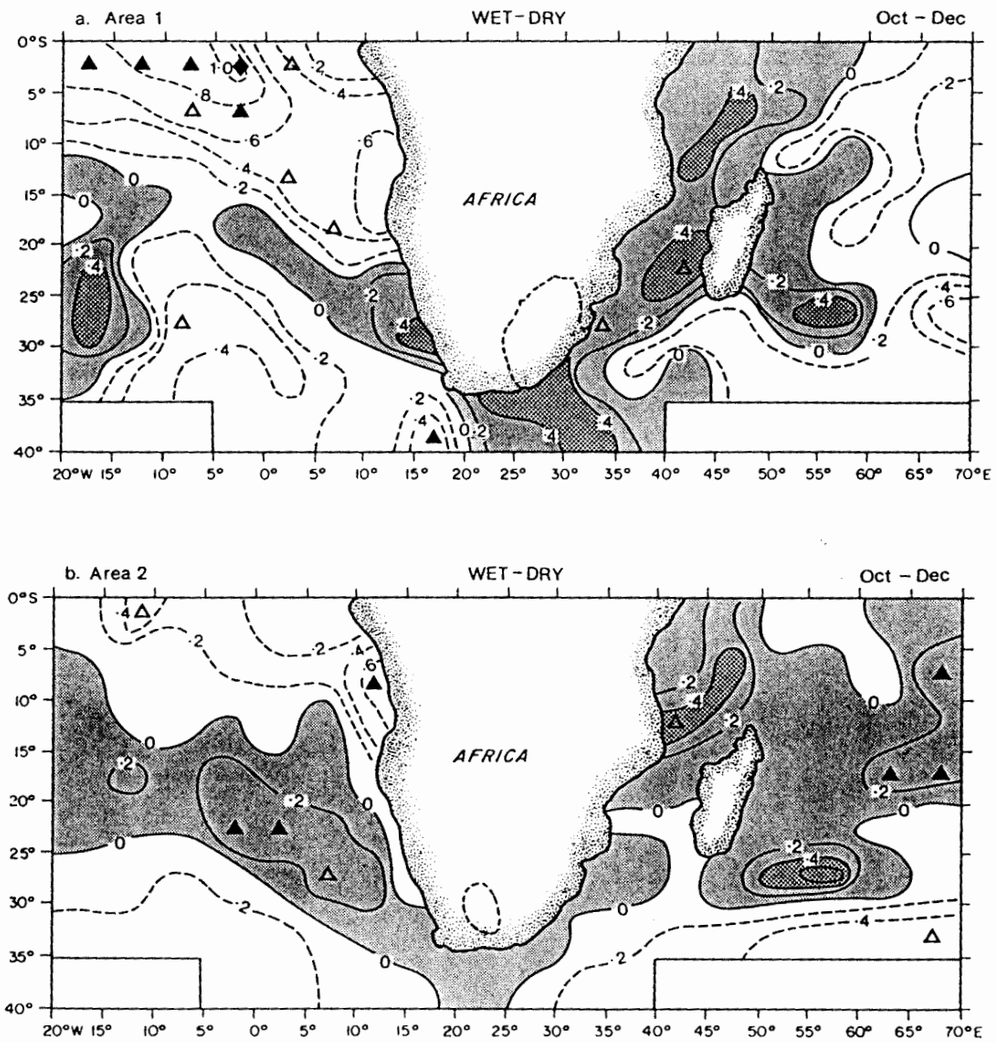

Figure 3.17 Composite SST differences (°C) between average WET and average DRY early summer seasons (WET minus DRY) for a) area 1 and b) area 2 (*SO influences on rainfall excluded*). Positive differences are shaded and differences exceeding 0.4°C are darkest. Dashed contours indicate negative differences. Differences significant above the 10% level are indicated and follow the convention given in Figure 3.15.

Lag associations for the early summer season were investigated through the use of correlation techniques and compositing as was done for the late summer. The correlations and WET-DRY differences were found to be less significant than those which described the simultaneous associations between SST and rainfall. Thus, they will not be presented here.

Compositing analyses: early summer

Circulations at temperate latitudes are thought to be more influential on rainfall variations over South Africa during early summer than during late summer (Harrison, 1986a,b,c; Schulze, 1965). It is, therefore, unfortunate that very little long-term SST information is available for these ocean areas. In this section, use will be made of high quality satellite-derived SSTs to assess SST distributions for contrasting rainfall regimes of early summer.

Monthly-averaged SSTs were obtained for 2.5° x 2.5° grid-squares over the period January 1982 through December 1985. During this time, areas 1 and 2 exhibited similar early summer rainfall behavior since the 1983 and 1985 seasons were very wet and the 1982 and 1984 seasons were comparatively dry (Figure 3.14). During 1985, area 2 experienced more rainfall than during any other early summer of the preceding 36-year period (Figure 3.14b). Three of the four early summers were accompanied by SOI values near zero. In contrast, the early summer of 1982 corresponded with an extreme low index phase of the SO.

Sea surface temperature distributions during contrasting rainfall regimes were assessed by subtracting the November SSTs of the DRY cases from the November SSTs of the WET cases (eg. 1983-1982 and 1985-1984). The mid-season month was used to illustrate SST distributions as the rainfall anomalies occurred after October. The SST differences corresponding to the WET minus DRY seasons are illustrated in Figure 3.18. In both cases, similar anomaly patterns were revealed. These included positive differences of 1° to 3°C south of the subcontinent within the Agulhas Retroflection region, positive differences of 1° to 3°C along the east coast of South America at the confluence of the Brazil and Falkland Current systems and negative differences of 1° to 2°C in the central South Atlantic. Contrasting SST differences were observed in the tropical Indian Ocean during the two cases. In the 1983/1982 case, negative differences of 1° to 2°C occurred, while the differences were positive in the 1985/1984 case.

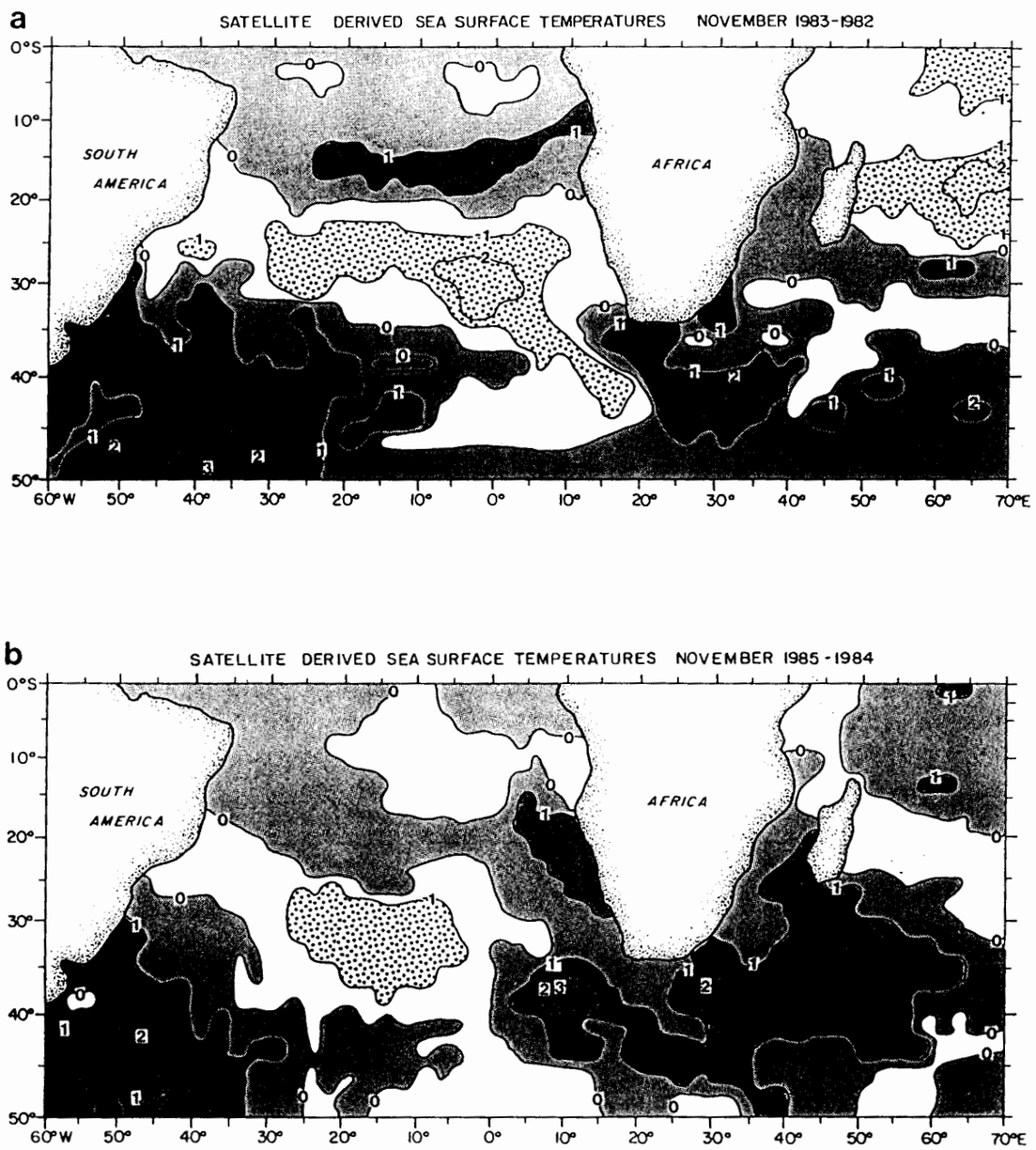

Figure 3.18 Satellite-derived November SST differences corresponding to WET and DRY early summer seasons a) 1983 (WET) - 1982 (DRY), b) 1985 (WET) - 1984 (DRY). Positive values are shaded and values exceeding 1°C are darkest. Negative values exceeding 1°C are dotted.

The observation of most direct interest to this study is that in both cases a large ocean area south of the subcontinent was considerably warmer (1°-3°C) in association with wetter conditions over the summer rainfall region. In the 1983/1982 case, SST gradients at the Subtropical Convergence/Agulhas interface southwest of South Africa were increased by at least 2°C during the WET 1983 season. An enhancement of meridional contrasts of wind shear and temperature within the marine boundary layer in association with the strong SST front near 40°S, 15°E could be inferred, a situation which would favor local cyclogenesis. In the 1985/1984 case, there was a marked westward shift in the SST difference field, the positive anomaly in 1985 having extended much further west into the southeast Atlantic Ocean. The positioning of this large-scale anomaly to the west of the country was closely associated in time with the 1985 rainfall anomaly over western portions of the summer rainfall area.

Monthly-averaged SST anomaly maps (National Environmental Satellite, Data and Information Service, NOAA, Washington, DC) confirmed that the differencing technique had isolated two major warm water events within the Agulhas Retroflection region south of the subcontinent. During October-December 1983, SST anomalies south of the subcontinent were 1 to 2°C above average and SST gradients near 15°E were about 3°C stronger than normal (Figures 1.7, 5.20). In October and November 1985, SST anomalies of 1° to 4°C were revealed in the 35° to 50°S zonal band between 8°E and 60°E (Figure 4.3), thus confirming that an extensive warm event occurred within southern reaches of the Agulhas Current system and extended a considerable distance into the South Atlantic. The SST anomaly maps suggested that SST anomalies along the west coast ranged from 1° to 2°C.

The use of high quality satellite information has revealed two major Agulhas warm events which were closely related in time with wet early summer seasons over much of the interior. In both cases, easterly wind anomalies within the southwest Indian Ocean south of 20°S were associated with and preceded the warm water events south of the subcontinent (*Climate Diagnostics Bulletin*, Climate Analysis Center, Washington, DC). In Chapter 4, the ocean-atmosphere interactions involved in the evolution of the more intense 1985 event will be considered. In Chapter 5, the synoptic systems responsible for the anomalous rainfall in 1983 and 1985 will be investigated.

CHAPTER 4

OCEAN-ATMOSPHERE INTERACTIONS ON SEASONAL AND MONTHLY TIME SCALES

Surface winds, heat fluxes and marine boundary layer characteristics were investigated to obtain insights into the possible ocean-atmosphere coupling mechanisms associated with the identified SST-rainfall relationships. Attention was focused on the season of maximum rainfall, January to March, and rainfall seasons least associated with the Southern Oscillation were considered. The previously defined WET and DRY seasons provided the basis for all compositing analyses within this chapter.

Surface Winds Associated with Contrasting Rainfall Regimes

Late summer wind behavior

Surface winds across the oceans were investigated in order to assess atmospheric circulations associated with SST-rainfall relationships involving the Mozambique/Agulhas region, the Agulhas Retroflection area and the Benguela Current region. The wind components were obtained from VOS data and stratified according to WET and DRY seasons of each rainfall area. Zonal (U) and meridional (V) component fields were constructed by averaging the seasonal means over all years within the WET and DRY groups. The average U and V components corresponding to area 1 WET seasons are illustrated for reference purposes in Figures 4.1a and 4.2a, respectively. The average U and V components corresponding to area 2 are not shown as they were virtually undistinguishable from those of area 1. Positive U components represent increased westerly winds and positive V components indicate increased southerly winds during the wetter seasons. The Kruskal-Wallis test was used to assess whether the WET season values were significantly different from the DRY ones. Significance levels of 10% and 5% are indicated on the difference maps as open and solid triangles respectively. Due to the small sample sizes, physically relevant patterns may not always have attained statistical significance. Thus, spatially coherent features will also be discussed.

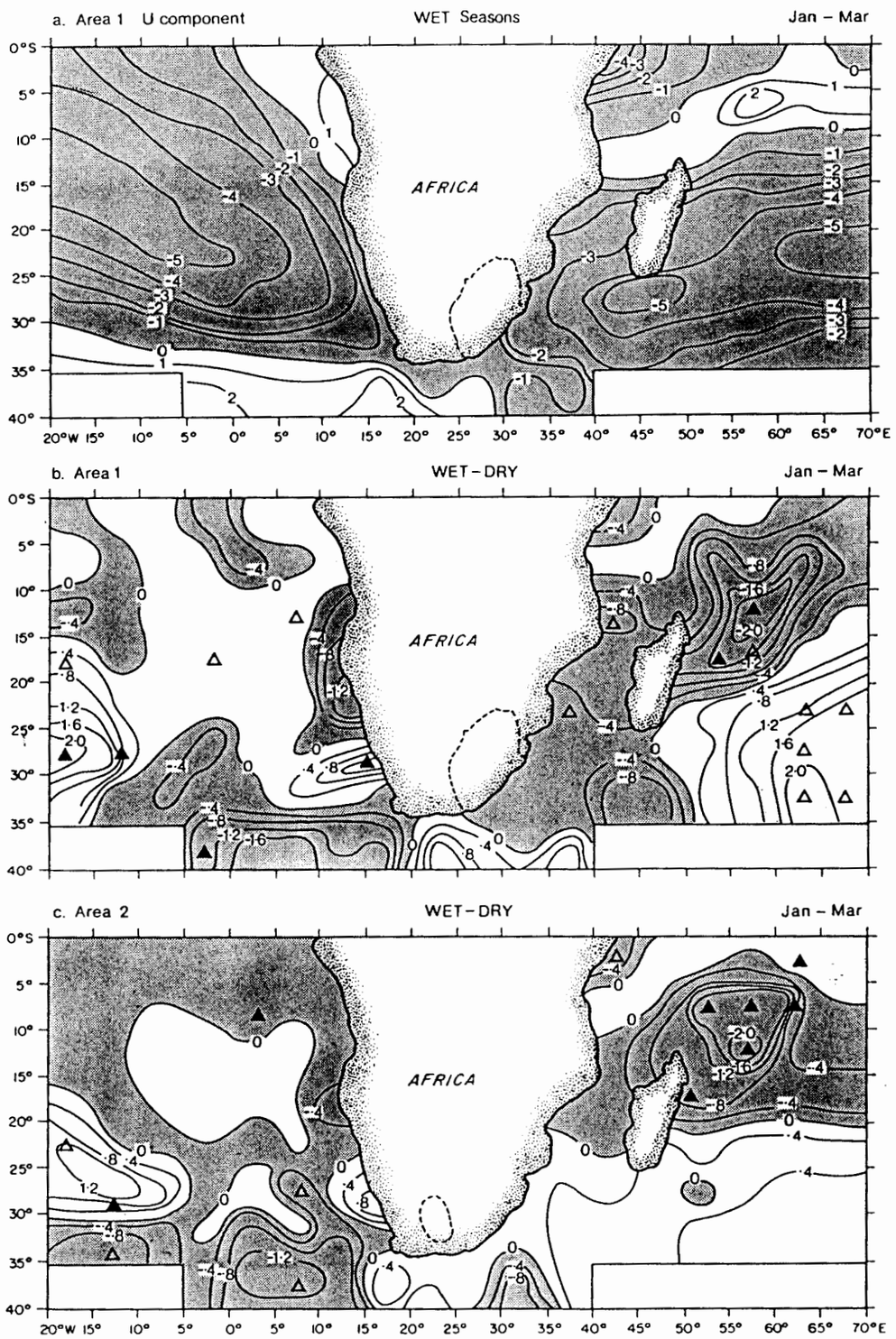

Figure 4.1 a) Average zonal (U) wind components (m/s) corresponding to the WET seasons of area 1 b) U wind component differences between average WET and average DRY late summer seasons of area 1 c) U component differences between average WET and average DRY late summer seasons of area 2. Negative values are shaded and represent easterly flow or easterly differences. Differences significant above the 10% and 5% levels are indicated by open and filled triangles respectively.

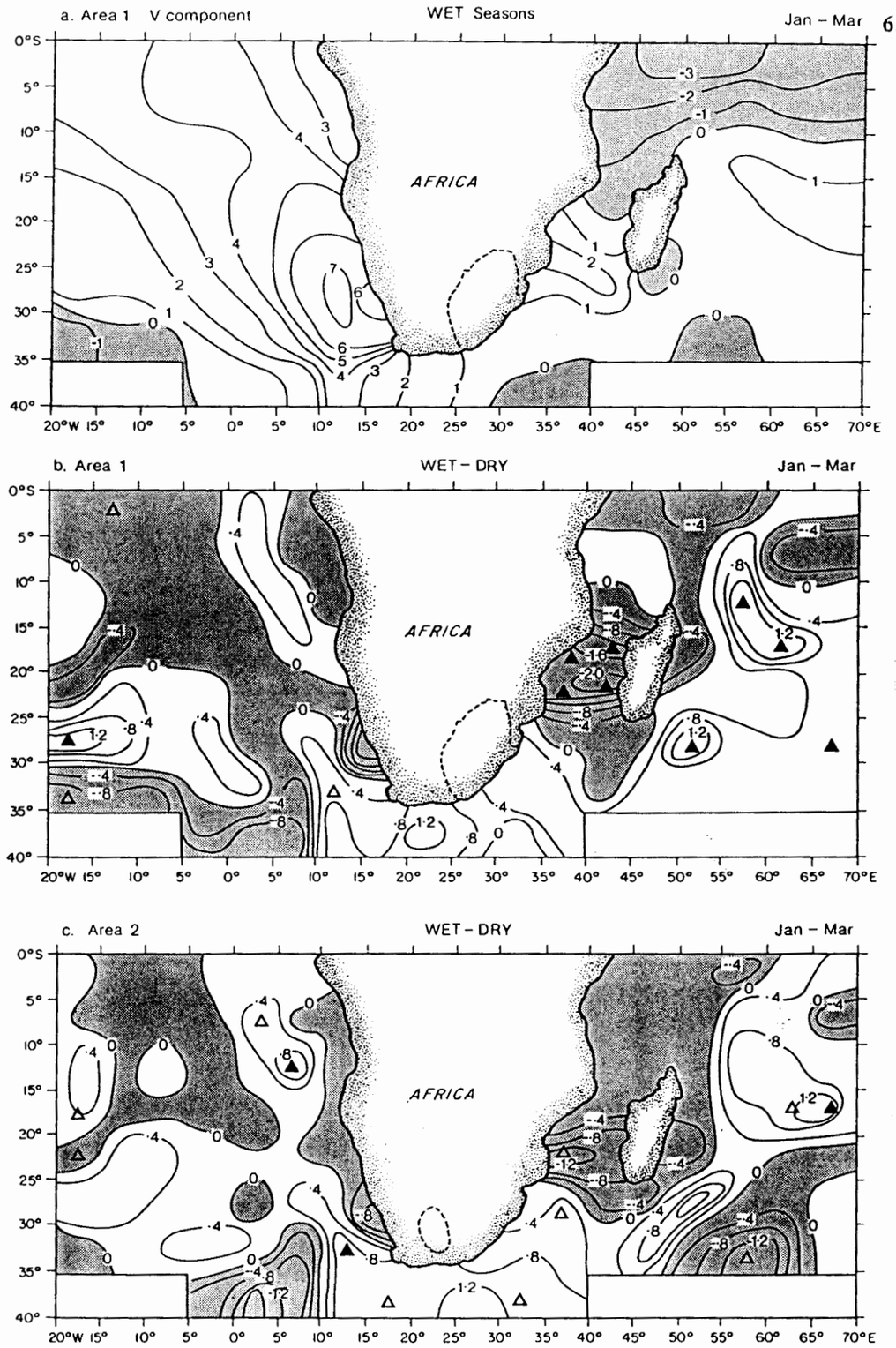

Figure 4.2 a) Average meridional (V) wind components (m/s) corresponding to the WET seasons of area 1 b) V wind component differences between average WET and average DRY late summer seasons of area 1 c) V component differences between average WET and average DRY late summer seasons of area 2. Negative values are shaded and represent northerly flow or northerly differences. Differences significant above the 10% and 5% levels are indicated by open and filled triangles respectively.

The average zonal wind components corresponding to the WET seasons of area 1 (Figure 4.1a) revealed a prevalence of easterly flow across the Indian Ocean south of 10°S and north of 5°S. Strongest easterly winds were observed within the zonal band from 15° to 30° S with maximum speeds having occurred near 45°E and 65°E. In terms of the average meridional components (Figure 4.2a), a transition from southerly to northerly winds was observed along the African east coast near 15°S, probably revealing the mean location of the Intertropical Convergence Zone. Surface winds were markedly different across the southwest Indian Ocean during the composite WET and DRY seasons. Easterly winds were significantly increased during the wetter seasons within the 5°-25°S zonal band (Figure 4.1b,c). The zonal component differences attained a maximum value of 2 m/s and were most significant northeast of Madagascar. Southerly flow was simultaneously increased in this region (Figure 4.2b,c), indicating that the trade winds were stronger during wetter seasons. In the area 1 case, zonal wind differences were noted along the east African coast from 10° to 35°S. Significant differences were identified within the Mozambique Channel (Figure 4.1 b). Meridional wind differences were closely associated with these zonal wind changes (Figure 4.1, 4.2). The net result was an increased prevalence of northeasterly and easterly flow rather than southeasterly flow during wetter seasons. In the case of area 1, WET-DRY merdional component differences exceeded 2 m/s (Figure 4.2b). The identified wind changes along the east coast suggest a poleward displacement of the Indian Ocean Anticyclone and the Intertropical Convergence Zone during wetter seasons.

An increased prevalence of northerly and easterly flow was observed south of Madagascar in close proximity to the East Madagascar Current area, corresponding to an easterly wind maximum within the Indian Ocean area (Figure 4.1a). In the area 2 composite case, winds were also more northerly southeast of Madagascar near 30° to 35°S and 50° to 65°E during wetter seasons (Figure 4.2c), also suggesting southward displacement of the Indian Ocean Anticyclone. A similar pattern was, however, not identified for the area 1 case in which increased southerly winds were observed to occur over a large ocean area southeast of Madagascar (Figure 4.2b). An inspection of the zonal wind differences in this same region revealed the prevalence of increased westerly flow during wetter seasons, particularly in the area 1 case. Based on these wind patterns it is suggested that anticyclonic circulation was strengthened in the western Indian Ocean adjacent to the east coast of southern Africa during the wetter seasons of area 1. Although the mean position of the South Indian Ocean Anticyclone during summer is near 85°E, high pressure cells are often situated along the southeast coast. Taljaard and van Loon (1984) have described the ocean area southeast of Africa as an area of anticyclonesis, where sudden intensification of anticyclones occurs. Their analysis of 5 year's data revealed two distinct regions where anticyclones occur most

frequently, one centered on 37°S, 40°E and the second near 35°S, 95°E. They suggest that the anticyclone center off the southeast coast of Africa is not revealed on average summer atmospheric pressure maps as the actual pressures are higher further east. The presence of anticyclones near the east coast of southern Africa assists in the advection of moist maritime air onto the plateau, a situation often associated with rainfall. The wind patterns corresponding to area 2 suggested primarily north-south instead of east-west circulation changes between contrasting rainfall regimes.

South of the subcontinent between 10°E and 30°E, spatially coherent and significant differences in meridional wind components were identified (Figure 4.2 b,c). Increased southerly flow occurred during the wetter seasons. To the west of 15°E, westerly flow was considerably weaker in the 30°-40°S zonal band revealing a poleward displacement of the zonal westerlies (Figure 4.1).

West of southern Africa, increased southerly winds occurred during wetter seasons in the southern Benguela system (30° - 35°S) and also further north (5°-15°S) (Figure 4.2a-c). Along the west coast from 25° to 30°S, onshore flow increased significantly during wetter seasons (Figure 4.1b). Near 25° to 30°S and 20°W to 10°W, both zonal and meridional components were significantly different, revealing enhanced southwesterly flow corresponding to wetter seasons. Within this ocean area, relatively high SSTs also occurred (Figure 3.11) perhaps indicating an area of enhanced cyclogenesis during wetter seasons. Additional support for this suggestion is provided by the February 1988 case study analysis to be discussed in Chapter 5.

Early summer wind behavior

Figure 4.3 illustrates the WET-DRY wind component differences one season before the late summer rainfall composites for area 1. The map corresponding to area 2 was very similar and is not shown. The WET-DRY zonal wind differences revealed an increased prevalence of easterly winds across the southwest Indian Ocean during wetter seasons. The largest differences of 0.8 m/s were observed to the east and south of Madagascar (Figure 4.3a). In terms of meridional wind differences (Figure 4.3 b), winds were less southerly in the western part of the basin during wetter seasons. In contrast, east of 55°E and north of 10°S winds were more westerly during wetter seasons. This pattern suggests an increased prevalence of anticyclonic circulation in the vicinity of the southeast coast of southern Africa one season before wetter late summer seasons. The meridional wind differences were significant over source regions for the Mozambique and Agulhas currents. Easterly wind anomalies were also present within the Indian Ocean during the previous season of July to September.

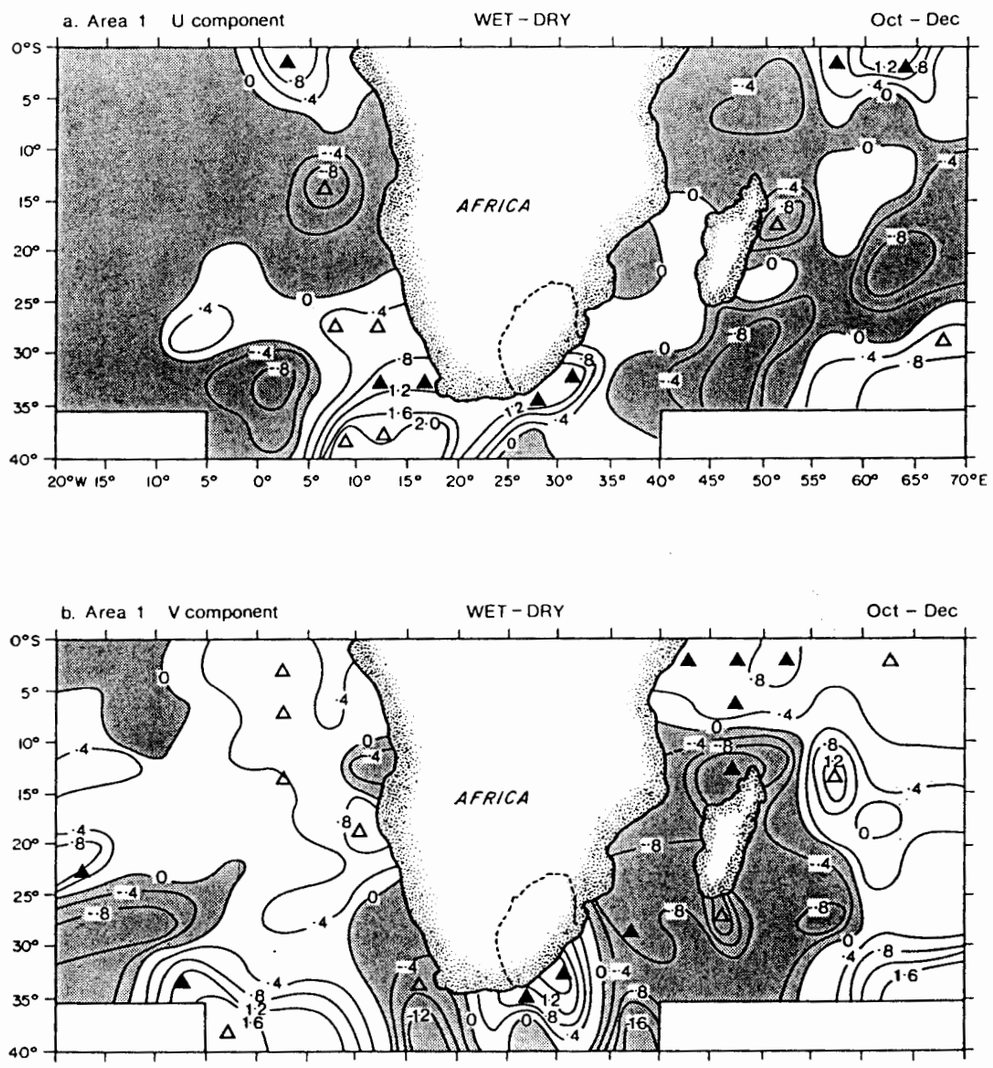

Figure 4.3 Composite early summer wind component differences (m/s) preceding WET and DRY late summer seasons (average WET minus average DRY). a) zonal (U) component differences b) meridional (V) component differences. Negative values are shaded and represent easterly and northerly differences. Open and filled triangles show in which grid-squares differences attained significance above 10% and 5%, respectively.

Adjacent to the subcontinent south of 30°S, surface winds were more westerly over a large area one season in advance of wet seasons (Figure 4.3a). Along the southeast coast southerly winds increased during wetter seasons, whereas southwest of the subcontinent between 10° and 20°E northwesterly winds increased (Figure 4.3 a,b). West of 10°E and throughout much of the southeast Atlantic Ocean, southerly and easterly winds were stronger in association with wetter seasons.

The early summer wind patterns have revealed intensified trade winds over both oceans in the vicinity of southern Africa during wetter seasons, from which a strengthening and poleward displacement of subtropical anticyclones is inferred. Within the southwest Indian Ocean, easterly and northeasterly winds increased over source regions of the Mozambique and Agulhas Current at least one season prior to wetter seasons. These atmospheric circulation changes within the southwest Indian Ocean would favor enhanced poleward flow within the Agulhas current system and its source regions.

Generation mechanisms for southern Agulhas "warm events"

The increased easterly wind forcing across the southwest Indian Ocean and over source regions for the Agulhas Current during and before wetter seasons would serve to increase its poleward flow at least in the surface layers. Modeling studies have demonstrated that a poleward shift in the westerlies and wind stress curl zero line south of the subcontinent would facilitate westward penetration of Agulhas current waters into the southeast Atlantic (de Ruijter, 1982; de Ruijter and Boudra, 1985). These studies have indicated that without the fast latitudinal variation in the wind stress curl south of Africa, the Agulhas Current could flow directly into the southeast Atlantic Ocean. A mere latitudinal shift of 1° in the wind stress curl zero line could alter inter-ocean exchange of Agulhas waters by about 6 x 10^6 m^3 s^{-1} (de Ruijter, 1982), a transport equivalent to previous estimates of the total inter-ocean exchange (Harris and van Foreest, 1978). These results clearly demonstrate the importance of changes in atmospheric circulations south of the subcontinent to local oceanic circulations (and SST characteristics). An increased prevalence of Agulhas Current waters within the southeast Atlantic Ocean could alter the heat content of the upper ocean considerably. Increased inter-ocean flux of Agulhas Current waters through the Retroflection region may help to explain the presence of relatively warm waters northwest of the Retroflection region and in the southern and central Benguela region during wetter seasons (Figure 3.11). Suggestions have previously been made that Agulhas Current water occasionally

influences the Benguela Current system as far north as 25°S (Darbyshire, 1966; Agenbag and Shannon, 1987).

The Agulhas Current "warm events" which preceded and co-occurred with wetter summers were a consequence of intensification of the prevailing easterlies across the southwest Indian Ocean and a poleward displacement of the westerlies. A positive ocean-atmosphere feedback system may have evolved whereby the presence of abnormally warm waters south of the subcontinent induced a poleward shift of SST fronts south and southeast of Africa. Such a shift would alter meridional contrasts of wind shear, temperature and humidity within the atmospheric marine boundary layer which could, perhaps, further facilitate poleward displacement of the zonal westerlies.

This proposed feedback mechanism may have played a role in the evolution of the 1985 southern Agulhas "warm event". In Figure 4.4, SST and wind anomalies are shown for the months of September, October and November 1985. Easterly wind forcing throughout the western Indian Ocean was abnormally strong and sustained over the three months (Figure 4.4b). The core of the wind anomaly (5 m/s), which was of similar magnitude to the average zonal wind (Figure 4.1a), moved from east of Madagascar in September towards the southwest and, by November, was situated directly south and east of South Africa. The atmospheric circulation anomaly was associated with intensification of the westerlies which were displaced poleward in sympathy with the poleward and westward displacement of the South Indian Anticyclone. The SST anomalies from 35° to 45°S intensified and moved south and west together with the surface wind anomalies. By early November, Agulhas Current waters had penetrated the South Atlantic Ocean to 10°E (Figure 4.4c). Subsequent to this westward penetration, western parts of the country experienced copious rains yielding the *highest early summer rainfall since 1949* (Figure 3.14). An inspection of published atmospheric information for the months preceding this event (*Climate Diagnostic Bulletin*, Climate Analysis Center) revealed the presence of anomalous trade winds across the southwest Indian ocean near 20°S and positive geopotential height anomalies in the western Indian Ocean as early as July 1985. Large-scale SST anomalies of + 1.0°C were in evidence within the southern Agulhas region as early as August 1985. The positioning of the SST anomaly to the west of the geopotential height anomaly suggests that the SST anomaly evolved primarily through anomalous southwestward advection within the western boundary current system. However, altered surface heat fluxes may have contributed to its intensity.

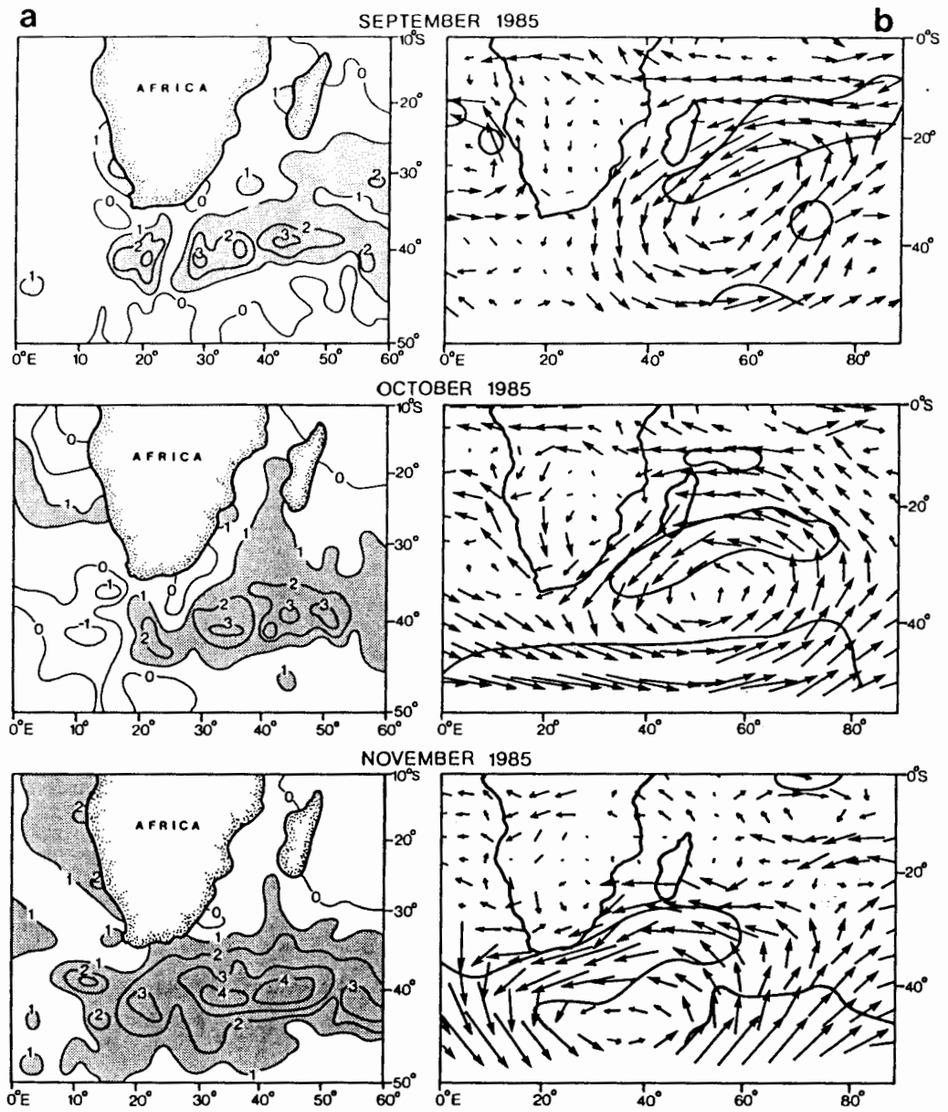

Figure 4.4 Time history of the evolution of a large-scale "warm event" within the southern Agulhas Current system during 1985; a) SST anomalies (°C) and b) wind anomalies (m/s) during September 1985, October 1985 and November 1985. SST anomalies exceeding + 1.0°C are shaded. Wind vector lengths of 5° of longitude represent wind speed anomalies of 3.125 m/s. Wind anomalies of 5 m/s are contoured. (National Environmental Satellite, Data and Information Service (NOAA) and *Climate Diagnostics Bulletin*, Climate Analysis Center). SST anomalies are based on a 1° x 1° grid and 20-year climatology.

Surface Heat Fluxes and Boundary Layer Adjustments Associated With Contrasting Rainfall Regimes

In this section, surface heat fluxes and boundary layer characteristics are investigated to obtain insight into ocean-atmosphere coupling mechanisms associated with the SST-rainfall relationships involving local ocean areas. The question of whether SSTs exert a direct influence on atmospheric processes influencing rainfall is addressed. An alternative scenario would be that the SST patterns were symptomatic of large-scale wind and pressure patterns conducive to rainfall. Certainly the wind analysis and inferred pressure distributions revealed conditions known to co-occur with wetter periods over the interior. These include poleward displacement of pressure systems over both oceans (Tyson, 1981; Taljaard, 1981; Harrison, 1986a; Taljaard, 1986b), enhanced easterly air flow along the east coast (Tyson, 1984; Taljaard, 1986a) and increased onshore flow along the south and west coasts (Tyson, 1981; Taljaard, 1981; 1985; 1986a). It has been suggested that the Indian Ocean air masses provide most of the moisture supplying the rain-producing systems (Taljaard, 1986a), whereas cooler southerly winds south of the subcontinent enhance low-level convergence, necessary to initiate convective processes (Taljaard, 1981).

The prevalence of higher SSTs adjacent to southern Africa during the wetter seasons suggests the possibility of positive ocean-atmosphere feedbacks as a result of boundary layer modification processes. Thus, surface latent and sensible heat fluxes and temperature/humidity conditions have been investigated in key ocean areas through the use of compositing techniques. The data were compiled by month to gain a better insight into ocean-atmosphere interactions and possible feedback mechanisms.

Five key grid-squares along the east and west coasts were chosen for the analysis. All squares were situated south of 20°S within major shipping lanes. Only two will be discussed to avoid redundancy. The east coast grid-square (20°-25°S, 35°-40°E) was situated within the Mozambique/Agulhas SST-rainfall teleconnection region (Figure 3.10 a, 3.11a) and was influenced by an easterly flow regime from more tropical regions during the WET seasons (Figure 4.1b, 4.2b, 4.3). The west coast grid-square (20°-25°S, 10°-15°E) was located within the Benguela SST-rainfall teleconnection region (Figure 3.10b, 3.11b), where minimal wind direction changes were identified between the composite WET and DRY seasons.

The investigation of ocean-atmosphere heat fluxes within the Agulhas Retroflection region differed from that of the east and west coast areas which were fortuitously situated within major shipping lanes. Available measurements in the region are considered insufficient for studying interannual variations in heat fluxes (Walker and Mey, 1988). Thus, heat flux processes were investigated under conditions of a positive SST anomaly (+1.0°C) within the region and then compared with climatological heat flux values. Mean atmospheric conditions were used in the calculations but the VOS wind data results were considered in the interpretation. This simple analysis provided information concerning the relative importance of sensible and latent heat fluxes in the presence of a southern Agulhas warm event. This type of approach was considered more advantageous than totally excluding the area from the discussion due to poor data coverage.

Agulhas/Mozambique region

The key meteorological parameters and computed surface heat fluxes were stratified by month according to the previously defined WET and DRY late summer seasons corresponding to area 1. Monthly-averaged data for the WET and DRY groups are illustrated in Figure 4.5. Information is also included for the months July through December of the previous year. SST differences were observed as early as September, however, the largest differences were evident from December through March (Figure 4.5a). Dry bulb and dew point temperature differences were observed from November through February. For dry bulb temperature, significant WET-DRY differences occurred from November through January. In the case of dew point temperature, significant differences occurred in November and December. Vapor pressures were 2 mb higher during WET seasons and the WET-DRY differences were most significant during the early summer months of November and December (Figure 4.5a).

Latent heat flux was significantly lower during the months of November, December, January and March corresponding to wetter seasons (Figure 4.5b). Sensible heat flux contributed about 10% to the total heat flux and conformed with the latent heat flux pattern as higher oceanic heat losses occurred during the drier composite months (Figure 4.5b). These results were not unexpected as a large reduction in southerly flow was experienced during wetter seasons (Figure 4.5b). The advection of relatively warm moist air over the area during wetter seasons reduced sea-air temperature and humidity gradients despite the elevated SSTs. Although flux magnitudes were observed to be lower during wetter seasons, both heat and water vapor transfer processes were operative. Latent heat flux in excess of 100 W/m^2 was sustained

from December through March, corresponding to oceanic water losses of 0.4 - 0.5 cm/day. Thus, oceanic heat and water vapor losses associated with the elevated coastal temperatures contributed to boundary layer modifications along the east coast and a significantly warmer, moister air mass was present during wetter seasons.

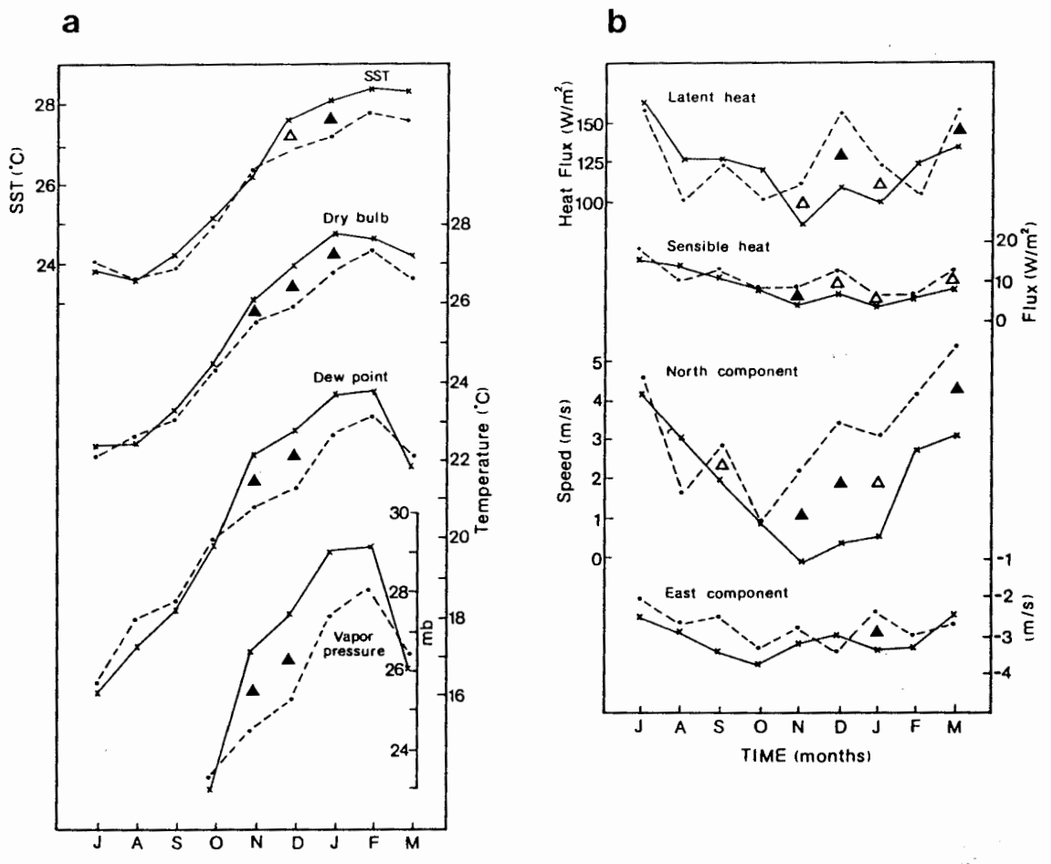

Figure 4.5 Atmospheric parameters, surface heat fluxes and wind components from July through March along the east coast (20° to 25°S, 35° to 40°E), corresponding to WET and DRY late summer seasons of area 1. a) SST (°C), dry bulb temperature (°C), dew point temperature (°C) and vapor pressure (mb); b) latent heat flux (W/m^2), meridional wind component (m/s), zonal wind component (m/s). Positive components are southerly and westerly. Positive heat fluxes represent losses from ocean to atmosphere. Open and filled triangles indicate differences significant above the 10% and 5% levels, respectively.

Inspection of Figure 4.5 revealed that the SST differences lagged those of the atmospheric parameters by one month. This information indicates that reduced ocean-atmosphere heat fluxes may have contributed to the higher SSTs during WET seasons at this site. In addition, a portion of the SST changes may have owed their origin to altered ocean currents. The observation that both oceanic and atmospheric differences persisted for several months suggested that ocean-atmosphere coupling via positive feedback mechanisms had occurred.

Benguela Current region

A similar analysis was performed for the Benguela Current system from 20° to 25°S. The only difference was that monthly data were stratified according to the WET and DRY seasons corresponding to rainfall area 2. The relevant atmospheric data and heat flux estimations are given in Figure 4.6. This analysis revealed WET-DRY differences in SSTs from August through March, although the differences were very small before January (Figure 4.6a). Dry bulb temperature differences corresponded with those of SST and were significant in January. The dew point temperature differences were less than the dry bulb temperature differences, an observation which contrasts with the east coast results. Vapor pressure differences were small and non-significant except in October preceding the wetter seasons (Figure 4.6a). A comparison of east coast and west coast vapor pressures during January revealed a 10 mb difference during wetter seasons (29 and 19 mb, respectively).

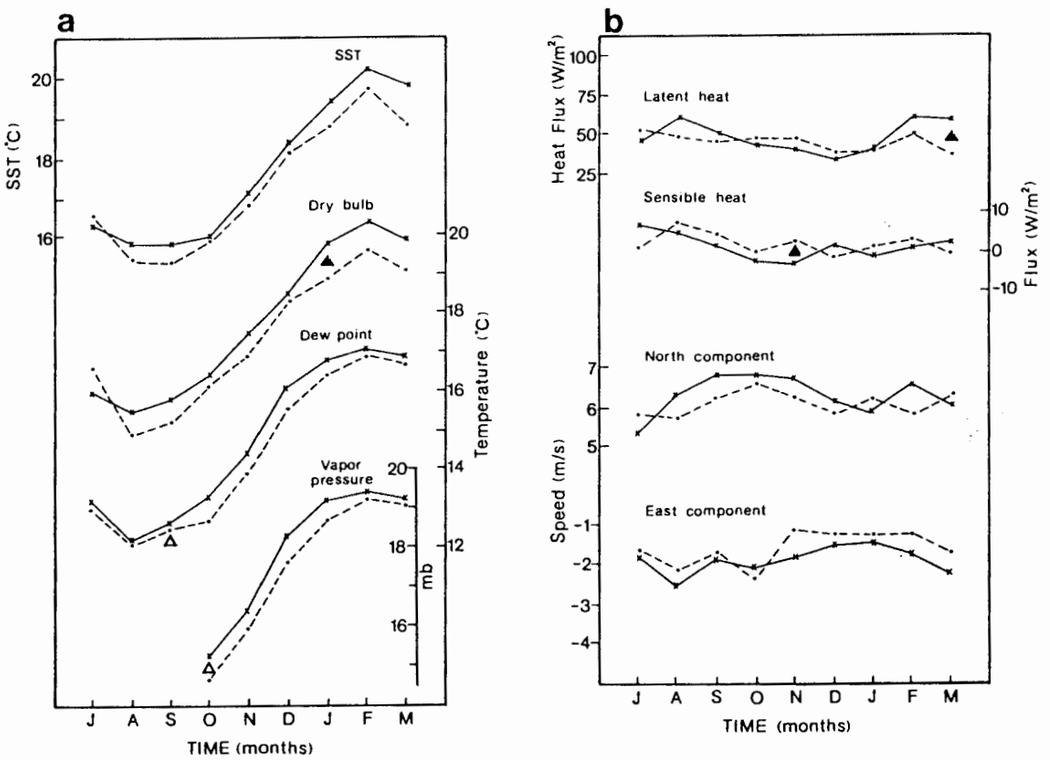

Figure 4.6 Atmospheric parameters, surface heat fluxes and wind components from July through March along the west coast (20°-25°S, 10°-15°E), corresponding to WET and DRY late summer seasons of area 2 a) SST (°C), dry bulb temperature (°C), dew point temperature (°C) and vapor pressure (mb) b) latent heat flux (W/m^2), sensible heat flux (W/m^2), meridional wind component (m/s), zonal wind component (m/s). Positive components are southerly and westerly. Positive heat fluxes represent losses from ocean to atmosphere. Open and filled triangles indicate differences significant above the 10% and 5% levels respectively.

Latent heat fluxes were higher during August, September, February and March in association with wetter seasons, however, the identified differences only attained significance in March (Figure 4.6b). Sensible heat flux differences were small and insignificant. The wind component differences showed a general trend of increased southerly and easterly flow during wetter seasons, however, in no month did the differences attain significance (Figure 4.6b).

In comparison with the east coast analysis, relatively minor changes were identified in the near-surface boundary layer along the west coast during wetter seasons. In this region, the prevalence of enhanced offshore flow during wetter seasons argues against a direct link between the observed boundary layer changes and rainfall variations over the interior. Under suitable conditions of onshore flow, however, SST anomalies along the west coast might influence rainfall variations at least locally.

The Agulhas Retroflection region

This region supports the highest oceanic latent and sensible heat losses within the study area, 85% of which result from evaporation (Walker and Mey, 1988). For this analysis, summer season averages (December-February) of meteorological parameters were available covering the area 35° to 41°S and 10° to 30°E. The data were compiled into 2° x 2° grid-squares. Latent and sensible heat fluxes were computed for each grid-square with the climatological SST and atmospheric forcing parameters (1960 through 1984) and then with the imposition of a +1°C SST anomaly. The resulting differences are expressed as percentages in Figure 4.7.

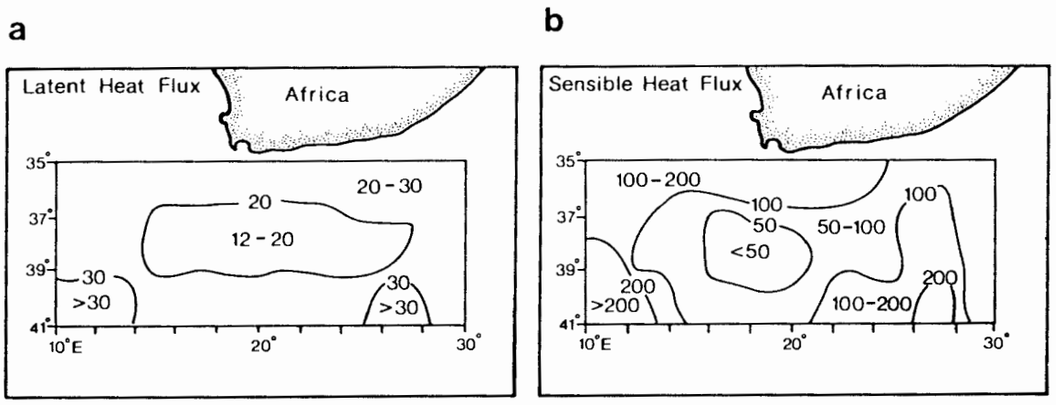

Figure 4.7 Percentage changes in a) latent heat flux and b) sensible heat flux within the Agulhas Retroflection region associated with the imposition of a +1.0°C SST anomaly on climatological values.

Latent heat flux increased over the entire region by an average value of 23% (Figure 4.7a). The largest percentage changes were observed in areas exhibiting relatively low fluxes, e.g. outside the high heat flux core region (Figure 1.9). Associated water losses over the entire region were 15 cm/month (0.5 cm/day), yielding a net increase of 3 cm/month. Sensible heat flux, which influences stability within the lower troposphere, was increased by an average value of 100%. Thus, potentially large changes in low-level stability can occur over large ocean areas in association with a relatively small positive SST anomaly. Although percentage changes in sensible heat flux were 2 to 7 times more than latent heat flux changes, the actual changes in terms of flux magnitudes were more similar since latent heat flux contributes about 85% to the total flux. These values are most likely underestimates of heat flux changes as they were determined using climatological wind data. The previous wind analyses revealed increased southerly flow over this region during wetter seasons, a situation which would further increase oceanic heat losses as well as its onshore transport.

This analysis has revealed that relatively large changes in surface fluxes and stability of the marine boundary layer are possible in the presence of a modest +1°C SST anomaly. The implications of these results to rainfall variations will receive further attention in Chapter 6.

CHAPTER 5

RAIN-PRODUCING SYSTEMS DURING LOCAL "WARM EVENTS"

The systems responsible for rainfall over the subcontinent are not always reflected in monthly or seasonal means of atmospheric variables (Jackson, 1952; Taljaard, 1981; Harrison, 1986a; Terblanche and Taljaard, 1987). For this reason, a case-study approach has been adopted in an attempt to understand the processes by which SST anomalies may influence atmospheric marine boundary layer characteristics and circulations leading to increased rainfall. To attain this objective, the major rain-producing synoptic systems during local oceanic warm events were identified and studied with regard to local air-sea interaction processes. Two late summer and two early summer case-study periods were chosen. They were restricted to the 1980's as relatively high quality oceanic and atmospheric data obtained by satellites were available. As in Chapter 3, the late summer period is discussed first.

January 1981 Episode

During the late summer season of 1981, above-average rainfall was experienced in both areas 1 and 2 (Figure 3.8, Table 3.2). Most of the abnormal rainfall occurred during January and February. The month of January was chosen for investigation as tropical-temperate trough formation and interior rainfall reaches a maximum at this time.

Oceanic and atmospheric anomalies

Monthly SST anomalies for December 1980, compiled from VOS data, revealed that SSTs were well above average over large ocean areas surrounding southern Africa prior to the copious rains (Figure 5.1a). SST anomalies exceeded 0.8°C along the east, south and west coasts south of 20°S. SST gradients southwest of the country were enhanced near 20°E. In addition, waters were observed to be particularly warm west of 10°W in the southeast Atlantic Ocean. As satellite anomaly maps were not yet being produced in 1981, surface temperatures of the 1980/81 wet summer are compared with those of the 1981/82 dry summer for the region south of the country (Figure 5.1b). Major differences were observed in the latitudinal position of the 15°C isotherm, which

reveals the approximate position of the Subtropical Convergence. From December 1980 through March 1981, the 15°C isotherm was positioned approximately 5° further south, suggesting WET-DRY differences of several degrees Celsius within the Agulhas Retroflection Region (ARR). The satellite data indicated that surface waters were abnormally warm within the ARR to at least 45°S and SST gradients were more intense during 1981 than during the dry season of 1982.

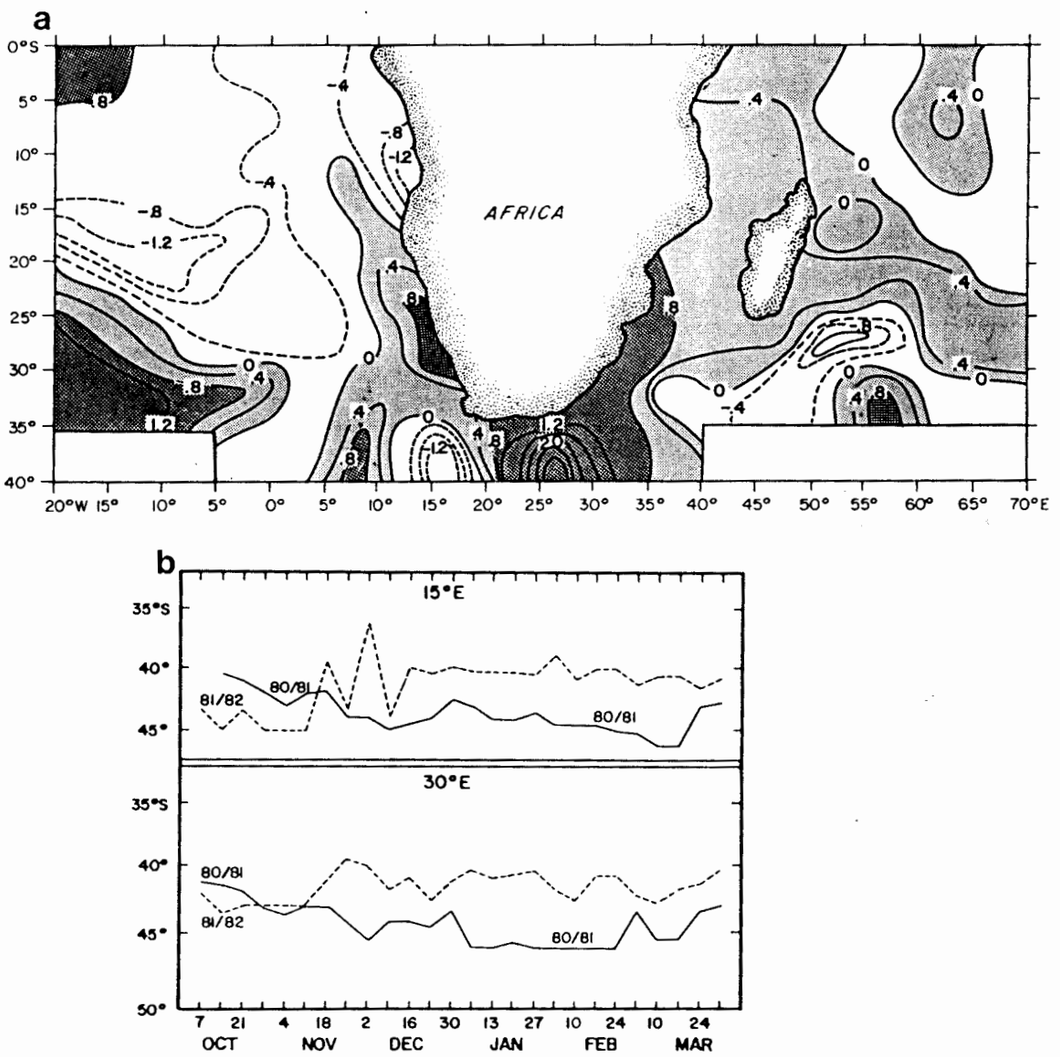

Figure 5.1 a) SST anomalies for December 1980 as determined from VOS data. Light shading represents positive anomalies and darker shading indicates anomalies in excess of 0.8°C. b) Meridional location of the 15°C isotherm at 15°E and 30°E from October through March of the 1980/81 WET summer and 1981/82 DRY summer (National Environmental Satellite, Data, and Information Service).

VOS wind data revealed that surface easterly winds were abnormally strong across the southwest Indian Ocean during January 1981, with maximum anomalies occurring within the Mozambique Channel (anomaly = +1 m/s), on the north side of Madagascar (2.7 m/s) and east of Madagascar (2.7 m/s). Vapor pressures were 10-30% higher than normal along the east coast and at interior stations (*Monthly Climatic Data for the World*). This condition may have resulted from increased moisture flux convergence over the eastern interior as a consequence of the onshore advection of abnormally warm and moist air. Easterly wind anomalies over both oceans were also present south of 30°S. In contrast, westerly anomalies were present directly south of the country.

Sea level pressure anomaly maps (S.A. Weather Bureau) revealed that surface pressures were above average in the southwest Indian Ocean between southern Madagascar and the African coast and also in the southeast Atlantic Ocean east of Gough Island (Figure 5.2a). Surface pressures were lower than normal southeast of land and, at upper levels, pressures were lower south of the subcontinent (Figure 5.2 a-c). Thus, subtropical anticyclones were relatively intense and displaced poleward of their average January position. They were separated by an area of increased cyclonic activity south of the subcontinent.

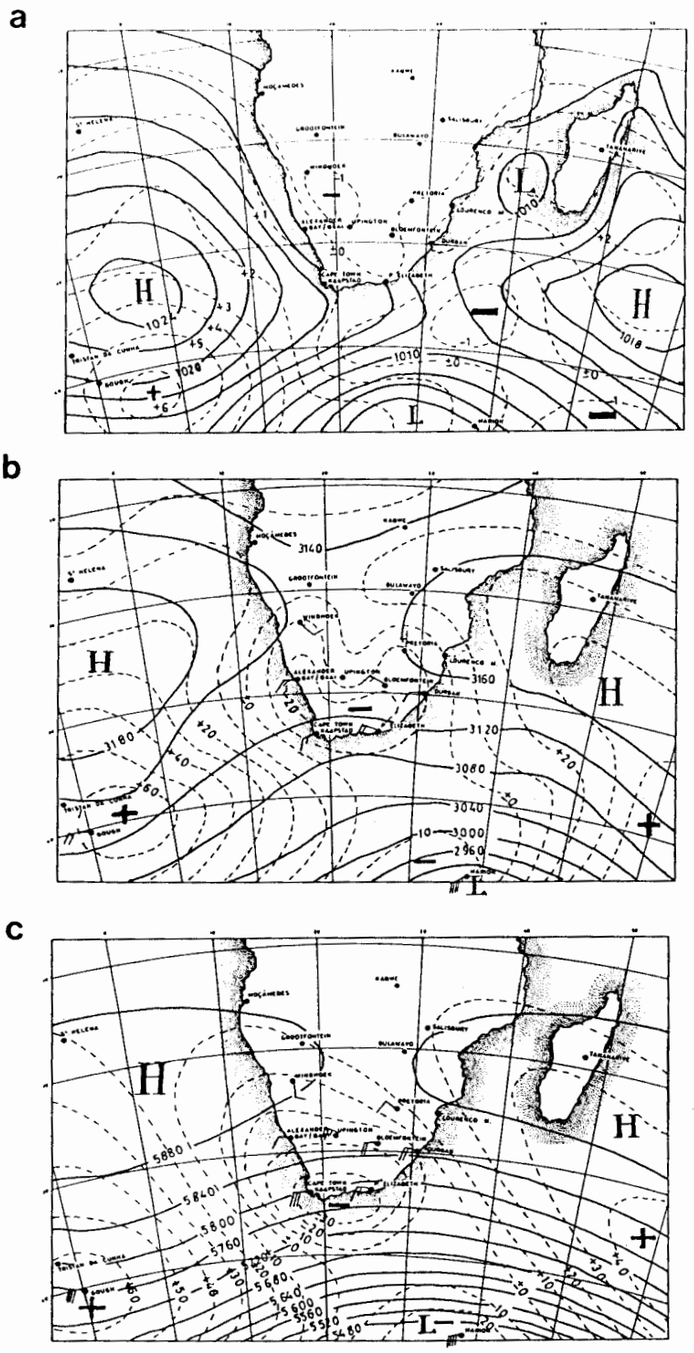

Figure 5.2 Pressure distributions (solid lines) and anomalies (dashed lines) during January 1981. a) Sea level pressure over the ocean and 850 mb contours over land b) 700 mb contours c) 500 mb contours (S.A. Weather Bureau Monthly Newsletter).

Rain-producing systems

Daily rainfall estimates were compiled for both areas of the summer rainfall region (Figure 5.3). The major rainfall episode occurred in the latter part of the month from January 23 to 26, when areas 1 and 2 experienced 33% and 95% of their monthly precipitation, respectively. Thermal infrared satellite imagery revealed that a well-developed tropical-temperate cloud band was present throughout the rainfall episode. Prior to its development, copious rains were experienced on January 21 over eastern parts of the country as a result of a truncated-trough system. This rain-producing system was marked by a cloud band connecting an interior low to a coastal depression. Truncated-trough systems often develop ahead of tropical-temperate troughs although the latter supply more rainfall to the interior (Harrison, 1984; 1986a). Developmental characteristics of the main rain-producing system, from January 23 to 26 have been studied through the use of satellite imagery, synoptic charts and associated SST distributions (Figures 5.4 to 5.6).

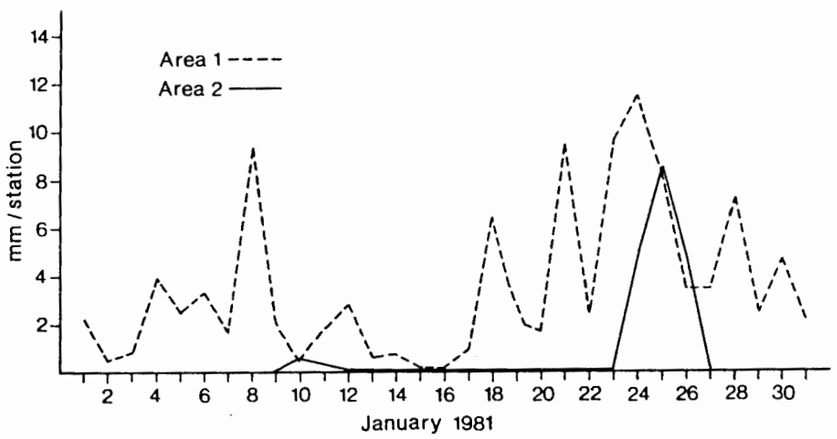

Figure 5.3 Time series of daily rainfall within areas 1 and 2 during the month of January 1981, expressed as mm/reporting station. (S.A. Weather Bureau Daily Weather Bulletins).

On January 22, a surface cold front and westerly wave were situated southwest of the subcontinent and the associated temperate low was located near 48°S, 21°E (not shown). Low pressure was in evidence over the subcontinent and convective showers occurred in the eastern part of area 1. Between mid-day of January 22 and 23, intensification of the westerly wave occurred as three new low pressure cells developed south of the country. Cyclogenesis occurred in close proximity to the Agulhas/Subtropical Convergence SST front near 40°S, 20°E producing what will be termed an "Agulhas low". A cut-off low, most clearly evident above 700 mb, had developed behind the Agulhas low (Taljaard, 1985) (Figure 5.4c) and a coastal depression had formed ahead of the cold front. The original temperate low pressure cell

continued on its eastward course, whereas the Agulhas low moved northeastwards towards warmer water. The Agulhas low was situated over 18°-20°C waters on the 23rd and the coastal depression ahead of it overlay water of 20°-22°C (Figure 5.4a).

A tropical-temperate cloud band had formed by January 23rd, linking the surface cold front system and convective cells over the subcontinent (Figure 5.4b). Convection was intense over the southeast coastal and interior regions as a result of strong surface convergence associated with the cold front, the coastal depression and a poleward flow of moist tropical air over the eastern interior. Convective rains of area 1 increased by an order of magnitude after cloud band formation. By January 24, convection (as determined by cloud cover and temperature) had increased substantially over the southern Agulhas ocean area from 20° to 40°E (Figure 5.5b) and the eastern interior. Ridging of the South Atlantic Anticyclone south of Africa maintained the onshore flow along the southern coastal areas in the lee of the cold front. The coastal depression and Agulhas low provided the main extratropical links within the tropical-temperate trough as connections with the temperate low appeared to have weakened considerably by January 24. Extensive cloud masses were in evidence over ocean areas where SSTs ranged from 18° to 20°C and over the interior in the vicinity of strongly convergent surface airflow. In contrast to many tropical-temperate trough systems which show strong connections with temperate lows south of 40° (Harrison, 1984), this system demonstrated strongest links with two locally generated Agulhas lows.

On January 25 convection persisted over the southern Agulhas system. Moist tropical air continued to be advected polewards along the eastern side of the interior low, which had moved westward (Figure 5.6). As a consequence, rainfall over area 2 reached a maximum on January 25. The cut-off low to the west had also intensified and was readily apparent on the satellite image (Figure 5.6b). It was responsible for heavy rainfall and flooding over the extreme western parts of the country (west of area 2) on January 24 and 25 (Taljaard, 1985), and is better known in South Africa as the disastrous "Laingsburg flood" when more than 100 people drowned (Estie, 1981). On January 26, poleward flow of moist tropical air continued between the surface anticyclone and tropical lows over the subcontinent. Cloudiness persisted over the ARR until January 27 when the cloud band finally dissipated. The effects of the tropical-temperate trough system lasted 4 days and resulted in the only significant rainfall over area 2 during the month.

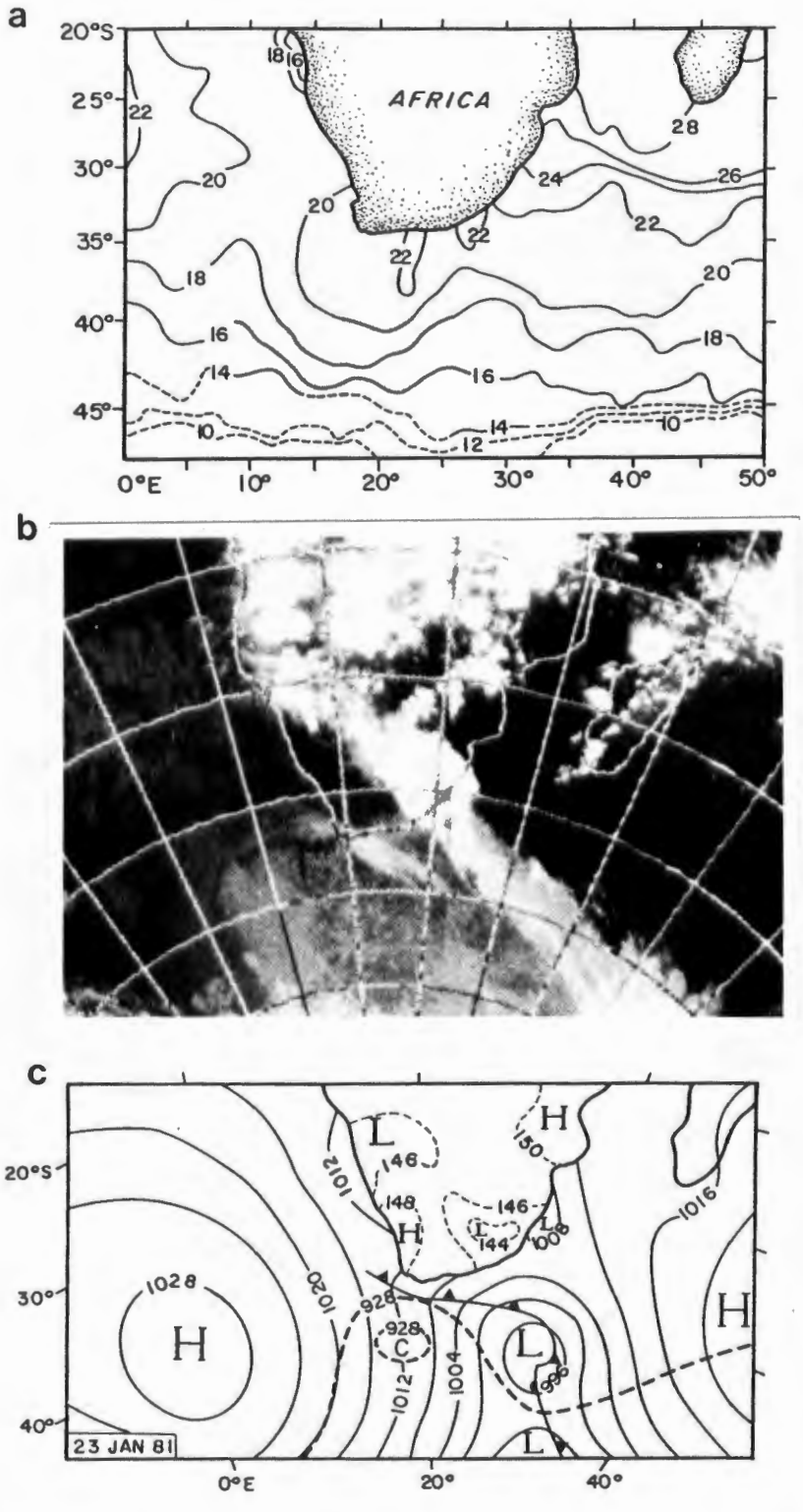

Figure 5.4 a) Satellite-derived SST distributions for the week ending 20 January 1981 b) Thermal infrared hemispheric satellite mosaic for 23 January 1981 (17h00 UTC) illustrating a cloud band linking the tropical low, coastal depression, and temperate low c) Synoptic information for 23 January (12h00 UTC) (From Taljaard, 1985). Solid lines represent isobars of sea level pressure (mb) and dashed lines over the continent represent contours of the 850 hPa surface. Over the oceans, bold dashed lines depict the position of the westerly trough and cut-off low as revealed by the 1000-300 mb thickness of 928 geopotential decameters.

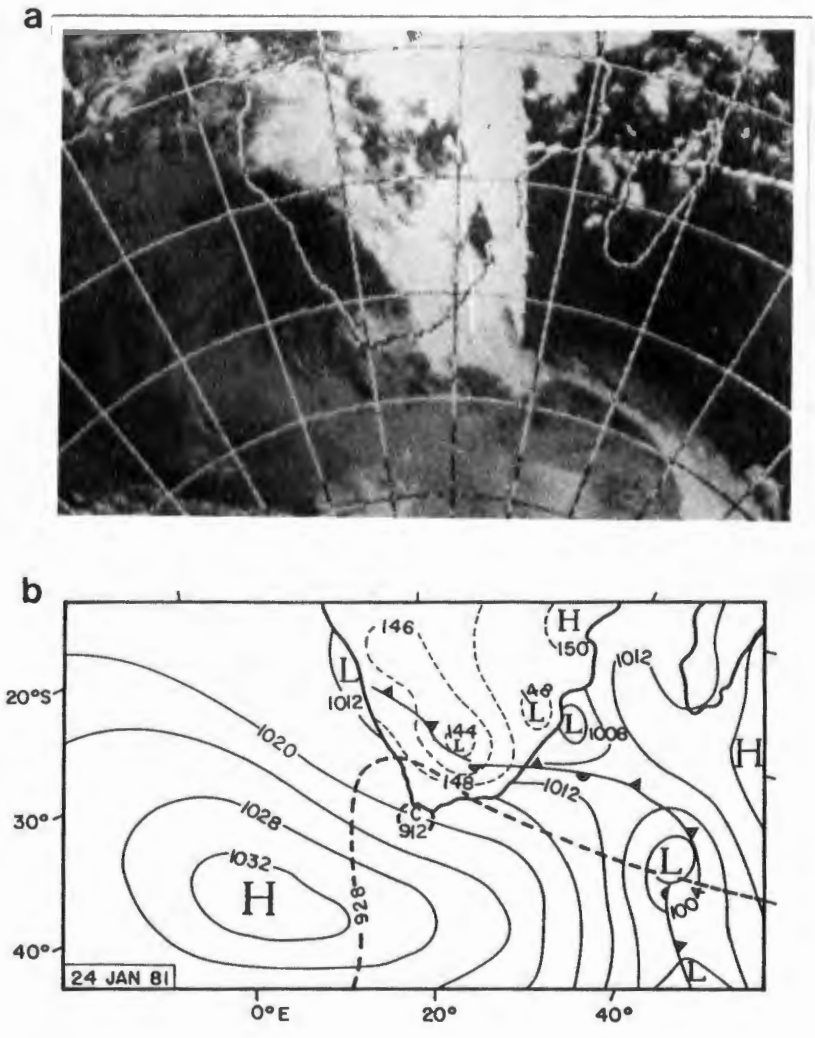

Figure 5.5 a) As in Figure 5.4b for 24 January 1981. b) As in Figure 5.4c for 24 January 1981.

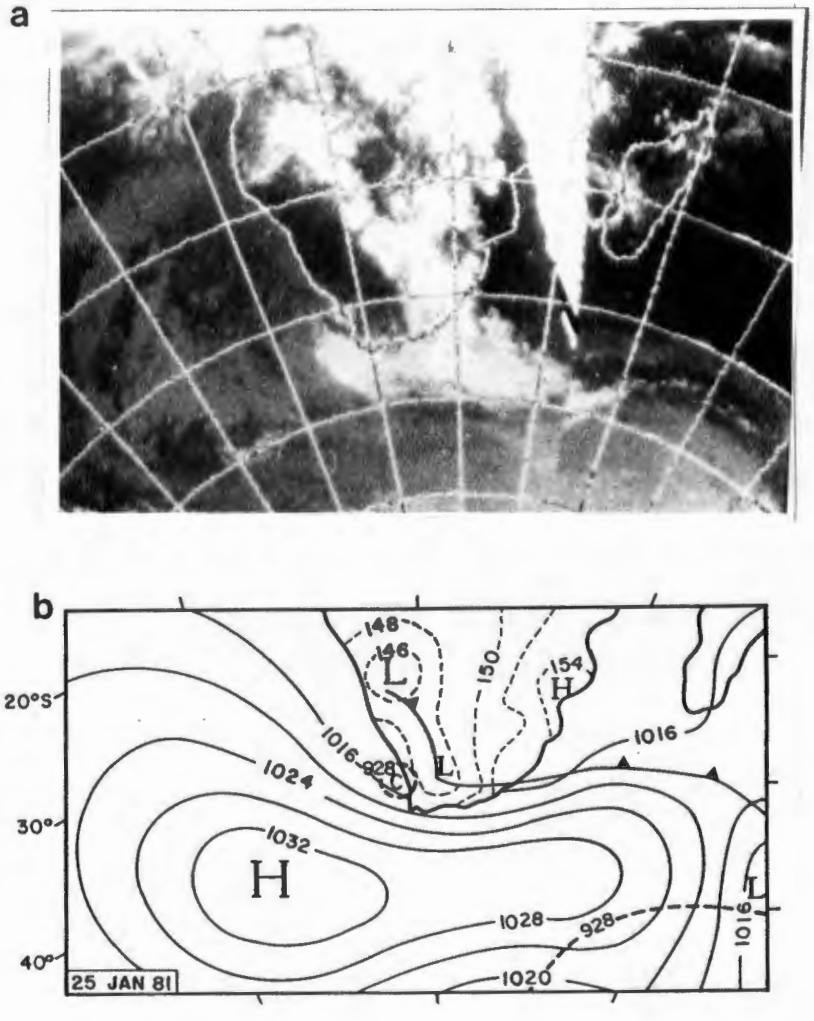

Figure 5.6 a) As in Figure 5.4b for 25 January 1981. b) As in Figure 5.4c for 25 January 1981.

Taljaard (1985) reviewed the development of this particular cut-off low and suggested that the temperate system was unusually strong for mid-summer. The fact that intensification of the westerly wave and the development of three low pressure

systems (one being the cut-off low) occurred in close association with an extensive warm water anomaly of the southern Agulhas system suggests that air-sea interactions may have played a prominent role in the sequence of events. Southwest of the country, air masses undergo rapid modification upon encountering the warm water zone of the ARR (Jury and Walker, 1988). The presence of abnormally warm waters and enhanced SST gradients southwest of Africa could have provided a "trigger" mechanism for the rapid intensification of the trough. Anomalous equatorward advection of cold air behind the cold front would have deepened the trough while poleward advection of warm air ahead of the cold front would simultaneously have built the preceding ridge. The presence of abnormally warm waters west of 5°W (Figure 5.1a) would have contributed to warm air advection within the South Atlantic Anticyclone. The net result would have been an intensification of the ridge/trough system, contributing to the observed wave intensification and cyclogenesis. In addition, the relatively warm, moist and unstable air mass over the southern Agulhas system could have enhanced convective processes within the trough system as a consequence of latent heat release at upper levels.

Tropical-temperate troughs have been observed to form only during times of active tropical convection over the subcontinent leading Harrison (1984) to suggest that the troughs are tropically forced by latent heat release over the subcontinent. In this case, satellite imagery revealed the presence of extensive cloud cover north of 20°S in advance of tropical-temperate trough formation. However, maximum rainfall occurred only after coupling of the tropical and temperate components, indicating that the westerly wave played a crucial role in the system's development over South Africa. Synoptic information indicated that the tropical lows over land were strengthened after linkage with the temperate system.

The Flood-Producing Systems of February/March 1988

During February and March 1988 exceptionally heavy rainfall was experienced over the interior of southern Africa which resulted in widespread flooding (van Heerden, 1988; Estie, 1988), described by Quinn (1988) as "the worst in living memory". It is of interest that the episodic rainfall was not adequately predicted by the ECMWF General Circulation Model (van Heerden, 1988). The prevalence of SST anomalies in previously identified SST-rainfall "teleconnection" areas suggests that oceanic influences may have contributed to the anomalous rainfall events. In this section the major rain-

producing systems are identified and their developments studied in relation to SST and wind anomalies surrounding southern Africa.

Rainfall behavior

The major rainfall episodes between mid-February and mid-March were identified from daily rainfall measurements which were subjectively grouped into four areas covering the summer rainfall region (Figure 5.7). The northwest-southeast orientation of the areas was chosen to conform to the preferred positioning of tropical-temperate cloud bands across the interior. Area-averaged rainfall estimates revealed that most of the rain fell within areas 2 and 3, where more than 160 mm/station were recorded on average over the 30 days (Figure 5.7b). The time series of daily rainfall data are depicted for the two areas in Figure 5.8. Two distinct high-rainfall episodes were clearly revealed by the analysis: February 20-21 and March 10-11 when similar precipitation amounts were recorded.

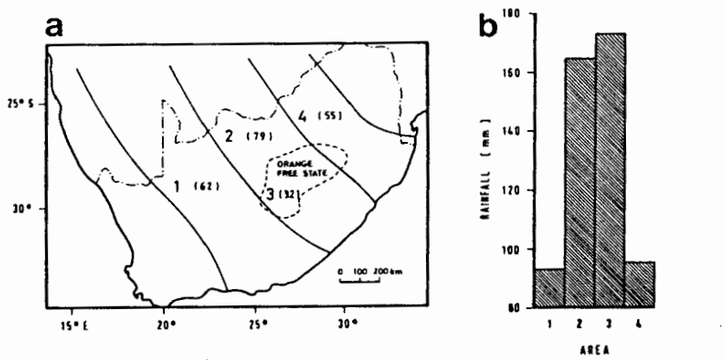

Figure 5.7 a) South Africa with subjectively-defined areas 1 to 4 for which rainfall statistics were calculated. Figures in parentheses indicate the number of rainfall stations within each area. b) Area-averaged rainfall for the four areas during the period 14 February to 14 March 1988. (From Walker and Lindesay, 1989).

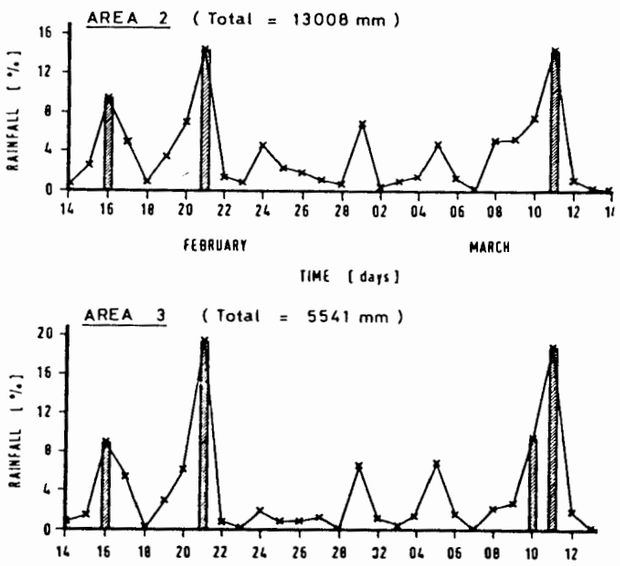

Figure 5.8 Time series of daily rainfall totals for areas 2 and 3 (Locations, Figure 5.7), expressed as a percentage of the total rainfall for each area from 14 February to 14 March 1988. Vertical bars indicate daily rainfall in excess of 8% of the period total for the area (From Walker and Lindesay, 1989).

Oceanic and atmospheric anomalies

Satellite-derived SST anomalies for February and March 1988 (Figure 5.9) clearly indicated above-normal SSTs over large expanses of ocean surrounding southern Africa. During February, SST anomalies exceeded + 1°C across most of the subtropical South Atlantic, maximum departures of + 2-3°C (Figure 5.9, 5.11) having occurred near 25°-35°S, 10°-20°W. SST departures in this region were previously found to be positively correlated with rainfall departures of both areas 1 and 2 (Figure 3.10). SSTs were also above-normal along the west African coast north of 20°S.

Throughout the southwest Indian Ocean, February SSTs were unusually high and SST anomalies exceeded + 1°C in several areas within the tropics and subtropics (Figure 5.9a). SST anomalies moved towards the African coast between February and March, so that during March nearshore anomalies exceeded + 1°C (Figure 5.9b) within a portion of the Agulhas Current system along the east coast. Similarly SST anomalies exceeding +1°C were present along the west coast from 10° to 30°S (Figure 5.9b). Satellite imagery of March 3 revealed that warm coastal waters were prevalent in the central Benguela Current system where cold upwelled waters are usually found at this time of year.

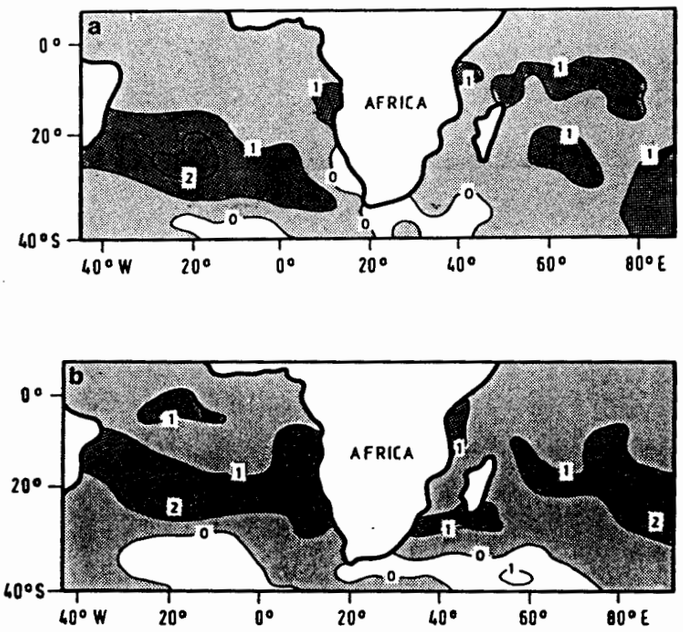

Figure 5.9 Satellite-derived SST anomalies for a) February and b) March 1988. Shading indicates regions of above-normal sea surface temperature; darker shading regions where anomalies exceeded 1°C. Anomalies are based on 30-year climatology and a 2° x 2° grid (Climate Analysis Center) (From Walker and Lindesay, 1989).

Available coastal temperature measurements supported the satellite-derived SST data analyses. Along the Natal coast, at Durban, monthly-averaged nearshore temperatures during February exceeded available 6-year means by more than 1°C and these differences increased somewhat during March. In both months, maximum surface temperatures exceeded the previously recorded extreme monthly maxima. Surface temperatures within the Agulhas Current were 28°-29°C. Along the west coast at Luderitz, both February and March SSTs exceeded long-term means (11-year climatology) by 1°-2°C. Further south at Lamberts Bay a warm water intrusion of 19°C occurred along the coast by 4 March, yielding a monthly-mean anomaly of + 2.6°C. Southward advection of relatively warm Orange River water may have contributed to this extreme positive anomaly at the coast (Shillington et al., 1989).

Easterly wind anomalies of 2-3 m/s occurred in February along the east coast north of 20°S and south of 30°S. Over the interior, northeasterly anomalies were experienced from 20° to 25°S. Easterly wind anomalies were also present in March. At east coast stations near 20°S and 30°S, vapor pressures were 2-3 mb above normal during February and March. Simultaneously, vapor pressure anomalies were experienced over interior regions of Zimbabwe and South Africa. These relatively high humidity levels may be attributed to the combined influence of abnormally strong

easterly winds crossing the east coast (*Climate Diagnostic Bulletins*) and the relatively high SSTs offshore.

Pressure anomaly maps showed that the subtropical anticyclones were displaced poleward and the influence of the Indian Ocean Anticyclone was relatively more intense during both months. Geopotential heights were lower than normal throughout the troposphere over the interior (*S.A. Weather Bureau Newletters*).

The rainfall episode of 19-21 February 1988

The main rain-producing synoptic system during February was a distinctive tropical-temperate trough marked by a cloud band lying from northwest to southeast across southern Africa. The system was most active for three days, from the 19th to the 22nd, (Figure 5.10), during which time monthly rainfall reached a maximum (Figure 5.8). Circulation over tropical southern Africa was dominated by a deep low which formed over Botswana on the 17th and extended through most of the troposphere on the 19th. Heavy rains were recorded over Zimbabwe in association with this tropical low and a southward excursion of the Intertropical Convergence Zone (Zimbabwe Dept. of Meteorological Services). The low pressure cell providing the temperate link for the tropical-temperate system developed in the subtropical Atlantic Ocean at the southern margin of the extensive SST anomaly near 35°S, 20°W (Figure 5.11a). The surface low remained in close proximity to the anomalous SSTs for 4 days, from February 13-16, then moved rapidly southeastward. Abnormally strong meridional SST gradients in the region (Figure 5.11b) may have contributed to development within the baroclinic system. On February 19, linkage of circulation between the temperate and tropical low pressure systems resulted in the formation of a tropical-temperate trough and impressive cloud band (Figure 5.10a).

Figure 5.10 Upper: Thermal infrared METEOSAT images for a) 19 February, b) 20 February and c) 21 February, illustrating the position of the tropical-temperate trough responsible for the copious rainfall which led to the February floods in central South Africa. Middle: Simplified surface synoptic charts for d) 19 February e) 20 February and f) 21 February 1988. Solid lines represent contours of the 850 hPa surface over the subcontinent and dashed lines isobars of sea level pressure. Lower: Upper-level synoptic charts for g) 19 February, h) 20 February and i) 21 February 1988. Solid lines represent contours of the 700 hPa surface and pecked lines contours of the 300 hPa surface (gpm). Vector winds are at 700 hPa (open circles) and 300 hPa (filled circles). All charts are at 12h00 UTC. (From Walker and Lindesay, 1989).

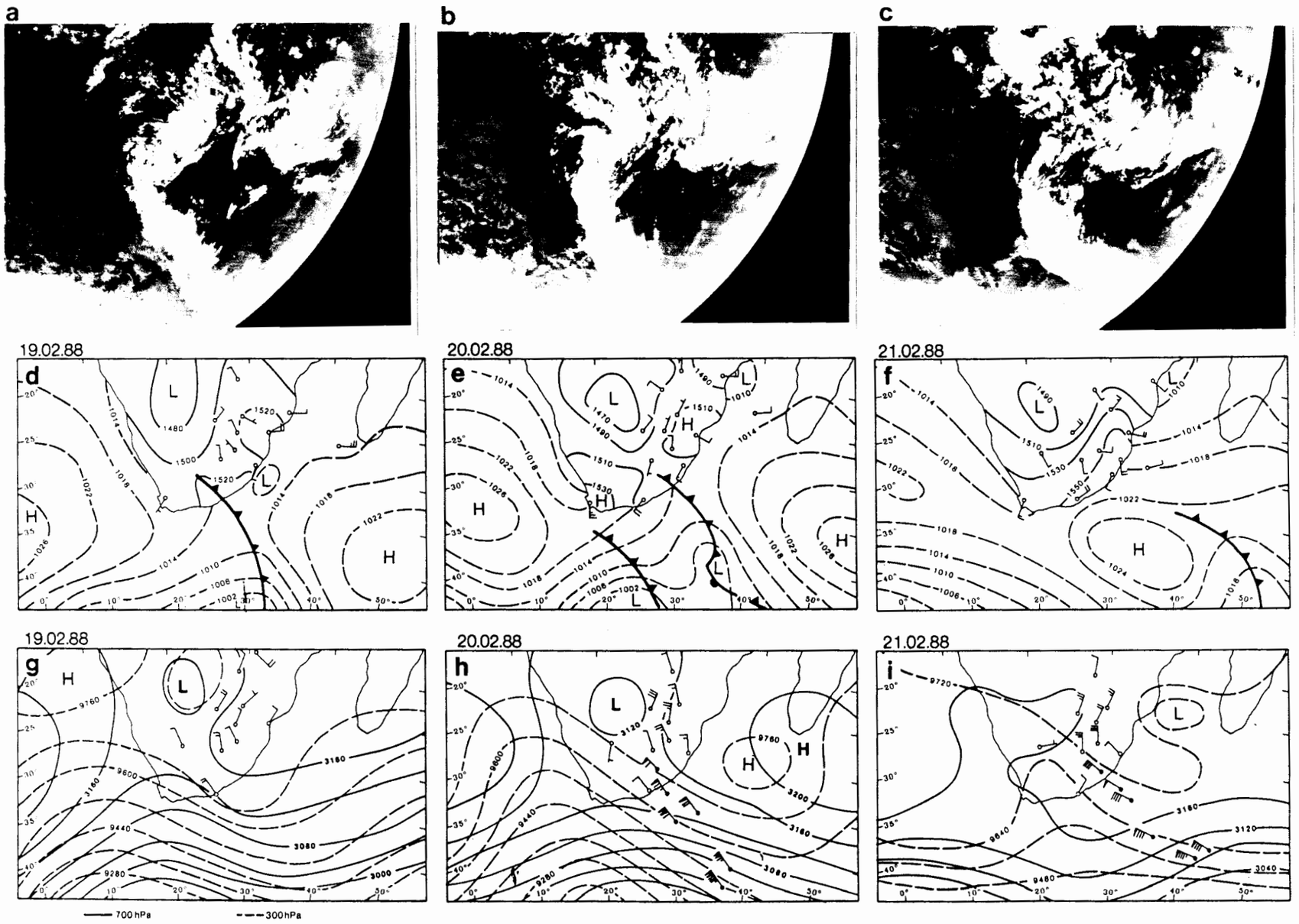
a
b
c
19.02.88
d
20.02.88
e
21.02.88
f
19.02.88
g
20.02.88
h
21.02.88
i
700 hPa
300 hPa

By February 20, cyclogenesis had again occurred along the leading edge of the trough in close proximity to a distinct SST front at the southern edge of the Agulhas Retroflection (Figure 5.11b). Wave intensification occurred south of the subcontinent between the 19th and 20th as revealed by a steepening of the trough and lowering of geopotential heights from the surface to 300 mb cloud masses (Figure 5.10e,h). Over the interior, convective activity was fueled by low-level convergence of tropical northerly flow with strong onshore flow in association with the cold front. Along the leading edge of the westerly wave at 300 mb, strong northwesterly winds prevailed. They were enhanced by poleward flow of tropical air along the eastern side of the interior low (Figure 5.10e,h). This strong poleward flow within the trough system at upper levels provided a conduit for the transport of heat, moisture and momentum out of the tropics into temperate latitudes.

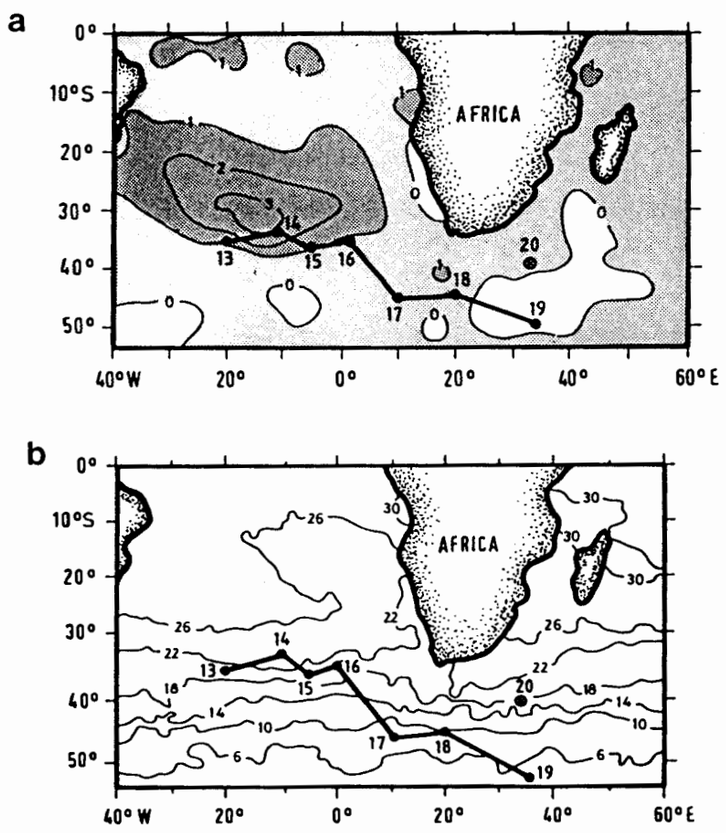

Figure 5.11 a) Satellite-derived SST anomalies for 1-15 February 1988 and daily positions of the extratropical cyclone which formed the temperate link within the tropical-temperate trough system on 19-21 February. The approximate location of cyclogenesis on 20 February is indicated. b) Satellite-derived SST distributions for 1-15 February, otherwise as in (a). SST distributions and anomalies on 1° x 1° grid, anomalies based on 20-year climatology (National Weather Service).

By mid-day on February 21, the temperate low pressure cell had moved eastward and a conspicuous bend was apparent in the cloud band. Areas of active convection had apparently shifted poleward and expanded over the southern interior and adjacent ocean areas along the southeast and east coasts (Figure 5.10 c,f,i). Surface easterly airflow across the east coast, associated with a high pressure system southeast of the subcontinent, enhanced surface convergence and increased convective activity within the tropical-temperate trough system, as was apparent from the strong poleward flow at upper levels (Figure 5.10i). Maximum rainfall was experienced over the interior on February 21. By February 22 the tropical-temperate linkage had weakened and both convective activity and rainfall had diminished.

Tropical-temperate cloud bands develop in regions of forced low-level convergence between airflows around two eastward-moving anticyclones in conjunction with a baroclinically-unstable atmosphere (Johnson, 1969; Harrison, 1986a). In this case, both the tropical and extratropical components of the rain-producing system were well developed. The easterly airflow entering from the Indian Ocean was abnormally warm and moist as revealed by the anomalous vapor pressures during February. SST anomalies along the east coast, extending southward at least to 30°S, may have influenced the intensity of the ridge/trough system by feeding warm air southward ahead of the trough. In addition, the temperate low had developed over abnormally warm waters and an intensified SST front within the South Atlantic Ocean, suggesting that low-level temperature, humidity and instability may have been abnormally high, thus contributing to convection within the westerly wave. Van Heerden (1988) has suggested that Conditional Instability of the Second Kind (CISK) contributed to development of this abnormally intense rainfall-producing system.

The rainfall episode of 10-11 March 1988

The March rainfall episode was not attributable to a tropical-temperate trough, but rather to the combined influence of several distinctive weather systems. Superpositioning of a surface low pressure cell along the southwest coast with an upper level westerly wave (Figure 5.12) resulted in a system which has been termed a west coast cyclone (Harrison, 1986a). These systems generally occur in association with a relatively intense high pressure cell along the east coast and resultant strong easterly air flow, both of which were observed to occur during this event. Between mid-day of March 10 and 11 the west coast cyclone intensified and moved southward in concert

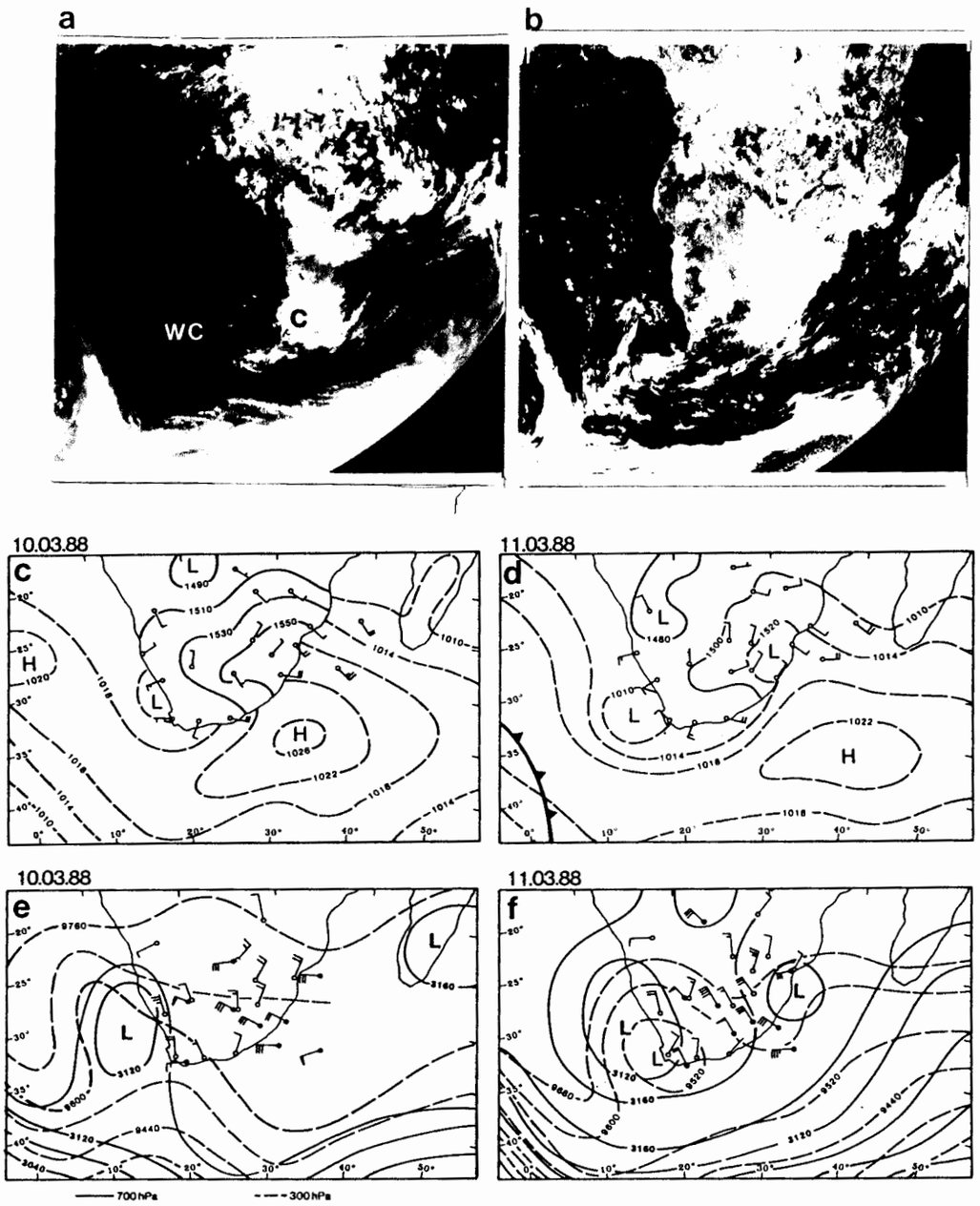

Figure 5.12 Upper: a) Thermal infrared and b) visible METEOSAT images for 11 March 1988, illustrating the west-coast cyclone (WC) and convective cell (C) responsible for the heavy rainfall over central southern Africa on 10-11 March. Middle: Simplified surface synoptic charts for c) 10 March and d) 11 March 1988. Solid lines represent contours of the 850 hPa surface over the subcontinent and dashed lines isobars of sea level pressure. Lower: Upper-level synoptic charts for e) 10 March and f) 11 March 1988. Solid lines represent contours of the 700 hPa surface and dashed lines contours of the 300 hPa surface (gpm). Vector winds are at 700 hPa (open circles) and 300 hPa (filled circles). All charts are at 12h00 UTC. (From Walker and Lindesay, 1989).

with a low over the western interior. Rain-bearing cloud masses formed over major areas of surface convergence along the eastern edge of the cyclone wave with onshore flow across the west coast contributing to surface convergence over the interior (Figure 5.12c,d). The infrared image vividly illustrates the cloud masses responsible for the interior rainfall which peaked on March 11 (Figure 5.12a). The west coast cyclone is readily evident only in the visible image as a result of the relatively warm cloud-top temperatures of this system (Figure 5.12b). Additional cyclogenesis occurred along the south coast by 12 March and subsequent eastward movement of the systems resulted in extensive rains over the eastern parts of the country.

As in the February situation, northerly airflow prevailed over the subcontinent at the surface and throughout the troposphere (Figure 5.12c-f), funneling moist tropical air over the country. The presence of the west coast cyclone adjacent to the coast facilitated the poleward and westward flow of tropical air over the interior on March 10 and 11. The heavy rainfall was associated with interaction between tropical air masses and cyclonic circulation systems south of the subcontinent.

The close correspondence in time and space between development of the west coast cyclone and the prevalence of anomalously warm waters along the west coast is intriguing. A reduction in low-level stability over the anomalously warm waters along the west coast could have contributed to its development. The South Atlantic Anticyclone was extremely weak during March, enabling intensification of the low pressure system. The South Indian Anticyclone adjacent to the east coast played a prominent role as it provided the onshore flow of moist tropical air which fueled convective cells over the subcontinent. As in February, coastal and interior vapor pressures were abnormally high as a result of southward displacement of pressure systems and increased moisture convergence over the interior.

Discussion

During both flood-producing events, extratropical oceanic cyclones were involved which developed over abnormally warm waters within the South Atlantic Ocean. An equally important aspect of the flood events was the prevalence of moist, tropical, easterly airflow along the east coast originating over abnormally warm waters. In both cases, anticyclonic airflow within the southwest Indian Ocean dominated the scenario, whereas the South Atlantic Anticyclone was weak. Anticyclonic circulation along the east coast enabled southward penetration of moist air into the subtropics which under suitable conditions of surface convergence and upper divergence produced the exceptional rainfall over the South African interior.

Rainfall Events Associated with the 1985 Agulhas Anomaly

In Chapter 3, an extensive SST anomaly of 2°-4°C was identified south of the subcontinent during the early summer of 1985. Maximum expression of this anomaly southwest of the country occurred in November 1985 (Figure 4.4, 5.13b) after a major westward intrusion of Agulhas Current waters had occurred into the southeast Atlantic Ocean, in early November (Figure 5.13a). The evolution of anomalous SSTs south of 35°S by intense easterly wind forcing within the southwest Indian Ocean was described in Chapter 4. SST anomalies exceeding 1°-2°C were also present along the west coast of

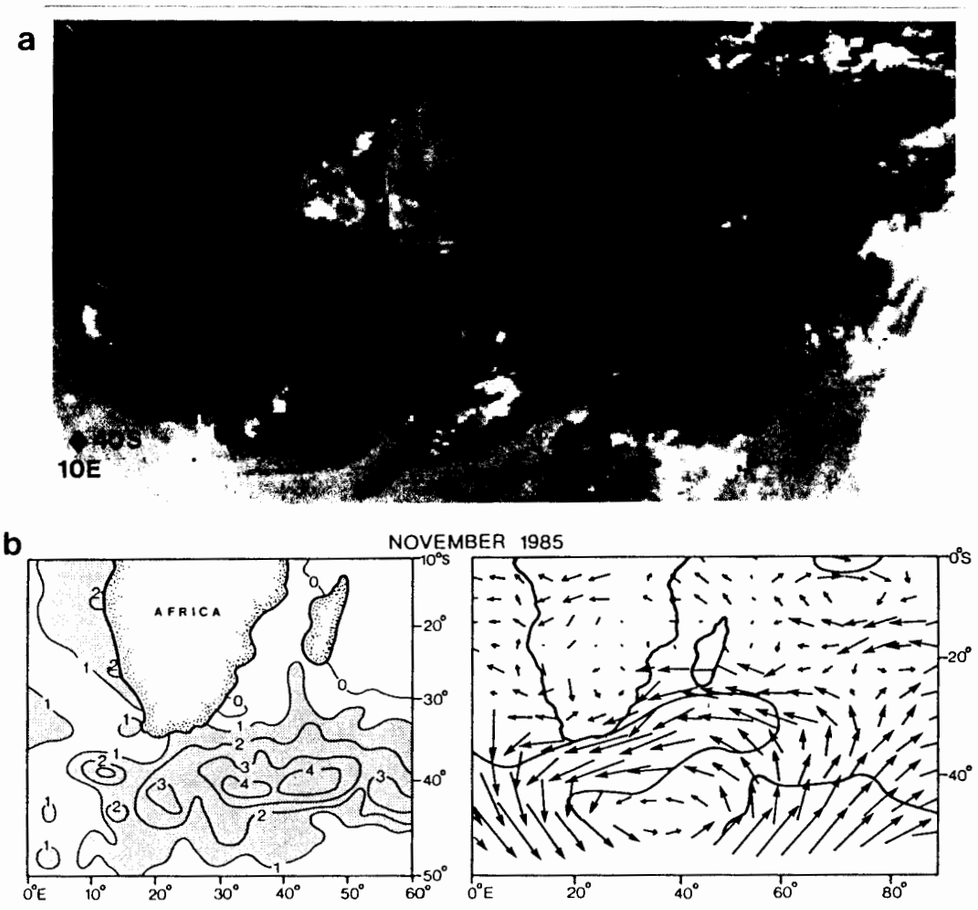

Figure 5.13 a) De-clouded METEOSAT image from 3 November 1985 illustrating an extreme westward penetration of Agulhas Current waters into the southeast Atlantic Ocean. Warmer waters are represented by darker hues. De-clouding was performed by the Satellite Remote Sensing Centre, CSIR by retaining the warmest pixels of several scenes over the day. b) November 1985 SST and wind anomalies (see Figure 4.4 for more details).

southern Africa (Figure 5.13b). Early summer rainfall of area 2 was exceptionally high, exceeding that of all previous 36 years (Figure 3.14b). December's rainfall was the most anomalous with a positive normalized departure of 2.2, whereas departures during the preceding two months were close to unity. Rainfall of area 1 was also exceptionally high during the early summer, ranking third within the 1949-1985 period (Figure 3.14a). The normalized departure of area 1 rainfall in December was 0.4. Unlike area 2, the eastern area experienced its most anomalous rainfall in October.

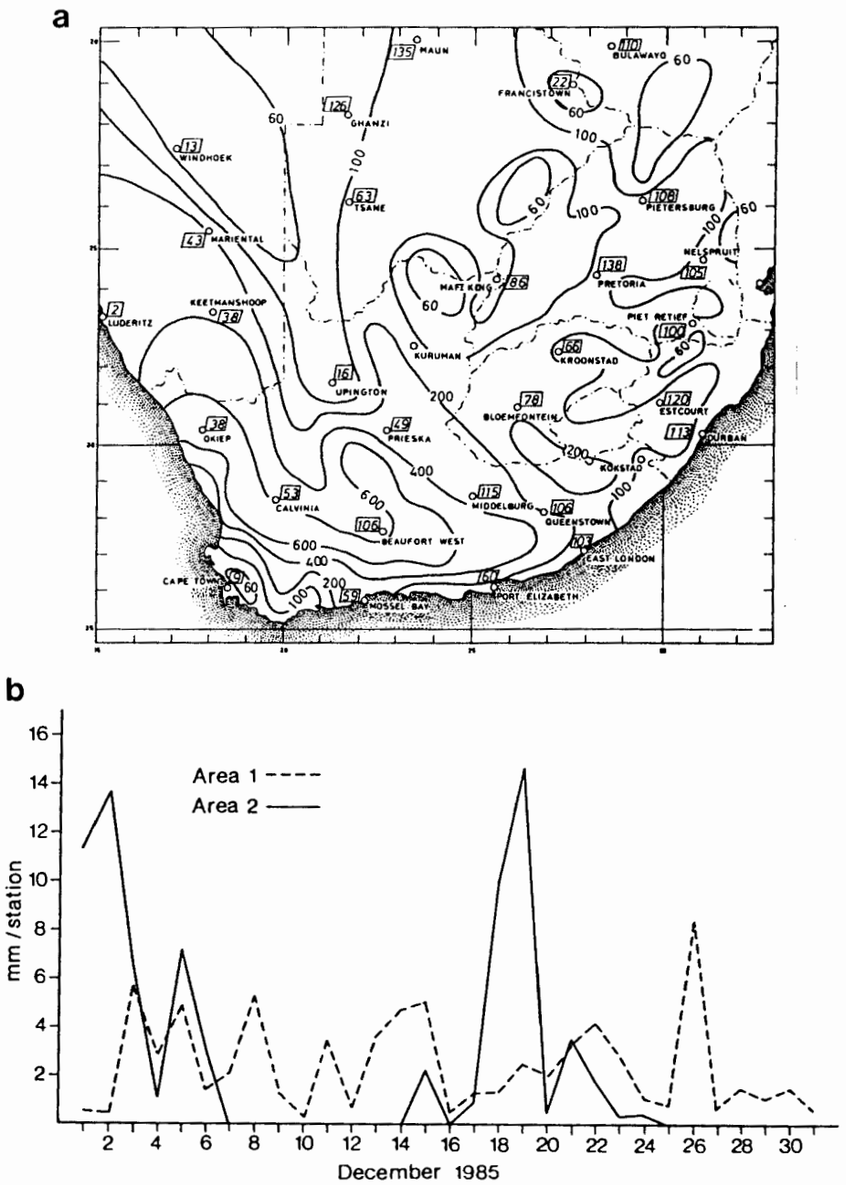

Figure 5.14 a) Rainfall anomalies for December 1985 over the entire country expressed as a percentage of the long-term mean (S.A. Weather Bulletin Monthly Newsletter). b) Time series of daily rainfall, area-averaged over areas 1 and 2 and expressed as mm/ reporting station within each area.

In this section, the synoptic systems reponsible for the anomalous December rainfall in the western parts of the country will be investigated. December rainfall anomalies (expressed as percentages of normal) across the country, based on all S.A. Weather Bureau reporting stations showed a localization of the rainfall over the central and western interior (as well as south and west coast regions) (Figure 5.14a). Rainfall over the entire western half of the country was 200% to 600% above normal. For area 2, daily rainfall data clearly revealed two main rain-producing events: 1-3 December and 18-19 December (Figure 5.14b). In contrast, rainfall of area 1 was distributed fairly evenly throughout the month.

Rain-producing systems of 1-3 December 1985

During this period, strong links between tropical and extratropical circulations were identified. A west coast cyclone figured prominently during the event and enabled a southward flux of moisture across the western interior beginning on December 1 (Figure 5.15). By the following day, a distinctive tropical-temperate trough system had formed as the cold front system passed south of the country (Figure 5.16). By December 3 an interesting synoptic situation was observed in which a T-shaped cloud band linked air masses in the tropics with low pressure cells along the east and west coasts (Figure 5.17). The developments and circulation characteristics of these systems are described in more detail below.

On November 30 low pressure was widespread along the west coast in association with relatively warm surface temperatures. Two separate low pressure cells were indicated on the surface synoptic chart, however, only the northernmost system was apparent above 700 mb (not shown). Further south, a westerly wave and surface cold front approached from the southwest. By December 1 (12h00 UTC), two additional low pressure cells were apparent from the surface synoptic information. Cyclogenesis had occurred south of the intense SST front near 42°S, 20°E and a low pressure cell had also developed along the south coast, ahead of the cold front (Figure 5.15 b,c). SST distributions for the first week of December (Figure 5.15a) revealed that all low pressure cells intensified over waters in excess of 20°C. Danard (1986) has demonstrated that 18°C is a critical threshold value above which intensification of extratropical cyclones is facilitated. In association with these synoptic conditions, moist tropical air crossed the east coast near 20°S, along the northern limb of a local anticyclone situated along the east coast. The tropical airflow recurved southward over the interior towards the low pressure systems along both the west and south coasts. Cloud masses extended across the central interior and southward over the marine low pressure cells (Figure 5.15

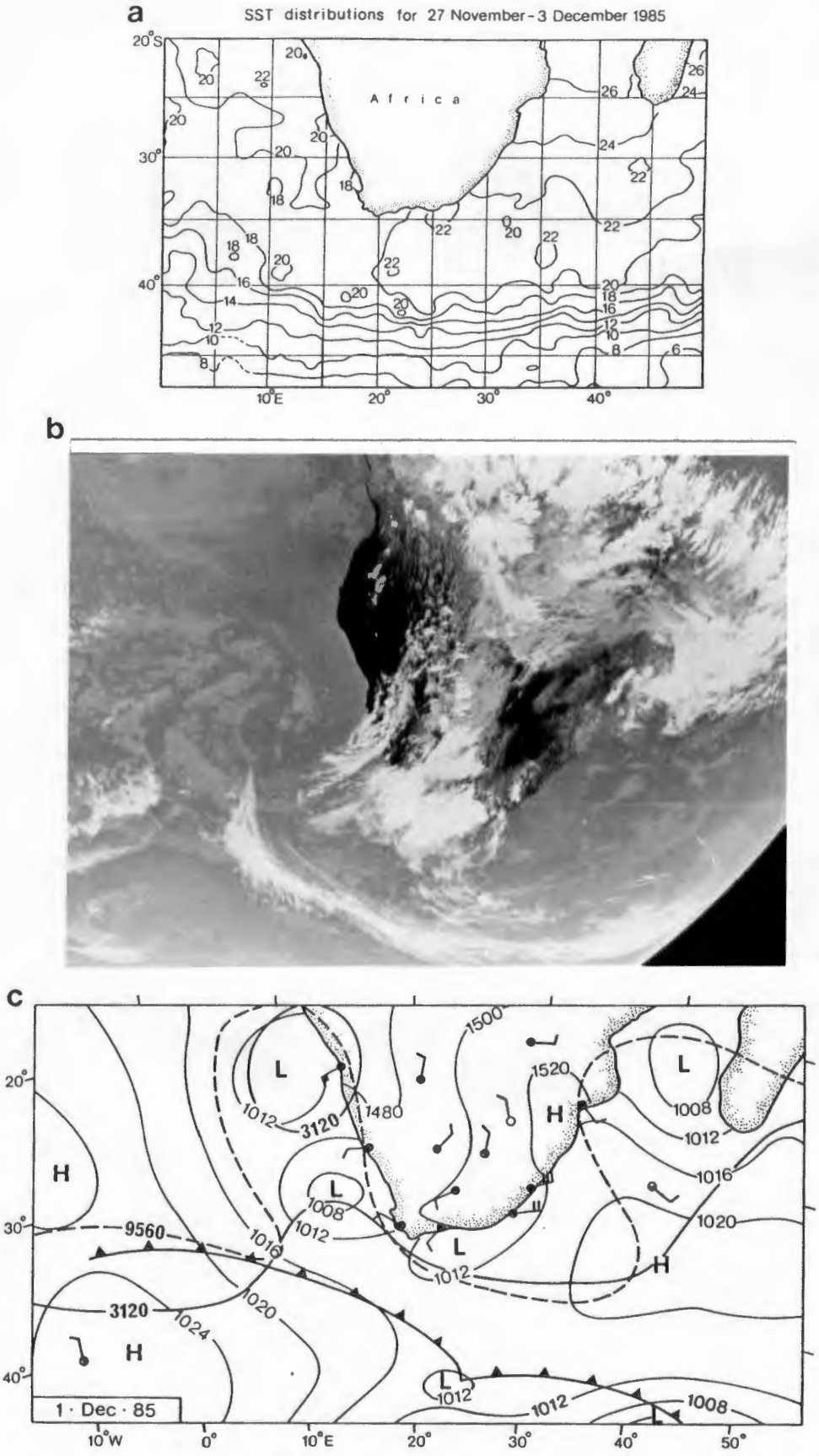

Figure 5.15 a) Satellite-derived SST distributions for the week ending 3 December 1985. b) Thermal infrared METEOSAT image for 1 December 1985 (10h00 UTC) c) Surface synoptic chart for 1 December 1985 (12h00 UTC) where solid lines represent isobars of sea level pressure over the ocean and the 850 hPa surface over land. Vector winds show sea level and 850 hPa winds. Bold solid and dashed lines represent selected contours of the 700 and 300 hPa surfaces respectively.

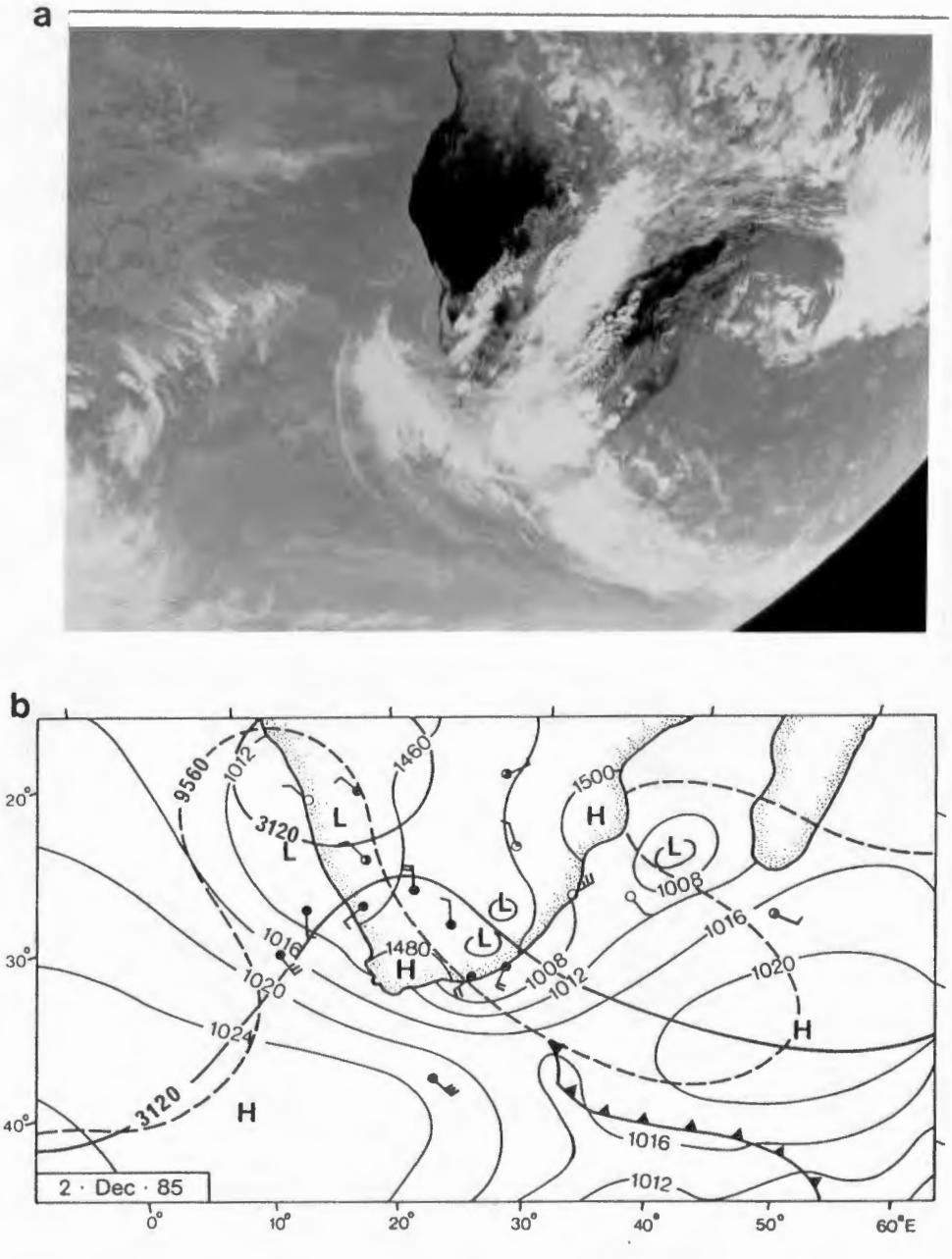

Figure 5.16 a),b) As in Figure 5.15 (b,c) for 2 December 1985.

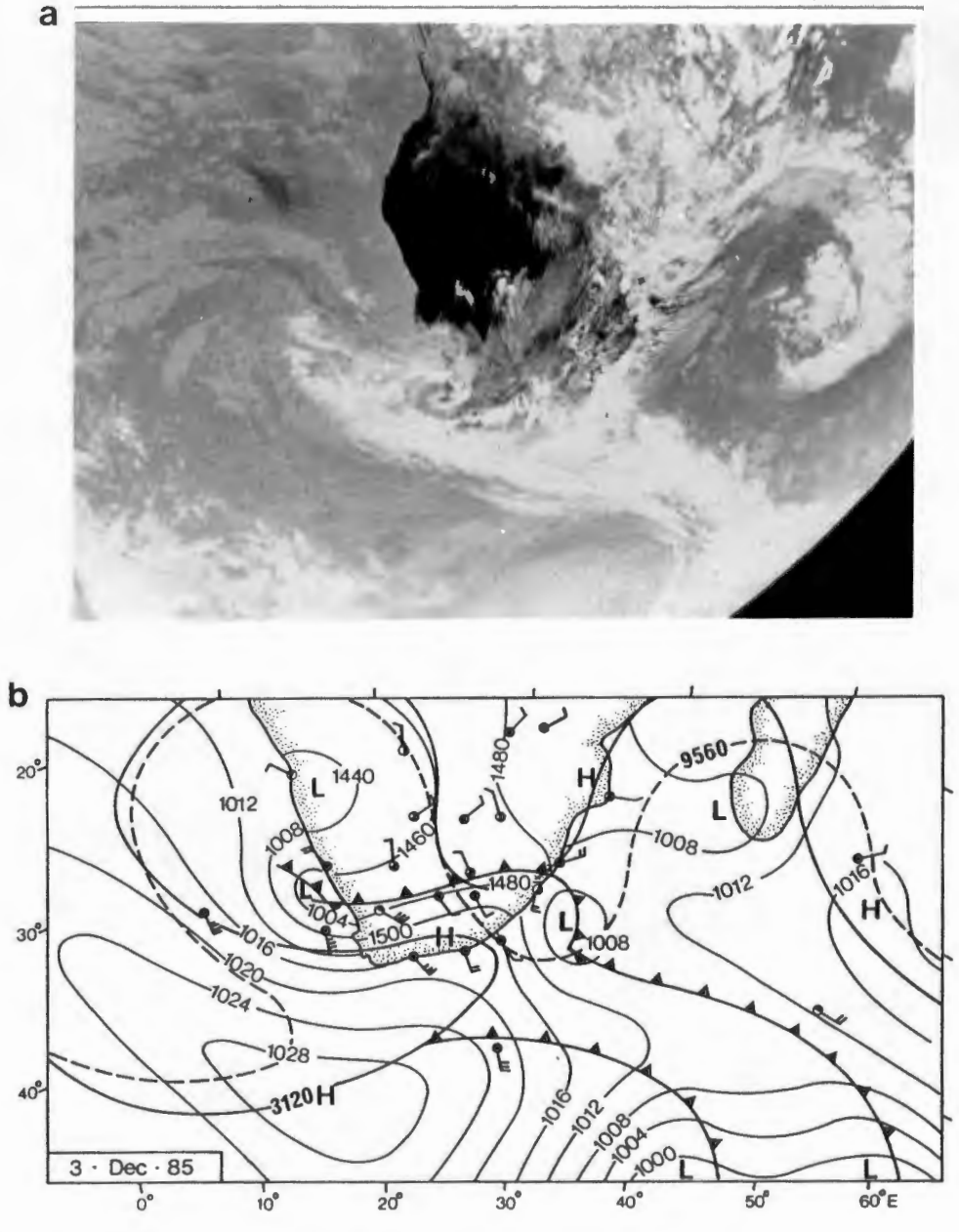

Figure 5.17 a),b) As in Figure 5.15 (b,c) for 3 December 1985.

b,c). Rainfall over the western interior was exceptionally high on December 1, exceeding 11 mm/station. This is considerably more than the maximum rainfall recorded over the same area during the January 1981 episode.

Over the next 24 hours, the locally formed Agulhas low moved northeastward towards warmer waters and by 12h00 UTC was situated at 38°S, 32°E over waters of

20°-22°C (Figure 5.15a, 5.16b). The west coast cyclone and westerly trough also moved northeastward. Thermal infrared satellite imagery (Figure 5.16a) revealed that a distinctive tropical-temperate trough system had developed, forming a crescent-shaped cloud band extending across the interior of southern Africa and terminating at a temperate low south of 45°S (Figure 5.16 a,b). Northerly flow prevailed down the axis of the subcontinent only at the surface. An anticyclone above 700 mb over the eastern interior confined northerly flow to the western parts of the country. Convective activity (as estimated from cloud amount and temperature) reached a maximum over the coastal low pressure cells and adjacent land areas on December 2 (Figure 5.16a). As a consequence, the low along the south coast had deepened over the 24 hours and additional low pressure cells had formed over land in close proximity to the coastal low. Rainfall reached a maximum over the western interior on December 2 however eastern parts of the country received little rain despite the extensive cloud cover. Convection was most pronounced over ocean areas, suggesting that the oceanic supply of moisture actively supplied latent heat which was released at the upper levels.

By December 3, the westerly wave and cold front system had undergone further intensification. The sea level pressure at Marion Island (47°S) had dropped 12 mb and an additional cold front system had formed behind the first, indicating intensification of the surface westerlies (Figure 5.17 a,b). The South Atlantic Anticyclone, situated southwest of the country, had moved eastward and intensified. A most unusual circulation pattern developed, marked by a T-shaped cloud band which linked tropical airflows with cyclonic flows along both west and east coasts. A distinct line of surface convergence traversed the subcontinent from west to east and rainfall continued to fall over the western interior. Inspection of the 300 mb chart revealed divergence zones overlying the main areas of surface convergence (not shown).

In summary, the anomalous rain period of 1-3 December 1985 resulted from intense interaction between tropical and extratropical circulations over southern Africa. Three extratropical low pressure systems developed over positive SST anomalies south and west of the subcontinent. They provided strong onshore airflow along the south and west coasts which converged with the more tropical air being advected onshore and polewards along the northwest side of an anticyclone resident along the east coast. The resulting tropical-temperate trough system produced the anomalous rainfall over western parts of the country.

Rain-producing system of 18-19 December 1985

The main synoptic elements contributing to the occurrence of abnormally high rainfall were a west coast cyclone, a low pressure system over adjacent continental areas and an intense high pressure system southeast of the country. Maximum rainfall occurred under the influence of strong coupling between tropical and extratropical circulations on the 19th.

On December 18 a relatively intense anticyclone (surface to 700 mb) was situated southeast of the subcontinent. To the west the westerly wave had become disfigured and a closed low pressure cell was noted at 700 mb (Figure 5.18c). In association with intensification of the ridge/trough system south of land, tropical lows had moved southward and a relatively deep low was in evidence over the western parts of the country (Figure 5.18c). As during the previous rain event, easterly airflow entering the interior near 15° to 20°S recurved southward into central South Africa as a consequence of a locally well-developed high pressure cell. In addition, intense easterly winds were experienced along the South African east coast from 30° to 35°S along the northern limb of the anticyclone whose center was situated near 40°S, 30°E. Cloud masses covered most of southern Africa (Figure 5.18 a,b) and copious rainfall occurred over the western interior as a result.

By midday on December 19 the low southwest of land had separated from the main westerly flow and coupling between tropical and temperate systems had become more organized. A cloud band was observed across the interior, terminating at the west coast cyclone (Figure 5.19 a,b,c). In association with an approaching cold front, which intensified near the western edge of the Agulhas anomaly (40°S, 8°E), pressure gradients intensified and northerly flow of tropical air increased over the central interior (Figure 5.19c). Consequently the anticyclone in the east and the cyclone to the southwest became better developed. Convergent airflow was apparent at the surface and at 700 mb in association with the area of maximum rainfall. By December 20, the cold front had reached the southwest tip of land, and the west coast cyclone had moved eastward ahead of it. A double cloud band linkage was observed on the 20th when the west coast cyclone cloud band became aligned with the cold front (not shown). This additional linkage, involving a temperate low south of 45°S, formed over the ocean off the east coast, therefore continental rain did not result.

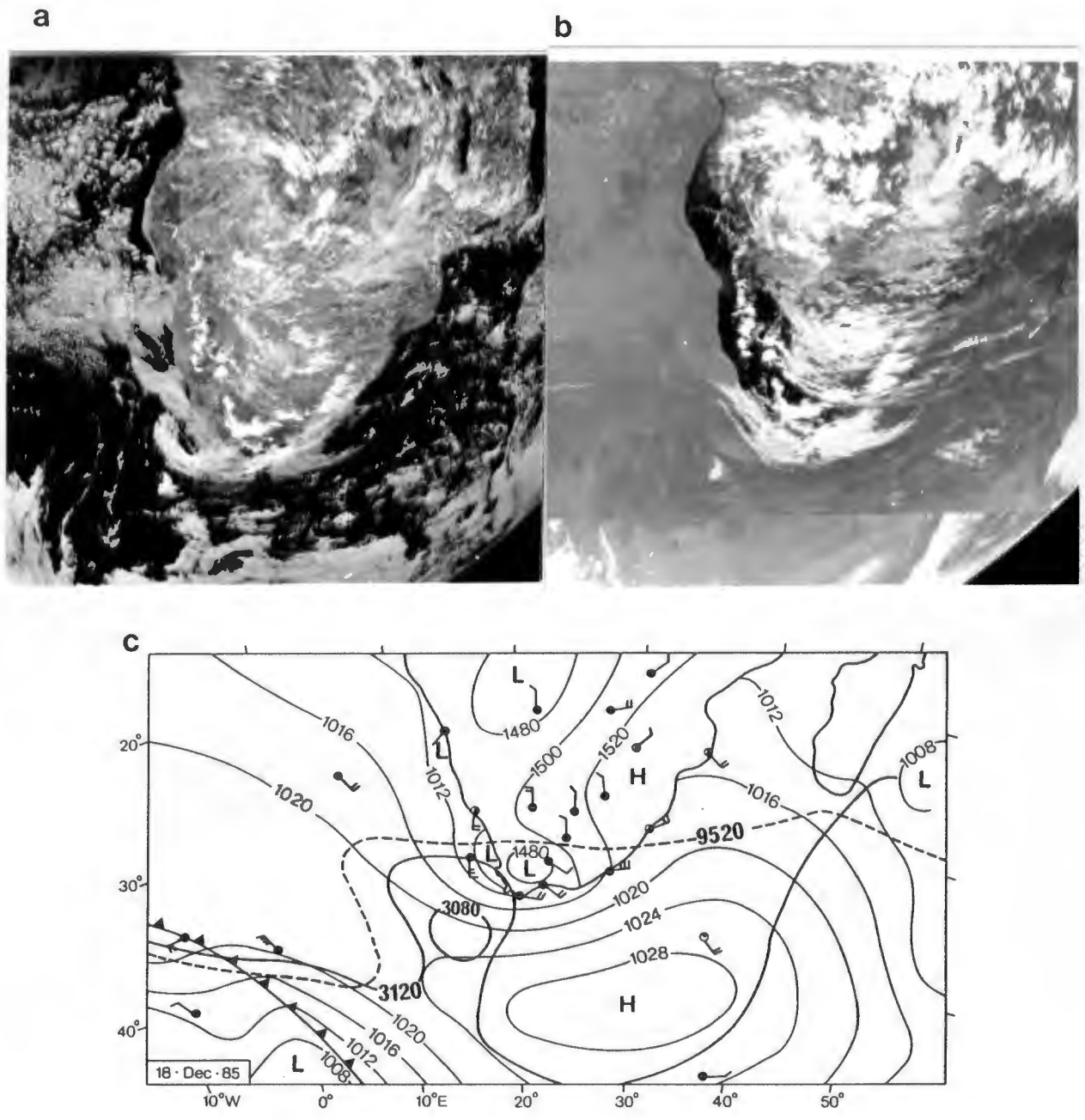

Figure 5.18 a) Visible and b) thermal infrared METEOSAT images for 18 December 1985 (10h00 UTC). c) Surface synoptic chart for 18 December 1985 (12h00 UTC) where solid lines represent isobars of sea level pressure over the ocean and contours of the 850 hPa surface over land. Vector winds are at sea level and 850 hPa. Bold solid and dashed lines represent selected contours of the 700 and 300 hPa surfaces, respectively.

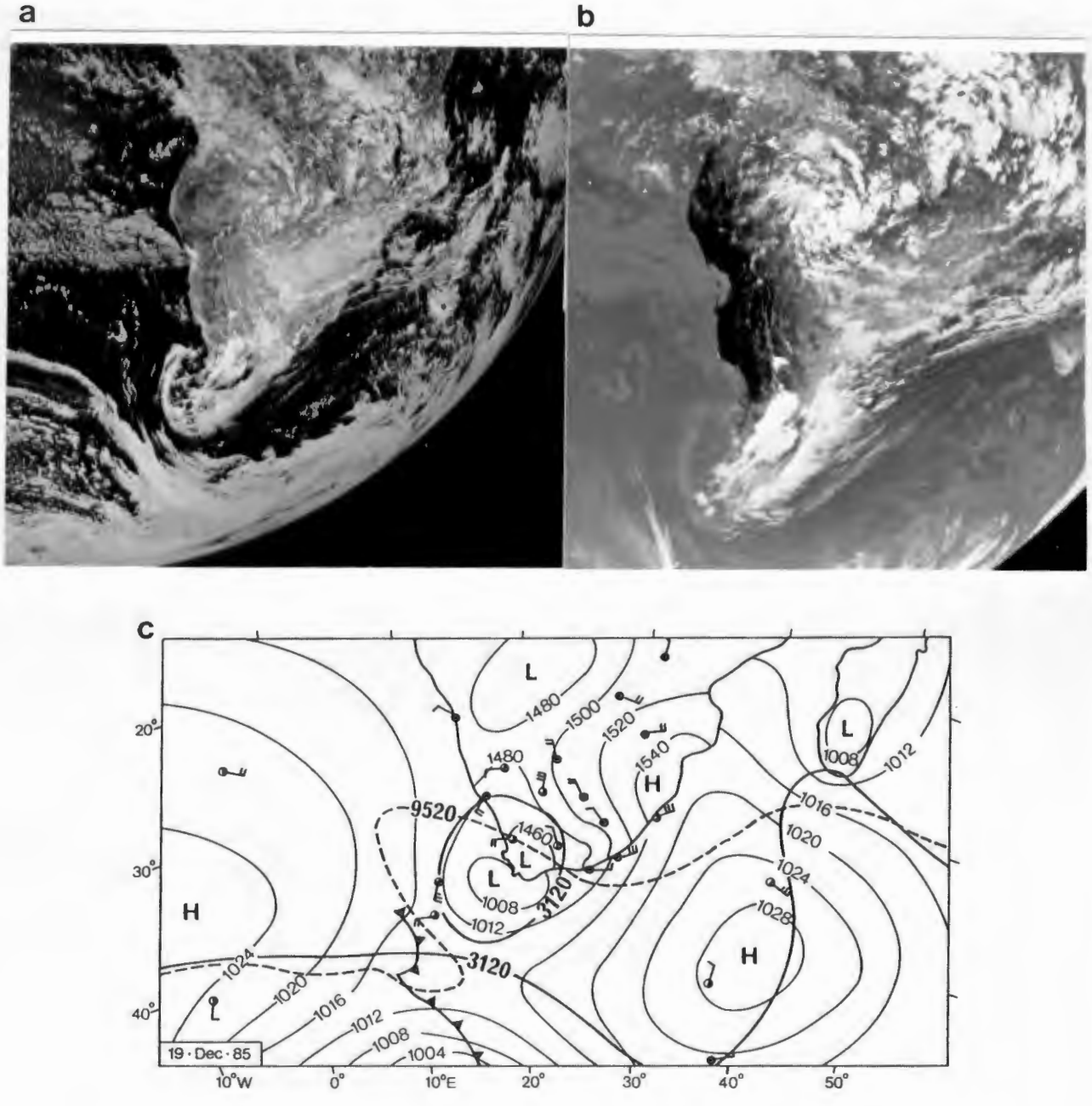

Figure 5.19 As in Figure 5.18 for 19 December 1985.

An evaluation of locally available synoptic information and satellite imagery revealed that tropical-extratropical coupling resulted in the copious rains over the interior during December 1985. In both cases, anticyclonic airflow predominated along the east coast whereas cyclonic flow prevailed along the west coast. The net result was a poleward flux of moist tropical air over the interior and strong surface convergence along all coasts. In contrast to February 1988, poleward flow at 300 mb was confined to western parts of the country. In both December episodes, westerly waves were intensified in close proximity to abnormally warm waters within the ARR and along the west coast, while temperate lows were situated south of 45°S, remote from land.

In Chapter 4, surface heat flux anomalies over the ARR were estimated for a +1°C SST anomaly. Sensible heat fluxes were found to increase by about 100% while latent heat fluxes increased by about 23% over a large region south of Africa (Figure 4.7). Increased surface fluxes have important implications for extratropical cyclone intensification. Modeling studies have demonstrated that sensible heating is important to cyclone development as it increases moisture convergence within the boundary layer (Danard, 1986). In addition, the vertical distribution of latent heating has a significant effect on cyclone deepening, with a lower level of maximum heating producing greater intensification (Anthes and Keyser, 1979; Anthes et al., 1983). Therefore, the prevalence of low pressure systems over large-scale SST anomalies of several degrees during December 1985 would have facilitated their developments and, subsequently, those of the rain-bearing systems.

Rain-producing Systems of November 1983

Oceanic and atmospheric anomalies

In Chapter 3, results obtained from analyzing SST differences during WET and DRY early summer seasons revealed that the wet 1983 season was associated with warmer waters south of the country in the ARR and enhanced SST gradients, compared with conditions in the dry 1982 season (Figure 3.18). During the mid-season month of November 1983, SSTs were 1°-2°C higher within the ARR and SST gradients were enhanced by 3°-4°C. Both eastern and western rainfall areas received above-average rainfall during the 1983 early summer season, as indicated by normalized departures of 0.62 and 1.32 for areas 1 and 2, respectively (Table 3.3). Inspection of the monthly values revealed that November rainfall departures were highest in both areas. Whereas area 2 continued to experience heavy rainfall in December, rainfall in area 1 was near normal.

Monthly-averaged SST anomalies for October 1983, preceding the anomalous rainfall, confirmed that above-average SSTs of 1°-2°C were present within the Agulhas Retroflection region (Figure 5.20a). Further west, below-average SSTs were encountered which in limited areas exceeded -2°C. These anomaly features resulted in SST gradient enhancement of 3°-4°C along the western margin of the ARR. Weekly SST distributions for the 1st week of November showed that the strongest front (10°C/200 km) was situated near 42°S, 17°E (Figure 5.20b).

In terms of the general atmospheric circulation, November surface pressure anomalies were well above average south of land, with major centers of +7 and +8 mb within the South Atlantic and South Indian Oceans, respectively (S.A. Weather Bureau Newsletter). Easterly winds were abnormally strong south and southeast of Madagascar along the northern limb of the local anticyclone and northerly wind anomalies occurred over the African interior (*Climate Diagnostics Bulletin*, Climate Analysis Center).

The major rain-producing systems were identified from daily rainfall data compiled for areas 1 and 2 (Figure 5.21). Precipitation in area 2 occurred in two main episodes after the 18th, whereas that of area 1 was more evenly distributed throughout the month. This discussion focuses on the evolution and circulation features of two main events: 6-7 and 26-28 November 1983.

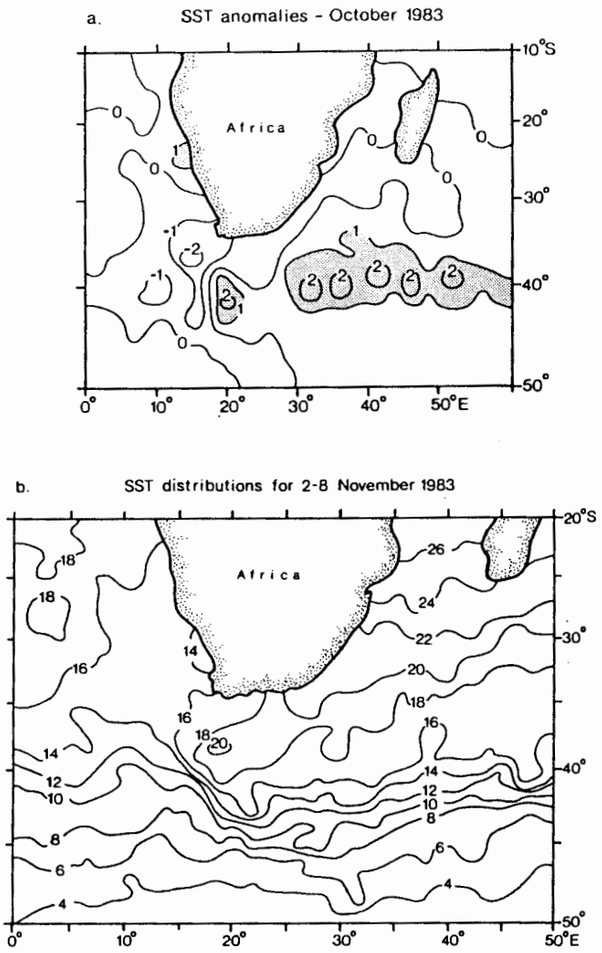

Figure 5.20 a) Satellite-derived SST anomalies for October 1983 b) SST distributions for the 1st week of November 1983 illustrating an intense SST front southwest of the subcontinent near 40°S and 15°E.

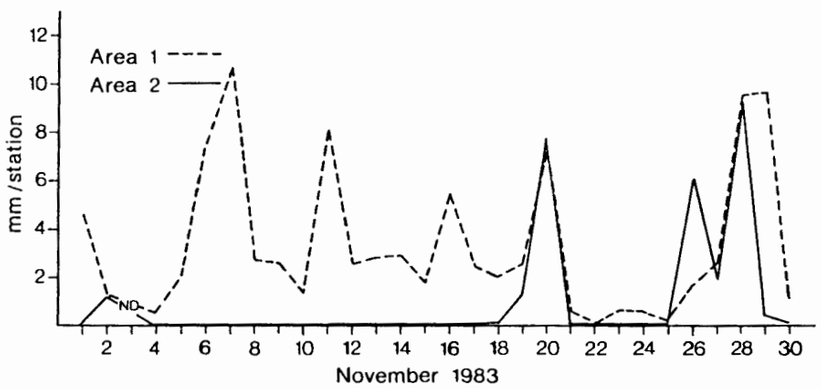

Figure 5.21 Time series of daily rainfall during November 1983, area-averaged over areas 1 and 2 and expressed in mm/reporting station within each area.

Close inspection of visible and thermal infrared imagery, in tandem with synoptic information, revealed several cases of cyclogenesis southwest of the subcontinent near 40°S, 15°E, in close proximity to the abnormally intense SST gradients during the month. These cyclones formed ahead of, or in association with, existing frontal systems but the depression track lay south of 45°S. In addition, intensification of low pressure systems occurred over the warmer Agulhas waters further to the northeast. The rain-producing systems during the early part of the month were temperate in origin, whereas after November 16 combined tropical-temperate activity was observed. In terms of the classification scheme of Harrison (1984, 1986a), east coast troughs and tropical-temperate troughs were responsible for most of the rainfall.

Rain-producing systems of 6-7 November 1983

Development of the frontal system which caused extensive rainfall on the 6th and 7th is illustrated in Figures 5.22 through 5.24. Between November 3 and 4 cyclogenesis and frontogenesis occurred near 40°S, 15°E in the lee of an intense high pressure system southeast of the country and ahead of an approaching cold front (Figure 5.22c). Cloud development was extensive over the newly formed system, extending northeastward over the axis of the warm Agulhas current (Figure 5.22 a,b). By November 5 the anticyclone had moved off to the east and low pressure prevailed southeast of the subcontinent where an additional low pressure cell had formed behind the cold front (Figure 5.23c). Over land, a reduction in pressure had occurred near the south coast ahead of the cold front. However, little cloud was observed over the southern subcontinent suggesting only weak tropical convection (Figure 5.23 a,b).

Copious rainfall on the 6th occurred in association with ridging of the South Atlantic Anticyclone behind the cold front system. Rain-bearing cloud masses were confined to near coastal areas where convergence of continental and maritime air masses occurred (Figure 5.24). By November 7, southerly flow was replaced by strong easterly flow as the anticyclone moved eastward and moisture convergence over the eastern interior increased. An additional low pressure cell had formed by mid-day of the 7th along the northern edge of the westerly wave south of the subcontinent. A kink in the wave was evident on November 6 (Figure 5.24c). Its presence in the upper troposphere resulted in divergence at upper levels which further contributed to conditions favourable for rainfall. Tropical cloud masses moved southeastward towards the frontal clouds along the coast, however, strong tropical-temperate coupling did not occur. This case-study thus suggests that rainfall resulted primarily from temperate influences, south of Africa.

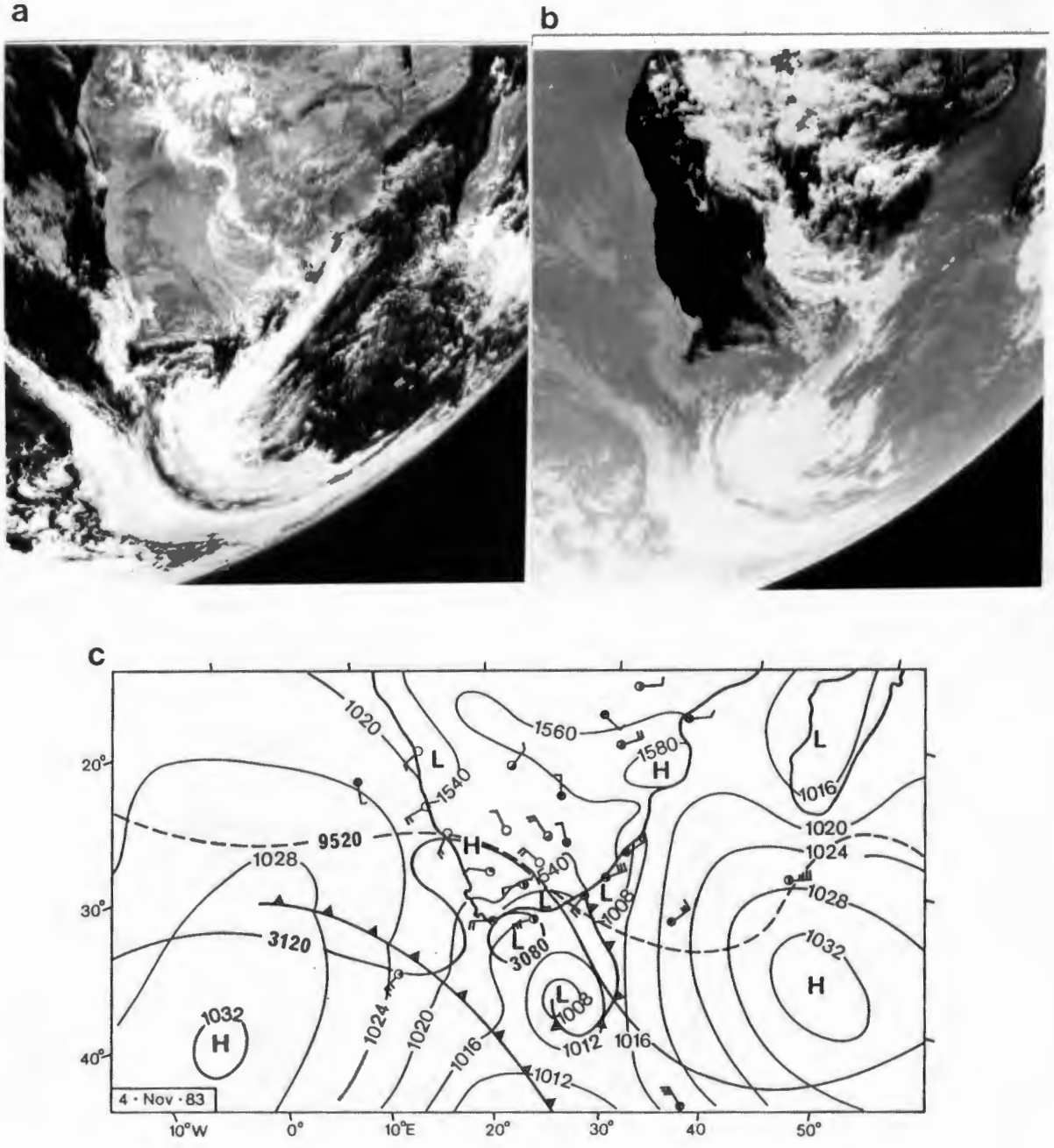

Figure 5.22 a) Visible and b) thermal infrared METEOSAT images for 4 November 1983 (10h00 UTC). c) Surface synoptic chart for 4 November 1983 (12h00 UTC) where solid lines represent isobars of sea level pressures over the ocean and contours of the 850 hPa surface over land. Vector winds are at sea level and 850 hPa. Bold solid and dashed lines represent selected contours of the 700 and 300 hPa surfaces, respectively.

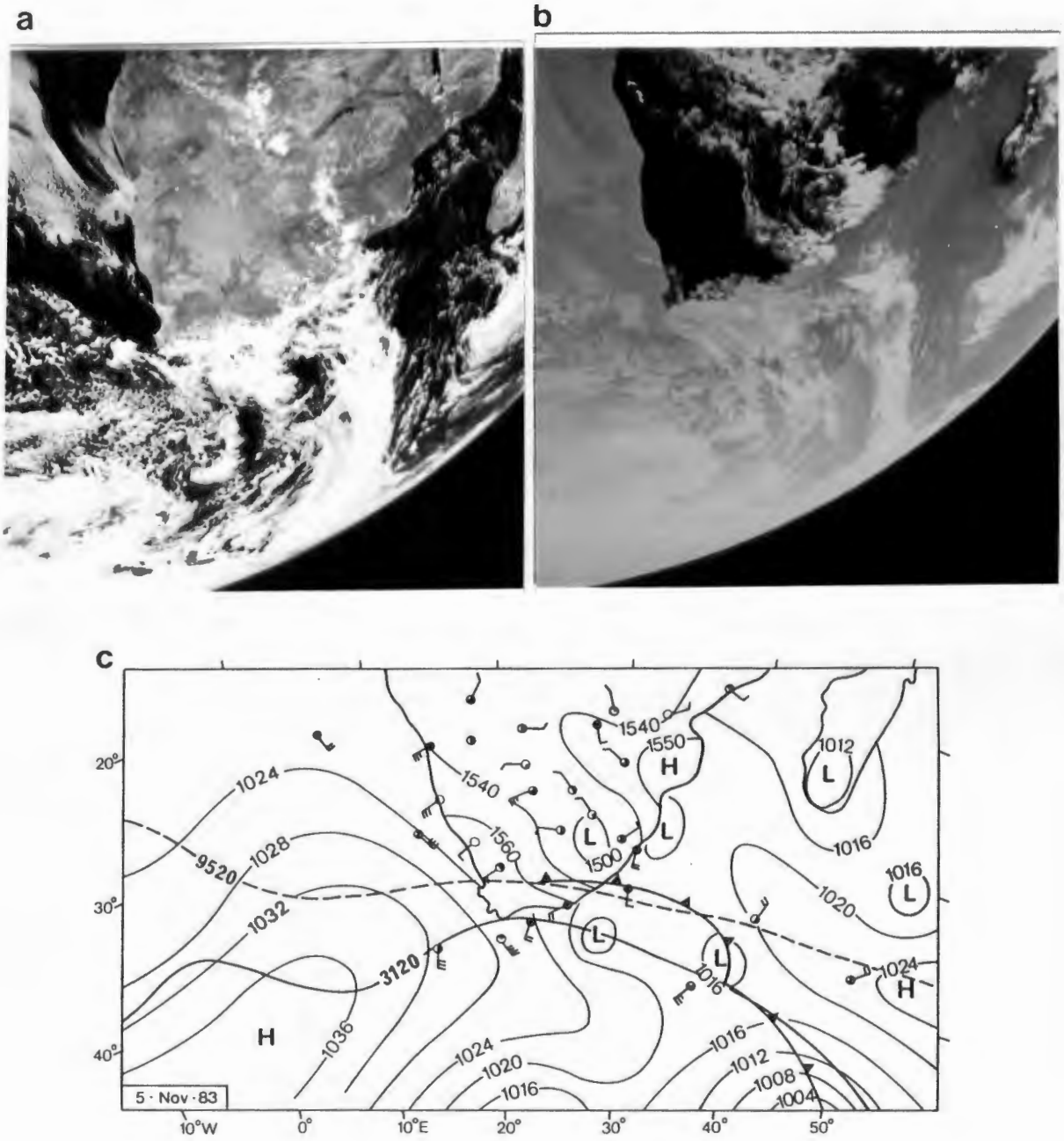

Figure 5.23 As in Figure 5.22 for 5 November 1983.

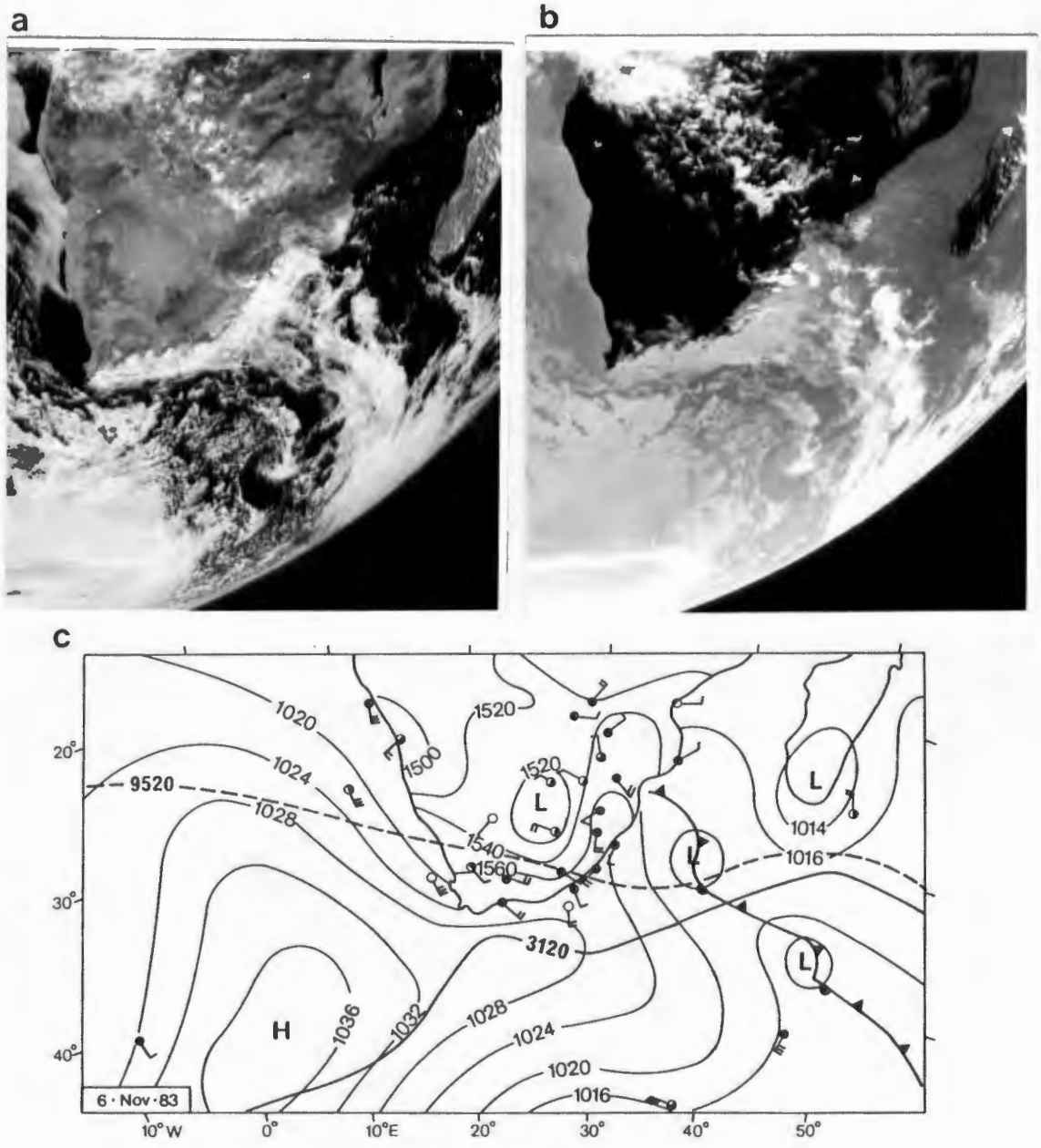

Figure 5.24 As in Figure 5.22 for 6 November 1983.

Rain-producing systems of 26-29 November 1983

This rainfall event was initiated by cyclogenesis southwest of the country and culminated in a tropical-temperate trough system which persisted from November 25 to 28. On November 22 a cold front was situated southwest of the subcontinent and a closed surface low (to 700 mb) was situated along the westerly wave near 38°S, 12°E. By November 23 the low had undergone intensification of 6 mb at the surface, had moved to 41°S, 17°E and extended vertically to 300 mb. On the 24th further development of the system occurred in association with intensification of the high pressure system to the southeast and enlargement of a coastal low pressure system ahead of the main low (Figure 5.25). Over the subcontinent, northerly flow prevailed at the surface and 700 mb level along the western limb of an anticyclone situated over the east coast. High pressure prevailed at the surface and at upper levels on November 24 except in the southern coastal areas where low pressure had developed over land in close proximity to oceanic low pressure cells.

Over the next 24 hours, the main Agulhas low moved southeastward, aligning meridionally with the coastal low pressure system. A distinctive cloud band was observed on the 25th, extending from the western interior to the locally formed Agulhas low, situated near 44°S, 24°E (Figure 5.26). Little rain was associated with the cloud band system until the following day (November 26) when low pressure had displaced the high pressure previously resident over the southern subcontinent and the flow across the west coast became more northerly in association with a closed low at 700 mb near 25°S, 10°E (Figure 5.27). Rainfall associated with the tropical-temperate linkage was maintained through the 28th when it reached maximum values as a result of increased onshore airflow associated with ridging of high pressure south of the country.

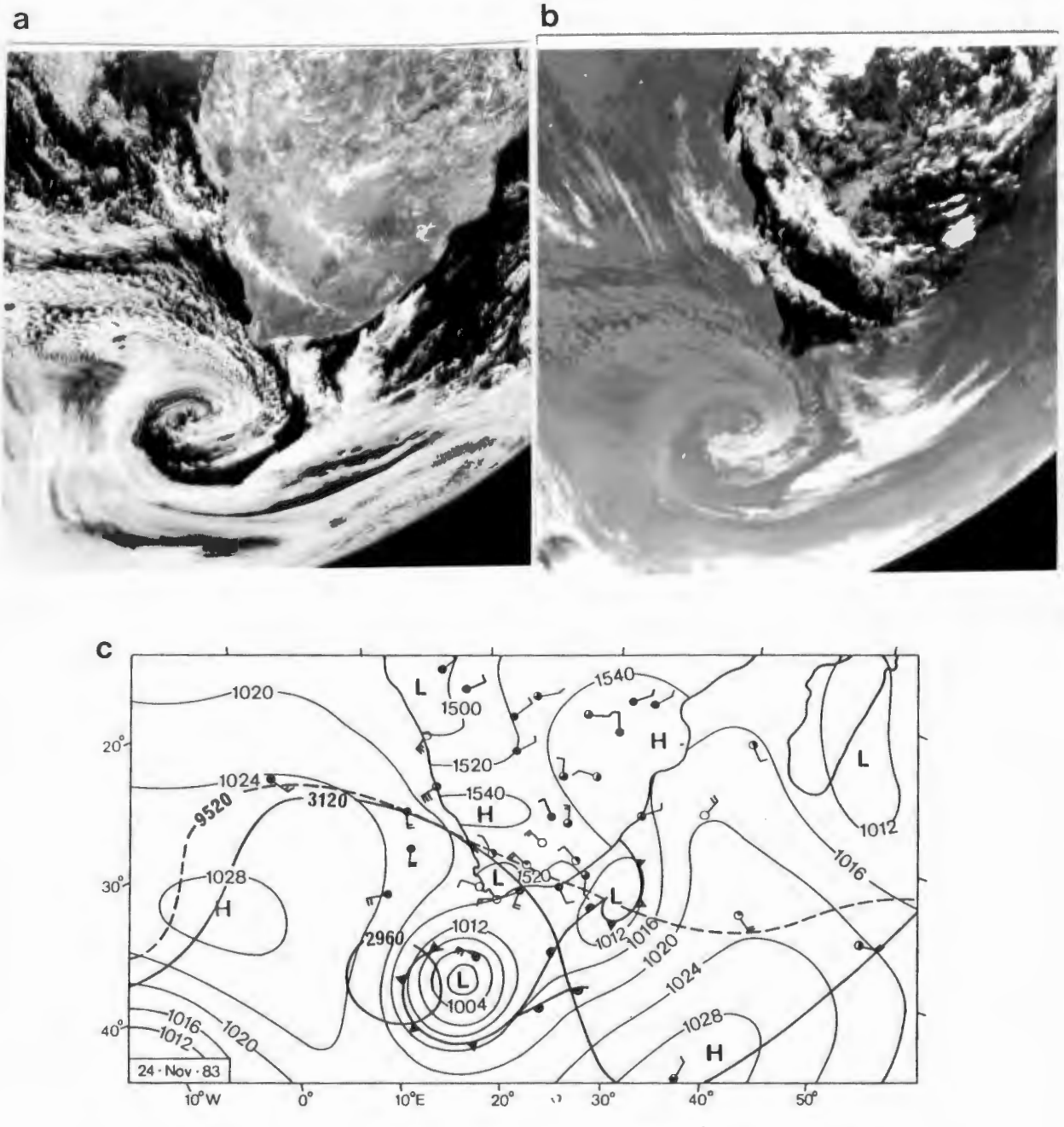

Figure 5.25 a) Visible and b) thermal infrared METEOSAT images for 24 November 1983 (10h00 UTC). c) Surface synoptic chart for 24 November 1983 (12h00 UTC) where solid lines represent isobars of sea level pressures over the ocean and contours of the 850 hPa surface over land. Vector winds are at sea level and 850 hPa surface over land. Bold solid and dashed lines represent selected contours of the 700 and 300 hPa surfaces, respectively.

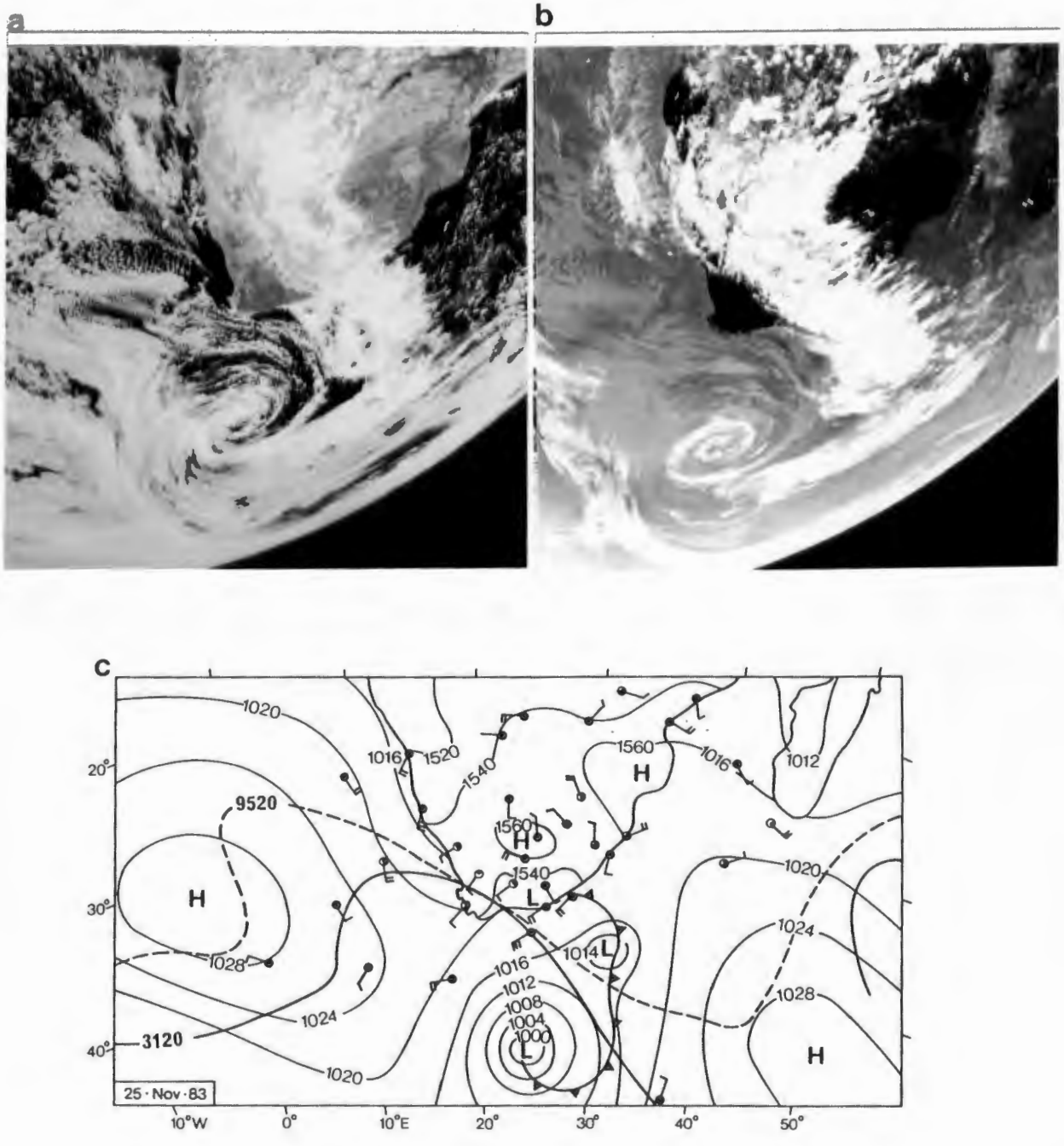

Figure 5.26 As in Figure 5.25 for 25 November 1983.

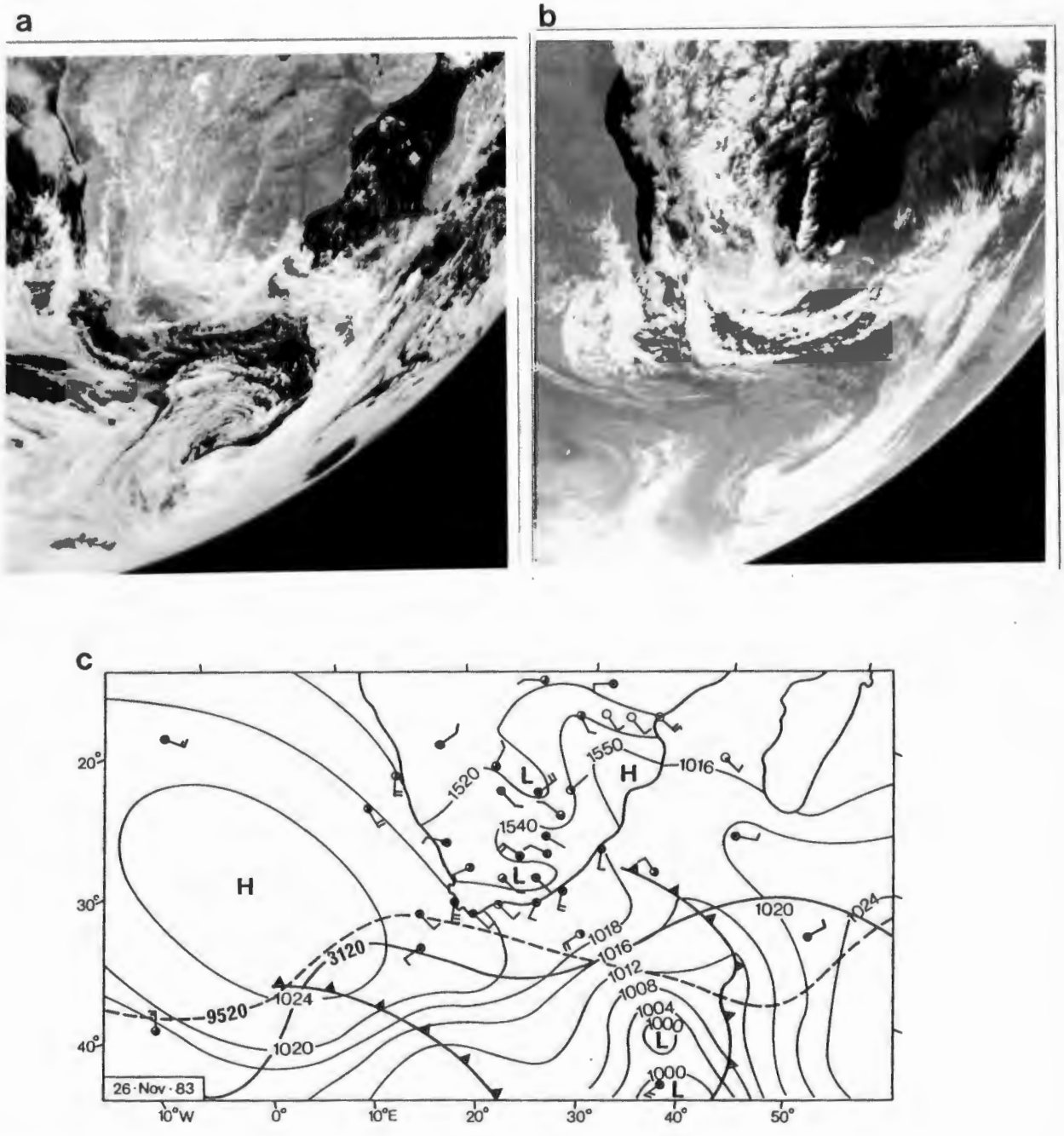

Figure 5.27 As in Figure 5.26 for 26 November 1983.

On November 29, an extensive cloud mass was observed over the southern Agulhas system and over eastern coastal areas, conforming closely to what Harrison (1984, 1986a) termed a coastal depression. In association with this system, surface convergence increased through the interaction of airflows between a high southeast of land and a continental low pressure cell, which had moved southeastward across the subcontinent since the previous day. Rainfall abruptly ended on the 30th.

This rainfall event was thus initiated by an extratropical cyclone which developed and intensified near abnormally strong SST gradients southwest of the subcontinent. Rainfall occurred only after coupling of the tropical and temperate circulations, suggesting that the individual systems were relatively weak. The intensification of tropical activity over the South African interior lagged that over oceanic regions suggesting that the baroclinic system was instrumental in the initiation of convection over South Africa. This statement is supported by research of Smith (1985) which suggests that tropical cloud masses move south over Zimbabwe from Zambia only when strong mid-level troughing occurs due to cold front passage. The coupling of tropical and temperate systems is evidently essential for maximization of rainfall over the central interior of southern Africa.

The prevalence of positive SST anomalies and enhanced SST gradients southwest of land in November 1983 facilitated coupling between tropical and temperate systems by enhancing the baroclinic component. The presence of ocean anomalies in this region during early summer thus enables tropical-temperate coupling to occur earlier in the rainfall season and perhaps more frequently.

CHAPTER 6

DISCUSSION

Over the past decade, considerable climatic research has focused on understanding the mechanisms by which anomalous ocean temperature distributions can affect atmospheric circulations and climate variations. Pertinent theoretical and modeling results will be briefly summarized to provide a foundation for the forthcoming discussions. This synthesis draws on published research and review articles, including those of Namias (1973, 1974), Gill (1980), Namias and Cayan (1981), Webster (1981,1982), Phillips and Semtner (1984), Phillips (1984), Frankignoul (1985) and Shukla (1986).

An abnormally warm sea surface can provide more heat and moisture to the overlying atmosphere through sensible and latent heat fluxes at the air-sea interface. However, only through the generation of a circulation anomaly or altered flow field can the full effects of the SST anomaly be realized (Shukla, 1986). The probability of this occurring is much greater near the equator where easterly winds prevail and rotational influences are reduced. Thus, a positive SST anomaly in the tropics can generate a localized circulation anomaly as a consequence of low-level convergence into the heating region and subsequent upper-level divergence over the SST anomaly (Webster, 1981). The magnitude and structure of the convergence pattern will depend on the magnitude and structure of the SST pattern. Atmospheric Kelvin waves transmit information rapidly eastward which then provides positive feedback to the circulation anomaly via enhancement of the easterly trade winds. A zonal circulation results with ascent over the heat source and descent to the east. Although much slower, planetary waves transmit information westward increasing surface westerlies to the west of the heating anomaly. A low pressure system is generated at the southwestern margin (Southern Hemisphere) of the heating zone as a result of the intiation of cyclonic flow (Gill, 1980).

Outside the tropical easterly wind regime, the influence of an SST anomaly of a similar magnitude is reduced because the prevailing westerly flow provides negative feedback to the original circulation anomaly (Webster, 1981). The circulation anomaly is thus destroyed by atmospheric advection currents away from the original heating anomaly. Because of this advective limitation, midlatitude and subtropical SST anomalies exert their maximum influence on atmospheric circulations during summer

months, when zonal westerly flow is reduced as a consequence of the poleward shift in the depression track (Webster, 1982; Phillips and Semtner, 1984).

The magnitude and structure of the SST anomaly as well as the climatological SST on to which it is imposed are crucial factors in determining whether a given SST anomaly will produce a heating anomaly (Shukla, 1986). If the anomaly occurs within the tropics where sea surface temperatures are relatively high, the potential changes in saturation vapor pressure are much greater than if the anomaly is located in a cooler ocean region. Within the extratropics, an anomaly may yield more influence if located within a region of strong SST gradients (Sanders and Gyakum, 1980; Palmer and Sun, 1985; Nuss and Anthes, 1987).

The location of the SST anomaly in relation to the large-scale flow field is of paramount importance. If located under the ascending branch of the Hadley or Walker cell in the tropics, it can increase moisture convergence and heating. The same anomaly under the descending portion of such a cell will not facilitate moisture convergence even given enhanced evaporation over the anomaly. Through the use of General Circulation Models (GCMs), Palmer and Mansfield (1984) have shown how this concept applies to extratropical responses to SST anomalies in the tropical east and west Pacific. Mansfield (1986) has demonstrated that anomalies of less than +1° C can have marked local and midlatitude effects particularly on the western side of tropical ocean basins. Thus in the southern African context, tropical and subtropical SST anomalies along the east coast would be expected to influence atmospheric circulations and moisture processes more than similar anomalies along the west coast.

Considerable controversy has arisen on the extent to which extratropical SST anomalies influence atmospheric circulations due to ambiguous and sometimes contradictory modeling results. Many experiments using GCMs have yielded non-significant results when using realistic SST anomaly values. This contradiction stems from the fact that the various GCMs incorporate different parameterization schemes as well as different initial and mean flow conditions (Frankignoul, 1985). Basic uncertainties still exist concerning the influence of diabatic heating in midlatitudes and the parameterization of cumulus convection, thus questioning the validity of some model results. The grid-resolution of GCMs presents another problem, as sea surface temperature fronts are not adequately resolved and the generation of baroclinic disturbances such as polar lows and comma clouds would not be incorporated in the results (Gronas et al., 1987).

Nevertheless, observational evidence (Namias, 1974; 1976; Davis, 1978; Harnack and Broccoli, 1979; Namias and Cayan, 1981; Palmer and Sun, 1985) and modeling

results (Simpson and Downey, 1975; Kutzbach et al., 1977; Shukla and Bangaru, 1978; Rowntree, 1979; Chervin et al., 1980; Hendon and Hartmann, 1982; Palmer and Sun, 1985) have demonstrated that midlatitude SST anomaly patterns can influence atmospheric circulations locally and downstream.

Chervin et al. (1976, 1980) and Kutzbach et al. (1977) used "superanomalies" of +6 to 12 K as input in the six-layer National Center for Atmospheric Research (NCAR) GCM and showed both local and hemispheric effects for a positive SST anomaly in the North Pacific. The response consisted mainly of a relative direct thermal circulation over the positive anomaly with lower troposphere pressure falls, upper troposphere pressure rises, increased vertical motion, cyclonic activity and precipitation. A surface anticyclone was observed downstream of the SST and precipitation anomalies (Figure 6.1). Time-averaged responses to the midlatitude SST anomaly exhibited downstream wave-like changes, whereas the subtropical SST anomaly response was more spatially confined (Chervin et al., 1980). A change in planetary waves primarily at wave numbers 3 and 4 was suggested by the model results. Blackmon and Lau (1980) pointed out that, if better simulations of transient variability had been included in the NCAR model, significant results may have been obtained with more realistic anomaly values.

Palmer and Sun (1985) obtained analogous atmospheric responses over the North Atlantic using the Bracknell Meteorological Office 5-level GCM and more realistic SST anomaly patterns. An SST anomaly of 2° to 3°C produced distinctive pressure patterns, namely a surface high pressure anomaly downstream over the North Atlantic and a low pressure anomaly over Europe (Figure 6.2). They proposed that the warm SST anomaly situated southeast of Newfoundland moved the zone of maximum baroclinic instability poleward, inducing a similar poleward shift in storm tracks and simultaneously intensified the westerlies. Their modeling results were supported by simultaneous observational analyses using historical data.

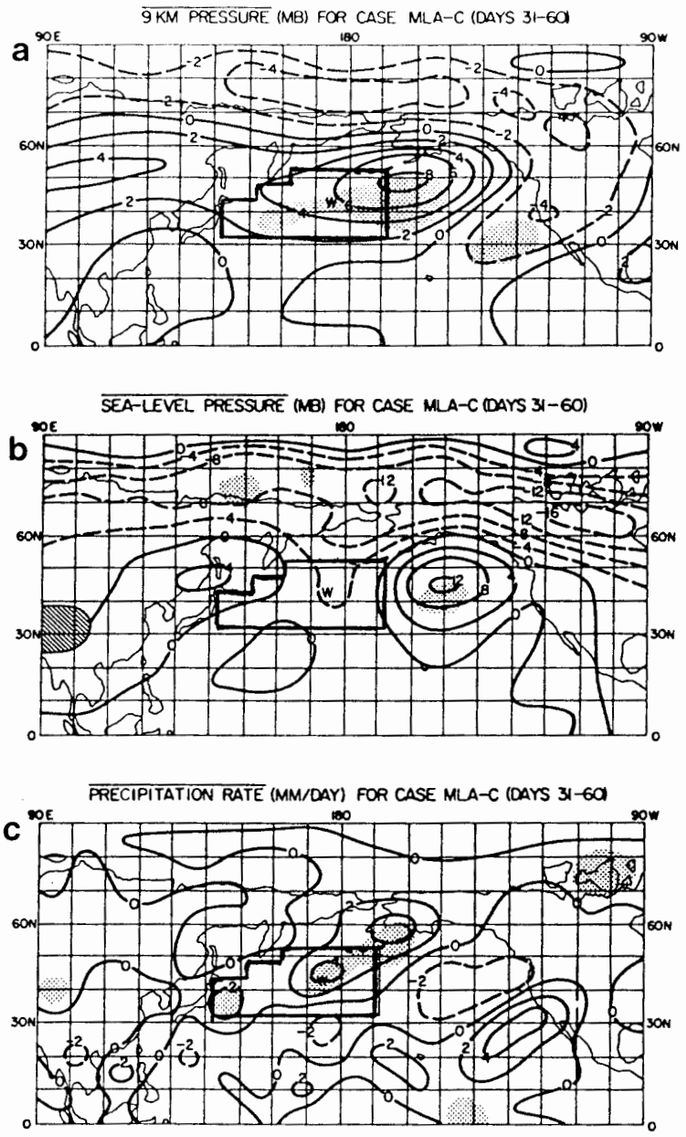

Figure 6.1 Geographical distribution of prescribed change response for the mid latitude anomaly minus control case, averaged in time over the interval Days 31-60 for a) 9 km pressure (mb), b) sea-level pressure (mb) and c) precipitation rate (mm/day). Stippled areas indicate statistically significant differences at the 5% level. The prescribed change region (SST anomaly) is boldly outlined and labeled 'W' for warm anomaly (From Chervin et al., 1980).

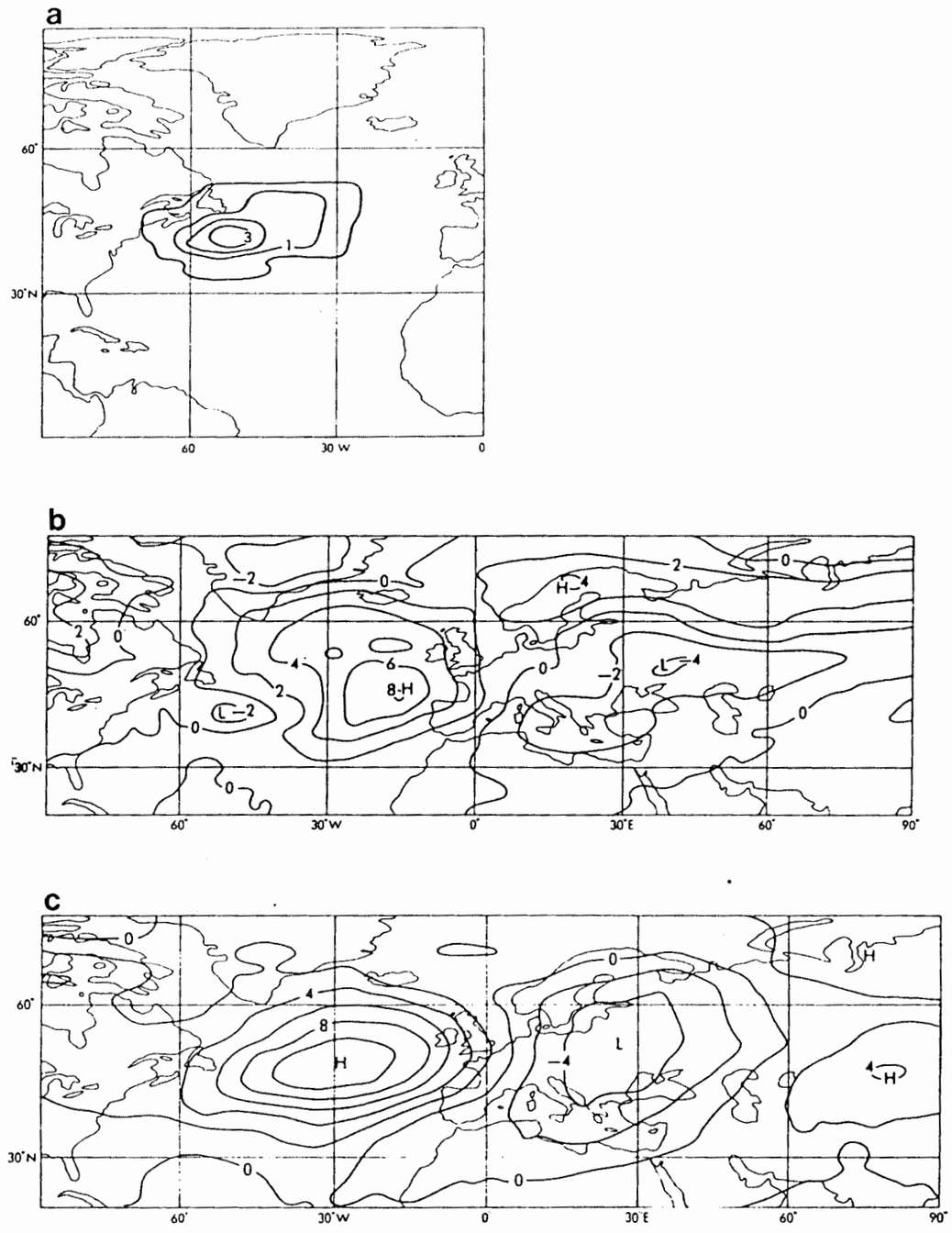

Figure 6.2 a) Full SST anomaly (K) used for the model integrations and anomaly added to climatological values (^{o}C); b) Geopotential height difference (dam) averaged over the four pairs of integrations at 1000 mb; c) Same as (b) but for 500 mb. Each pair of integrations consisted of one 50 day run with the SST anomaly of (a) and one run with the negative of this SST anomaly. The mean of days 21-50 are shown (From Palmer and Sun, 1985).

Feedback Mechanisms within Tropical/Subtropical Regions

Several researchers have demonstrated that the major rain-producing synoptic systems over southern Africa in summer have strong links with tropical convective processes (Harrison, 1984; 1986a; Taljaard, 1986a; Tyson, 1986). The case-study analyses presented in Chapter 5 supported these previous results. In most cases, active tropical convection was apparent over southern Africa north of 20°S in advance of the development of the major rain-producing systems. Only in November 1983 did temperate systems produce rainfall over the subcontinent in the absence of local tropical influences. It is thus appropriate to investigate ocean-atmosphere interactions and feedback mechanisms within tropical and subtropical regions along the east coast of southern Africa.

In Chapter 3 it was shown that tropical and subtropical SSTs along the east coast were higher during and before wetter late summer seasons (Figures 3.10 - 3.13). A contrasting situation was noted further east in the Indian Ocean tropics where cooler SSTs co-occurred with wetter seasons. The occurrence of warmer water in the western portion of the basin was accompanied by the presence of airflow from lower latitudes. The combined effect of these two factors would be an enhancement of moisture and moisture convergence over the subcontinent south of 15°S. This hypothesis is tested by comparing oceanic vapor pressures along the east coast (20°-25°S) with vapor pressures over the eastern interior (Bulawayo, Zimbabwe) and central interior (Bloemfontein, South Africa) of southern Africa during contrasting rainfall regimes (Figure 6.3).

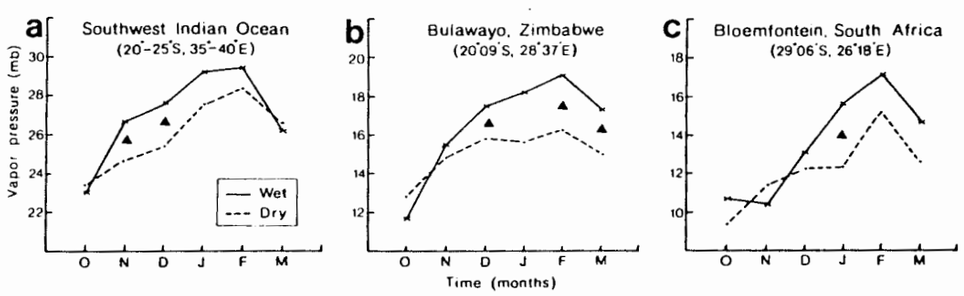

Figure 6.3 Monthly-averaged vapor pressures associated with and preceding composite WET and DRY late summer seasons of area 1 for a) the 5° x 5° grid-square adjacent to the east coast from 20° to 25°S and 35° to 40°E b) Bulawayo, Zimbabwe (20°09'S, 28°37'E) and c) Bloemfontein, South Africa (29°06'S, 26°18'E). Filled and open triangles reveal statistically significant WET-DRY differences exceeding the 5 % and 10% levels respectively.

Vapor pressures were averaged for months pertaining to WET and DRY late summer seasons of area 1 (Figure 3.8a). Over the interior, vapor pressures were found to be significantly higher during the composite WET seasons. At Bulawayo near 20°S, WET-DRY differences were significant in December, February and March, the maximum difference of 3 mb occurring in February. Further south at Bloemfontein, a maximum difference of 4 mb occurred in January. Further inspection of the data revealed that the WET-DRY differences were larger over the interior than over the adjacent ocean area to the east. The most likely explanation for this is an increased convergence of moisture over these interior regions during wetter seasons. It is interesting to note that statistically significant vapor pressure differences over land lagged those over the ocean by one to two months (Figure 6.3). Maximum values occurred over both environments in February, although the continental values were 30% to 40 % lower.

Onshore advection of abnormally moist tropical air originating over the southwest Indian Ocean would fuel convective processes over land. Generation of a positive feedback loop is postulated whereby increased near-surface moisture convergence over the eastern interior would reduce atmospheric stability and favor vertical circulations leading to convection, rainfall and latent heat release. The establishment of active convection within the mid and upper troposphere would facilitate more onshore flow of moist maritime air, further fueling precipitation processes and latent heat release. As suggested by Holton (1979), the large-scale flow would provide the latent heat supply for the convection and the convective heating in turn would produce the large-scale pressure field maintaining the low-level inflow. The occurrence of Conditional Instability of the Second Kind (CISK), resulting from linkages between cumulus scale convection and the large-scale flow, could further increase the circulation anomaly (Holton, 1979; Shukla, 1986). The net result would be the development of a zonal circulation cell through which centralization and strengthening of convection over the eastern interior could occur. The wind analyses in Chapter 4 revealed pronounced convergence of airflow near 15° to 25° S during the wetter seasons (Figure 4.2).

The SST and easterly wind anomalies along the east coast strengthened from early to late summer indicating that the suggested ocean-atmosphere feedback mechanisms were operative. Coupling mechanisms pertinent to development of active tropical convection over the eastern interior are summarized in Figure 6.4. Similar interactions have been suggested as important to initiation and intensification of the southwest monsoon over India (Kershaw, 1988).

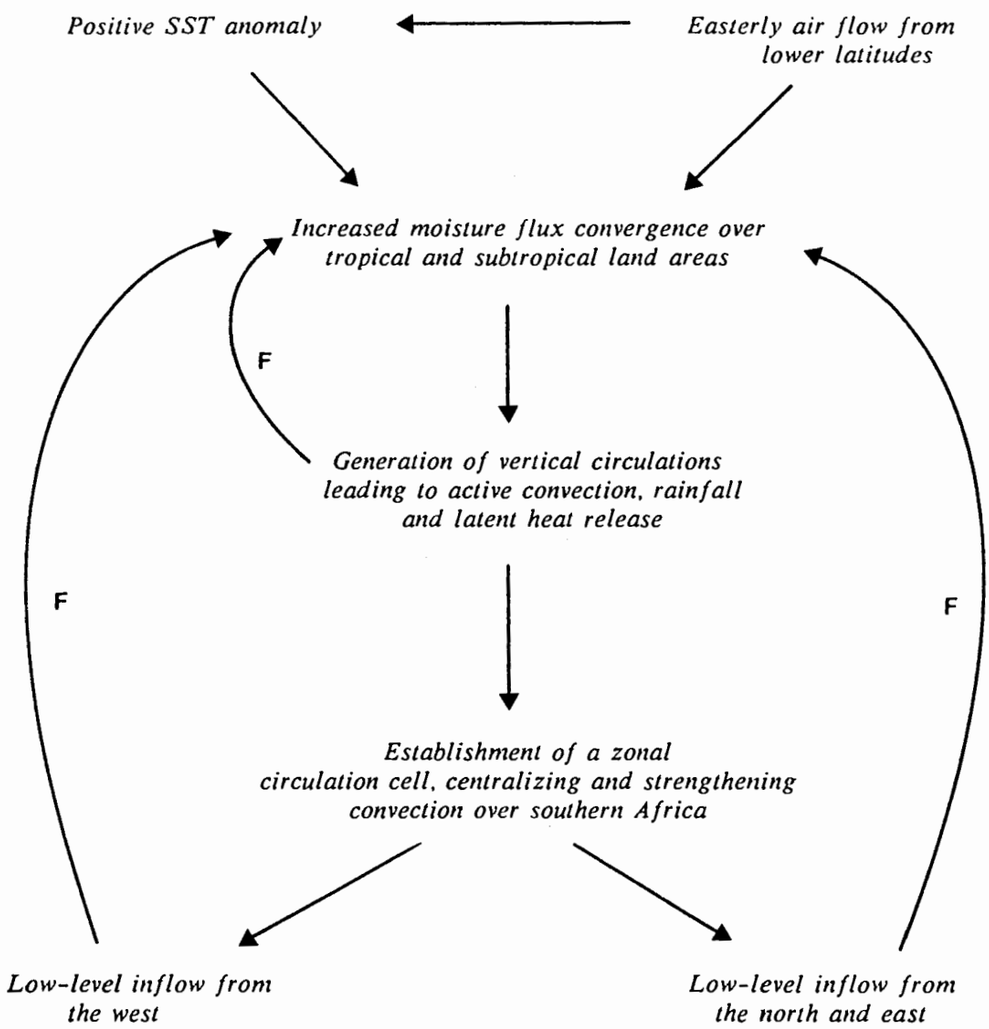

Figure 6.4 Proposed ocean-atmosphere feedback mechanisms operating along the east coast of southern Africa (10°-25°S) during wetter seasons. 'F' denotes a feedback loop.

Positioning of the SST anomaly near the ascending branch of the Hadley cell and upstream from a major global heat source (Vonder Haar, 1968) (Figure 6.5) would facilitate maximum development of active tropical convection in the vicinity of the Intertropical Convergence Zone (ITCZ). Positive SST anomalies were apparent within the western southwest Indian Ocean tropics and subtropics one season in advance of wetter summer seasons over South Africa (Figure 3.12, 3.13). Poleward displacement of the SST anomaly and concurrent easterly wind forcing south of 15°S would have facilitated poleward displacement of the ITCZ over the eastern parts of the subcontinent. Over east Africa, from 0°-10°S, rainfall occurs semi-annually as the ITCZ is moving either north or south (transitional months of both hemispheres). Cadet and Beltrando (1987) have reported on preliminary research that indicates an enhancement of rainfall over tropical east Africa during early austral summer in association with positive SST departures in the western equatorial Indian Ocean. Their observational evidence gives further confirmation of the direct links between positive SST anomalies along the African east coast and enhanced tropical convection.

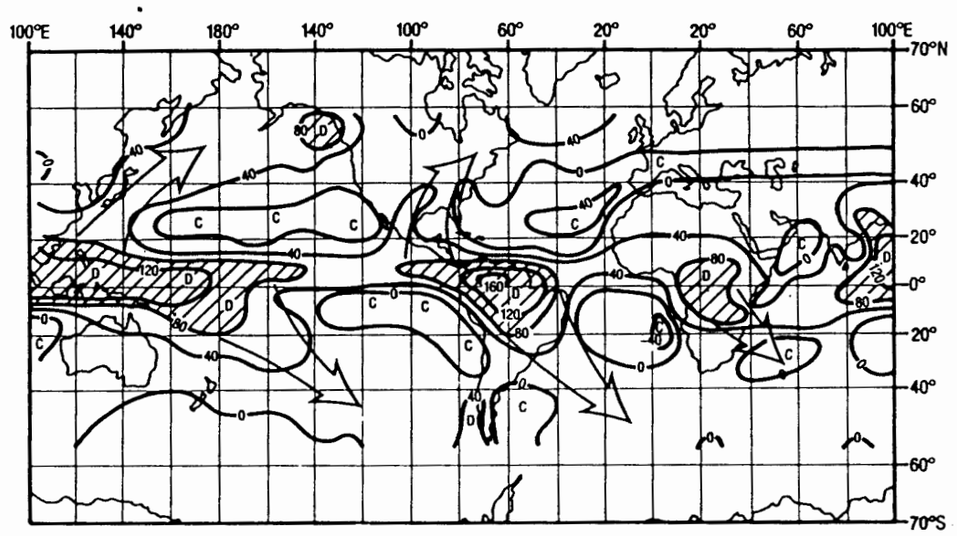

Figure 6.5 Divergence of non-latent energy in the annual mean atmosphere estimated from satellite data (Vonder Haar, 1968). Units are kcal cm^{-2} $year^{-1}$ and shading marks major areas of energy divergence, 'D', and sources of energy export. Regions of upper level convergence are designated as 'C' (From Tyson, 1986 (after Vonder Haar, 1968)).

The hypothesized SST-wind-convection feedback system was further investigated through the use of Outgoing Longwave Radiation (OLR) measurements available for the 1981 (wet) and 1982 (dry) summer. They provide a good measure of cloudiness which reflects atmospheric conditions ranging from tropical convection to extratropical wave disturbances (Lau and Chan, 1983). Lower OLR values represent increased cloud cover. These two seasons were included in the WET and DRY composites of both areas 1 and

2 (Figure 3.8 a,b). SSTs were warmer (0.5° - 1.0°C) along the east coast from 10° to 25°S during the October to March period of 1980/81 and the associated wind field was more northerly (less southerly). SSTs within the Agulhas Retroflection region were 1°-2°C higher during the wetter season (Figure 5.1). Monthly mean OLR measurements are illustrated in Figure 6.6 for the two January months and also for the previous Novembers. In January 1981 low OLR values (< 220 W/m^2) were concentrated over the interior north of 20°S (Figure 6.6a), whereas in January 1982 low OLR values were widespread over the tropics, extending eastward to 55°E (Figure 6.6b). The monthly-averaged OLR distributions for January 1981 revealed the presence of tropical-temperate trough activity over southeastern Africa, previously revealed in the case study analysis (Figure 5.4-5.6). During January 1982, however, cloud cover and tropical-temperate trough formation were shifted eastward over Madagascar, an observation confirmed by an inspection of satellite mosaics for the month.

During November 1980 and 1981, similar OLR values were apparent over much of the region (Figure 6.6 c,d). However during November 1980 (preceding the wet January), very low OLR values were observed along the eastern side of the subcontinent from 20°S to 25°S, indicating persistent convection in this area. Thus, as early as November, intensification and southward displacement of active convection was present in tropical/subtropical areas. These results further confirm the reality of the hypothesized SST-wind-convection feedback mechanisms operating along the east coast.

The major rain-producing synoptic systems identified by the case study analyses were not only tropical in nature, but were also closely affiliated with baroclinic systems south of the subcontinent. Therefore, air-sea interactions and feedback mechanisms involving extratropical systems are discussed in the next section.

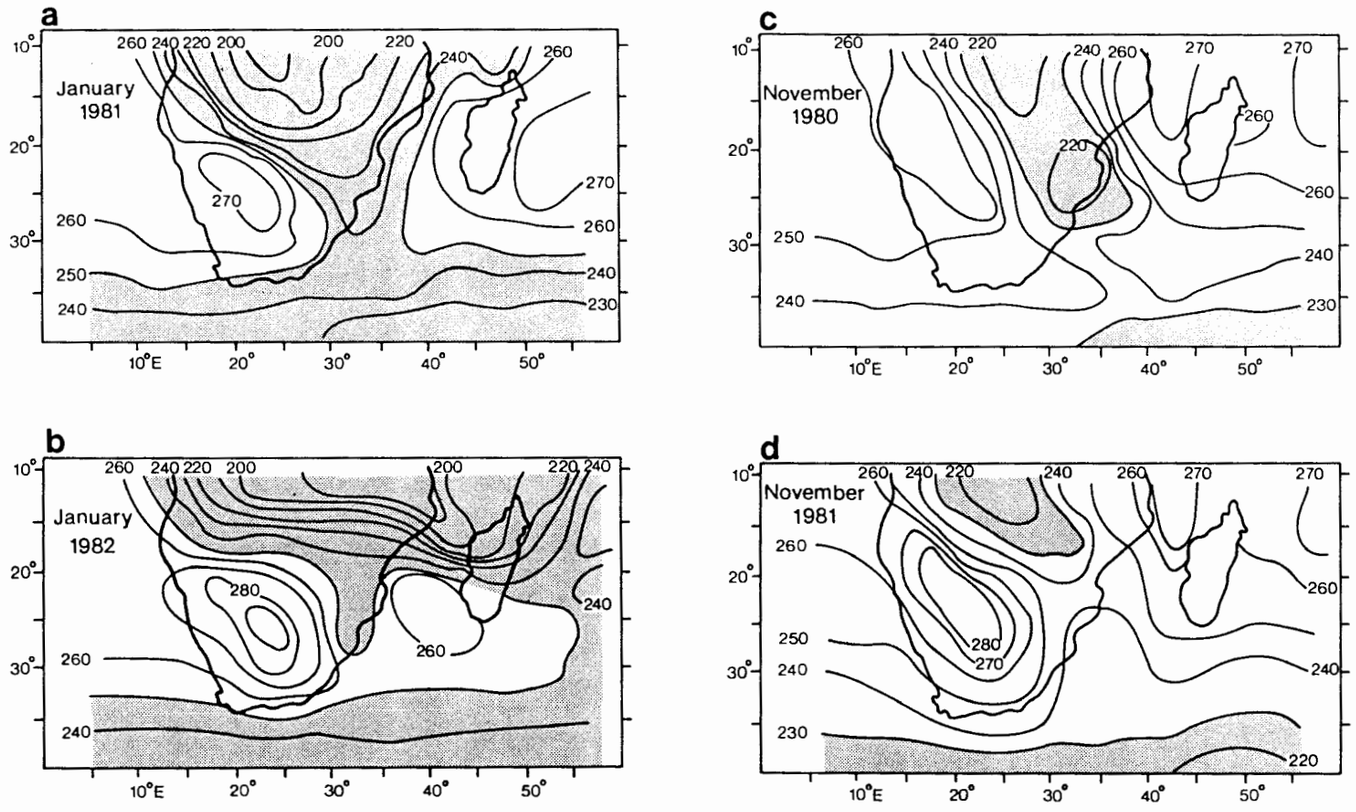

Figure 6.6 Outgoing Longwave Radiation (OLR) in W/m^2 for a) January 1981 of a WET season b) January 1982 of a DRY season c) November 1980 preceding the WET season and d) November 1981 preceding the DRY season. Shading is used to facilitate comparisons of monthly values.

Feedback Mechanisms South of Africa

During the early summer case-studies of November 1983 and December 1985, surface cyclogenesis frequently occurred from 35° to 45°S south and southwest of the subcontinent. Most of the low pressure systems formed or intensified in close proximity to relatively intense SST fronts formed at the confluence of warm Agulhas and colder sub-Antarctic waters at the Subtropical Convergence. This SST frontal zone is at times the strongest within the Southern Hemisphere westerly wind belt (Harrison et al., 1989). James and Anderson (1984) have demonstrated that baroclinic disturbances, with periodicities of 2 to 6 days, dominate meridional transports of heat and momentum within the Southern Hemisphere, a situation which contrasts with that of the Northern Hemisphere where long waves are most important. Their analyses revealed a region of relatively high eddy kinetic energy in the South Atlantic from 20°W to 20°E, which they suggested was a region of strong baroclinic growth in transient disturbances. They referred to this region as the "storm track", distinct from the main "depression track" of westerly lows further south. Although not discussed in their paper, the occurrence of intense SST gradients in the eastern portion of this region may partially explain the observed prevalence of cyclogenesis.

Cyclogenesis occurs frequently east of North America in close proximity to intense SST fronts associated with the confluence of warm Gulf Stream waters and colder Labrador Current waters (Sanders and Gyakum, 1980), a situation somewhat analogous to that encountered south of Africa. In the Northern Hemisphere the frequency of cyclogenetic events increases during spring and winter when ocean-atmosphere heat fluxes reach a maximum as a result of the intrusion of cold, dry continental air from the northwest. The Agulhas Retroflection region harbors similarly high heat losses but with less of an annual cycle due to the prevalence of westerly winds and intrusions of relatively cold and dry air within high pressure systems throughout the year. As in the Northern Hemisphere, heat losses attain maximum values under cold-air outbreak synoptic situations (Mey et al, 1989). Maximum horizontal heat flux gradients occur in summer at the southwestern margin of the Agulhas Retroflection region (Hoflich, 1984; Walker and Mey, 1988), a condition which would facilitate cyclogenesis locally.

Atmospheric measurements obtained during summer within the Retroflection region (Jury and Walker, 1988; Mey, Walker and Jury, 1989) have confirmed the presence of ideal conditions for surface cyclogenesis, namely low static stability and strong low-level baroclinicity (Reed and Albright, 1986; Nuss and Anthes, 1987). Aircraft measurements during February 1987 revealed the presence of distinct

thermodynamic and kinematic changes within the atmospheric marine boundary layer (MBL) across the edge of the Agulhas Current southwest of Africa. Westerly winds accelerated across the SST front in an ageostrophic seabreeze-like circulation as a result of reduced boundary layer stability and turbulence associated with increased oceanic heat losses over the warmer waters (Jury and Walker, 1988). Hsu (1984) has described similar circulations across SST fronts of the Gulf Stream system. Adjustments in atmospheric temperature, moisture and boundary layer thickness also occurred across this SST front. In Figure 6.7, the changes in boundary layer thickness on crossing the front (from cool to warm) are shown for three case-study days. An average change of 390 meters was observed across a 6.4°C front under the influence of high pressure. Associated average changes in air temperature, dew point temperature and wind speed were 3.6° C, 2.6°C and 7 m/s (Jury and Walker, 1988; Table 2).

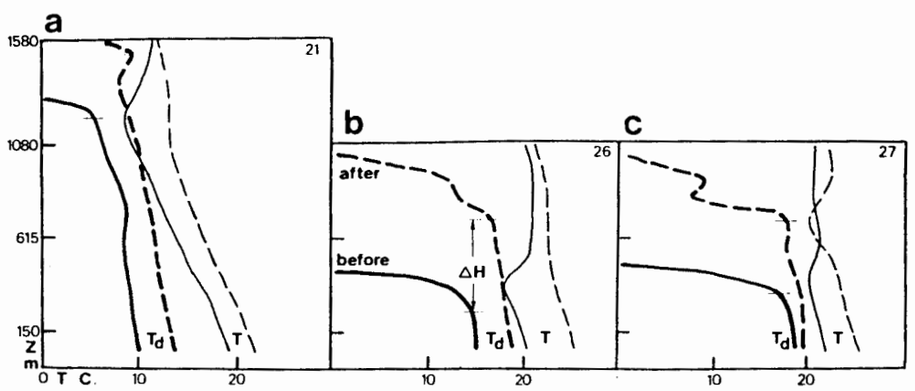

Figure 6.7 Vertical profiles of air temperature (T, thin lines) and dew point temperatures (T_d, thick lines) before (solid lines) and after (dashed lines) Agulhas modification on a) February 21 b) February 26 and c) February 27, as determined from aircraft measurements across the edge of the Agulhas Current southwest of Africa in 1987 (From Jury and Walker, 1988).

Further south under the influence of the prevailing westerlies, marked MBL changes were observed across an SST front of 8.7°C/35 km near 44°S, 20°E (Figure 6.8). Surface wind speed doubled across the front (from 8 to 16 m/s) in association with the initiation of oceanic heat losses and turbulence over warmer waters (Figure 6.8 a,b,d). As a consequence of the altered boundary layer conditions, baroclinically enhanced westerly airflow paralleled the SST front over 18° to 20°C waters (Mey et al., 1989).

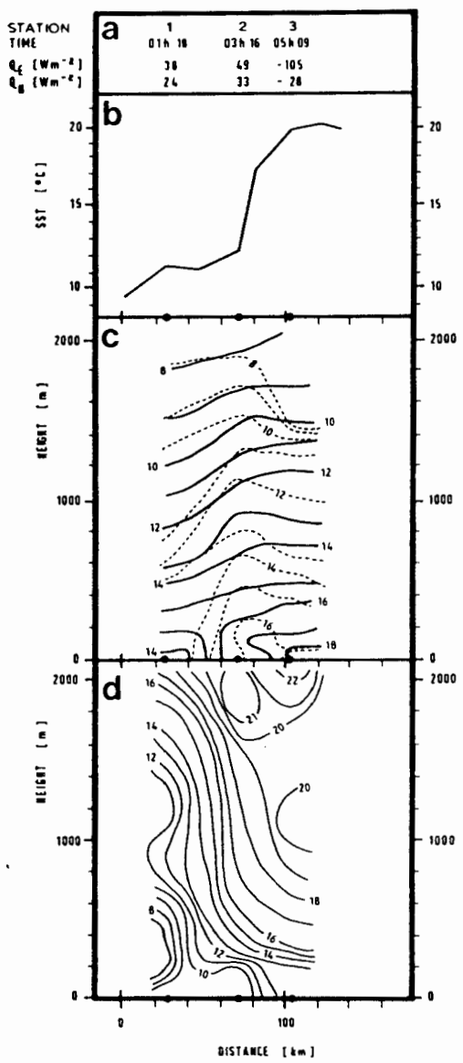

Figure 6.8 Ocean-atmosphere heat fluxes and atmospheric marine boundary layer characteristics on 27 February 1987 across the Agulhas/Subtropical Convergence SST front of 8.7°C/35 km situated near 44°S, 20.5°E. a) Sensible (Q_H) and latent (Q_E) heat fluxes at the three stations crossing the SST front. *Negative* values represent oceanic heat *losses*. b) SST (°C) across the front. c) Air (solid lines) and dew point temperature (dashed lines) in °C d) Wind speed (m/s). Winds are west-northwesterly (From Mey, Walker and Jury, 1989).

These few available boundary layer measurements have revealed that SST distributions within the region provide conditions conducive to cyclogenesis and intensification of baroclinic systems south of the country. The presence of SST anomalies within the Agulhas Retroflection region would reduce low-level stability within the boundary layer (as shown in chapter 4) and provide heating at low levels within the troposphere, a situation conducive to maximum cyclone deepening (Anthes and Keyser, 1979; Anthes et al., 1983). Associated enhancement of SST gradients would strengthen baroclinicity within the boundary layer thus favoring cyclogenetic processes. The zonal location of the SST anomaly or SST gradient anomaly would affect the site of cyclogenesis south of Africa.

Along the Agulhas/Subtropical Convergence SST front, low pressure system formation and westerly trough amplification would occur through differential temperature and thickness advection within the troposphere (Holton, 1979). Poleward advection of warm moist air ahead of the low would build the preceding ridge while equatorward advection of relatively cold air would deepen the following trough. In this way, the ridge/trough system would intensify. The often observed half-sine wave SST feature formed by a wave in the Agulhas/Subtropical Convergence SST front southwest of land (Figure 1.7a), would increase low level thermal advection and vertical velocities within developing low pressure systems as a result of increased low level temperature advection (Nuss and Anthes, 1987). This mechanism would operate most efficiently for Rossby waves of a similar length scale, i.e. wave numbers 5 to 8 (Mey et al, 1989). The South Atlantic Anticyclone could also be expected to undergo intensification as a result of this process. The case-studies of January 1981 and November 1983 provided observational evidence of such occurrences. An increased meridional index of low-level airflow would result in enhanced southerly flow along the south coast providing additional surface convergence over land. The presence of such a circulation during wetter seasons was suggested by the VOS wind data analysis (Figure 4.2, 4.3). The net result of cyclogenesis and westerly wave intensification would be an increase in rainfall and latent heat release within the frontal system. These ocean-atmosphere interactions and feedback processes are summarized in Figure 6.9.

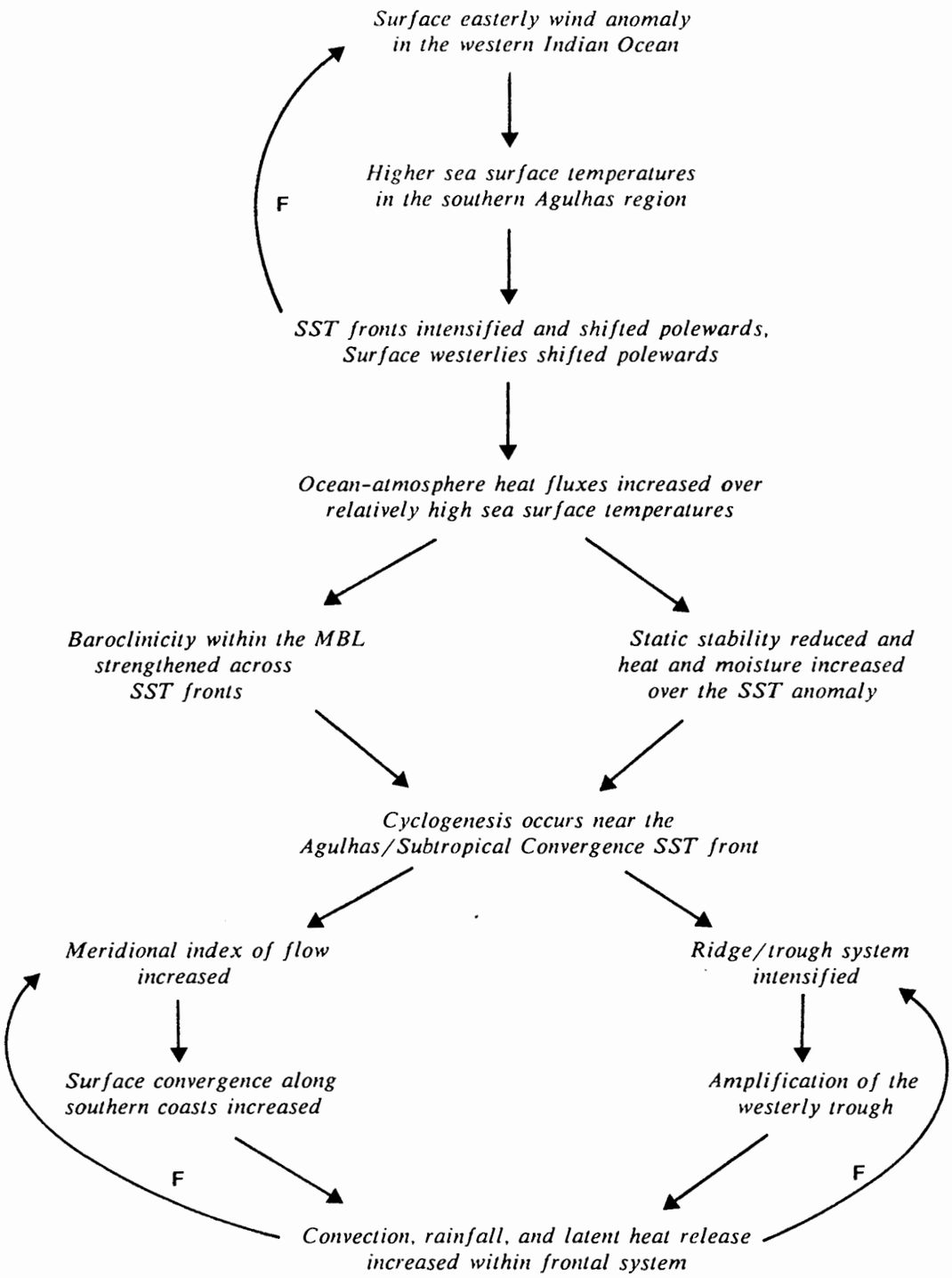

Figure 6.9 Proposed ocean-atmosphere feedback mechanisms south of Africa. 'F' denotes a feedback loop.

Based on previous observational and modeling results (Namias, 1974; Chervin et al., 1980; Palmer and Sun, 1985), lowered pressure and increased rainfall would be expected in close proximity to an extensive positive SST anomaly in the subtropics and extratropics. In addition, a high pressure system would be expected downstream from the anomaly. The case-studies provided evidence of the presence of such circulations. An ocean temperature anomaly southeast of the subcontinent would intensify if subjected to enhanced easterly and northerly air flow in the presence of anticyclonic circulation in the western Indian Ocean ahead of the surface low. Low-level baroclinicity within the MBL would shift poleward enabling an enhancement of the original atmospheric anomaly. The 1985 Agulhas warm event provided observational evidence that this self-enhancing ocean-atmosphere feedback mechanism can persist for several months and move westward across the Indian Ocean. A similar situation would not be found west of the Agulhas Retroflection where positive SST anomalies would tend to exhibit relatively short residence times. Intense wind mixing (de Ruijter and Boudra, 1985) and rapid surface cooling (Walker and Mey, 1988) would rapidly eliminate the abnormally warm surface layer unless the inter-ocean flux persisted. Large latitudinal shifts in the site of Agulhas Current retroflection occur on average every 30 to 55 days, in association with ring formation (Lutjeharms and van Ballegooyen, 1988). This periodicity could have important implications to intra-seasonal rainfall variations over the subcontinent.

The ocean-atmosphere interactions identified within this region would directly influence rainfall processes during early summer when temperate forcing is strongly established and also during the latter summer months in association with tropical influences. The tropical-temperate circulation interactions will be considered in detail in the next section.

Tropical-Temperate Interactions

The importance of tropical-temperate interactions to rainfall processes during both late and early summer seasons was clearly demonstrated in the case-study analyses. Although this study has concentrated on South African rainfall, spatial coherency of rainfall anomalies over southern Africa south of 10°S has been identified by Nicholson (1986) and attributed to the effects of tropical-temperate troughs. In this study, the central and western interior regions of southern Africa were found to be particularly dependent upon strong synoptic scale forcing as provided by tropical-temperate coupling during early and late summer. The spatial distribution of rainfall anomalies across the country during Mozambique/Agulhas warm events reflects the effects of

tropical-temperate trough systems. In Figure 6.10a, average rainfall departures for the 6 warmest January-March seasons within the Mozambique/Agulhas region (defined by PC 1 of Indian Ocean) over the 36 years are illustrated. A distinctive northwest to southeast orientation of positive rainfall departures across the central and western interior is apparent. In addition, the high-lying northeastern parts of the country received abnormally high rainfall. The stability of these rainfall patterns is confirmed through the use of linear correlation analyses (Figure 6.10b). These distinctive rainfall patterns over South Africa suggest enhanced moisture flux across the northeast parts of the country and an increased prevalence of tropical-temperate trough formation, thereby increasing rainfall across the central and western interior, as well as, over south coast areas during Mozambique/Agulhas warm events. The lower rainfall along the east coast suggests that relatively high pressure extended westward over land from the Indian Ocean, a commonly observed circulation feature of the case-studies.

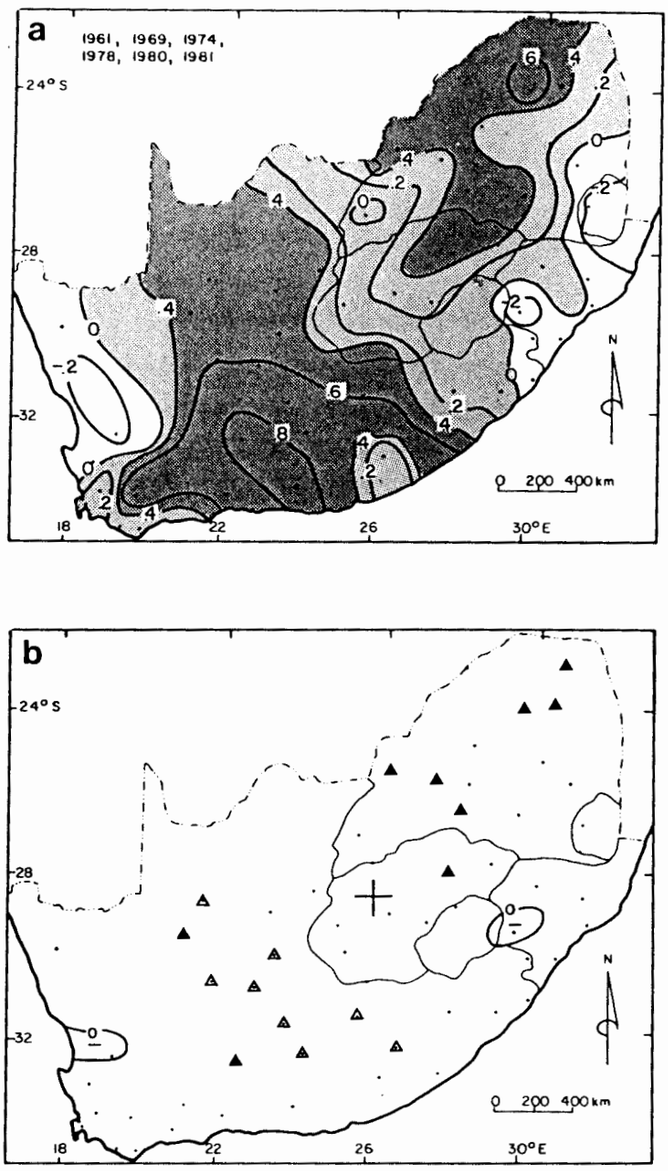

Figure 6.10 Spatial distribution of rainfall departures associated with east coast oceanic "warm events" a) Standardized station rainfall departures averaged over the 6 warmest January-March seasons within the Mozambique/Agulhas Current system (PC 1 of the Indian Ocean analysis, Location in Figure 3.1) b) Linear correlations between rainfall departures and SST anomalies in the same area as (a). Triangles depict correlations significant above the 10% level (r=0.29) and filled triangles those above the 5% level (r=0.34).

Within the Southern Hemisphere during summer, tropical heat release is centered over Indonesia, South America and Africa and excess energy is transported from these areas to the southeast (Vonder Haar, 1968) (Figure 6.5). Most of this energy is transported within tropical-temperate troughs, marked by cloud bands extending from the tropics to midlatitudes. The major hemispheric cloud band within the Indian Ocean exhibits the largest seasonal and interannual variability in median locations (Streten, 1973). A unique feature of this band is that its location is in opposite phase to that of the anticyclone. In summer it most frequently extends from tropical Africa or Madagascar southeastwards into the ocean to the west of the anticyclone, whereas in winter it is located to the east of the anticyclone which has shifted westwards. This annual shift may be related to the establishment of tropical convection over southern Africa during summer (Streten, 1973). On the interannual time scale, the bands have been observed to form over southern Africa during wetter seasons and further west over Madagascar during drier ones (Harrison, 1983). The preferential positioning of the tropical-temperate cloud bands over southern Africa has previously been explained in terms of enhanced upper air easterly flow over tropical/subtropical southern Africa accompanying high index phases of the Southern Oscillation (Harrison, 1983; Harrison, 1986a; Lindesay, 1988 a,b).

This study has demonstrated that positioning of the tropical-temperate troughs over southern Africa can also be explained in terms of surface circulation changes and ocean-atmosphere interactions in the southern African region. Intensification and westward positioning of the Indian Ocean Anticyclone during early or late summer would favor a westward positioning of the Indian Ocean cloud band. Oceanic warm events along the east coast and in the southern Agulhas current system accompany local intensification of anticyclonic circulation in the western Indian Ocean. The presence of these positive SST anomalies and attendant circulations would increase the likelihood of tropical-temperate trough formation over southern Africa by intensifying both tropical and extratropical circulation components. The contribution provided by each component within the coupled system would be influenced by the position and magnitude of the SST anomaly as well as the moisture flux convergence anomaly. In this regard, the western limit of abnormally warm waters or intense SST gradients would influence the location of cloud band formation. The ocean-atmosphere coupling mechanisms associated with local oceanic warm events within the Mozambique/Agulhas area and the Agulhas Retroflection region are presented schematically in Figure 6.11. The relative contributions of tropical and temperate circulations to tropical-temperate trough formation is also influenced by the season of occurrence. Baroclinic forcing is dominant in early summer when energy is exported from the extratropics to maintain the kinetic energy of the tropical circulation (Harrison, 1986c). Later in summer,

thermal forcing is more important than baroclinic forcing. The warm events south of Africa should thus provide more control over tropical-temperate trough formation during early summer months.

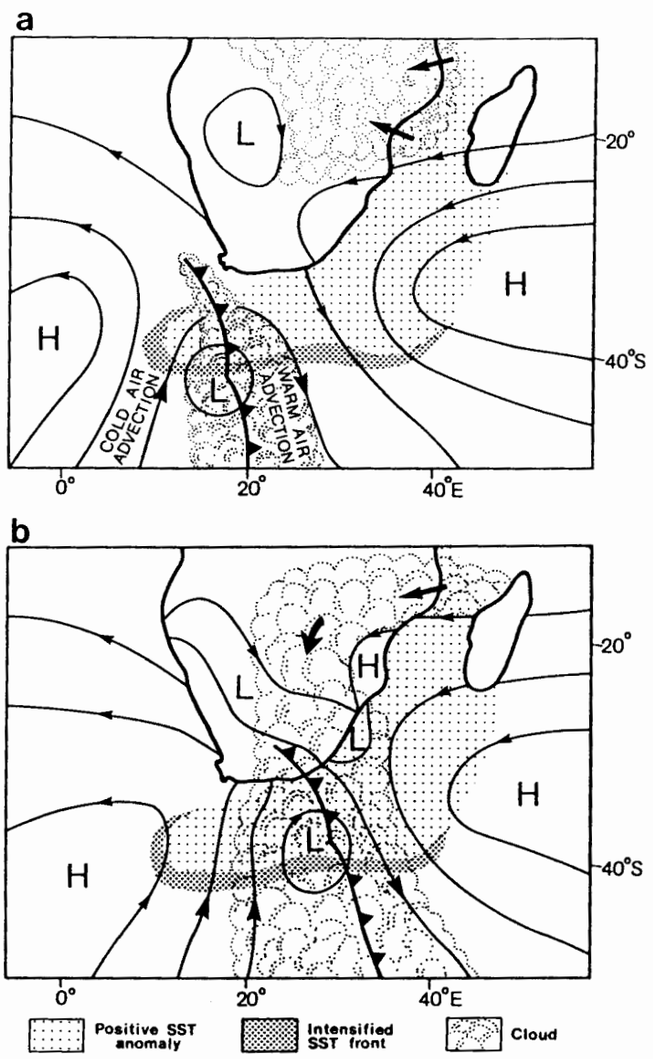

Figure 6.11 Schematic representation of enhanced tropical and extratropical circulations associated with SST anomalies within the Mozambique/Agulhas and Agulhas Retroflection regions. a) Tropical convection north of 25°S over eastern parts of the subcontinent is fueled by abnormally moist, tropical air entering from the Indian Ocean. Further south, cyclogenesis occurs in association with abnormally warm waters and enhanced SST gradients along the western and southern margins of the Agulhas Retroflection region. Westerly waves amplify through differential thermal advection within the ridge/trough system b) Surface convergence and upper air divergence intensifies through latent heat release as tropical and temperate circulations are coupled producing a tropical-temperate cloud band across the interior of southern Africa. Sea level pressures are shown over the ocean and 850 mb contours over the subcontinent.

The efficiency of precipitation processes over southern Africa would also depend on the residence time of the tropical-temperate trough system over the subcontinent. Organized deep convection within the baroclinic component over warm Agulhas waters could be expected to slow the system's eastward progression (Reed and Duncan, 1987), thereby prolonging its life span over the subcontinent. In addition, the presence of strong anticyclonic circulation within the western Indian Ocean would retard movement of the cold front and westerly trough, further prolonging the effects of the tropical-temperate coupling over southern Africa. A synthesis of these proposed coupling mechanisms and ocean-atmosphere feedbacks pertinent to tropical-temperate interactions are presented in Figure 6.12.

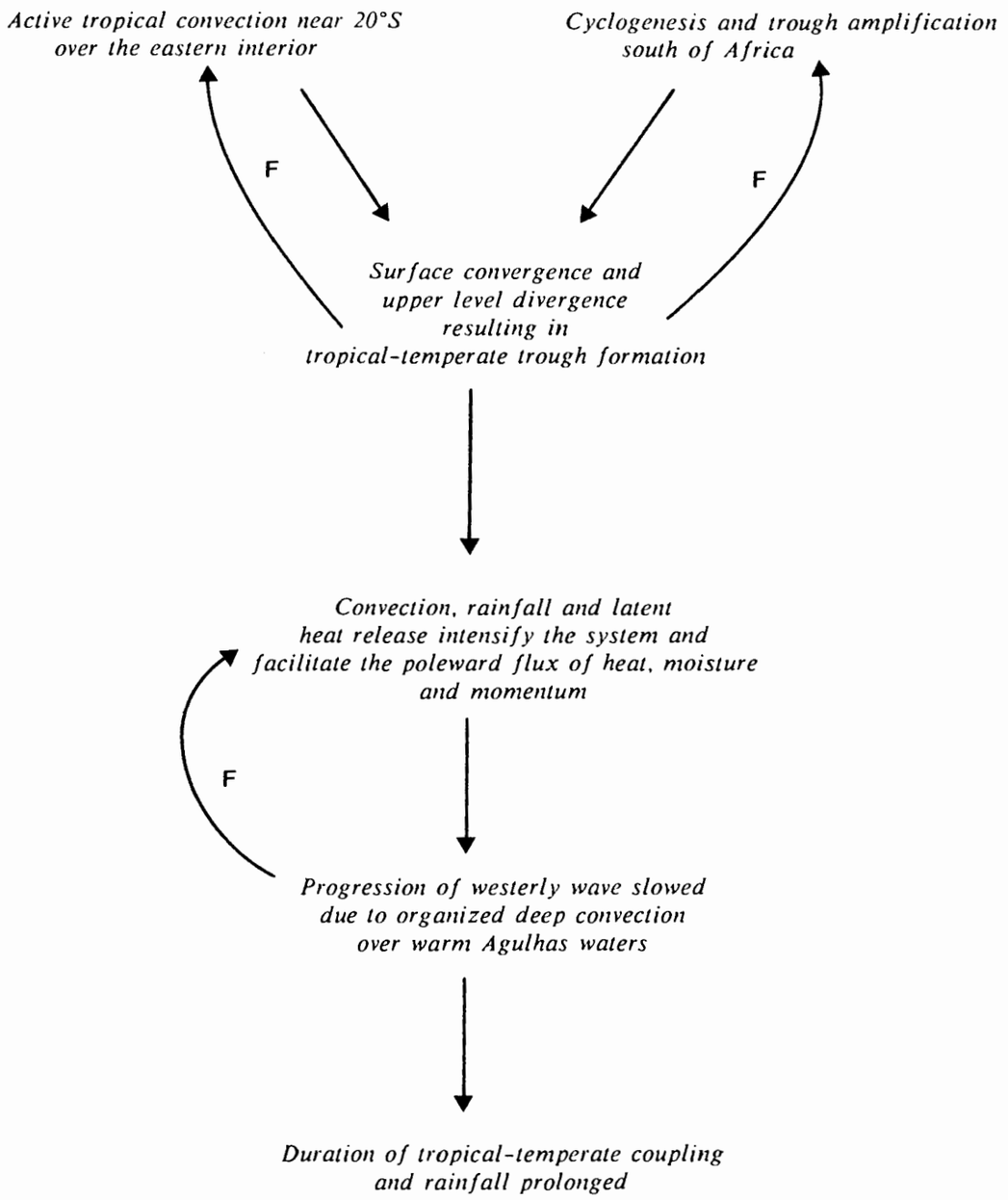

Figure 6.12 Tropical-temperate coupling and feedback mechanisms pertinent to rainfall over southern Africa. 'F' denotes a feedback mechanism.

CHAPTER 7

SUMMARY AND CONCLUSIONS

Sea surface temperature-rainfall relationships and associated ocean-atmosphere coupling mechanisms have been investigated on seasonal to synoptic time scales using statistical, observational and theoretical approaches. Exclusion of the rainfall anomalies which were closely associated with the Southern Oscillation facilitated this study of local ocean-atmosphere coupling mechanisms. In Chapter 3, the statistical relationships between ocean temperatures and summer rainfall were analyzed in detail. In Chapter 4, atmospheric circulations, surface heat fluxes and boundary layer modifications were assessed under contrasting SST and rainfall regimes. In Chapter 5, the SST-rainfall relationships and associated air-sea interactions were investigated in more detail by identifying the synoptic weather systems responsible for the rainfall anomalies during local oceanic "warm events". Results of the various approaches were synthesized in Chapter 6 and conceptual models were proposed for the ocean-atmosphere coupling mechanisms contributing to tropical, extratropical and tropical-temperate circulations during local oceanic warm events. The main conclusions reached from this research are detailed below.

1. Sea surface temperatures of the Mozambique, Agulhas and Benguela Current systems from 1949 through 1984 are positively correlated with summer rainfall over South Africa, such that warmer (cooler) waters co-occur with wetter (dryer) rainfall seasons. The positive relationships are stronger and more significant during both early and late summer seasons when rainfall anomalies associated with the Southern Oscillation are not considered. Before excluding Southern Oscillation influences, the strongest spatially coherent SST-rainfall correlations are negative and involve the tropical Indian Ocean, east of 50°E.

2. Statistical analyses, compositing analyses and case-studies suggest that future prediction efforts for summer rainfall over South Africa will benefit from a consideration of local SST anomaly patterns in combination with other atmospheric indices. During early summer (October-December), positive SST anomalies and intensified SST gradients south of Africa preceded abnormal rain events on a time-scale of weeks to months. Therefore, ocean dynamics within the Agulhas Current Retroflection region may play a decisive role in weather modification processes on relatively short time-scales. Wetter late summer

seasons (January-March) were preceded by positive SST anomalies in the Agulhas Current recirculation region east of South Africa during the previous season (October-December). The time-scales of interaction between SST anomalies and rainfall variations deserve more detailed study in the future.

3. Easterly wind anomalies across the southwest Indian Ocean and over source regions of the Agulhas Current precede and co-occur with positive SST anomalies along the east coast, south of 15°S, and in the southern Agulhas current system, including the Agulhas Retroflection region. The SST anomalies south of 30°S are generated primarily by abnormal southwestward transport within the southern Agulhas Current system and provide positive feedback to the initial atmospheric anomaly. Anticyclonic circulation southeast of Africa intensifies through differential thermal advection within the troposphere and a poleward shift in baroclinicity within the atmospheric marine boundary layer. Both processes facilitate a poleward displacement of the zonal westerlies enabling increased westward transport of Agulhas Current waters into the Retroflection region and the southeast Atlantic Ocean.

4. Along the east coast from 15° to 30° S, marine boundary layer characteristics are significantly different during WET and DRY seasons. In association with positive SST anomalies and more tropical airflow, atmospheric temperature and humidity increase considerably. A conceptual model is proposed to explain how these altered boundary layer conditions and surface wind changes enhance tropical convection in the vicinity of the Intertropical Convergence Zone. Briefly stated, increased moisture flux convergence over eastern tropical Africa leads to increased vertical circulations and latent heat release which augment tropical/subtropical rainfall. A positive feedback loop develops whereby the initial circulation anomaly generates a zonal circulation cell, intensifying convection over the eastern interior of the subcontinent.

5. An SST anomaly within the Agulhas Retroflection region produces relatively large surface heat flux changes as compared with the east and west coast areas. In association with an SST anomaly of +1°C, sensible heat flux increases by about 100% and latent heat flux by 23% over the region 35° to 41°S, 10° to 30°E. The higher SSTs and the enhanced horizontal heat flux gradients across the Agulhas/Subtropical Convergence SST front facilitate cyclogenesis and intensification of baroclinic disturbances by reducing low-level stability and increasing meridional contrasts of temperature, moisture and wind speed in the lower troposphere. Differential temperature and thickness advection intensify the

ridge/trough systems south of the subcontinent, thus increasing surface convergence along the south coast and convection, rainfall and latent heat release within the frontal system.

6. Along the west coast within the northern Benguela system (20°-25°S), boundary layer characteristics are only marginally different during contrasting rainfall regimes. It is concluded that in this area little ocean-atmosphere coupling takes place which directly influences rainfall over the summer rainfall region.

7. Tropical-temperate trough systems account for most of the abnormal rainfall during local oceanic warm events along the east coast and within the Agulhas Retroflection region. This is particularly the case for the western part of the country where rainfall is more event-related. The presence of positive SST anomalies to the east and south of Africa increases the likelihood of tropical-temperate trough formation over southern Africa by intensifying the tropical and extratropical components. The contribution provided by each component is influenced by the position and magnitude of the SST anomaly as well as the season of occurrence. An extreme westward placement of the positive Agulhas anomaly south of the country shifts the region of cyclogenesis and trough amplification westward, thus influencing the location of tropical-temperate cloud band formation across southern Africa.

In this research, ocean-atmosphere forcing mechanisms have been identified which contribute to rainfall variations over southern Africa in summer. Although the emphasis has been on obtaining insight into local SST-rainfall relationships and ocean-atmosphere coupling mechanisms in the absence of strong Southern Oscillation influences on rainfall, air-sea interactions may also provide some control over atmospheric circulations associated with high and low index phases of the Southern Oscillation.

The conclusions and conceptual models which have been presented await further testing with more sophisticated tools such as general circulation and coupled ocean-atmosphere models. As many of the atmospheric processes and air-sea interaction mechanisms are still inadequately understood, observational analyses must be continued to obtain further insight into the ocean-atmosphere interactions which affect weather and climate in the southern African region.

REFERENCES

Acharya, U.R. and N.S. Bhaskara Rao, 1981: Meteorology of Zambia : Parts I and II, Government Printers, Lusaka.

Aceitano, P., 1988: On the functioning of the Southern Oscillation in the South American Sector. Part I: Surface Climate, *Monthly Weather Review*, 116, 505-524.

Agenbag, J.J. and L.V.S. Shannon, 1987: Preliminary note on a recent perturbation in the Agulhas Current retroflection area, *Tropical Ocean-Atmosphere Newsletter*, 37, 10-11.

Anthes, R.A. and D. Keyser, 1979 : Tests of a fine-mesh model over Europe and the United States, *Monthly Weather Review*, 107, 1045-1078.

Anthes, R.A., Y.-H Kuo and J.R. Gyakum, 1983: Numerical simulation of a case of explosive marine cyclogenesis, *Monthly Weather Review*, 111, 1174-1188.

Bang, N.D., 1970: Dynamic interpretation of a detailed surface temperature chart of the Agulhas Current retroflexion and fragmentation area, *South African Geographical Journal*, 52, 67-76.

Barnett, T.P., 1981: Statistical prediction of North American air temperatures from Pacific predictors, *Monthly Weather Review*, 109, 1021-1041.

Barnett, T.P. 1983: Interaction of the monsoon and Pacific trade wind system at interannual time scales. Part 1. The equatorial zone, *Monthly Weather Review*, 111, 756-773.

Barnett, T.P., 1984: Long-term trends in surface temperature over the oceans, *Monthly Weather Review*, 112, 303-312.

Bhalotra, Y.P.R., 1973: Disturbances of the summer season affecting Zambia, *Technical Memorandum*, 3, Zambia Meteorological Department, Lusaka, 7pp.

Bjerknes, J., 1966: A possible response of the atmospheric Hadley circulation to equatorial anomalies of ocean temperatures, *Tellus*, 18, 820-829.

Bjerknes, J., 1969: Atmospheric teleconnections from the equatorial Pacific, *Monthly Weather Review*, 97, 163-172.

Blackmon, M.L. and N.C. Lau, 1980: Regional characteristics of the Northern Hemisphere wintertime circulation: a comparison of the simulation of a GFDL general circulation model with observations, *Journal of the Atmospheric Sciences*, 37, 497-514.

Blanc, T.V., 1987: Accuracy of bulk-method-derived flux, stability, and sea surface roughness, *Journal of Geophysical Research*, 92, 3867-3876.

Bretherton, F., 1981: The ocean surface energetics - a need for climate understanding. *Applications of existing satellite data to the study of the ocean surface energetics*, C. Gautier, Ed., University of Wisconsin Press, 5-14.

Bunker, A.F., 1976: Computations of surface energy flux and annual air-sea interaction cycles of the North Atlantic Ocean, *Monthly Weather Review*, 104, 1122-1140.

Bunker, A.F. and L.V. Worthington, 1976: Energy exchange charts of the North Atlantic Ocean, *Bulletin of the American Meteorological Society*, 57, 670-678.

Cadet, D.L., 1985: The Southern Oscillation over the Indian Ocean, *Journal of Climatology*, 5, 189-212.

Cadet, D.L. and B.C. Diehl, 1984: Interannual variability of surface fields over the Indian Ocean during recent decades, *Monthly Weather Review*, 112, 1921-1935.

Cadet, D.L. and G. Beltrando, 1987: *Report of the third session of the CCCO Indian Ocean climate related studies panel*, Vacoas, Mauritius, April 1987.

Chen, W.Y., 1982: Assessment of Southern Oscillation sea-level pressure indices, *Monthly Weather Review*, 110, 800-807.

Chervin, R.M., W.M. Washington and S.H. Schneider, 1976: Testing the statistical significance of the response of the NCAR general circulation model to North Pacific Ocean surface temperature anomalies, *Journal of the Atmospheric Sciences*, 33, 413-423.

Chervin, R.M., J.E. Kutzbach, D.D. Houghton and R.G. Gallimore, 1980: Response of the NCAR general circulation model to prescribed changes in ocean surface temperature. Part II. Midlatitude and subtropical changes, *Journal of the Atmospheric Sciences*, 37, 308-332.

Danard, M., 1986: On the sensitivity of predictions of maritime cyclogenesis to convective precipitation and sea temperature, *Atmosphere-Ocean*, 24, 52-72.

Darbyshire, M., 1966: The surface water near the coasts of southern Africa, *Deep-Sea Research*, 13, 57-81.

Davis, R.E., 1976: Predictability of sea surface temperature and sea level pressure anomalies over the North Pacific Ocean, *Journal of Physical Oceanography*, 6, 249-266.

Davis, R.E., 1978: Predictability of sea level pressure anomalies over the North Pacific Ocean, *Journal of Physical Oceanography*, 8, 233-246.

de Ruijter, W.P.M., 1982: Asymptotic analysis of the Agulhas and Brazil current systems, *Journal of Physical Oceanography*, 12, 361-373.

de Ruijter, W.P.M. and D.B. Boudra, 1985: The wind-driven circulation in the South Atlantic-Indian Ocean, I. Numerical experiments in a one-layer model, *Deep-Sea Research*, 32, 557-574.

Dyer, T.G.J., 1974: The frequency distribution of annual precipitation totals for South Africa, *South African Journal of Science*, 70, 180-182.

Dyer, T.G.J., 1975: The assignment of rainfall stations into homogeneous groups: an application of principal component analysis, *Quarterly Journal of the Royal Meteorological Society*, 101, 1005-1013.

Earle, M.D., 1985: Statistical comparisons of ship and buoy marine observations. *MEC Systems Corp. Rep. MEC-85-8* [Available from NESDIS/NOAA].

Estie, K.E., 1981: The Laingsburg flood disaster of 25 January 1981, *South African Weather Bureau Newsletter*, 383, 19-32.

Estie, K.E., 1984: Forecasting the formation and movement of coastal lows, Abstracts and summary of the Coastal Low Workshop, Institute of Maritime Technology, Simonstown, 17-27.

Estie, K.E., 1988: Floods in the northern and north-eastern Free State - 10 to 12 March 1988, *South African Weather Bureau Newsletter*, 470, 6-7.

Folland, C.K., D.E. Parker and F.E. Kates, 1984: Worldwide marine temperature fluctuations 1856-1981, *Nature*, 310, 670-673.

Folland, C.K., T.N. Palmer and D.E. Parker, 1986: Sahel rainfall and worldwide sea temperatures, 1901-85, *Nature*, 320, 602-607.

Frankignoul, C., 1985: Sea surface temperature anomalies, planetary waves, and air-sea feedbacks in the middle latitudes, *Reviews of Geophysics*, 23, 357-390.

Garstang, M., B.E. Kelbe, G.D. Emmitt and W.B. London, 1987: Generation of convective storms over the escarpment of northeastern South Africa, *Monthly Weather Review*, 115, 429-443.

Gill, A.E., 1980: Some simple solutions for heat-induced tropical circulation, *Quarterly Journal of the Royal Meteorological Society*, 106, 447-462.

Gillooly, J.F. and N.D. Walker, 1984: Spatial and temporal behaviour of SST in the South Atlantic, *South African Journal of Science*, 80, 97-100.

Graham, A.E., 1982: Winds estimated by the Voluntary Observing Fleet compared with instrumented measurements at fixed positions, *Meteorological Magazine*, 111, 312-327.

Gronas, S., A. Foss and M. Lystad, 1987: Numerical simulation of polar lows in the Norwegian Sea, *Tellus*, 39A, 334-353.

Gründlingh, M.L., 1978: Drift of a satellite-tracked buoy in the southern Agulhas Current and Agulhas Return Currnt, *Deep-Sea Research*, 25, 1209-1224.

Guttman, L., 1954: Some necessary conditions for common-factor analysis; *Psychometrika*, 19, 149-161.

Harangozo, S., and M.S.J. Harrison, 1983: On the use of synoptic data in indicating the presence of cloud bands over southern Africa, *South African Journal of Science*, 79, 413-414.

Harnack, R.P. and A.J. Broccoli, 1979: Associations between sea surface temperature gradient and overlying mid-tropospheric circulations in the North Pacific region, *Journal of Physical Oceanography*, 9, 1232-1242.

Harnack, R.P. and J. Harnack, 1985: Intra-and inter-hemispheric teleconnections using seasonal Southern Hemisphere sea level pressure, *Journal of Climatology*, 5, 283-296.

Harris, T.F.W., 1972: Sources of the Agulhas Current in the spring of 1964, *Deep-Sea Research*, 19, 633-650.

Harris, T.F.W.and D. van Foreest, 1978: The Agulhas Current in March 1969, *Deep-Sea Research*, 25, 549-561.

Harrison, M.S.J., 1983: The Southern Oscillation, zonal equatorial circulation cells and South African rainfall, *Preprints of the 1st International Conference on Southern Hemisphere Meteorology*, American Meteorological Society, 302-305.

Harrison, M.S.J., 1984: A generalized classification of South African summer rain-bearing synoptic systems, *Journal of Climatology*, 4, 547-560.

Harrison, M.S.J., 1986a: A synoptic climatology of South African rainfall variations, *Unpublished Ph.D. Thesis, University of the Witwatersrand*, 341 pp.

Harrison, M.S.J., 1986b: Circulation variations on a semi-annual cycle over southern Africa, *Preprints of the 2nd International Conference on Southern Hemisphere Meteorology*, American Meteorological Society, 382-385.

Harrison, M.S.J., 1986c: Verification of the Eliassen-Palm relationship over southern Africa, *Preprints of the 2nd International Conference on Southern Hemisphere Meteorology*, American Meteorological Society, 283-286.

Harrison, M.S.J., S.R. Juhnke and N.D. Walker, 1989: Circulation differences between one wet and one dry month of October and January over the interior of South Africa, *Journal of Climatology*, submitted.

Hastenrath, S., 1984: Interannual variability and the annual cycle: mechanisms of circulation and climate in the tropical Atlantic sector, *Monthly Weather Review*, 112, 1097-1107.

Hastenrath, S., 1985: *Climate and Circulation of the Tropics*, D. Reidel, Dordrecht, 455 pp.

Hastenrath, S. and P.J. Lamb, 1979: *Climatic Atlas of the Indian Ocean, Parts I and II.*, University of Wisconsin Press, Wisconsin.

Hellerman, S. and M. Rosenstein, 1983: Normal monthly wind stress over the World Ocean with error estimates, *Journal of Physical Oceanography*, 13, 1093-1104.

Hendon, H.H. and D.L. Hartmann, 1982: Stationary waves on a sphere: sensitivity to thermal feedback, *Journal of the Atmospheric Sciences*, 39, 1906-1920.

Hirst, A.C. and S. Hastenrath, 1983: Atmosphere-ocean mechanisms of climate anomalies in the Angola-tropical Atlantic sector, *Journal of Physical Oceanography*, 13, 1146-1157.

Höflich, O., 1984: Climate of the South Atlantic Ocean, in *World Survey of Climatology*, V.15, edited by H. van Loon, 1-132, Elsevier, New York.

Holton, J.R., 1979: *An Introduction to Dynamic Meteorology*, Academic Press, New York, 391 pp.

Horel, J.D., 1981: A rotated principle component analysis of the interannual variability of the Northern Hemisphere 500 mb height field, *Monthly Weather Review*, 109, 2080-2092.

Horel, J.D. and J.M. Wallace, 1981: Planetary-scale atmospheric phenomena associated with the Southern Oscillation, *Monthly Weather Review*, 109, 813-829.

Hsu, S.A. 1984: Sea breeze-like winds across the north wall of the Gulf Stream: An analytical model, *Journal of Geophysical Research*, 89, 2025-2028.

Jackson, S.P. 1952: Atmospheric circulation over South Africa, *South African Geographical Journal*, 34, 48-60.

James, I.N. and L.T. Anderson, 1984: The seasonal mean flow and distribution of large-scale weather systems in the Southern Hemisphere: effects of moisture transports, *Quarterly Journal of the Royal Meteorological Society*, 110, 943-966.

Johnson, D.H., 1969: The role of the tropics in the global circulation, in *The Global Circulation of the Atmosphere*, Ed. Corby, G.A., Royal Meteorological Society, 113-136.

Jury, M.R., F.A. Shillington, G. Prestidge and C.D. Maxwell, 1984: Meteorological and oceanographic aspects of a winter storm over the southwestern Cape Province, South Africa, *South African Journal of Science*, 82, 315-319.

Jury M. and N.D. Walker, 1988: Marine boundary layer modification across the edge of the Agulhas Current, *Journal of Geophysical Research*, 93, 647-654.

Kaiser, H.F., 1958: The varimax criterion for analytic rotation in factor analysis, Psychometrika, 23, 187-200.

Keen, C.S. and P.D. Tyson, 1973: Seasonality of South African rainfall: a note on its regional delimitation using spectral analysis, *Archiv. für Meteorologie Geophysik und Bioklimatologie, Series B.*, 21, 207-214.

Kelbe, B.E., 1988: Features of westerly waves propagating over southern Africa during summer, *Monthly Weather Review*, 116, 60-70.

Kendall, M., 1975: Multivariate Analysis, Charles Griffin, 210 pp.

Kershaw, R., 1988: The effect of a sea surface temperature anomaly on a prediction of the onset of the south-west monsoon over India, *Quarterly Journal of the Royal Meteorological Society*, 114, 325-345.

Kondo, J., 1975: Air-sea bulk transfer coefficients in diabatic conditions, *Boundary Layer Meteorology*, 9, 91-112.

Kraus, E.B., 1977: Subtropical droughts and cross-equatorial energy transports, *Monthly Weather Review*, 105, 1009-1018.

Kumar, S., 1978: Interaction of upper westerly waves with the Intertropical Convergence Zone and their effect on the weather over Zambia during the rainy season, Government Printer, Lusaka, 36 pp.

Kutzbach, J.E., 1967: Empirical eigenvectors of sea-level pressure, surface temperature and precipitation complexes over North America, *Journal of Applied Meteorology*, 6, 791-802.

Kutzbach, J.E., R.M. Chervin and D.D. Houghton, 1977: Response of the NCAR general circulation model to prescribed changes in ocean surface temperature, Part I. Mid-latitude changes, *Journal of the Atmospheric Sciences*, 34, 1200-1213.

Lamb, P.J. 1978: Large-scale tropical Atlantic surface circulation patterns associated with SubSaharan weather anomalies, *Tellus*, 30, 240-251.

Lau, K.M. and P.H. Chan, 1983: Short-term climate variability and atmospheric teleconnections from satellite-observed outgoing longwave radiation. Part II. Lagged correlations, *Journal of the Atmospheric Sciences*, 40, 2751-2767.

Lindesay, J.A., 1984: Spatial and temporal rainfall variability over South Africa, 1963 to 1981, *South African Geographical Journal*, 66, 168-175.

Lindesay, J.A., 1988a: South African rainfall, the Southern Oscillation and a southern hemisphere semi-annual cycle, *Journal of Climatology*, 8, 17-30.

Lindesay, J.A., 1988b: The Southern Oscillation and atmospheric circulation changes over southern Africa, *Unpublished PhD. Thesis*, University of the Witwatersrand, 284 pp.

Lindesay, J.A. and M.S.J. Harrison, 1986: The Southern Oscillation and flow fields over southern Africa, *Preprints of the 2nd International Conference on Southern Hemisphere Meteorology*, American Meteorological Society, 457-460.

Lindesay, J.A. M.S.J. Harrison and M.P. Haffner, 1986: The Southern Oscillation and South African rainfall, *South African Journal of Science*, 82, 196-198.

Liu, W.T., K.B. Katsaros, and J.A. Businger, 1979: Bulk parameterization of air-sea exchanges of heat and water vapor including the molecular constraints at the interface, *Journal of the Atmospheric Sciences*, 36, 1722-1735.

Lough, J.M., 1986: Tropical Atlantic SST and rainfall variations in Sub-Saharan Africa, *Monthly Weather Review*, 114, 561-570.

Lutjeharms, J.R.E., 1972: A quantitative assessment of year-to-year variability in water movement in the Southwest Indian Ocean, *Nature Physical Science*, 239, 59-60.

Lutjeharms, J.R.E., 1988: Examples of extreme circulation events at the Agulhas retroflection, *South African Journal of Science*, 84, 584-586.

Lutjeharms, J.R.E., N.D. Bang, and C.P. Duncan, 1981: Characteristics of the currents east and south of Madagascar, *Deep-Sea Research*, 28A, 879-899.

Lutjeharms, J.R.E. and H.R. Valentine, 1984: Southern Ocean thermal fronts south of Africa, *Deep-Sea Research*, 31, 1461-1475.

Lutjeharms, J.R.E. and A.L. Gordon, 1987: Shedding of an Agulhas ring observed at sea, *Nature*, 235, 138-140.

Lutjeharms, J.R.E. and R.C. van Ballegooyen, 1988: Retroflection of the Agulhas Current, *Journal of Physical Oceanography*, 18, 1570-1583.

Malkus, J.S., 1962: Large-scale interactions, in *The Sea* V. 1, Physical Oceanography, edited by M.N. Hill, Wiley Interscience, New York, 88-285.

Mansfield, D.A., 1986: The skill of dynamical long-range forecasts, including the effects of sea surface temperature anomalies, *Quarterly Journal of the Royal Meteorological Society*, 112, 1145-1176.

Mardia, K.V., J.T. Rent and J.M. Bibby, 1979: *Multivariate Analysis*, Academic Press, London, 519 pp.

Markham, C.G. and D.R. Mclain, 1977: Sea surface temperature related to rain in Ceara, north-eastern Brazil, *Nature*, 265, 320-323.

Mason, S.J. 1988: The nature of sea surface temperature changes in the Agulhas Current and their influence upon precipitation variability over South Africa, *Unpublished Honours Thesis*, Hertford College, United Kingdom, 158 pp.

McGee, O.W. and S.L. Hastenrath, 1966: Harmonic analysis of the rainfall over South Africa, *Notos*, 15, 79-89.

McLain, D.R., R.E. Brainard and J.G. Norton, 1985: Anomalous warm events in Eastern Boundary Current systems, CalCOFI Report, Vol. XXVI, 51-64.

Mey, R.D., N.D. Walker and M.R. Jury, 1989: Surface heat fluxes and marine boundary layer modification in the Agulhas Retroflection region, *Journal of Geophysical Research*, submitted.

Mobley, C.D. and R.W. Preisendorfer, 1985: Statistical analysis of historical climate data sets, *Journal of Climate and Applied Meteorology*, 24, 555-567.

Moura, A.D. and J. Shukla, 1981: On the dynamics of droughts in northeastern Brazil: Observation, theory and numerical experiments with a General Circulation Model, *Journal of Atmospheric Sciences*, 38, 2653-2675.

Namias, J., 1973: Thermal communication between the sea surface and the lower troposphere, *Journal of Physical Oceanography*, 3, 373-378.

Namias, J., 1974: Longevity of a coupled air-sea-continent system, *Monthly Weather Review*, 102, 638-648.

Namias, J., 1976: Negative ocean-air feedback systems over the North Pacific in the transition from warm to cold seasons, *Monthly Weather Review*, 104, 1107-1121.

Namias, J. and R.M. Born, 1970: Temporal coherence in North Pacific sea surface temperature patterns, *Journal of Geophysical Research*, 75, 5922-5955.

Namias, J. and D.R. Cayan, 1981: Large-scale air-sea interactions and short-period climatic fluctuations, *Science*, 214, 869-876.

Newell, R.E., R. Selkirk and W. Ebisuzaki, 1982: The Southern Oscillation: sea surface temperature and wind relationships in a 100-year data set, *Journal of Climatology*, 2, 357-373.

Nicholls, N., 1980: Long-range weather forecasting: value, status and prospects, *Reviews of Geophysics and Space Physics*, 18, 771-788.

Nicholson, S.E., 1980: The nature of rainfall fluctuations in subtropical west Africa, *Monthly Weather Review*, 108, 473-487.

Nicholson, S.E., 1986: The nature of rainfall variability in Africa south of the Equator, *Journal of Climatology*, 6, 515-530.

Nicholson, S.E. and D. Entekhabi, 1987: Rainfall variability in equatorial and southern Africa: relationships with sea surface temperatures along the southwestern coast of Africa, *Journal of Climate and Applied Meteorology*, 26, 561-578.

Nuss, W.A. and R.A. Anthes, 1987: A numerical investigation of low-level processes in rapid cyclogenesis, *Monthly Weather Review*, 115, 2728-2743.

Onesta, P.A. and P. Verhoef, 1976: Annual rainfall frequency distributions for 80 rainfall districts in South Africa, *South African Journal of Science*, 72, 120-122.

Palmer, T.N. and Zhaobo Sun, 1985: A modelling and observational study of the relationships between SST in the Northwest Atlantic and atmospheric general circulations, *Quarterly Journal of the Royal Meteorology Society*, 111, 947-975.

Palmer, T.N. and D.A. Mansfield, 1984: The response of two atmospheric general circulation models to sea surface temperature anomalies in the tropical east and west Pacific, *Nature*, 310, 483-485.

Parrish, R.H., A. Bakun, D.M. Husby and C.S. Nelson, 1983: Comparative climatology of selected environmental processes in relation to eastern boundary current pelagic fish reproduction, In, *Proc. Expert consultation to examine changes in abundance and species of neritic fish resources*, San José, Costa Rica, April 1983, FAO Fish Rept, No 291, part 3, edited by G.D. Sharp and J. Csirke, 731-777.

Pearce, A.F., 1977: Some features of the upper 500m of the Agulhas Current, *Journal of Marine Research*, 35, 731-753.

Pearce, A.F. and M.L. Gründlingh, 1982: Is there a seasonal variation in the Agulhas Current?, *Journal of Marine Research*, 40, 177-184.

Philips, M.J., 1986: The improved SADCO marine climatology database, *CSIR Technical Report* T/SEA 8606, 7 pp.

Phillips, T.J. 1984: The seasonal response of the Held-Suarez Climate Model to prescribed ocean temperature anomalies. Part II. Dynamical analysis, *Journal of the Atmospheric Sciences*, 41, 2918-2933.

Phillips, T.J. and A.J. Semtner, Jr, 1984: The seasonal response of the Held-Suarez climate model to prescribed ocean temperature anomalies. Part I. Results of decadal integrations, *Journal of the Atmospheric Sciences*, 41, 2605-2619.

Picaut, J., J. Servain, P. Lecomte, M. Seva, S. Lukas and G. Rougier, 1985: *Climatic Atlas of the Tropical Atlantic Wind Stress and Sea Surface Temperture 1964-1979*. Université de Bretagne Occidentale (Laboratoire d'Oceanographie Physique)/University of Hawaii (Joint Institute for Marine and Atmospheric Research): 467 pp.

Pittock, A.B., 1973: Global meridional interactions in the stratosphere and troposphere, *Quarterly Journal of the Royal Meteorological Society*, 99, 424-437.

Priestly, C.H.B., 1964: Rainfall-SST Associations on the New South Wales Coast, *Australian Meteorology Magazine*, 47, 15-25.

Quinn, S.J., 1988: The weather of February 1988, *S.A. Weather Bureau Newsletter*, 467, 20-26.

Ramage, C.S., 1983: Teleconnections and the siege of time, *Journal of Climatology*, 3, 223-231.

Ramage, C.S., 1984a: Climate of the Indian Ocean north of 35°S, In: *World Survey of Climatology*, V.15, edited by H. van Loon, 603-672.

Ramage, C.S., 1984b: Can shipboard measurements reveal secular changes in tropical air-sea heat flux?, *Journal of Climate and Applied Meteorology*, 2, 187-193.

Ramage, C.S., 1987: Secular changes in reported surface wind speeds over the oceans, *Journal of Climate and Applied Meteorology*, 26, 525-528.

Rasmusson, E.M. and T.H. Carperter, 1982: Variations in tropical sea surface temperature and surface wind fields associated with the Southern Oscillation/El Nino, *Monthly Weather Review*, 110, 354-384.

Reed, R.J. and C.N. Duncan, 1987: Baroclinic instability as a mechanism for the serial development of polar lows: A case study, *Tellus*, 39A, 376-384.

Reed, R.J. and M.D. Albright, 1986: A case study of explosive cyclogenesis in the Eastern Pacific, *Monthly Weather Review*, 114, 2297-2319.

Richman, M.B., 1986: Rotation of principal components, *Journal of Climatology*, 6, 293-335.

Richman, M.B. and P.J. Lamb, 1985: Climatic pattern analysis of three-and seven-day summer rainfall in the central United States: Some methodological considerations and a regionalization, *Journal of Climate and Applied Meteorology*, 24, 1325-1343.

Rogers, J.C., 1976: Sea surface temperature anomalies in the eastern North Pacific and associated wintertime atmospheric fluctuations over North America, 1960-1973, *Monthly Weather Review*, 104, 985-993.

Rowntree, P.R., 1979: The effects of changes in ocean temperature on the atmosphere, *Dynamics of Atmospheres and Oceans*, 3, 373-390.

Sanders, F. and J.R. Gyakum, 1980: Synoptic-dynamic climatology of the "bomb", *Monthly Weather Review*, 108, 1589-1606.

Saur, J.F.T., 1963: A study of the quality of sea water temperatures reported in logs of ships' weather observations, *Journal of Applied Meteorology*, 2, 417-425.

Schulze, B.R. 1965: *Climate of South Africa: Part 8: General Survey, WB28*, South African Weather Bureau, 330 pp.

Shannon, L.V., 1985: The Benguela Ecosystem Part I. Evolution of the Benguela, physical features and processes, *Oceanography and Marine Biology Annual Review*, 23, 105-182.

Shannon, L.V., A.J. Boyd, G.B. Brundrit and J. Taunton-Clark, 1986: On the existence of an El Nino-type phenomenon in the Benguela system, *Journal of Marine Research*, 44, 495-520.

Shaw G. and D. Wheeler, 1985: *Statistical techniques in Geographical Analysis*, John Wiley and Sons, United Kingdom, 364 pp

Shillington, F.A., G.B. Brundrit, A. Boyd, J.J. Agenbag, L.V. Shannon and J.R.E. Lutjeharms, 1989: The coastal current circulation during the Orange River flood 1988, *Proceedings of the Royal Society of South Africa*, submitted.

Shukla, J. 1986: SST anomalies and blocking, In *Anomalous Atmospheric Flows and Blocking*, Advances in Geophysics, 29, 443-452.

Shukla J. and B. Bangaru, 1979: Effect of a Pacific SST anomaly on the circulation over North America: A numerical experiment with the GLAS model, *GARP Publication Ser.* 22, 501-518.

Simpson, R.W. and W.K. Downey, 1975: The effect of a warm mid-latitude SST anomaly on a numerical simulation of the general circulation of the Southern Hemisphere, *Quarterly Journal of the Royal Meteorological Society*, 101, 847-867.

Smith, A.V., 1985: Studies of the effects of cold fronts during the rainy season in Zimbabwe, *Weather*, 40, 198-203.

Stoeckenius, T., 1981: Interannual variations of tropical precipitation patterns, *Monthly Weather Review*, 109, 1233-1247.

Streten, N.A., 1973: Some characteristics of satellite-observed bands of persistent cloudiness over the Southern Hemisphere, *Monthly Weather Review*, 101, 486-495.

Streten, N.A., 1981: Southern Hemisphere sea surface temperature variability and apparent associations with Australian rainfall, *Journal of Geophysical Research*, 86C, 485-497.

Strong, A.E. and E.P. McClain, 1984: Improved ocean surface temperatures from space-Comparisons with drifting buoys, *Bulletin of the American Meteorology Society*, 65, 138-142.

Taljaard, J.J. 1972: Synoptic Meteorology of the Southern Hemisphere, In *Meteorology of the Southern Hemisphere*, Ed. Newton, C.W., Meteorological Monographs, 139-213.

Taljaard, J.J., 1981: The anomalous climate and weather systems of January to March 1974, *South African Weather Bureau Technical Paper, No.* 9, 92 pp.

Taljaard, J.J., 1985: Cut-off lows in the South African region, *South African Weather Beureau Technical Paper, No.* 14, 153 pp.

Taljaard, J.J., 1986a: Change of rainfall distribution and circulation patterns over southern Africa in summer, *Journal of Climatology*, 6, 579-592.

Taljaard, J.J. 1986b, Contrasting atmospheric circulation during dry and wet summers in South Africa, *South African Weather Bureau Newsletter*, 445, 1-5.

Taljaard, J.J. and H. van Loon, 1984: Climate of the Indian Ocean south of 35°S, In: *World Survey of Climatology*, V.15, edited by H. van Loon, 505-601.

Terblanche, D.E. and J.J. Taljaard, 1987: Reënvalkontraste oor Suiden Suidwes-Afrika en anomalieë van die atmosferiese sirkulasie in Desember 1986 en Januarie en Februarie 1987, *South African Weather Bureau Newsletter*, 456, 4-12.

Torrance, J.D., 1979: Upper windflow patterns in relation to rainfall in South-east central Africa, *Weather*, 34, 106-115.

Trenberth, K.E., 1976: Spatial and temporal variations of the Southern Oscillation, *Quarterly Journal of the Royal Meteorological Society*, 102, 639-653.

Trenberth, K.E., 1981: Observed Southern Hemisphere eddy statistics at 500 mb: frequency and spatial distribution, *Journal of the Atmospheric Sciences*, 38, 2585-2605.

Troup, A.J. 1965: The 'Southern Oscillation', Quarterly Journal of the Royal Meteorological Society, 91, 490-506.

Tyson, P.D., 1981: Atmospheric circulation variations and the occurrence of extended wet and dry spells over southern Africa, *Journal of Climatology*, 1, 115-130.

Tyson, P.D., 1984: The atmospheric modulation of extended wet and dry spells over South Africa, 1958-1978, *Journal of Climatology*, 4, 621-635.

Tyson, P.D. 1986: *Climatic Change and Variability in Southern Africa*, Oxford University Press, Cape Town, 220 pp.

Tyson, P.D., T.G. Dyer and M.N. Mametse, 1975: Secular changes in South African rainfall: 1880 to 1972, *Quarterly Journal of the Royal Meteorological Society*, 101, 817-833.

van Heerden, J., 1988: A season of floods over South Africa, July 1987 to June 1988, *Floods in Perspective Conference Proceedings*, Paper 1.2, Division of Hydraulic and Water Engineering of the S.A. Institute of Civil Engineers, Pretoria, South Africa, October, 1988.

van Heerden, J., D.E. Terblanche and G.C. Schulze, 1988: The Southern Oscillation and South African summer rainfall, *Journal of Climatology*, 8, 577-597.

van Loon, H., 1967: The half-yearly oscillations in middle and high southern latitudes and the coreless winter, *Journal of the Atmospheric Sciences*, 24, 472-486.

van Loon, H. and R.L. Jenne, 1969: The half-yearly oscillations in the tropics of the Southern Hemisphere, *Journal of the Atmospheric Sciences*, 26, 218-232.

van Loon, H. and R.L. Jenne, 1970: On the half-yearly oscillations in the tropics, *Tellus*, 22, 391-398.

van Loon, H. and R.A. Madden, 1981: The Southern Oscillation Part I: Global associations with pressure and temperature in northern winter, *Monthly Weather Review*, 109, 1150-1162.

Vonder Haar, T.H., 1968: Variations of the Earth's radiation budget in meteorological satellite instrumentation and data processing, Final Report, Contract NASW-65, 1958-68, Dept of Meteorology, University of Wisconsin, 179 pp.

Vowinckel, E., 1955: Southern Hemisphere weather map analysis; five-year mean pressures, *Notos*, 4, 17-50.

Walker, N.D., 1986: Satellite observations of the Agulhas Current and episodic upwelling south of Africa, *Deep-Sea Research*, 33, 1083-1106.

Walker, N.D., 1987: Interannual sea surface temperature variability and associated atmospheric forcing within the Benguela system, *The Benguela and Comparable Ecosystems. South African Journal of Marine Science*. 5 (special issue), Eds. Payne, A.I.L. J.A. Gulland and K.H. Brink, 121-132.

Walker, N.D., J. Taunton-Clark and J. Pugh, 1984: Sea temperatures off the South African west coast as indicators of Benguela warm events, *South African Journal of Science*, 80, 72-77.

Walker, N.D. and R.D. Mey, 1988: Ocean-atmosphere heat fluxes within the Agulhas Retroflection Region, *Journal of Geophysical Research*, 93C, 15473-15483.

Walker, N.D.and J.A. Lindesay, 1988: Ocean-atmosphere interactions relating to the February-March 1988 flood events, *Floods in Perspective Conference Proceedings*, Paper 1.3, Division of Hydraulic and Water Engineering of the S.A. Institute of Civil Engineers, Pretoria, South Africa, October 1988.

Walker, N.D. and J.A. Lindesay, 1989: Preliminary observations of oceanic influences on the February-March 1988 floods in central South Africa, *South African Journal of Science*, in press.

Walsh, J.E. and M.B. Richman, 1981: Seasonality in the associations between surface temperatures over the United States and the North Pacific Ocean, *Monthly Weather Review*, 109, 767-783.

Walsh, J.E., M.B. Richman and D.W. Allen, 1982: Spatial coherence of monthly precipitation in the United States, *Monthly Weather Review*, 110, 272-286.

Weare, B.C. 1977: Empirical orthogonal analysis of Atlantic Ocean surface temperatures, *Quarterly Journal of the Royal Meteorological Society*, 103, 467-478.

Weare, B.C., 1979: A statistical study of the relationships between ocean surface temperatures and the Indian Monsoon, *Journal of the Atmospheric Sciences*, 36, 2279-2291.

Webster, P.J. 1981: Mechanisms determining the atmospheric response to sea surface temperature anomalies, *Journal of the Atmospheric Sciences*, 38, 554-571.

Webster, P.J. 1982: Seasonality in the local and remote atmospheric response to sea surface temperature anomalies, *Journal of the Atmospheric Sciences*, 39, 41-52.

Wright, P.B., 1986: Precursors of the Southern Oscillation, *Journal of Climatology*, 6, 17-30.

APPENDIX A

Standardized Sea Surface Temperature Time Series

The principal component amplitudes corresponding to the rotated components of non-seasonal SST variability for the southwest Indian and southeast Atlantic Oceans are shown. The associated spatial loadings are illustrated in Figure 3.1.

PC1 INDIAN OCEAN 1949–1984

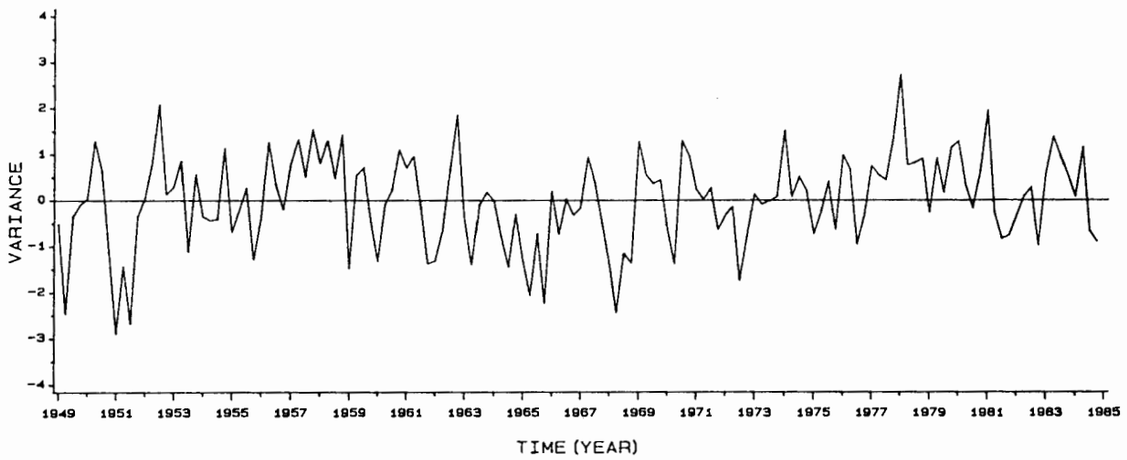

PC2 INDIAN OCEAN 1949–1984

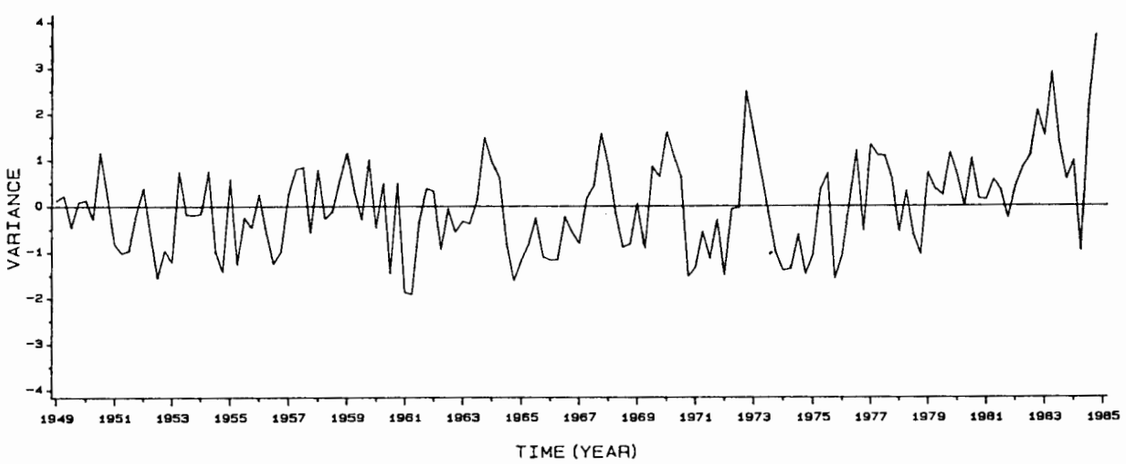

PC3 INDIAN OCEAN 1949–1984

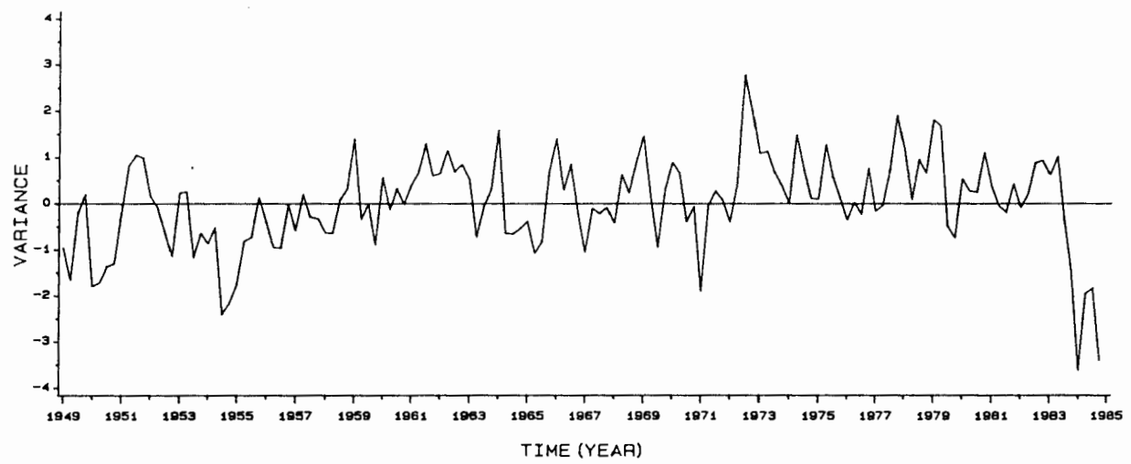

PC4 INDIAN OCEAN 1949–1984

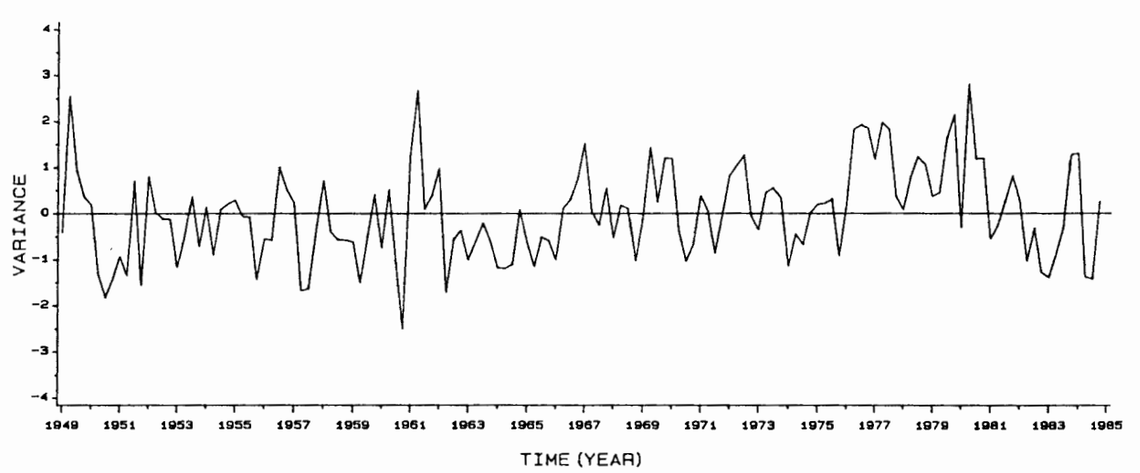

PC5 INDIAN OCEAN 1949–1984

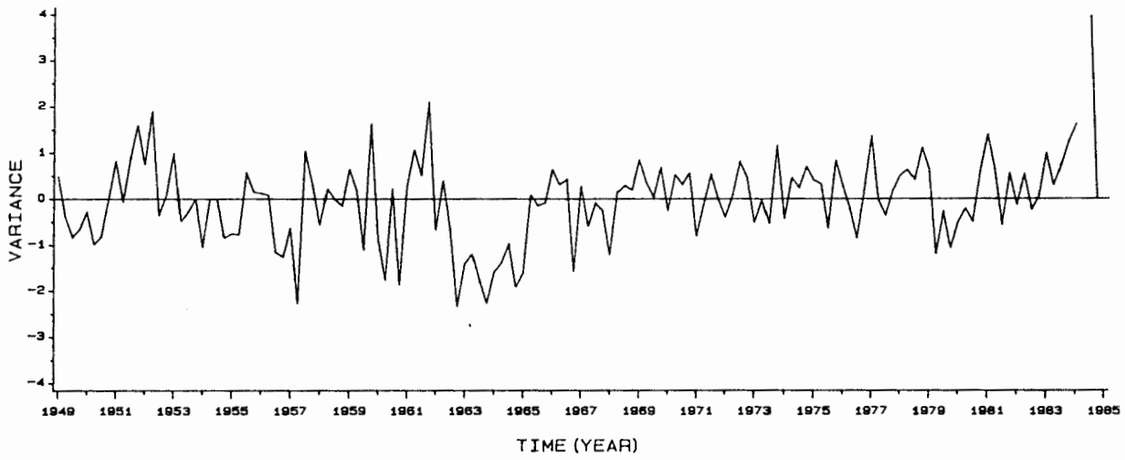

PC6 INDIAN OCEAN 1949–1984

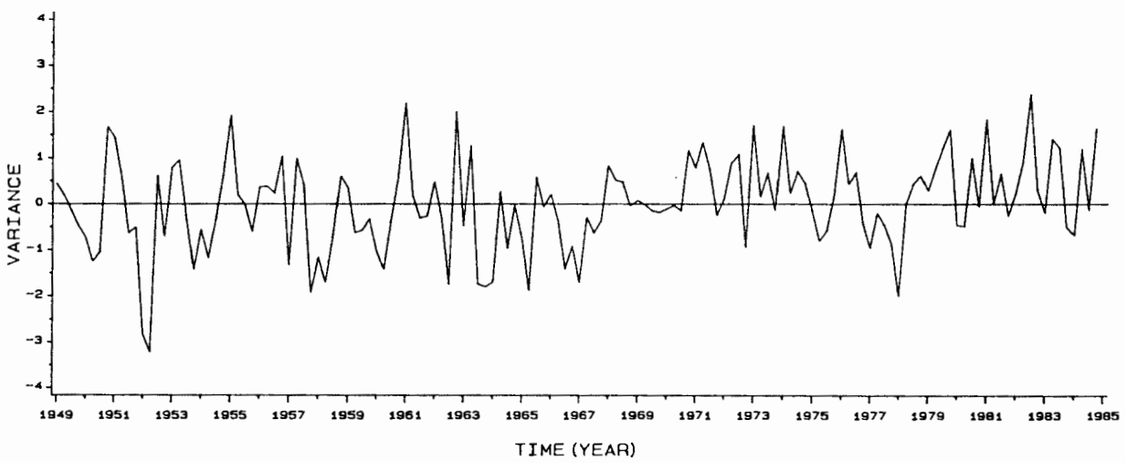

PC7 INDIAN OCEAN 1949–1984

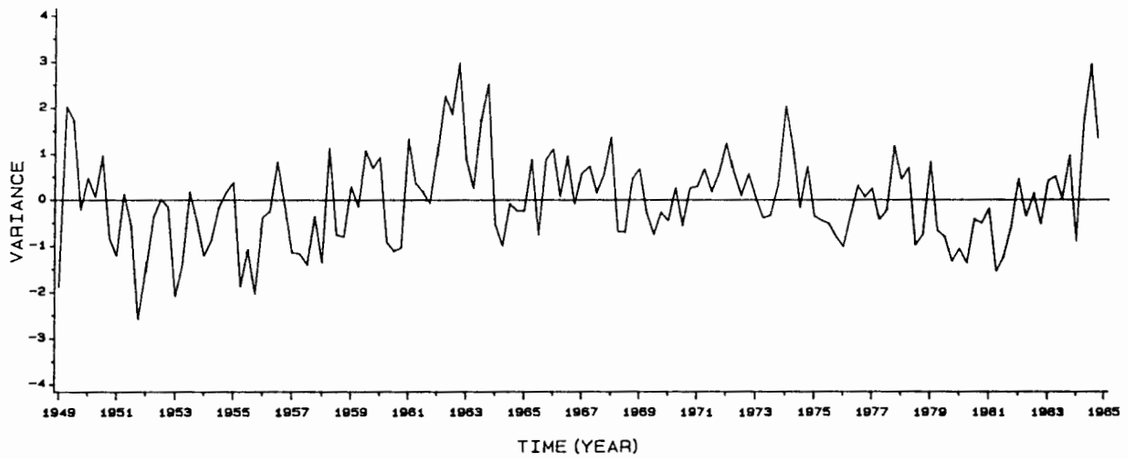

PC8 INDIAN OCEAN 1949–1984

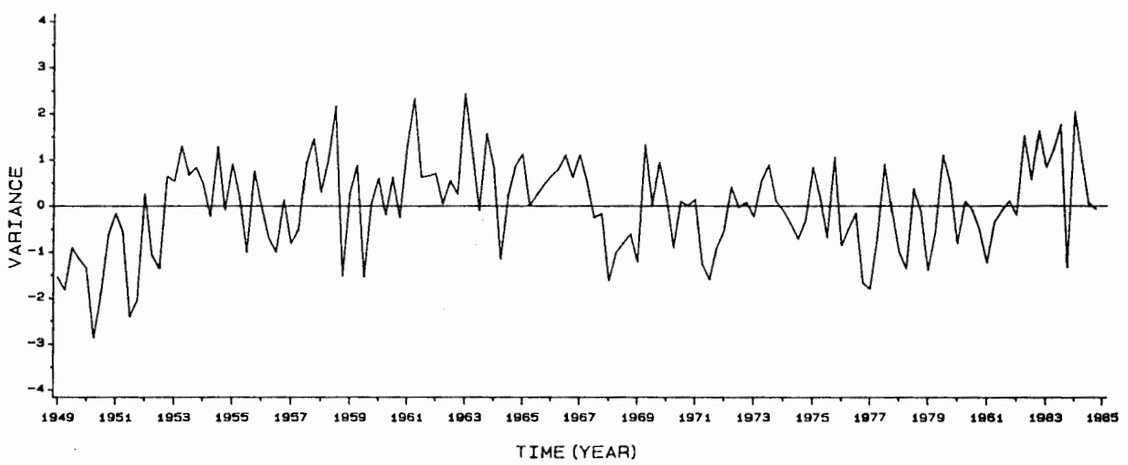

PC1 ATLANTIC OCEAN 1949–1984

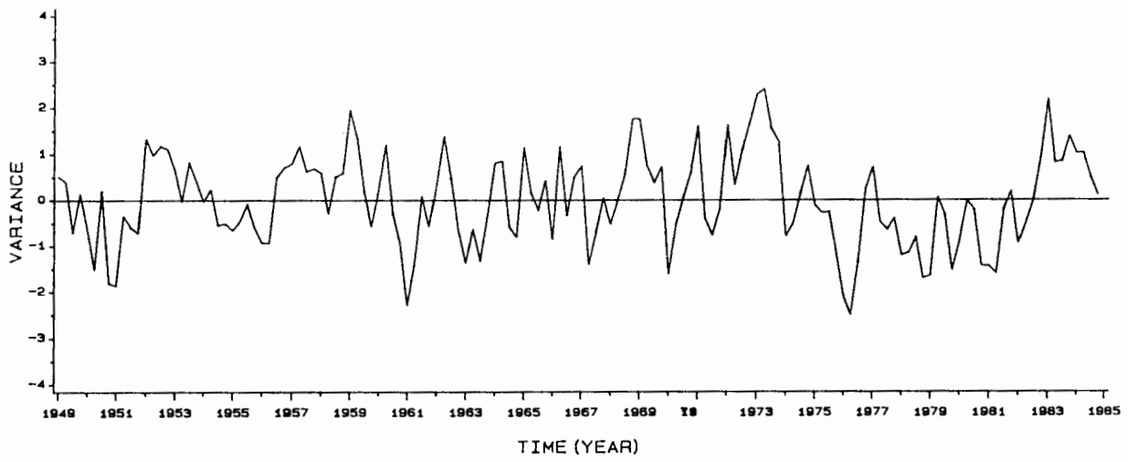

PC9 INDIAN OCEAN 1949–1984

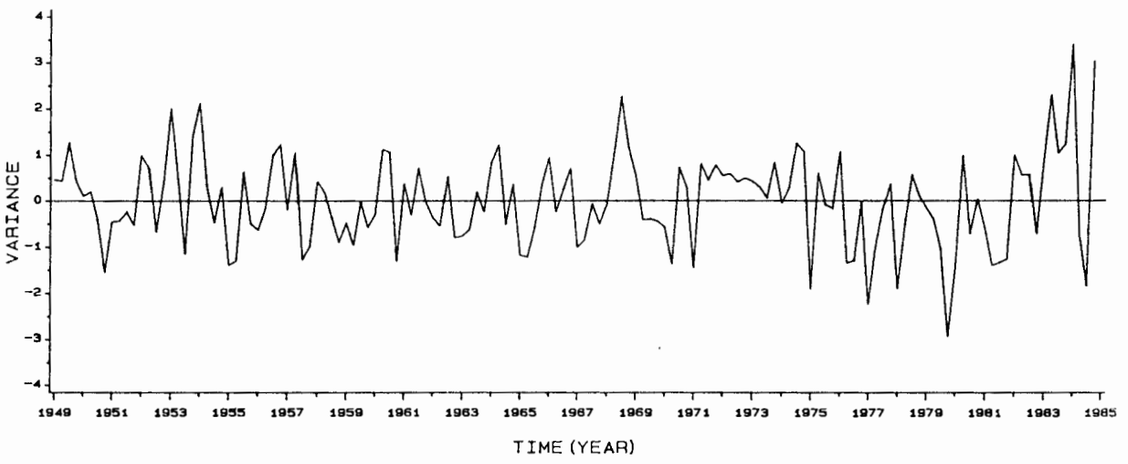

PC2 ATLANTIC OCEAN 1949–1984

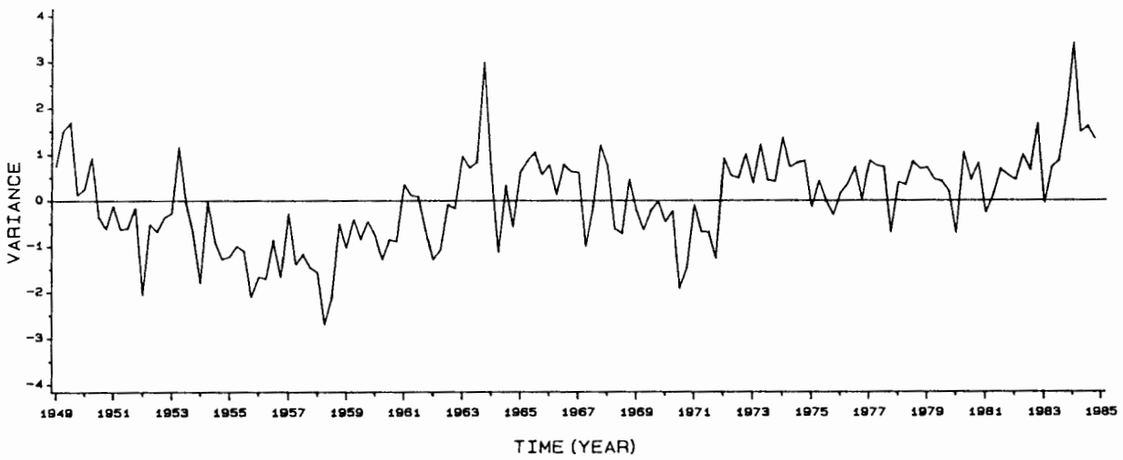

PC3 ATLANTIC OCEAN 1949–1984

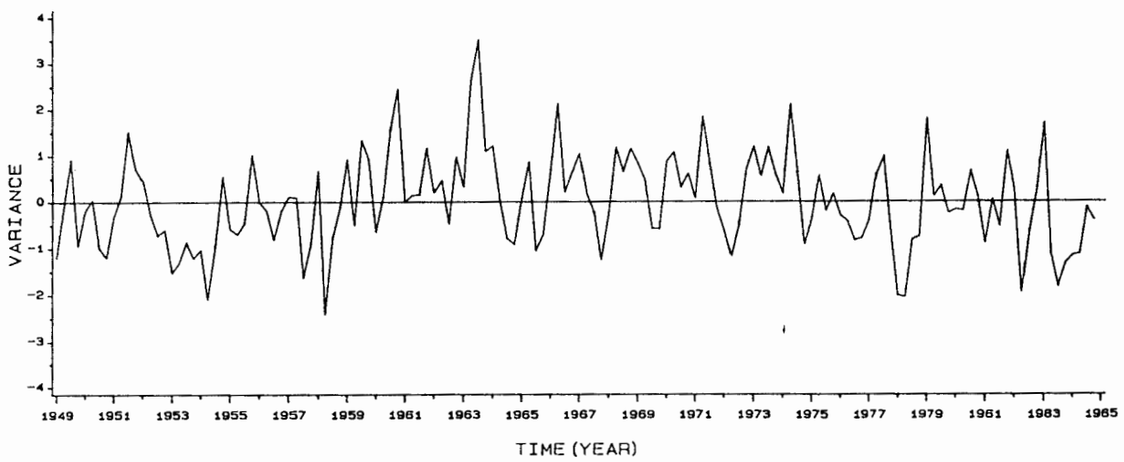

PC4 ATLANTIC OCEAN 1949–1984

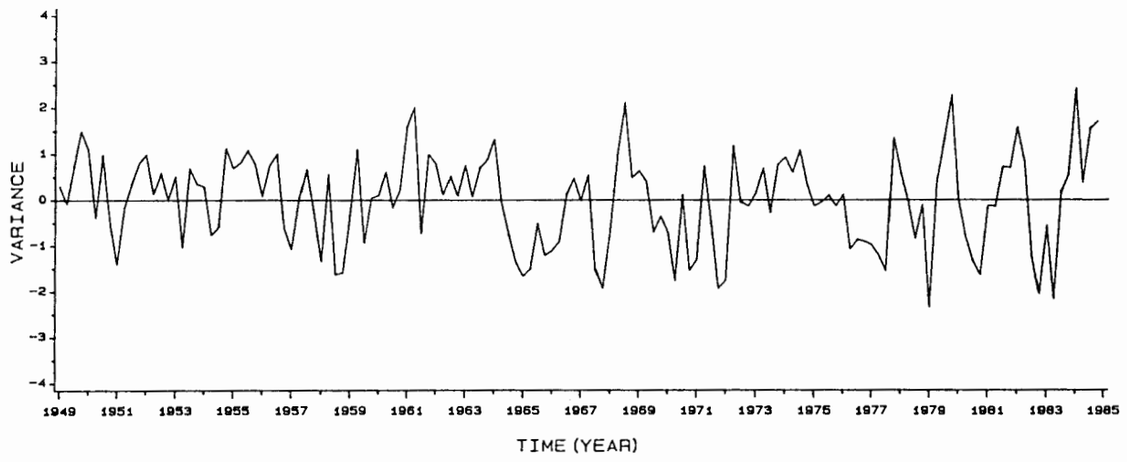

PC5 ATLANTIC OCEAN 1949–1984

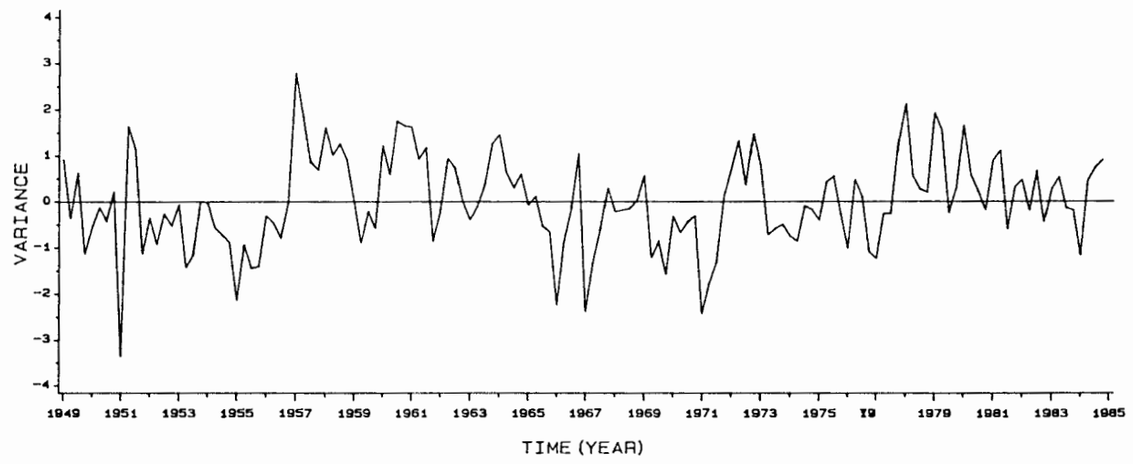

PC6 ATLANTIC OCEAN 1949–1984

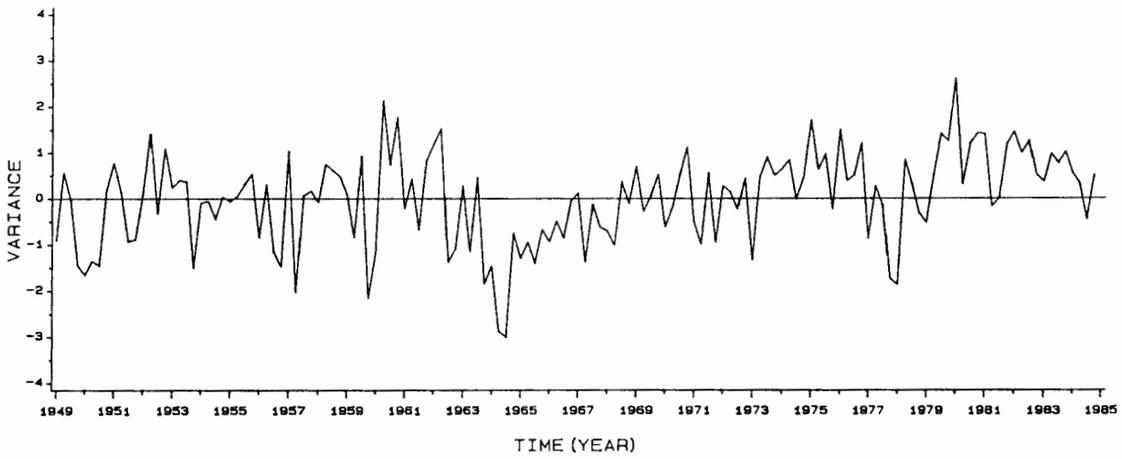

PC7 ATLANTIC OCEAN 1949–1984

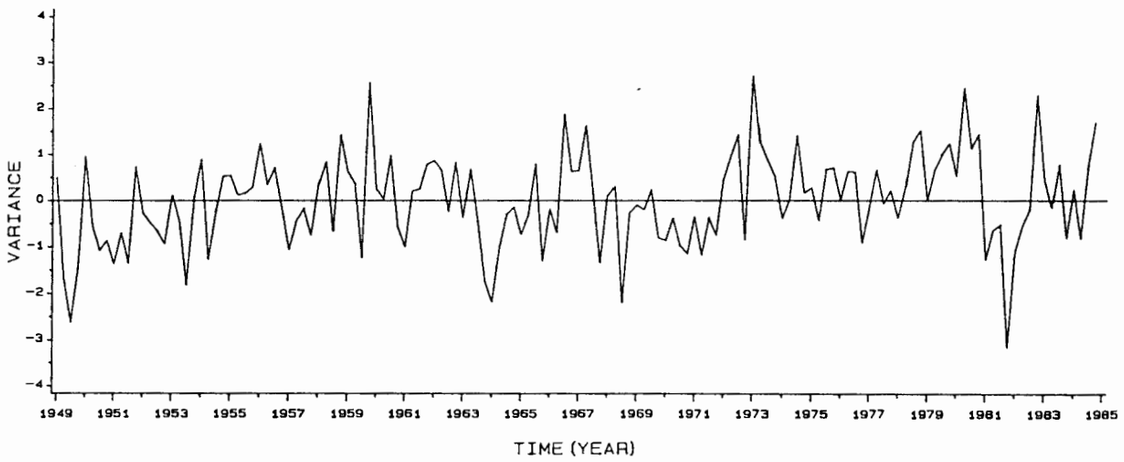

PC8 ATLANTIC OCEAN 1949–1984

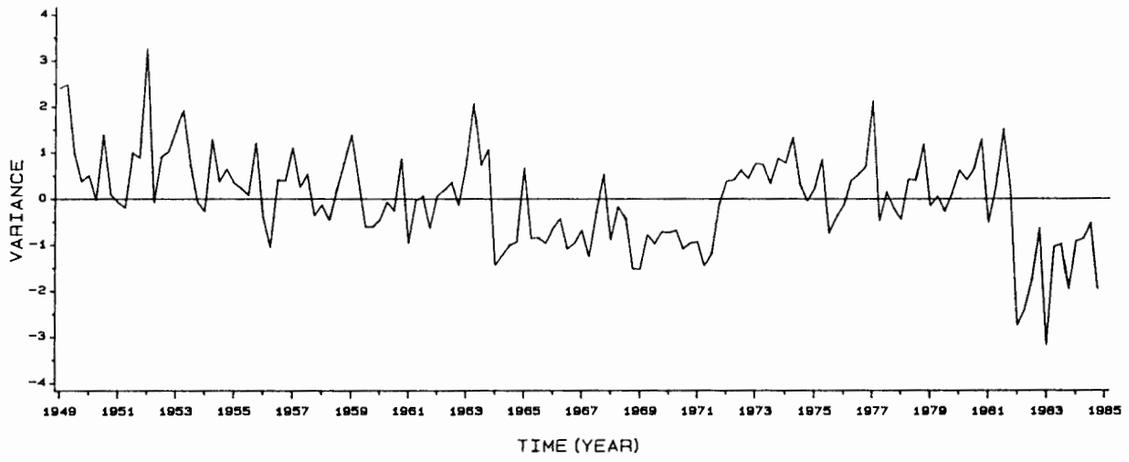

PC9 ATLANTIC OCEAN 1949–1984

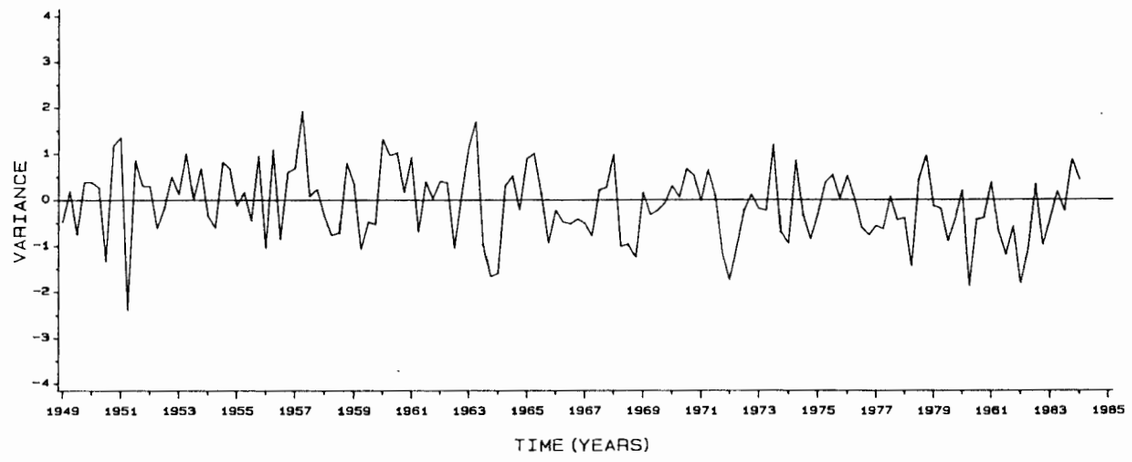

APPENDIX B

Standardized Rainfall Time Series

The 36-year time series of standardized station rainfall data, averaged over areas 1 and 2 (Figure 2.3) are shown for the early summer season (October-December) and the late summer season (January-March).

OND RAIN – AREA1

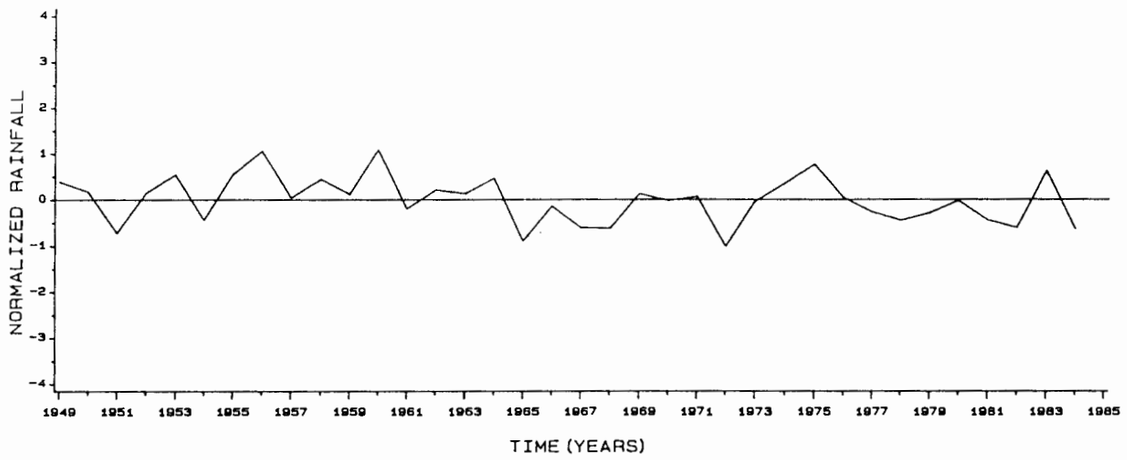

OND RAIN – AREA2

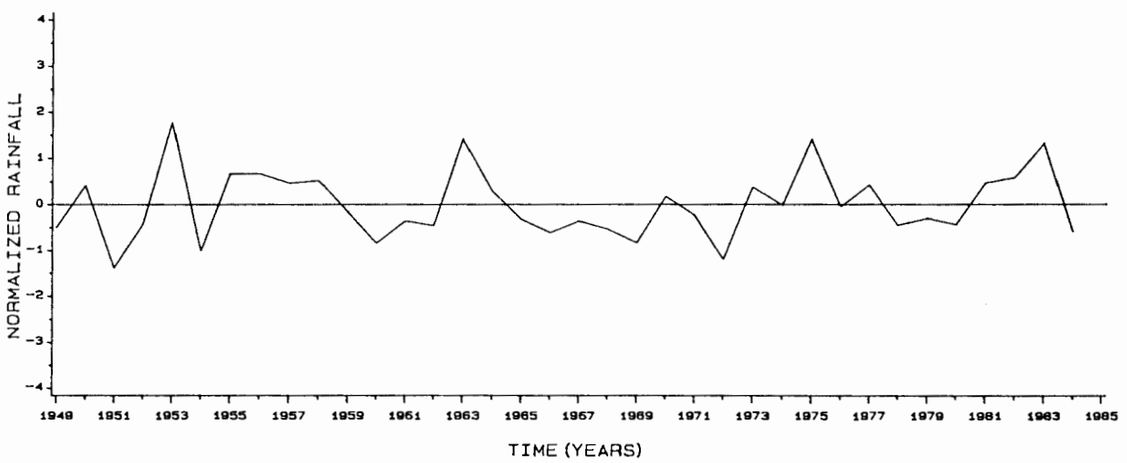

JFM RAIN – AREA1

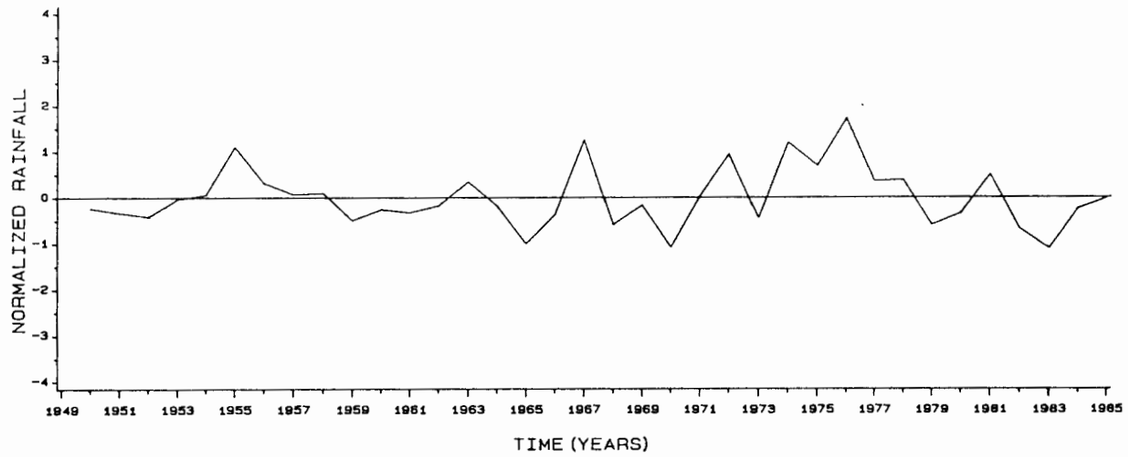

JFM RAIN – AREA2

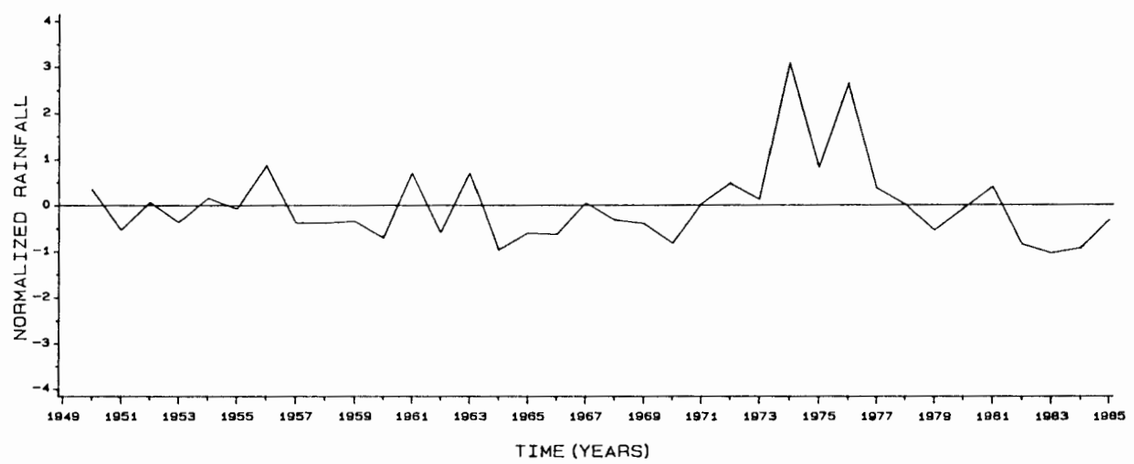

APPENDIX C

Southern Oscillation Index

SOUTHERN OSCILLATION INDEX

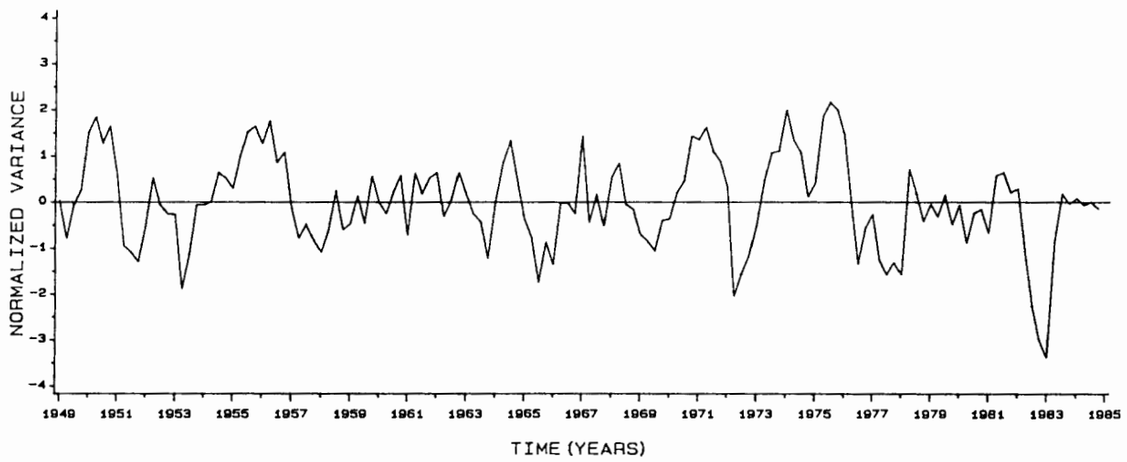

S.O.I. – OND

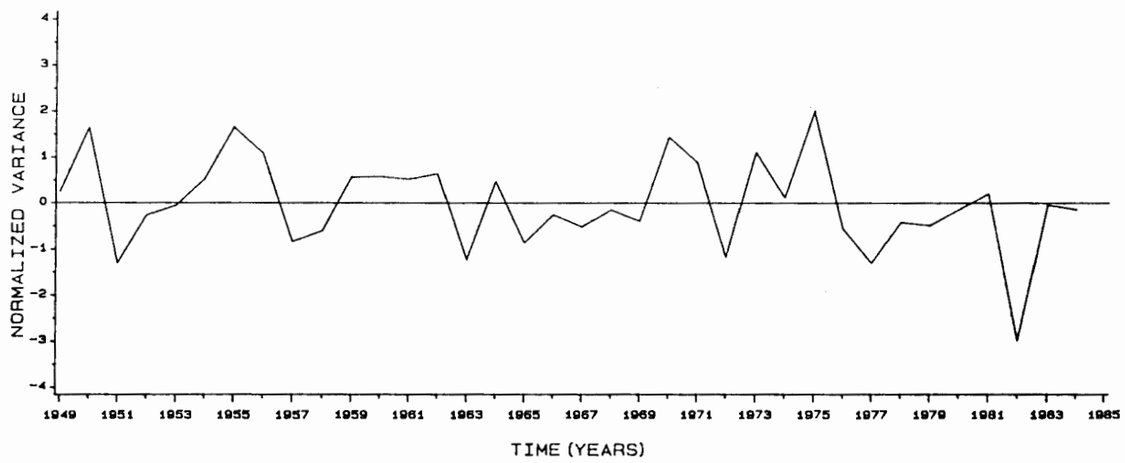

S.O.I. – JFM

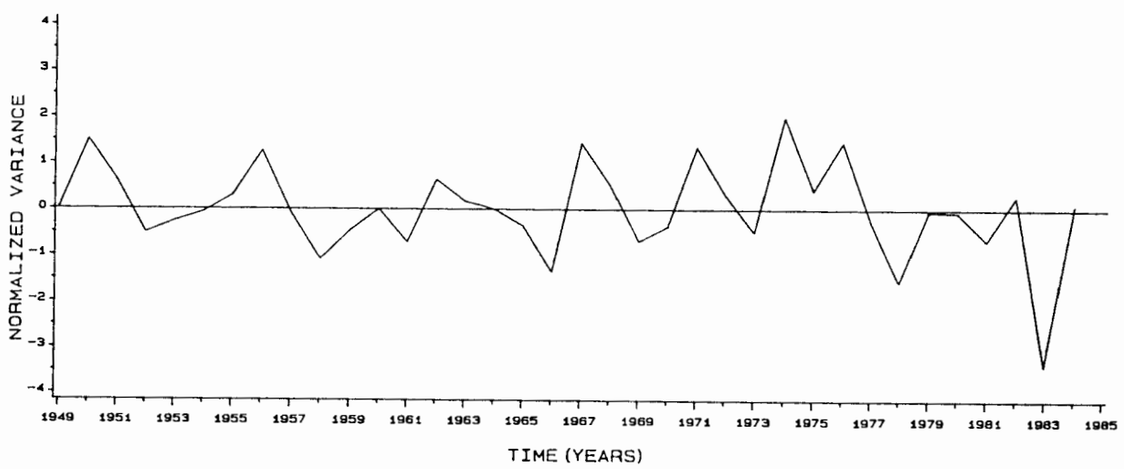

APPENDIX D

Statistical Significance Testing

Autocorrelation

Time series are often characterized by a dependence or similarity of successive observations. An investigation of autocorrelation within the individual time series is required before performing cross-correlations between time series. If autocorrelation exists, the degrees of freedom need to be reduced to obtain "effective" degrees of freedom. The following technique, from Quenouille (p. 168)[1] is useful in estimating the effective degrees of freedom (Hirst and Hastenrath, 1983; Aceituno, 1988). If the serial correlation coefficients in two series of N_1 terms are r_1,r_2 and r_3 and r_1' , r_2', and r_3'... the effective number of independant observations can be derived from

$$N/(1 + 2r_1r_1' + 2r_2r_2' + \dots)$$

If the serial correlations in either series are small or zero, no correction is needed. This results from the fact that if either series is random or near random each observation in that series contributes new information on the value of the correlation coefficient.

Autocorrelation tests, performed on both the sea surface temperature and rainfall data series, revealed that adjustments to the degrees of freedom were not necessary. The use of time series containing single seasons per year substantially reduces autocorrelation.

Field Significance of Correlation Patterns

A neglected aspect of statistical testing in a large number of geophysical studies has been the evaluation of collective significance of a finite set of individual significance tests. In hopes of ameliorating this situation, Livezey and Chen (1983)[2] have clearly outlined tests which should be performed to assess whether identified

---

1 Quenouille, M.H., 1952: *Associated Measurements*, Butterworths, 242pp.

2 Livezey, R.E. and W.Y. Chen, 1983: Statistical field significance and its determination by Monte Carlo techniques, *Monthly Weather Review*, 111, 46-59.

correlation patterns over space display "field" significance. They suggest the use of two tests.

The first test concerns finiteness and the binomial distribution, assuming independence of the individual time series. The percentage area of statistically significant correlations within the data field is determined and tested against the binomial distribution. The field significances of figures 3.3, 3.6, 3.10, 3.12 and 3.16 were assessed using figures 3 and 6 of Livezey and Chen[2]. In figure 3.3 (p.32), field significance was obtained for both rainfall areas at the 5% and 10% levels. In figure 3.6 (p.39) only the area 1 map attained field significance at both the 5% and 10% levels. Figure 3.10 (p. 47) displays SST-rainfall correlations after SO-rainfall associations were excluded. The area 1 map attained field significance at the 5% level, however, the area 2 map did not. The similarity of correlation patterns associated with the two areas suggests that area 2 correlations may not be random. Figure 3.12 (p. 50), displays lag correlations between SST and late summer rainfall. Neither map attained field significance at the 5% level, however, both maps faired better at the 10% level. Again, the similarity of correlation patterns for the two rainfall areas suggests that the identified correlations may not be spurious. Lag correlations may show greater significance on monthly or bi-monthly time scales and could be investigated in future work. Figure 3.16 (p. 56) shows correlations between early summer rainfall and simultaneous sea surface temperatures after exclusion of SO-rainfall relationships. Only the area 1 rainfall map attained field significance. All in all, the area 2 correlations were not as significant as those of area 1, particularly during early summer. This observation may be related to the fact that the western area receives very little rainfall in early summer. In addition, area 2 experiences rainfall which is more event-related than area 1. In contrast to the statistical results, case study analyses revealed a close correspondence between major warm events within the Agulhas Retroflection region and area 2 rainfall anomalies, even in early summer.

The second field significance test suggested by Livezey and Chen[2] involves evaluating and adjusting for interdependence between individual time series. This is advisable as large cross-correlations in a field reduce the degrees of freedom in a similar manner as large autocorrelations reduce the number of effective samples in a time series. As multivariate techniques are not always applicable to relatively short geophysical series, Monte Carlo simulations are the only recourse[2]. This second test for field significance was not explored in this study, however, detailed and laborious Monte Carlo techniques should be explored in future work.

VITAE

Nan Delene Walker-van Heerden was born on 9 October 1953 in Freeport, Texas. In 1972, she graduated from the Graded American High School in Sao Paulo, Brazil. She attended Duke University and graduated cum laude in 1976 with a Bachelor of Science degree, having specialized in marine sciences. She was awarded a NASA Graduate Student Research Fellowship in 1980 and completed her Master of Science degree within the Marine Sciences Department, Louisiana State University, in 1982. The thesis was entitled "Physical responses of southern Florida and northern Bahama lagoon waters to severe cold air outbreaks and effects on hermatypic reef corals". Subsequently, she moved with her husband, Dr. Ivor L. van Heerden, to Cape Town, South Africa where she has headed research projects at the Sea Fisheries Research Institute and the National Research Institute for Oceanology/CSIR in Stellenbosch. She enrolled in a Ph D program in the Physical Oceanography Department of the University of Cape Town in May 1987.